UNITED STATES DEPARTMENT OF COMMERCE
DANIEL C. ROPER, Secretary
NATIONAL BUREAU OF STANDARDS
Lyman J. Briggs, Director

✦

Journal of Research

of the

National Bureau of Standards

✦

Volume 20, No. 5

May 1938

Published with approval of the Director of the Budget

UNITED STATES
GOVERNMENT PRINTING OFFICE
WASHINGTON : 1938

For sale by the Superintendent of Documents, Washington, D. C. - - - - - Price 25 cents
$2.50 per year on subscription

The prices of the separate Research Papers appearing in this JOURNAL are given on the front cover page. If 100 or more copies of any separate are ordered, a discount of 25 percent is allowed. Those who desire copies of separate Research Papers should send their orders and remittances without delay to the Superintendent of Documents, U. S. Government Printing Office, Washington, D. C. This will aid him to determine the number of copies to be printed for sale. Research Papers are not printed from electrotypes, and usually no more reprints can be had when the first and only printing is exhausted.

U. S. Department of Commerce National Bureau of Standards

RESEARCH PAPER RP1092

Part of Journal of Research of the National Bureau of Standards, Volume 20, May 1938

EFFECT OF CARBON ON THE CRITICAL COOLING RATE OF HIGH-PURITY IRON-CARBON ALLOYS AND PLAIN CARBON STEELS

By Thomas G. Digges

ABSTRACT

This report describes the preparation of a series of high-purity iron-carbon alloys and two series of plain carbon steels, the members of each series differing only in carbon content. Determinations of the austenitic grain size and critical cooling rates show how carbon affects the hardening properties and permit comparison of the hardenability of these alloys and steels.

CONTENTS

	Page
I. Introduction	571
II. Preparation of materials	572
1. Iron-carbon alloys	572
2. Carbon steels	574
III. Microscopic examination	575
IV. Chemical composition	576
V. Austenitic grain size	577
VI. Critical cooling rate	578
VII. Summary	585

I. INTRODUCTION

The composition and grain size of austenite are now recognized as factors that influence the critical cooling rate or hardenability of steel. In previous investigations on the effect of carbon on the critical cooling rate, carried out at the National Bureau of Standards [1] with plain carbon steels, and by other investigators [2] with high-purity iron-carbon alloys, due regard was not given to the simultaneous influence of the austenitic grain size. At the time the study was made at the National Bureau of Standards, it was recognized that wide variation existed in the hardening characteristics of different heats of plain carbon steels of apparently the same composition, but the marked influence of austenitic grain size on the hardenability of steel was not then recognized. The experiments described in the present report were made to determine the influence of carbon on the critical cooling rate of both high-purity iron-carbon alloys and plain carbon steels. The method of preparing the alloys and steels used in this study eliminated the quality factor and variables other than carbon in the composition. Determinations were made of the critical cooling rates for both

[1] H. J. French and O. Z. Klopsch, *Quenching diagrams for carbon steels in relation to some quenching media for heat treatment*, Trans. Am. Soc. Steel Treating **6**, 251–294 (1924).

[2] H. Esser, W. Eilender, and E. Spenle, *Quenching diagrams of the iron-carbon alloys*, Arch. Eisenhüttenw. **6**, 389–393 (1933).

series of alloys and steels, quenched directly from the temperatures required to establish a constant austenitic grain size with all carbon in solution. In these experiments, the only variable that influenced the critical cooling rate was the carbon content of the austenite, since the time-temperature relationship used was such as to produce complete solution and uniform distribution of carbon in austenite of constant grain size. However, the study was extended to include determinations of the critical cooling rates of the carbon steels quenched from the usually recommended hardening temperature range. In the latter experiments, the carbon content and grain size of the austenite and total carbon varied with the different steels.

II. PREPARATION OF MATERIALS

1. IRON-CARBON ALLOYS

A heat of high-purity iron was used as the basic material for the iron-carbon alloys. This heat was prepared by melting and solidifying electrolytic iron in vacuo in a crucible of chemically pure magnesia bonded with a solution of 2 to 3 percent of magnesium chloride in water. The ingot, about 1⅞ inches in diameter at the top, 1⅝ inches in diameter at the bottom, and 3¾ inches long, had the surface imperfections removed before being split longitudinally into two approximately equal sections preparatory to mechanical working. All the specimens of the iron-carbon alloys were prepared from this ingot.

Hot-working was carried out at an initial temperature of 2,100 to 2,200° F, and the split halves of the original ingot were forged until reduced in thickness to about 3/16 inch and then hot-rolled to bars about ⅛ inch thick. The scale formed on the surface of the bars during hot-working was removed by grinding, before cold-rolling to the final form of plates, 0.040 inch thick. Prior to carburizing, these plates were cut into strips and annealed at 1,100° F for ½ hour either in vacuo or in a reducing atmosphere, to remove the effects of cold-working.

The advantages of preparing high-purity iron-carbon alloys by carburization in gases have been pointed out by Mehl and Wells.[3] They prepared a series of high-purity alloys from hydrogen-purified carbonyl iron by carburization in mixtures of dipentene-hydrogen and dipentene-benzene-hydrogen. These alloys were homogeneous in the carburized condition.

In the present experiments with propane as the carburizer, a study was made of the effects of temperature, rate of flow, concentration, direction of flow, and agitation of the gas on the uniformity of carburization of the iron. The preliminary carburizing experiments with propane as the carburizer gave unsatisfactory results. However, benzene proved to be entirely satisfactory for uniformly carburizing the iron to the desired carbon content.

Specimens of the high-purity iron were carburized in a mixture of hydrogen and benzene (less than 0.003 percent of sulfur) within the temperature range of 1,670 to 1,700° F, with a gas flow of 90 to 100 milliliters per minute. The assembly of the apparatus used is shown in figure 1. The hydrogen was purified by passing it through Ascarite (*B*) and silica gel (*D*) contained in a vertical tube heated electrically to 1,300 to 1,475° F, and then through magnesium perchlorate (*E*) and phosphorus pentoxide (*F*). The dry hydrogen next passed through

[3] R. F. Mehl and Cyril Wells, *Constitution of high-purity iron-carbon alloys*, Metals Tech. T. P. 798, 4 (June 1937).

the benzene (*G*) maintained at a temperature of 60 to 65° F by a water bath (*I*) in a Dewar flask (*H*), then through the orifice (*K*) and around the specimen (*M*) suspended vertically in a quartz tube by a wire of the same material as the specimen, and finally into the air at the exhaust end (*N*) of the furnace.

The desired gas flow was maintained during carburizing by regulating the pressure of the system, as indicated by the oil manometer (*J*), with reducing and needle valves attached to the hydrogen tank.

The furnace, constructed especially to obtain uniform heating of the specimens, consisted essentially of an Alundum tube wound with Nichrome wire, with a compensating coil placed at each end of the furnace over the main heating coil. The temperature was adjusted and controlled by independent adjustment of the current in each of the three branches of the heating circuit. By preliminary tests made

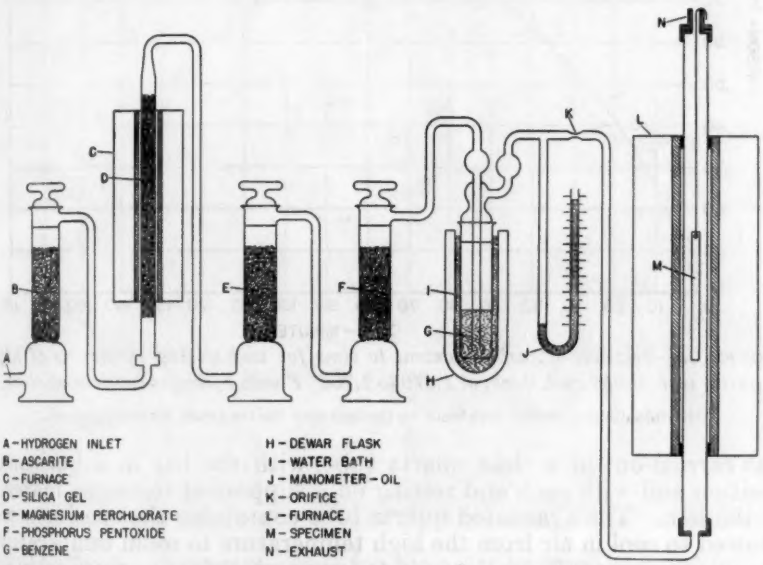

FIGURE 1.—*Diagram of apparatus used for carburizing with hydrogen-benzene mixture.*

prior to the carburizing treatment, the conditions necessary for establishing a uniform temperature were determined, and the current input necessary for maintaining equilibrium at the desired temperature was ascertained. The procedure for carburizing was as follows: After obtaining a uniform temperature in the carburizing zone of the furnace with the gas flowing at the required rate, the high-purity iron specimen (0.040 to 0.041 by 0.275 to 0.300 by 8 inches long) cleaned with 1G emery paper and washed in xylene, was inserted in the cold zone of the quartz tube at the top of the furnace. After remaining in this zone 1 to 2 minutes, the specimen was lowered without touching the walls of the tube into the carburizing zone, held for a predetermined time, and returned to the cold zone to cool in a reducing atmosphere to an estimated temperature of 200 to 400° F. It was finally allowed to cool to room temperature in air. The time of carburizing varied with the desired carbon content of the alloy, as is shown in figure 2.

The carburized bars were ground to a width of 0.250 inch, by removing approximately equal amounts from each edge, before being heated in vacuo at 1,670 to 1,700° F for 4 to 5 hours to produce uniform distribution of the carbon in the cross section. This heat treatment

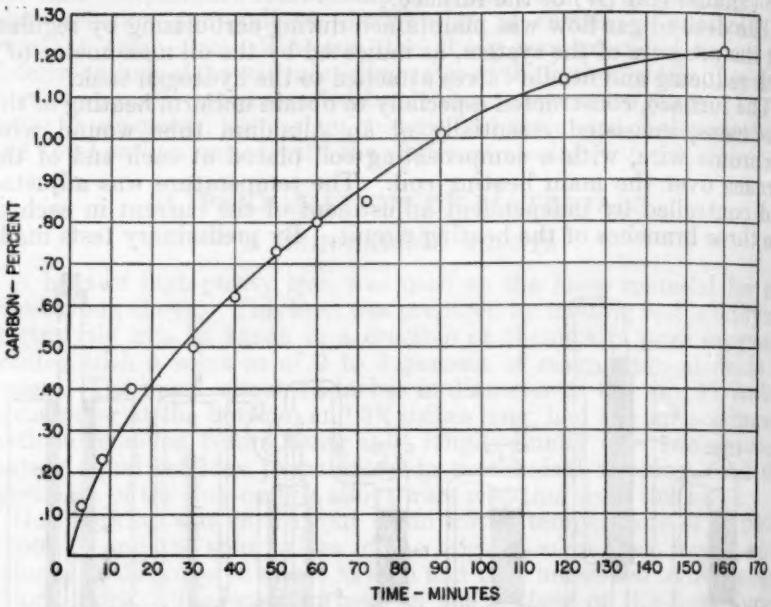

FIGURE 2.—*Relation of carbon content to time for carburizing specimens of high-purity iron, 0.040 inch thick, at 1,670 to 1,700° F with hydrogen-benzene mixture.*

Determinations of carbon were made on the bars after the treatment for homogeneity.

was carried out in a clear quartz tube, with the bar in a horizontal position and with each end resting on a support of the same material as the bar. The evacuated quartz tube containing the specimen was allowed to cool in air from the high temperature to room temperature. This cooling was sufficiently rapid to form sorbite (or fine pearlite) in the alloys, as is shown for the 0.23- and 1.21-percent carbon alloys in figure 3. Specimens subsequently used for the determination of the austenitic grain size and critical cooling rate had this initial structure of sorbite.

2. CARBON STEELS

A forging, 2 inches in diameter, of acid open-hearth steel containing 0.20 percent of carbon was the starting material for the preparation of the plain carbon steels. The composition of the forging is shown in table 1.

TABLE 1.—*Chemical composition of the steel used as the basic material for the carbon steels*

Element	Analysis	Element	Analysis
	Percent (by weight)		*Percent (by weight)*
Carbon	0.20	Chromium	0.02
Manganese	.46	Vanadium	Trace
Phosphorus	.043	Nickel	0.11
Sulfur	.025	Copper	.021
Silicon	.15	Arsenic	.012

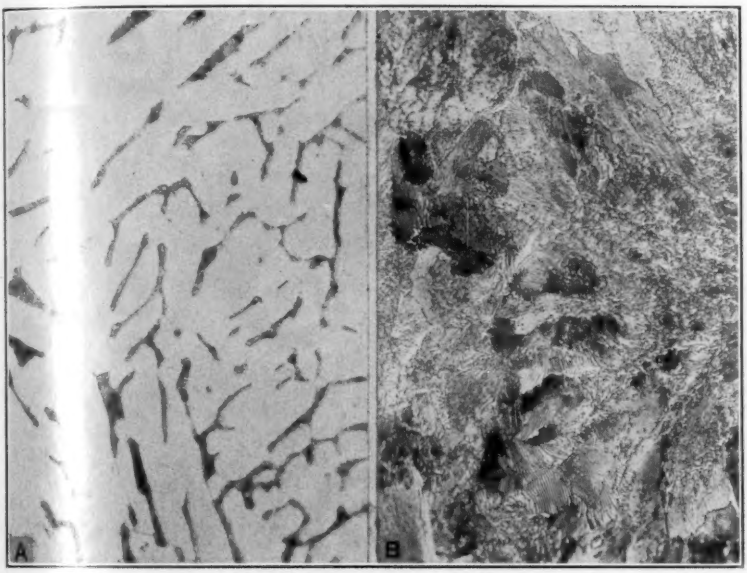

FIGURE 3.—*Structure of iron-carbon alloys after treatment for homogeneity.*

A, 0.23 percent of carbon; *B*, 1.21 percent of carbon. The sorbite, or fine pearlite, is representative of the initial structure of the alloys and steels for the determination of austenitic grain size and critical cooling rate. Etched with 1-percent nitric acid in alcohol. ×500.

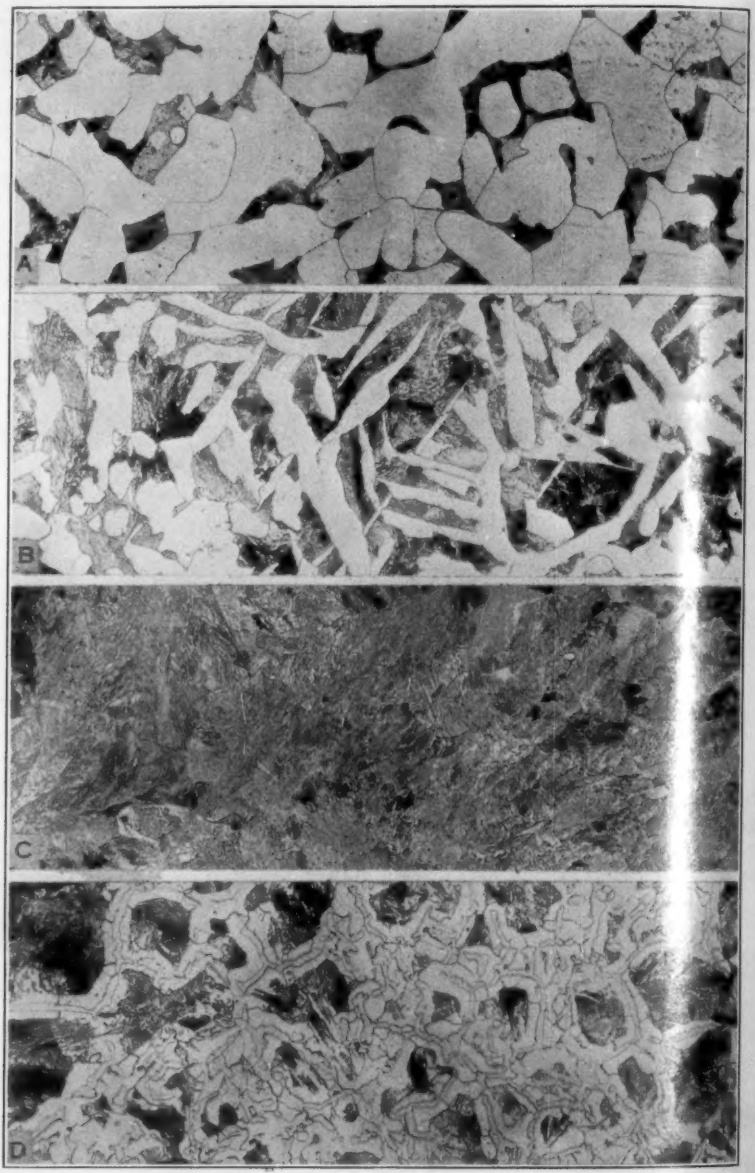

FIGURE 4.—*Structure of annealed iron-carbon alloys.*

A, 0.23 percent of carbon; *B*, 0.50 percent of carbon; *C*, 0.85 percent of carbon; *D*, 1.21 percent of carbon. Specimens annealed at 1,700° F. for 1 hour in vacuo after treatment for homogeneity. The length of the micrographs represents practically the entire thickness of the bars. The left border of the micrographs shows the structure at the extreme edge of the specimens. Etched with equal parts of nitric acid (1 percent) and picric acid (5 percent) in alcohol. ×100.

To minimize the influence of segregation, a ⅝-inch hole was drilled along the horizontal axis of this forging before preparing the specimens for carburizing. A disk from the cross section of the forging etched in hot acid showed no indications of segregation. However, subsequent microscopic examinations of the structures of the quenched specimens used in the determination of the critical cooling rates showed, in some of these specimens, indications of segregation of manganese sulfide inclusions or banding of ferrite and carbide. This factor evidently was responsible for the wide variation later observed in the structures of a few of the specimens prepared and quenched under identical conditions.

Two series of carbon steels were prepared from specimens cut from this forging. The first series was prepared by pack-carburizing specimens, 0.050 by 0.260 by 8 inches long, in a mixture of approximately 85 percent of wood charcoal and 15 percent of barium carbonate at 1,700° F for various periods of time. The carburized specimens were then pack-annealed at 1,700° F for 4 to 5 hours before normalizing from the usually recommended temperature range. The normalizing treatment produced a structure of sorbite in all the steels. The bars with this initial structure of sorbite were then ground to a thickness of 0.040 inch and a width of 0.250 inch, before preparing specimens for the determinations of the austenitic grain size and critical cooling rate.

With the procedure used in preparing the steels by pack-carburizing, pack-annealing, and normalizing difficulty was encountered in obtaining steels of the desired carbon content with the carbon uniformly distributed. Furthermore, pack-carburized specimens often show an appreciable increase in the oxygen content. Because of these factors, the second series of carbon steels was prepared by carburizing specimens of the 0.20-percent carbon steel in hydrogen and benzene, and homogenizing by heating in vacuo. These treatments were carried out under the same procedure as that already described for the high-purity iron-carbon alloys. Cooling the 0.040-inch-thick bars from the temperature used in the homogenizing treatment was sufficiently rapid to form sorbite in all the steels. The specimens subsequently used for determination of the austenitic grain size and critical cooling rate had this initial structure.

III. MICROSCOPIC EXAMINATION

Pieces, ¼ to ⅜ inch long, were discarded from each end of all the bars after the treatments for homogeneity. Microscopic examination of the cross section of each end of the bars (after the end pieces were removed) showed the carbon to be uniformly distributed. This is illustrated for the gas-carburized alloys and steels in figure 4, which shows the microstructure of four of the iron-carbon alloys annealed at 1,700° F for 1 hour in vacuo after the treatment for homogeneity. These micrographs show the structure of the bar from one surface almost to the opposite surface. (The actual cross sections were 0.040 to 0.041 inch thick.) This annealing treatment produced "abnormal" structures in all of the hypereutectoid iron-carbon alloys, as shown in the 1.21-percent carbon alloy by the coalesced masses of cementite partially or entirely surrounded by ferrite.

IV. CHEMICAL COMPOSITION

Spectrochemical and chemical analyses were made on specimens of the iron-carbon alloys and the determinations of gas content were made by the vacuum-fusion method. The arc spectrum of the alloy was examined for the sensitive lines of Ag, Al, As, Au, B, Ba, Be, Bi, Ca, Cb, Cd, Ce, Co, Cr, Cu, Fe, Ga, Ge, Hf, Hg, In, Ir, K, Li, Mg, Mn, Mo, Na, Ni, Os, Pb, Pd, Pt, Rh, Ru, Sb, Sc, Si, Sn, Sr, Ta, Th, Ti, Tl, U, V, W, Y, Zn, and Zr. The elements found present other than iron were Ca, Co, Cu, Mg, Mn, Ni, Pb, and Si (table 2).

TABLE 2.—*Impurities determined in the iron-carbon alloys*

Element	Analysis [1] (percent by weight)		
	Spectrochemical [2]	Chemical	Vacuum fusion
Manganese		0.002	
Phosphorus		<.001	
Sulfur		.004	
Silicon	0.001	.002	
Copper	<.001	Not detected	
Nickel	.006	.007	
Cobalt		.007	
Calcium	<.001		
Lead	probably <.001		
Magnesium	<.001		
Oxygen			0.003
Nitrogen			.001
Hydrogen			.0002

[1] Determinations were made on specimens from the bars after carburizing and heat treatment for homogeneity except as follows: Values of nickel, cobalt, and copper by chemical analysis were obtained from the electrolytic iron prior to melting, and the values of manganese and phosphorus by chemical analysis were obtained from the bars as carburized. Spectrochemical analyses were made by B. F. Scribner, chemical analyses by W. H. Jukkola and J. L. Hague, and vacuum-fusion analyses by V. C. F. Holm, all members of the staff of the National Bureau of Standards.

[2] Spectrum lines of cobalt and manganese were also found.

Chemical analyses of the electrolytic iron before and after vacuum fusion and of the carburized alloys showed no increase in silicon, sulfur, or manganese in the various operations incident to the preparation of the alloys. Likewise, analyses by the vacuum-fusion method showed no difference in the oxygen, nitrogen, or hydrogen contents as a result of working or carburizing of the high-purity iron.

The results of the analyses, given in table 2, show that sulfur, nickel, cobalt, and oxygen were the major impurities contained in the alloys. These elements amounted to about 0.021 percent, whereas the total percentage (by weight) for all impurities determined was about 0.030.

Carbon was also determined in specimens cut from opposite ends of the 7½-inch bars. Some of the alloys had the same carbon content at both ends. Maximum variation in the carbon value determined in any of the alloys was 0.04 percent. This, however, was an extreme case, and it is believed that the values for carbon for the entire bar are within 0.01 or 0.02 percent of the values shown in the various figures given in this report. In the alloys prepared later and in some of the carbon steels, the carbon was determined in only one section. This was adjacent to the specimens used for the determination of austenitic grain size and critical cooling rate.

Determinations of carbon in specimens from opposite ends of eight different carbon steels, prepared by carburizing in hydrogen and ben-

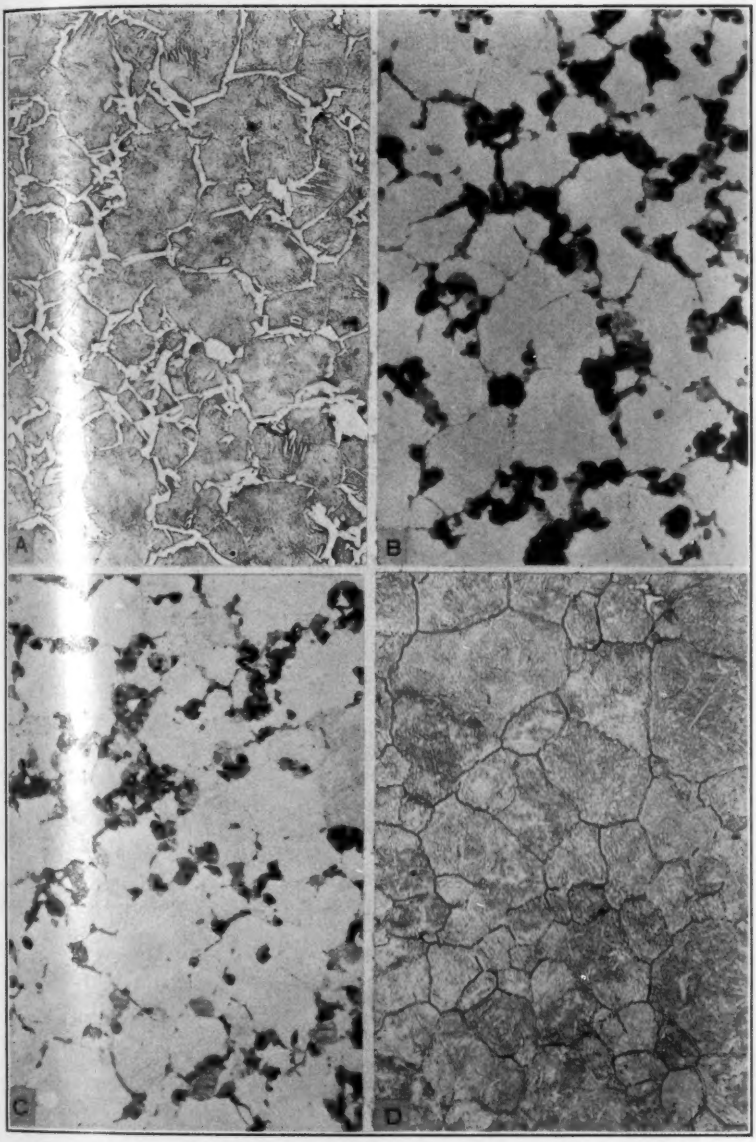

FIGURE 5.—*Grain size of iron-carbon alloys at 1,700° F.*

A, 0.23 percent of carbon; *B*, 0.62 percent of carbon; *C*, 1.01 percent of carbon; *D*, 1.21 percent of carbon. Austenitic grain size of 6 to 12 grains per square inch at 100 diameters (ASTM grain number 4). Etched with 1-percent nitric acid in alcohol. ×100.

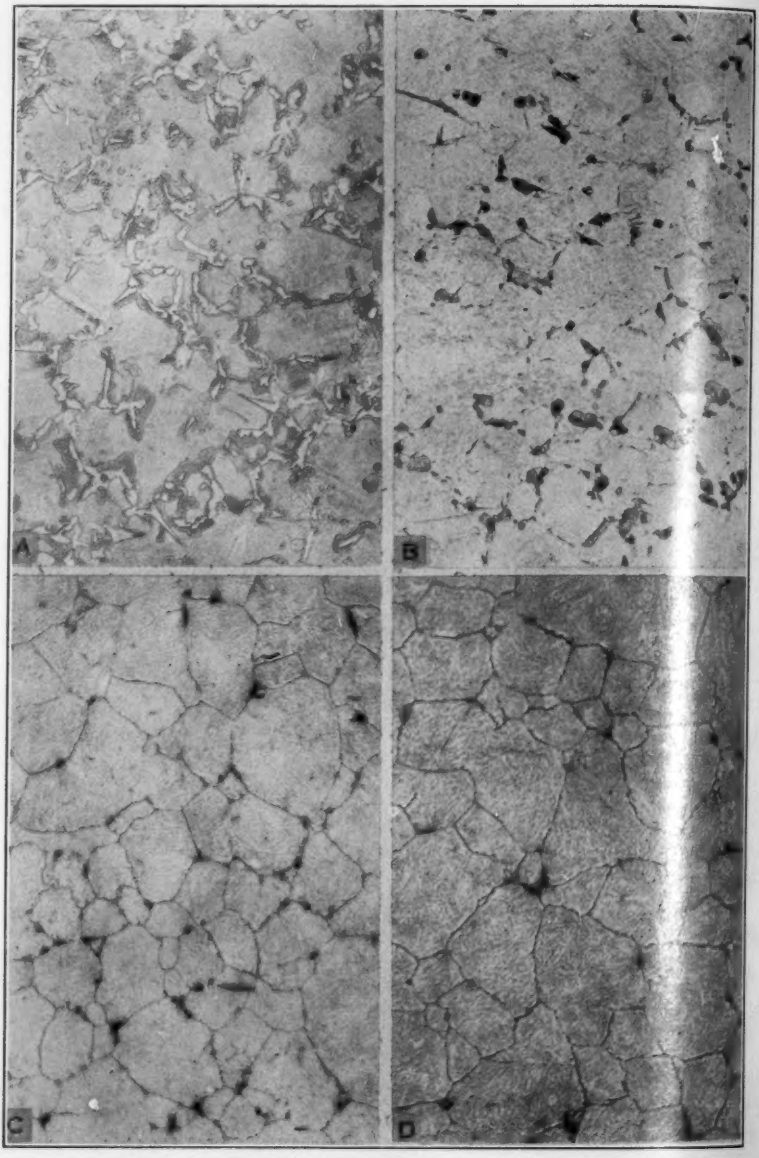

FIGURE 7.—*Grain size of carbon steels at different temperatures.*

A, 0.46 percent of carbon; *B*, 0.76 percent of carbon; *C*, 1.10 percent of carbon; *D*, 1.15 percent of carbon. Average grain size of 6 to 12 grains per square inch at 100 diameters at 1,625° F for the 0.46 percent of carbon, 1,660° F for the 0.76 percent of carbon, 1,680° F for the 1.10 percent of carbon, and 1,700° F for the 1.15-percent carbon steel. Etched with 1-percent nitric acid in alcohol. ×100.

zene, showed a maximum difference of 0.03 percent in any one steel. Variations in carbon of this same magnitude were also shown in the annealed bars of the selected steels, which were prepared by pack-carburizing. Further minor changes occurred in the carbon content of some of the latter steels during the normalizing treatment. The values determined after this treatment were used in preparing the various diagrams for this series of steels.

Complete analyses were not made on the carbon steels after the carburizing and homogenizing treatments. The proportions of the elements other than carbon, given in table 1, should not be materially affected by the various steps incident to the preparation of these steels. Possibly, the oxygen content varied for steels prepared by pack-carburizing. Variations in the oxygen content, however, had no detectable influence on the critical cooling rate of the steels.

V. AUSTENITIC GRAIN SIZE

The specimens for the determination of the austenitic grain size had the same initial structure and were of the same shape and size as

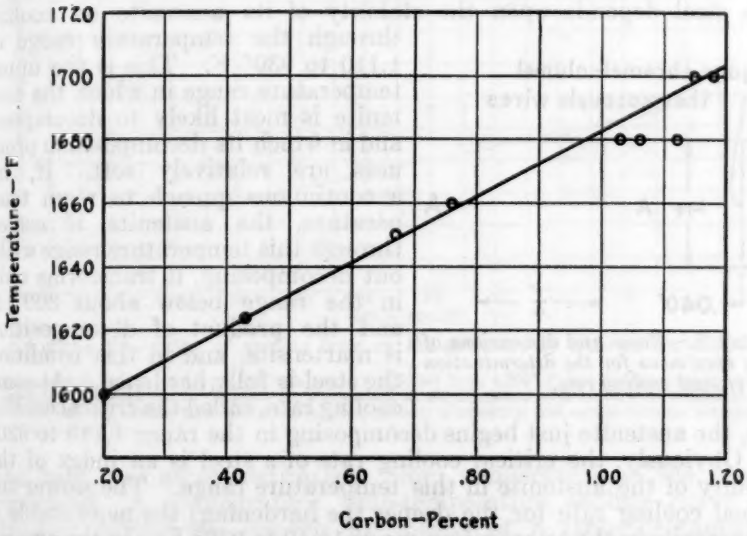

FIGURE 6.—*Relation of temperature to carbon content of the steels for establishing austenitic grain size of 6 to 12 grains per square inch at 100 diameters.*

those used for the determination of the critical cooling rate. They were heated in the same manner, held for the same time at the same temperature, and were then cooled in a manner suitable for outlining the grains.

The austenitic grain size at 1,700° F was determined for the highest-carbon alloy (1.21 percent of carbon). This temperature was sufficiently high to dissolve all the carbon. Subsequent tests on the lower-carbon alloys showed that variations in carbon did not affect the grain size at this selected temperature of 1,700° F.

Each of the iron-carbon alloys had an average grain size of 6 to 12 grains per square inch at 100 diameters (ASTM grain number 4) at

1,700° F. Figure 5 shows the grain size for the 0.23-, 0.62-, 1.01-, and 1.21-percent carbon alloys at 1,700° F. The grain size at 1,700° F was also determined for the 1.18-percent carbon steel. As shown in figure 6, lower temperatures were necessary to establish the same average grain size of 6 to 12 grains per square inch at 100 diameters in the lower carbon steels. Figure 7 shows that this grain size was obtained at 1,625° F for the 0.46-percent carbon steel, at 1,660° F for the 0.76-percent carbon steel, at 1,680° F for the 1.10-percent carbon steel, and at 1,700° F for the 1.15-percent carbon steel.

On heating within the usually recommended hardening temperature range, specimens of the hypoeutectoid carbon steels had approximately the same average grain size of 12 to 24 grains per square inch at 100 diameters (ASTM grain number 5).

No differences were observed between the temperature–grain-size-critical-cooling-rate relations of the carbon steels prepared by pack-carburizing and those prepared by carburizing in hydrocarbon.

VI. CRITICAL COOLING RATE

The work by Davenport and Bain [4] showed that the hardenability of a steel depends upon the stability of its austenite on cooling through the temperature range of 1,110 to 930° F. This is the upper temperature range in which the austenite is most likely to decompose, and in which its decomposition products are relatively soft. If, by a continuous quench to room temperature, the austenite is cooled through this temperature range without decomposing, it transforms only in the range below about 300° F and the product of decomposition is martensite, and in this condition the steel is fully hardened. At some cooling rate, called the critical cooling rate, the austenite just begins decomposing in the range 1,110 to 930° F. Obviously, the critical cooling rate of a steel is an index of the stability of the austenite in this temperature range. The slower the critical cooling rate (or the deeper the hardening) the more stable is its austenite in the temperature range 1,110 to 930° F. In the present experiments, the critical cooling rate was taken as the average cooling rate between 1,110 and 930° F, which produced in the quenched specimen a structure of martensite with nodular troostite (fine pearlite) in amounts estimated to be between 1 and 3 percent.

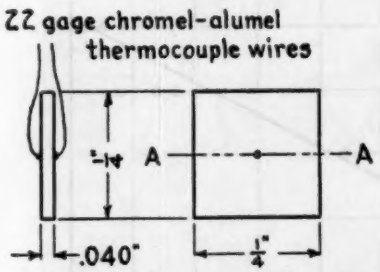

FIGURE 8.—*Form and dimensions of the specimens for the determination of critical cooling rate.*

For the determination of the critical cooling rate, specimens 0.25 inch square by 0.040 inch thick were quenched directly from the temperatures establishing the austenitic grain size. One wire of a 22-gage Chromel-Alumel thermocouple was spot-welded to the center of the flat face of the specimen and the other wire was spot-welded to the center of the opposite face (fig. 8). The specimens were heated in an atmosphere of nitrogen at a rapid rate, approximately 1 minute

[4] E. S. Davenport and E. C. Bain, *Transformation of austenite at constant subcritical temperatures*, Trans. Am. Inst. Mining Met. Engrs., Iron and Steel Div. **90**, 117–154 (1930).

being required to reach the desired temperature, held at that temperature for 15 minutes, and quenched in a bath which sealed the bottom end of the vertical tube of the heating furnace.

To minimize oxidation, the end of the furnace tube extending into the quenching bath was either closed by means of a slide, or the bath was covered with a layer of quenching oil during the entire time of heating the specimens of all the alloys and steels prepared by carburizing with hydrogen and benzene. This procedure was modified for the steels prepared by pack-carburizing. Specimens of the latter steels, quenched from the usually recommended hardening temperature range, were heated in an atmosphere of nitrogen, and those quenched from temperatures establishing a constant austenitic grain size were heated in an atmosphere of nitrogen and illuminating gas.

The desired cooling rates were obtained by quenching either in oil or in a sodium-silicate-water bath of varying concentration.

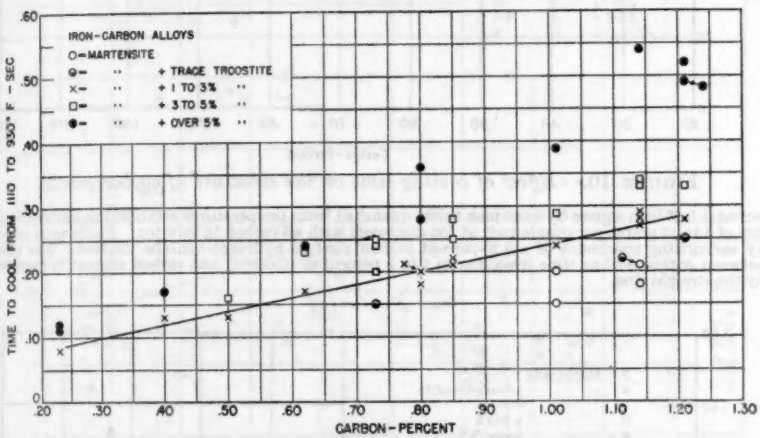

FIGURE 9.—*Effect of cooling time on the structure of iron-carbon alloys.*

Specimens 0.25 inch square by 0.040 inch thick, quenched from 1,700° F, the temperature establishing austenitic grain size of 6 to 12 grains per square inch at 100 diameters with all carbon in solution. The relation between cooling time (resulting in 1 to 3 percent of troostite) and carbon content is represented by the straight line.

The bath was at approximately room temperature at the time of quenching. A photographic time-temperature cooling curve was obtained during the quench by means of a string-galvanometer apparatus described in a previous report.[5]

For the correlation of critical cooling rate with structure, microscopic examinations were made of the quenched specimens on the cross section of the 0.040-inch-thick sheet, a short distance from the point of contact of the thermocouple wires (fig. 8).

The critical cooling rate was determined for iron-carbon alloys, ranging in carbon from 0.23 to 1.21 percent, and for carbon steels, ranging in carbon from 0.43 to 1.18 percent. Each specimen was quenched directly from the temperatures establishing a constant austenitic grain size with all the carbon in solution.

The relation between the time to cool from 1,110 to 930° F and the carbon content is shown for the iron-carbon alloys in figure 9, for the

[5] H. J. French and O. Z. Klopsch, *Quenching diagrams for carbon steels in relation to some quenching media for heat treatment*, Trans. Am. Soc. Steel Treating **6**, 251–294 (1924).

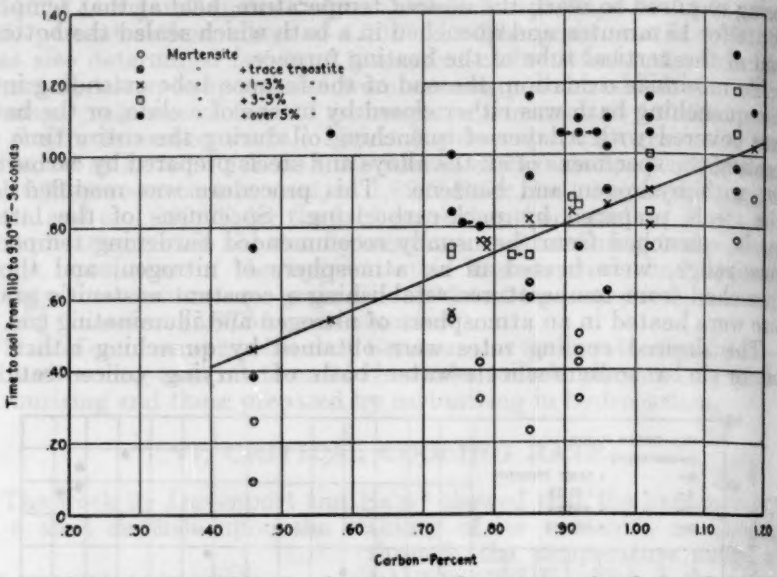

FIGURE 10.—*Effect of cooling time on the structure of carbon steels.*

Specimens 0.25 inch square by 0.040 inch thick, quenched from temperatures establishing austenitic grain size of 6 to 12 grains per square inch at 100 diameters with all carbon in solution. Steels were prepared by carburizing specimens of a 0.20-percent carbon steel in hydrogen-benzene mixture. The relation between critical cooling time (resulting in 1 to 3 percent of troostite) and carbon content is represented by the straight line.

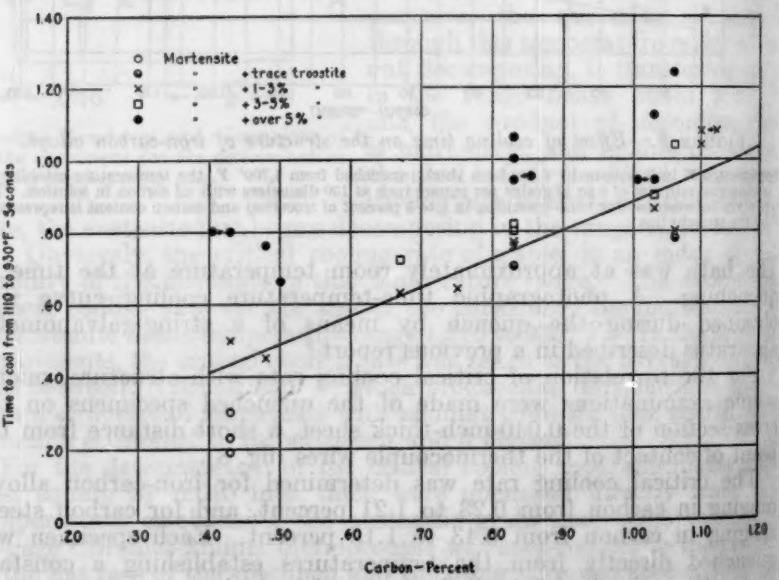

FIGURE 11.—*Effect of cooling time on the structure of carbon steels.*

Specimens 0.25 inch square by 0.040 inch thick, quenched from temperatures establishing austenitic grain size of 6 to 12 grains per square inch at 100 diameters. Steels were prepared by pack-carburizing specimens of a 0.20-percent carbon steel. The relation between critical cooling time (resulting in 1 to 3 percent of troostite) and carbon is represented by the straight line.

steels prepared by carburizing in hydrogen and benzene in figure 10, and for the steels prepared by pack-carburizing in figure 11. The estimated amounts of nodular troostite formed (1 to 3 percent for critical cooling time) with the various quenching rates are also shown in the figures, together with the curves representing the relation of critical cooling time to the carbon content.

The critical cooling rate was also determined for the carbon steels, varying in carbon from 0.43 to 1.38 percent, quenched from the usually recommended hardening temperatures. For these experiments, the austenitic grain size of the hypoeutectoid steels was constant (ASTM grain number 5) and all carbon was in solution. For the hypereutectoid steels the carbon content of the austenite

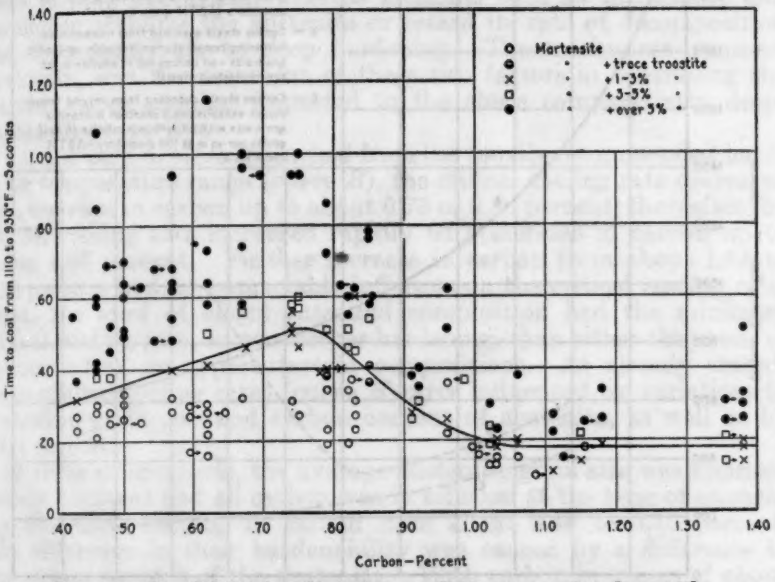

FIGURE 12.—*Effect of cooling time on the structure of carbon steels.*

Specimens 0.25 inch square by 0.040 inch thick, quenched from the usually recommended hardening temperature range. Steels were prepared by either pack-carburizing, or carburizing in hydrogen-benzene mixture, specimens of a 0.20-percent carbon steel. The relation between critical cooling time (resulting in 1 to 3 percent of troostite) and carbon content is represented by the curve.

was constant, but not all carbon was in solution and the average austenitic grain size was smaller than that of the hypoeutectoid steels. The critical cooling rates in these experiments, therefore, were influenced by three variables, namely, austenitic grain size, carbon content of austenite, and total carbon.

For the steels quenched from the usually recommended hardening temperatures, the relation between the time to cool from 1,110 to 930° F and the carbon content is shown in figure 12.

For convenient comparison, the relations of the critical cooling rate to carbon content of the alloys and steels are summarized in figure 13. For the selected conditions of constant austenitic grain size and solution of all carbon in the austenite, the critical cooling rate decreased continuously with increase in carbon, for both the high-purity iron-carbon alloys (curve *A*) and the plain carbon steel (curve *C*). That

is, the hypereutectoid alloys had slower critical cooling rates (were deeper hardening) than the alloys of either eutectoid or hypoeutectoid compositions, and the hypereutectoid steels were deeper hardening than the steels of eutectoid and hypoeutectoid compositions. However, the effect of a small change in carbon content of the austenite of the lower-carbon alloys and steels on the critical cooling rate was more marked than a corresponding change in the higher-carbon alloys and steels. For example, an increase in carbon from 0.23 to 0.33 percent of the alloys decreased the critical cooling rate by about 450° F per

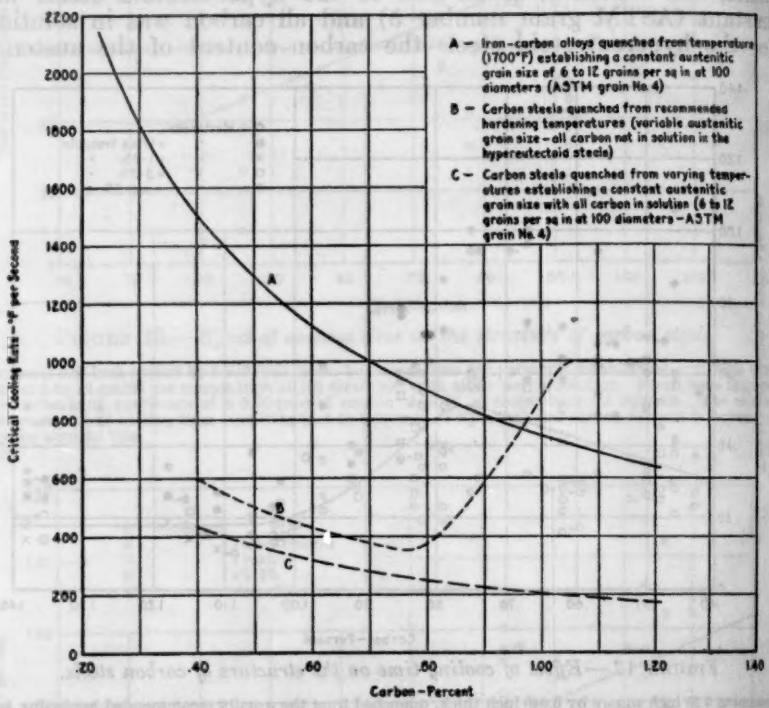
A — Iron-carbon alloys quenched from temperature (1700°F) establishing a constant austenitic grain size of 6 to 12 grains per sq in at 100 diameters (ASTM grain No. 4)
B — Carbon steels quenched from recommended hardening temperatures (variable austenitic grain size — all carbon not in solution in the hypereutectoid steels)
C — Carbon steels quenched from varying temperatures establishing a constant austenitic grain size with all carbon in solution (6 to 12 grains per sq in at 100 diameters — ASTM grain No. 4)
Critical Cooling Rate — °F per Second
2200
2000
1800
1600
1400
1200
1000
800
600
400
200
0
.20
.40
.60
.80
1.00
1.20
1.40
Carbon — Percent
A
B
C

FIGURE 13.—*Relation of critical cooling rate to carbon content of the iron-carbon alloys and carbon steels.*

second, whereas an increase in carbon from 1.10 to 1.20 percent decreased the critical cooling rate only about 50° F per second.

An important feature brought out in these experiments, therefore, is the influence of the carbon content of the austenite on hardenability. Since this was the only variable in the experiments on critical cooling rates of the alloys, the differences observed in their hardenability must be attributed to this factor. Likewise, the differences observed in the hardenability of the plain carbon steels (curve *C*) are also due solely to differences in carbon content of the austenite.

Comparisons of the critical cooling rates of the alloys and steels under similar conditions with respect to austenitic grain size, carbon content, and all carbon in solution (curves *A* and *C*, respectively) show that the alloys had considerably higher rates, that is, they were comparatively shallow hardening. For any selected carbon content

within the range investigated, and with austenitic grain size of 6 to 12 grains per square inch at 100 diameters, the ratio of the critical cooling rate of the alloys to that of the steels was approximately constant, and was of the order of 3.5 to 1.

The high-purity iron-carbon alloys differ from the plain carbon steels in the number of nonmetallic inclusions and amounts of manganese. The high-purity alloys were relatively free from nonmetallic inclusions and manganese. The carbon steels contained a relatively large number of nonmetallic inclusions and about 0.46 percent of manganese. These factors produce opposite effects on the critical cooling rate or hardenability. Nonmetallic inclusions act as nuclei for transformation of the austenite on cooling and thus tend to promote shallow hardening, whereas elements such as manganese and chromium stabilize the austenite or retard its rate of decomposition and thus contribute to deep hardening. The manganese content, obviously, was the dominant of these two factors in controlling the reaction rates and has imparted to the steels comparatively deep-hardening properties.

For the carbon steels quenched from the usually recommended hardening temperature range (curve *B*), the critical cooling rate decreased with increase in carbon up to about 0.75 or 0.80 percent; thereafter the critical cooling rate increased rapidly with increase in carbon up to about 1.05 percent. Further increase in carbon from about 1.05 to 1.40 percent had no appreciable influence on the critical cooling rate. Thus, the steel of about eutectoid composition had the minimum critical cooling rate, or was deeper hardening, than either the steels of hypoeutectoid or hypereutectoid compositions. As already stated, these critical cooling rates (curve *B*) were influenced by variations in austenitic grain size and carbon content of austenite, as well as by total carbon.

In these experiments, the average austenitic grain size was approximately constant and all carbon was in solution at the time of quenching the steels ranging in carbon from about 0.40 to 0.75 percent. The difference in their hardenability was caused by a difference in the carbon content of the austenite. With carbon in excess of about 0.80 percent, the carbon content of the austenite remained constant (quenching temperature of 1,425° F), but differences existed in the grain size, and in the undissolved or total carbon. The undissolved carbon or free carbides not only retard grain growth but also (like nonmetallic inclusions) act as nuclei for transformation during cooling. Furthermore, the reaction rate of the austenite is influenced by the number, size, and distribution of the free carbides. Assuming unformity in distribution and size of the carbide particles, the number will vary directly with increase in carbon above the saturation value for carbon in austenite at the quenching temperature. With steels containing carbon slightly above the eutectoid value, the free carbide particles, although relatively few in number, were sufficient to increase materially the reaction rates. The reaction rates continued to increase uniformly and rapidly as the number of free carbide particles increased until a value finally was reached (corresponding to a total carbon value of about 1.05 percent) beyond which further increase in the number of carbide particles had no marked effect on the critical cooling rate or hardenability. That is, the rapid increase in critical cooling rate with increase in carbon from about 0.80 to 1.05 percent

was due principally to variations in the number of free carbide particles.

The marked differences in critical cooling rates of the hypereutectoid steels (curves *B* and *C* of fig. 13) were caused by differences in austenitic grain size and undissolved carbides at the time of quenching. On heating to the usually recommended hardening temperature, the austenitic grain size was relatively small and some carbon remained undissolved. Both these factors contribute to shallow hardening. Obviously, to utilize full hardening power of the steel, it is necessary to heat the steel to a temperature sufficiently high to insure complete solution of the carbon.

This is further illustrated by comparison of the critical cooling rates of the hypereutectoid alloys and steels (curves *A* and *B*, respectively). As already shown, under similar conditions, the alloys were comparatively shallow hardening. However, the hypereutectoid alloys with the larger grain size and with all carbon in solution had slower critical cooling rates (were deeper hardening) than the carbon steels of similar total carbon content quenched from the recommended hardening temperature range.

The important role of austenitic grain size in controlling hardenability is shown by comparison of the critical cooling rates of the hypoeutectoid steels (curves *B* and *C* for carbon ranging from 0.40 to 0.75 percent). For a given carbon content within the range of 0.40 to 0.75 percent, the steel differed only in the size of the austenite grains at the time of quenching. The critical cooling rates represented by curve *B* were obtained with specimens having an average of 12 to 24 grains per square inch at 100 diameters (ASTM grain number 5) and those by curve *C*, with 6 to 12 grains per square inch at 100 diameters, (ASTM grain number 4). The smaller grain size steels obviously required the higher critical cooling rates. For example, increasing the average austenitic grain size from ASTM grain number 5 to 4 decreased the critical cooling rate of the 0.65-percent carbon steel from about 400 to 300° F per second, or by about 100° F per second. This change in critical cooling rate is equivalent to that resulting from increasing the carbon in solution from 0.45 to 0.65 percent (constant austenitic grain size of 6 to 12 grains per square inch at 100 diameters).

Attempts were also made to determine the critical cooling rate of the basic steel (table 1) used in preparing the carbon steels. For an austenitic grain size of 6 to 12 grains per square inch at 100 diameters the critical cooling rate of this 0.20-percent carbon steel would be expected to be in the neighborhood of 800 to 900° F per second. In fact, some of the experimental results showed it to be within this range. However, similar tests in which the specimens were cooled at considerably higher rates, observed values up to 12,000° F per second, produced in the quenched specimens some areas containing free ferrite. In the latter tests, the ferritic areas in the quenched specimens resulted from nonuniform distribution of the carbon in the austenite at the time of quenching. Regardless of cooling rates, complete hardening of these particular specimens should not be obtained until the ferrite or at least the very low carbon areas in the austenite were eliminated.

A structure containing nodular troostite was not observed in any of the quenched specimens of this particular 0.20-percent carbon steel. If transformation of the austenite on cooling occurred at temperatures

above the range where martensite was formed, then the transformation product was free ferrite, not nodular troostite. With the 0.23-percent carbon alloy, the transformation product was nodular troostite.

Results of investigations of the effect of carbon on critical cooling rate have been reported by Esser, Eilender, and Spenle [6] for high-purity iron-carbon alloys, and by French and Klopsch [7] for plain carbon steels. In the experiments by the former, the cooling rate between 1,470 and 1,290° F was determined by quenching thin wires of iron-carbon alloys in gas from about 1,800° F. These alloys were prepared from carbonyl iron and carbon. French and Klopsch determined the critical cooling rate at 1,330° F for the centers of cylinders 0.5 inch diameter by 2 inches long quenched from about 135° F above Ac_3 for hypoeutectoid steels and for about 135° F above Ac_1 for hypereutectoid steels.

They found that the critical cooling rates of both the high-purity iron-carbon alloys and plain carbon steels decreased with increase in carbon content up to about eutectoid compositions, but with further increase in carbon the critical cooling rates also increased. That is, when both the iron-carbon alloy and plain carbon steel were of about eutectoid compositions, they had the minimum critical cooling rates (were deeper hardening) than the hypoeutectoid or hypereutectoid alloys and steels. These results were influenced, however, by variables other than the carbon content of the materials. These two investigations were made without due regard for the influence of austenitic grain size and, in addition, the quenching temperatures used by French and Klopsch were not sufficiently high to insure complete solution of all the carbon in the highest-carbon steel.

VII. SUMMARY

High-purity iron-carbon alloys were prepared from hot- and cold-worked specimens of a heat of vacuum-fused electrolytic iron by carburizing in a hydrogen-benzene mixture. The carburized specimens were heated and cooled in vacuo to obtain uniform distribution of the carbon. Cooling during this homogenizing treatment was sufficiently rapid to form sorbite (or fine pearlite) in all of the alloys. Microscopic examination of the cross sections of the bars of the different alloys showed the carbon to be uniformly distributed.

The alloys studied contained 0.23, 0.40, 0.50, 0.62, 0.73, 0.80, 0.85, 1.01, 1.14, and 1.21 percent of carbon, respectively. These values are believed to be accurate within the limits of plus or minus 0.01 percent of carbon.

A series of plain carbon steels was also prepared by pack-carburizing specimens of a 0.20-percent carbon steel followed by pack-annealing and normalizing. A second series of plain carbon steels was prepared by carburizing specimens of the same 0.20-percent carbon steel in hydrogen and benzene and homogenizing by heating and cooling in vacuo.

The plain carbon steels varied in carbon from that of the basic material, 0.20 to 1.38 percent. These steels also contained about 0.46 percent of manganese and 0.15 percent of silicon.

[6] H. Esser, W. Eilender, and E. Spenle, *Quenching diagrams of the iron-carbon alloys*, Arch. Eisenhüttenw. 6, 389-393 (1935).

[7] H. J. French and O. Z. Klopsch, *Quenching diagrams for carbon steels in relation to some quenching media for heat treatment*, Trans. Am. Soc. Steel Treating 6, 251-294 (1924).

Spectrochemical and chemical analyses, as well as determinations of gas content by a vacuum-fusion method, showed that sulfur, nickel, cobalt, and oxygen were the major impurities in the iron-carbon alloys. The total of all the impurities determined was about 0.030 percent.

Abnormal structures were produced in the hypereutectoid alloys annealed in vacuo at 1,700° F.

All specimens used for determination of the austenitic grain size and critical cooling rate had an initial structure of sorbite (fine pearlite).

Austenitic grain size was determined for the highest-carbon alloy (1.21 percent of carbon) at a temperature sufficiently high to insure complete solution of all the carbon. Subsequent determinations on the lower-carbon alloys showed that variations in carbon did not affect the grain size at this selected temperature of 1,700° F. Each of the alloys at 1,700° F had an average grain size of 6 to 12 grains per square inch at 100 diameters (ASTM grain number 4).

The carbon steel containing 1.18 percent of carbon had the same grain size as the alloys at 1,700° F. Lower temperatures were necessary to establish the same austenitic grain size in the lower-carbon steels. On heating within the recommended hardening temperature range, specimens of the hypoeutectoid carbon steels had a constant average grain size of 12 to 24 grains per square inch at 100 diameters (ASTM grain number 5). No differences were observed in temperature–grain-size–critical-cooling relations of the carbon steels prepared by pack-carburizing and those carburized in hydrocarbon.

The critical cooling rate was taken as the average cooling rate, between 1,110 and 930° F, which produced in the quenched specimen a structure of martensite with nodular troostite (fine pearlite) in amounts estimated to be between 1 and 3 percent.

The critical cooling rate was determined for each of the iron-carbon alloys quenched directly from 1,700° F, and for the carbon steels varying in carbon from 0.43 to 1.18 percent, quenched also from the temperatures establishing a constant austenitic grain size with all carbon in solution.

For the selected conditions of constant austenitic grain size and solution of all carbon in the austenite, the critical cooling rate decreased continuously with increase in carbon, for both the high-purity iron-carbon alloys and plain carbon steels. That is, the hypereutectoid alloys had slower critical cooling rates (were deeper hardening) than the alloys of eutectoid and hypoeutectoid compositions, and the hypereutectoid steels were deeper hardening than the steels of eutectoid and hypoeutectoid compositions. However, a small change in the carbon content of the austenite of the lower-carbon alloys and steels had a more marked effect on the critical cooling rate than did a corresponding change in carbon of the high-carbon alloys and steels.

The carbon content of the austenite, therefore, had a pronounced influence on the hardenability of the alloys and steels. Under similar conditions with respect to austenitic grain size, carbon content, and with complete solution of the carbon in the austenite, the high-purity iron-carbon alloys hardened less deeply than did the plain carbon steels. This difference in hardenability was due principally to difference in manganese content of the alloys and steels.

For the carbon steels quenched from the usually recommended hardening temperature, the critical cooling rate decreased with increase in carbon up to about 0.75 to 0.80 percent, but increased rapidly with further increase in carbon up to about 1.05 percent. Changes in carbon from about 1.05 to 1.40 percent had no appreciable influence on critical cooling rate. These critical cooling rates, however, were influenced by variations in austenitic grain size, and carbon content of austenite as well as the total carbon content.

Full depth of hardening was obtained only when all the carbon was in solution in the austenite.

J. A. Bennett, a member of the staff of this Bureau, assisted in assembling the apparatus shown in figure 1 and in carrying out the carburizing experiments with gases.

WASHINGTON, February 11, 1938.

U. S. DEPARTMENT OF COMMERCE NATIONAL BUREAU OF STANDARDS

RESEARCH PAPER RP1093

Part of Journal of Research of the National Bureau of Standards, Volume 20, May 1938

HEAT OF COMBUSTION OF ISOPRENE

By Ralph S. Jessup

ABSTRACT

The heat of combustion of isoprene has been measured by means of a bomb calorimeter which was calibrated with benzoic acid. The mass of isoprene burned in each experiment was determined from the mass of CO_2 formed in combustion. As the result of seven measurements the value 3156.9 ±1.6 international kilojoules per mole was obtained for the heat of combustion of liquid isoprene at 25° C and under a constant pressure of 1 atmosphere, the products of combustion being liquid water and gaseous CO_2. Using the value 25.9 international kilojoules per mole calculated by Bekkedahl, Wood, and Wojciechowski for the heat of vaporization of isoprene, the heat of combustion of gaseous isoprene is calculated to be 3182.8 ±1.7 international kilojoules per mole at 25° C and under a constant pressure of 1 atmosphere, the products of combustion being liquid water and gaseous CO_2. Combining the data on isoprene with data reported previously on the heat of combustion of rubber hydrocarbon, there are obtained for the heats evolved in the reactions

$$x\mathrm{C_5H_8}(\text{liquid isoprene}) = (\mathrm{C_5H_8})_x(\text{rubber hydrocarbon})$$

and

$$x\mathrm{C_5H_8}(\text{gaseous isoprene}) = (\mathrm{C_5H_8})_x(\text{rubber hydrocarbon})$$

at 25° C and a constant pressure of 1 atmosphere, the values $(74.8 \pm 6.2)x$ and $(100.7 \pm 6.3)x$ international kilojoules respectively.

CONTENTS

		Page
I.	Introduction	589
II.	Previous work	590
III.	Apparatus and method	590
IV.	Calibration of calorimeter	590
V.	Material	591
VI.	Results and conclusions	592
VII.	References	597

I. INTRODUCTION

The work described in this paper was done as part of an investigation of thermodynamic properties of rubber hydrocarbon and related substances. In previous papers data have been reported on the heat of combustion [8] [1] and on the entropy and free energy of formation of rubber hydrocarbon [1]. Recently, data on the entropy of isoprene have been reported by Bekkedahl and Wood [2], who discuss the chemical similarity of isoprene and rubber hydrocarbon, and point out the desirability of a knowledge of the free energy of forma-

[1] Numbers in brackets relate to the literature references given at the end of this paper.

tion of isoprene for use in studying the thermodynamics of reactions involving the two substances. In order to use the entropy data in calculating the free energy of formation, an accurate value for the heat of combustion of isoprene is required.

II. PREVIOUS WORK

The only data on the heat of combustion of isoprene which have been found in the literature are those of Lebedev, Chochlovkin, and Kalacheva [10]. They report 11 measurements of the heat of combustion of liquid isoprene, the results of which range from 11,142 to 11,215 calories per gram, the mean result being 11,165 calories per gram. These authors do not give sufficient data to permit an estimate of the accuracy of their results, and they do not define their energy unit, so that accurate conversion of their data to the energy unit used for the entropy data is not possible. For these reasons a new determination of the heat of combustion of isoprene was desirable. If it is assumed that the calorie used by Lebedev, Chochlovkin, and Kalacheva is equal to 4.1833 international joules, their value for the heat of combustion of isoprene becomes 46.7 international kilojoules per gram, a value which is nearly 1 percent higher than that obtained in the present work.

III. APPARATUS AND METHOD

The bomb calorimeter and accessory apparatus, experimental procedure, and method of calculating results have been described in detail [4, 7, 9].

Samples of approximately 1 g of isoprene were inclosed in thin-walled glass bulbs which were flattened on opposite sides and filled completely with the liquid in the manner described by Richards and Barry [11]. The samples were ignited by means of an electric fuse of iron wire, as described previously [7]. The volume of the bomb used was determined to be 377 cm^3. One cm^3 of water was placed in the bomb before each experiment.

In most experiments the mass of isoprene burned was determined in two ways: (1) By weighing the sample of isoprene, and (2) by absorbing the CO_2 formed in combustion in Ascarite (a sodium hydroxide-asbestos mixture) and weighing it, and passing the remaining gas through a copper tube heated to redness to oxidize any CO which might be present, absorbing the resulting CO_2 in Ascarite and weighing [12, 7]. The mass CO_2 obtained by oxidizing the CO was very small, usually less than 0.01 percent of the total CO_2 formed in the bomb.

IV. CALIBRATION OF CALORIMETER

The calorimeter was calibrated with benzoic acid (NBS Standard Sample 39e), using for the heat of combustion of this material the value 26,414 international joules per gram mass under standard conditions [9]. These standard conditions are:

Temperature to which reaction is referred	30° C.
Initial absolute pressure of oxygen at 30° C	30 atm.
Mass of benzoic acid per liter of bomb volume	3 g.
Mass of water placed in bomb per liter of bomb volume	3 g.

The results of the calibration experiments are given in table 1. The uncertainty of the mean of the nine experiments (defined as $2\sqrt{\frac{\Sigma\Delta^2}{n(n-1)}}$, or about three times the "probable error") is 0.026 percent.

In the calibration experiments the final temperature of the calorimeter was 30° C, and as the value used for the heat of combustion of benzoic acid is that for 30° C, the values obtained for the energy equivalent of the calorimeter are for the initial system at the mean temperature of the experiments. In other words, the observed values of energy equivalent represent the energy per degree required to raise the temperature of the calorimeter from its initial to its final temperature (30° C) when the bomb contains 1 g of water, the charge of benzoic acid, and oxygen under a pressure of 30 atmospheres at 30° C. The values given in table 1 for the energy equivalent of the calorimeter are the observed values minus the heat capacity of the charge of benzoic acid (specific heat=1.26 j/g° C). In each experiment on isoprene the final temperature of the calorimeter was very nearly 30° C, and the value used for the energy equivalent was the mean value given in table 1, plus the heat capacity of the charge of isoprene (specific heat=2.25 j/g° C). Since the energy equivalent of the calorimeter is that of the initial system the observed values for the heat of combustion of the isoprene are for the final temperature of the calorimeter, or 30° C.

TABLE 1.—*Calibration of bomb calorimeter*

Experiment	Observed energy equivalent at 28.5° C	Deviation from mean		Experiment	Observed energy equivalent at 28.5° C	Deviation from mean	
	int. j/° C	int. j/° C	*Percent*		int. j/° C	int. j/° C	*Percent*
1	13498.6	−1.0	−0.007	7	13501.2	+1.6	+.012
2	13490.4	−9.2	−.068	8	13510.2	+10.6	+.079
3	13500.1	+0.5	+.004	9	13499.3	−0.3	−.002
4	13495.5	−4.1	−.030				
5	13499.5	−0.1	−.001	Mean	13499.6	±3.2	±0.024
6	13501.4	+1.8	+.013				

V. MATERIAL

The isoprene used was prepared by Bekkedahl, Wood, and Wojciechowski [3] by cracking dipentene vapor and was purified by fractional distillation. Their ebulliometric measurements on the freshly distilled isoprene indicated that the material was of a very high degree of purity. However, the measurements of CO_2 formed in combustion in the present investigation showed that the samples absorbed significant amounts of impurity upon exposure to the air during the filling of the glass bulbs used to contain the combustion samples. The isoprene was kept in glass bottles, closed in some cases by ground-glass stoppers, in others by cork stoppers, and it is possible that there was also some contamination of the isoprene as a result of leakage of air past the stoppers. Correlation of the results of the CO_2 determinations with the heat of combustion measurements indicated that there was little or no heat of mixing or combination of the impurity with the isoprene, the effect of the impurity being merely to reduce the heat

of combustion and the amount of CO_2 formed in combustion in the same proportion. For this reason values of heat of combustion of the isoprene obtained by using the mass of CO_2 formed in combustion as a measure of the mass of isoprene burned, should be fairly reliable in spite of the relatively large amounts of impurity in the samples.

The oxygen used was ordinary commercial oxygen from which combustible impurities were removed by passing the gas over copper oxide maintained at a temperature of 700 to 800° C. The oxygen was then passed through Ascarite before being admitted to the bomb in order to remove any CO_2 which might be present.

VI. RESULTS AND CONCLUSIONS

The results of heat of combustion measurements on several samples of isoprene are shown in table 2. Columns 1, 2, and 3 of this table give the sample number, experiment number, and mass (weight in vacuo) of isoprene burned in the experiment. Column 4 gives the

TABLE 2.—*Results of measurements on isoprene*

Sample	Experiment	Mass of charge	$\frac{CO_2 \text{ found}}{CO_2 \text{ calc}} = f$	Observed heat of combustion, Q_B	$\frac{Q_B}{f}$	Approximate Washburn correction	$-\Delta U_B$	Remarks
1	2	3	4	5	6	7	8	9
		g		int. j/g	int. j/g	int. j/g	int. j/g	
A_1	1	0.89065	0.99796	46,211	46,305	−12	46,293	Freshly distilled.
A_2	2	1.10090	.98303	45,588	46,375	−12	46,363	Same sample as A_1 but had been kept in a bottle at room temperature 17 days.
B	3	1.18103		44,724				Had been kept in a bottle for unknown length of time.
C_1	4	1.09362		46,318				Freshly distilled.
	5	0.96029	.99397	46,304	46,585	−13	46,572	
C_2	6	1.13093		46,218				Same lot of material as C_1 but had been kept in a bottle in icebox for 7 days.
	7	1.33751	.99235	46,224	46,580	−13	46,567	
D	8	1.18985		46,100				Freshly distilled into antioxidant.
E_1	9	1.07797	.99254	45,921	46,266	−11	46,255	Freshly distilled, bulbs filled immediately.
	10	1.00322	.99251	45,919	46,266	−11	46,255	
E_2	11	1.60296	.99229	45,917	46,274	−12	46,262	Same lot of material as E_1, bulb filled about 3 hours later.
E_3*	12	0.86821	.99268	46,202	46,543	−13	46,530	Same lot of material as E_1, bulbs filled about 26 hours later.
	13	1.06559	.99240	45,910	46,262	−11	46,251	
E_4*	14	0.97403	.99249	45,906	46,253	−11	46,242	Same lot of material as E_1, bulb filled 4 days later.
F	15	1.11085		46,028				Freshly distilled, bulbs filled immediately.
	16	1.14830		46,054				
	17	1.00269		45,996				
	18	1.18388	.99380	46,019	46,306	−10	46,296	

* Samples E_3 and E_4 were kept outdoors in a bottle at temperatures ranging from −3 to +11° C for 1 and 4 days, respectively.

ratio, r, of the mass of carbon dioxide formed in the complete combustion of the sample to the amount calculated from the mass of sample, assuming that the sample was pure isoprene. The atomic weights used in this calculation are C=12.01, H=1.0078, O=16.000. Column 5 of table 2 gives the observed heat of combustion per gram of isoprene (Q_s) under the conditions of the bomb process, when the amount of isoprene burned is taken as the mass determined by weighing the sample of isoprene. Column 6 gives values of Q_s/r, that is, the heat of combustion of isoprene under the conditions of the bomb process when the mass of isoprene burned in each experiment is calculated from the observed mass of carbon dioxide formed in combustion of the isoprene. The values of Q_s/r are therefore the values of Q_s corrected on the assumption that the departures from unity of the corresponding values of r are due to inert impurity in the isoprene. Column 7 gives Washburn's approximate correction [13], and column 8 the value of $-\Delta U_s$, that is, the energy decrease per gram of pure isoprene for the reaction

$$C_5H_8 \text{ (liq isoprene)} + 7\ O_2 \text{ (gas)} = 5\ CO_2 \text{ (gas)} + 4\ H_2O \text{ (liq)}$$

at 30° C and under a total pressure of 1 atmosphere, assuming again that the departures from unity of the ratio r are due to inert impurity.

Table 2 shows that the values of r are considerably lower than unity. There is also evidence that r decreased with time when the isoprene was kept in stoppered bottles, as previously mentioned. For example, for sample A the value of r dropped from about 0.998 to 0.983 when the sample was kept at room temperature for 17 days, and for sample C the value of r dropped from about 0.994 to 0.992 when the sample was kept in an icebox for 7 days. On the other hand, the value of r for sample E did not show any appreciable decrease when the sample was exposed to temperatures ranging from −3 to +11° C for 4 days.

It was thought that the departures from unity of the values of r might be caused by oxidation of the isoprene. To test this hypothesis a sample was distilled into a vessel containing an antioxidant, and one determination was made of the heat of combustion of the sample (experiment 8). Unfortunately, the attempt to measure the mass of CO_2 formed in combustion in this experiment was unsuccessful due to loss of part of the CO_2. However, the value obtained for the heat of combustion per gram of sample (Q_s) was so low as to indicate that this sample of isoprene contained more rather than less impurity than most of the other samples. It was concluded, therefore, that the impurity was not oxygen or an oxidation product but was probably water absorbed from the atmosphere. This conclusion is supported by unpublished data obtained by Bekkedahl and Wood in combustion analyses of sample E. The isoprene they used was contained in glass bulbs which were filled at the same time as some of those used in the calorimetric combustion experiments. The value for the ratio r obtained in their first experiment was 0.9926, which is in good agreement with the values of r for sample E in table 2. Their value for the hydrogen content of the sample was 11.83 percent as compared with the theoretical value 11.84 percent for pure isoprene. In a second combustion analysis part of the carbon dioxide was lost, but the observed hydrogen content was 11.79 percent. The fact that the carbon content of the isoprene was low and the hydrogen content

was nearly that for pure isoprene indicates that the impurity in the sample was water, since the hydrogen content of water is nearly the same as that of isoprene.

It will be seen from table 2 that the values $-\Delta U_R$ for most of the experiments are in satisfactory agreement, but that the values for experiments 5, 7, and 12, although consistent among themselves, are higher by about 0.63 percent than those for the remaining experiments. This is shown more clearly in table 3, where the results of experiments 5, 7, and 12 are listed separately from those of the other experiments.

TABLE 3.—*Comparison of the results of experiments 5, 7, and 12 with those of other experiments*

Experiment	$-\Delta U_R$	Deviation from mean	
	int. j/g	int. j/g	*Percent*
1	46, 293	+28	+0.061
2	(46, 363)		
9	46, 255	−10	−.022
10	46, 255	−10	−.022
11	46, 262	−3	−.006
13	46, 251	−14	−.030
14	46, 242	−23	−.050
18	46, 296	+31	+.067
Mean	46, 265	±17	±.037
5	46, 572	+16	+.034
7	46, 567	+11	+.024
12	46, 530	−26	−.056
Mean	46, 556	±18	±.039

The difference between the mean of experiments 5, 7, and 12 and the mean of the other group of experiments in table 3 was found to be about 85 percent of the energy of evaporation of isoprene, and this suggested that the glass bulbs used to contain the liquid isoprene had broken in experiments 5, 7, and 12 and allowed liquid to evaporate to fill the bomb with saturated isoprene vapor before the beginning of the calorimetric experiments. Unfortunately, an accurate calculation of the effect of evaporation of isoprene in the bomb is not possible, because no data are available on either (*a*) the effect on the partial pressure of the isoprene of the increase in concentration of water in the liquid phase resulting from evaporation of part of the isoprene, and possibly also from absorption of water from the water-saturated atmosphere in the bomb; or on (*b*) the effect of the pressure of the oxygen in the bomb on the density of the saturated isoprene vapor. However, it is possible to make fairly reasonable assumptions regarding the possible effects of factors (*a*) and (*b*), and to calculate the thermal effect of evaporation of isoprene in the bomb on the basis of these assumptions. In table 4 are given the results of recalculating the data of experiments 5, 7, and 12 on the assumption that the bomb was filled with isoprene vapor. The amount of isoprene in the vapor phase was calculated in the following three ways: (1) The effect of the factors (*a*) and (*b*) mentioned above was neglected. The vapor pressure of pure isoprene at the initial temperature of the calorimeter in each experiment was calculated from a vapor-pressure equation of the form $\log p = a - b/T$, where the constants were determined from values of boiling point and change of

boiling point with pressure reported by Bekkedahl, Wood, and Wojciechowski [3]. The actual pressure of the isoprene vapor in the bomb was assumed to be lower than the vapor pressure of pure isoprene by an amount calculated by means of Henry's law from the amount of impurity (assumed to be water) indicated by the observed values of r (table 2). The specific volume of the isoprene vapor was calculated by means of the relation PV/T=constant, where the constant was determined from the values of V and T at P=1 atmosphere [3]. (2) The liquid isoprene was assumed to have absorbed an amount of water sufficient to reduce the density of isoprene in the vapor phase to 80 percent of the density of vapor in equilibrium with pure liquid isoprene. The effect of the presence of oxygen in the bomb on the density of the isoprene vapor was neglected. (3) The presence of the oxygen in the bomb was assumed to have caused complete evaporation of the isoprene.

TABLE 4.—*Results of three methods of recalculating the data of experiments 5, 7, and 12*

Experiment	Recalculated values of $-\Delta U_R$ at 30° C		
	Method 1	Method 2	Method 3
	int. j/g	int. j/g	int. j/g
5	46,278	46,332	46,227
7	46,354	46,391	46,214
12	46,208	46,268	46,189
Mean	46,280	46,330	46,210

It will be seen from table 4 that the mean of the results recalculated by method 1 are in agreement within 0.03 percent with the mean of the first group of values given in table 3. The mean results obtained by methods 2 and 3 differ from the mean of the first group of values in table 3 by +0.14 and −0.12 percent, respectively. As the effects of the two factors neglected in method 1 are relatively small and of opposite sign they will partially cancel, and it may be concluded that the result obtained by method 1 is not seriously in error. The agreement of this result with the mean of the first group of values in table 3 may therefore be considered as confirmation of the hypothesis that the high values of $-\Delta U_R$ obtained in experiments 5, 7, and 12 were due to breaking of the glass bulbs containing the isoprene and the consequent evaporation of part of the isoprene.

In view of the above discussion, it appears justifiable to discard the results of experiments 5, 7, and 12, and to adopt as the value for the decrease in energy for the reaction

$$C_5H_8\ (liq)+7\ O_2\ (gas)=5\ CO_2\ (gas)+4\ H_2O\ (liq) \qquad (1)$$

at 30° C and under a pressure of 1 atmosphere, the value of $-\Delta U_R$ obtained from the first group of experiments of table 3, namely, 46,265 international joules per gram (weight in vacuo), or 3151.2 international kilojoules per mole of C_5H_8. The corresponding value of $-\Delta H$ for the above reaction is obtained by adding the value of $-\Delta(pv)$ for the reaction, 5.1 international kilojoules per mole, to the value of $-\Delta U_R$, giving for $-\Delta H$ the value 3156.3 international kilojoules per mole.

The uncertainty of the mean of the results given in the first group in table 3, defined as $2\sqrt{\frac{\Sigma\Delta^2}{n\ (n-1)}}$, is 0.035 percent. Combining this with the uncertainty of the energy equivalent of the calorimeter, 0.026 percent, and the estimated uncertainty, 0.023 percent, in the value used for the heat of combustion of benzoic acid, there is obtained for the uncertainty of the value given for the heat of combustion of liquid isoprene

$$\sqrt{(0.023)^2+(0.026)^2+(0.035)^2}=0.049 \text{ percent.}$$

Using for the specific heats at constant pressure of liquid isoprene, gaseous oxygen, gaseous CO_2, and liquid water the values 153.3 [2], 29.18 [5], 36.62 [5], and 75.18 [6] international joules per mole, respectively, there is obtained the value -0.126 kilojoule per mole degree centigrade for the temperature coefficient $(=d/dT\ (-\Delta H))$ of the heat of combustion of isoprene at constant pressure. Hence the value derived from this investigation for the heat of combustion of liquid isoprene at 25° C and a constant pressure of 1 atmosphere to form liquid water and gaseous CO_2 is 3156.9 ± 1.6 international kilojoules per mole. Adding to this the value for the heat of vaporization of isoprene calculated by Bekkedahl, Wood, and Wojciechowski [3], 25.9 ± 0.3 kilojoules per mole, there is obtained the value 3182.8 ± 1.7 international kilojoules per mole for the heat of combustion of gaseous isoprene at 25° C and at a constant pressure of 1 atmosphere, the products of combustion being liquid water and gaseous CO_2.

The data on the heat of combustion of isoprene can be combined with data reported previously [8] for the heat of combustion of rubber to calculate the heats evolved in the reactions.

$$x\text{C}_5\text{H}_8 \text{ (liq isoprene)}=(\text{C}_5\text{H}_8)_x\text{(rubber hydrocarbon)} \quad (2)$$

$$x\text{C}_5\text{H}_8 \text{ (gaseous isoprene)}=(\text{C}_5\text{H}_8)_x\text{(rubber hydrocarbon)} \quad (3)$$

Several values were reported in the reference cited for the heats of combustion of different samples of rubber. The value reported for the heat of combustion of "steam purified" rubber, which was the purest of the samples on which measurements were made, was 45239 ± 90 international joules per gram (weight in vacuo), or $(3081.3\pm6.0)x$ international kilojoules per mole at 30° C. Using the value $128.7x$ joules per mole degree centigrade reported by Bekkedahl and Matheson [1] for the specific heat of rubber hydrocarbon at 27.5° C, and the values given previously in this paper for the specific heats of gaseous oxygen, gaseous carbon dioxide, and liquid water, the temperature coefficient of the heat of combustion of rubber hydrocarbon is calculated to be $-0.151x$ international kilojoule per mole. The heat of combustion of rubber hydrocarbon at 25° C is therefore calculated to be $(3082.1\pm6.0)x$ international kilojoules per mole. Combining this value with the values given previously for the heats of combustion of liquid and gaseous isoprene there are obtained the values $(74.8\pm6.2)x$ and $(100.7\pm6.3)x$ for the heats evolved in the reactions (2) and (3), respectively, at 25° C and a constant pressure of 1 atmosphere.

VII. REFERENCES

[1] N. Bekkedahl and H. Matheson, J. Research NBS **15,** 503 (1935) RP844.
[2] N. Bekkedahl and L. A. Wood, J. Research NBS **19,** 551 (1937) RP1044.
[3] N. Bekkedahl, L. A. Wood, and M. Wojciechowski, J. Research NBS **17,** 883 (1936) RP951.
[4] H. C. Dickinson, Bul. BS **11,** 189 (1914) S230.
[5] Int. Critical Tables **5,** 80 (1929).
[6] Int. Critical Tables **5,** 113 (1929).
[7] R. S. Jessup, J. Research NBS **18,** 115 (1937) RP966.
[8] R. S. Jessup and A. D. Cummings, J. Research NBS **13,** 357 (1934) RP713.
[9] R. S. Jessup and C. B. Green, J. Research NBS **13,** 469 (1934) RP721.
[10] S. B. Lebedev, M. A. Chochlovkin, and A. V. Kalacheva, J. Applied Chem. (USSR) **9,** 1605 (1936).
[11] T. W. Richards and F. Barry, J. Am. Chem. Soc. **37,** 993 (1915).
[12] F. D. Rossini, BS J. Research **6,** 37 (1931) RP260.
[13] E. W. Washburn, BS J. Research **10,** 525 (1933) RP546.

WASHINGTON, February 4, 1938.

U. S. Department of Commerce National Bureau of Standards

RESEARCH PAPER RP1094

Part of Journal of Research of the National Bureau of Standards, Volume 20, May 1938

ELECTROMOTIVE FORCE OF SATURATED WESTON STANDARD CELLS CONTAINING DEUTERIUM OXIDE

By Langhorne H. Brickwedde and George W. Vinal

ABSTRACT

Saturated Weston standard cells in which deuterium oxide is substituted for some or all of the normal water may be expected to have electromotive forces slightly different from those made with normal water. A study has been made of the characteristics of 12 cells, prepared with identical materials, except for the isotopic composition of the water. The initial samples of water contained 0.018 (normal water), 1.036, 3.121, and 6.848 mole percent of D_2O. The ratios of moles of D_2O to H_2O in the finished cells were less than in the original samples, because of dilution by the water of crystallization of the cadmium sulphate. The constancy of the electromotive force of each of the 12 cells is shown by the small average deviation of single observations, extending over several months, from the respective mean values. In no case did it exceed 0.6 microvolt. The decrease in electromotive force as a result of using the D_2O amounted to 2.9 microvolts per mole percent. No significant difference was found in the temperature coefficient for the various D_2O concentrations. Hysteresis measurements indicate a slight superiority for the cells containing added D_2O. Measurements of the internal resistance of the cells at 20 and 28° C indicate a ratio of $R_{20}/R_{28}=1.24$. The cells containing D_2O are fully as reproducible and constant as those made with normal water, and in some respects they may be superior.

CONTENTS

		Page
I.	Introduction	599
II.	Experimental procedure	600
III.	Experimental results	601
IV.	Conclusions	605

I. INTRODUCTION

Saturated Weston standard cells in which deuterium oxide, D_2O, is substituted for some or all of the H_2O, may be expected to have an electromotive force slightly different from those made with normal water. The free-energy change, which determines the electromotive force of the cell, is the change accompanying the reaction:

$$Cd(10\%\ \text{amalgam}) + Hg_2SO_4(s) + 8/3H_2O(\text{in satd. } CdSO_4 \text{ soln.}) \rightleftarrows 2Hg(l) + CdSO_4.8/3H_2O(s)$$

Since water enters into a part of the cell reaction involving a free-energy change, the electromotive force developed should depend on the isotopic composition of the water present.

The three samples of deuterium oxide used in this work were prepared and standardized by the physical chemistry section of this

Bureau. These samples were of sufficient amount to construct several cells of the same size as those which are used customarily for primary standards of electromotive force.

II. EXPERIMENTAL PROCEDURE

A study has been made of the characteristics of a group of 12 saturated cells constructed on July 27, 1937. These cells were prepared in the same way and with identical materials except for the isotopic content of the water used in making the solutions of cadmium sulphate. The materials were purified according to methods described in an earlier publication,[1] and the cells were made in the usual manner. Four samples of water containing, respectively, 0.018 (normal water), 1.036, 3.121, and 6.848 mole percent of D_2O [2] were saturated with small $CdSO_4.8/3H_2O$ crystals. These crystals had been moistened with a small amount of H_2SO_4, so that the saturated $CdSO_4$ solution of normal water for the control cells was 0.0226 *N* in acid. Since the crystals were well mixed and since the same ratio of crystals to water was used in all cases, each solution should be of the same acidity. In accordance with this Bureau's practice of referring to the acidity of a cell as that of the acid before saturating with neutral $CdSO_4.8/3H_2O$, these cells are designated as 0.03 *N* acid.

The ratios of moles of D_2O to moles of water in the finished cells were less than in the samples initially. The dilution by the water of crystallization of the cadmium sulphate used in saturating the solution and added as excess solid to the cells is not definitely known because of lack of knowledge of the rate and extent of exchange between the H_2O of the solid $CdSO_4.8/3H_2O$ crystals and the D_2O of the liquid.

TABLE 1.—*Dilution of deuterium oxide by water of crystallization of the cadmium sulphate*

Cell No.	Initial D_2O concentration	ΔE difference from control cells	Assuming no exchange		Assuming complete exchange	
			D_2O concentration	ΔE per mole percent	D_2O concentration	ΔE per mole percent
	Mole %	*μv*	*Mole %*		*Mole %*	
956 to 958 [a]	0.018		0.018		0.018	
959 to 961	1.036	2.5	.85	2.9	.76	3.3
962 to 964	3.121	5.6	2.57	2.2	2.27	2.5
965 to 967	6.848	14.3	5.64	2.5	4.98	2.9
Mean				2.5		2.9

[a] Control cells, containing normal water.

If we assume no exchange between the liquid and crystals and attribute the dilution of the D_2O to the H_2O of the dissolved crystals alone, the D_2O mole percentages of the water in the solutions would

[1] G. W. Vinal, D. N. Craig, and L. H. Brickwedde. Trans. Electrochem. Soc. 58, 146 (1935).

[2] These compositions were calculated from the densities of the samples, using the equation $N_{D_2O}=9.2385\Delta S+0.2597\ (\Delta S)^2$. In this equation, which was obtained from the data of L. G. Longsworth, J. Am. Chem. Soc. 59, 1483 (1937), by least-square computation, N_{D_2O} is the mole fraction of deuterium oxide and

$$\Delta S \text{ is } d^{25}_{25}-1=\frac{d^{25}_{4}}{0.99705_4}-1,$$

in which 0.99705_4 is the density, d^{25}_{4}, of D_2O-free water.

be 0.018, 0.85, 2.57, and 5.64. If, on the other hand, we assume that the H_2O of the solid entered into an exchange with the liquid and came to an equilibrium such that the D_2O/H_2O ratio in the crystals is the same as in the solution, the mole percentages of D_2O in the solutions would be 0.018, 0.76, 2.27, and 4.98. The hydrogen added by the H_2SO_4 may be neglected since, in the most concentrated D_2O sample, it reduced the concentration of D_2O by only 0.002 mole percent.

In table 1 the mole percentages of the original samples are compared with the percentages in the finished cells on the assumptions of no exchange and complete exchange in the crystals. The difference in results based on these assumptions is of little importance since the variations in ΔE per mole percent are within the limits of scattering of the values in the various groups. From the standpoint of the present work it is immaterial, therefore, whether the exchange is complete, except as the constancy of electromotive force over a long period of time may be involved. In this paper we have assumed that the second of the above alternatives is correct and the mole percentages of D_2O in tables 2 to 5 are expressed on this basis. In continuing the work, however, according to plans for constructing cells containing much higher percentages of D_2O, this matter will become of increasing importance and a more definite answer, based on experimental results, is to be expected.

Another uncertainty in estimating the actual concentration of D_2O in the finished cells arises from the possible partial dehydration of the cadmium sulphate crystals on exposure to the air prior to using them for preparing the saturated solutions. Partial dehydration of the crystals would result in less dilution of the D_2O than is shown in table 1, but the uncertainty in the concentration would hardly be great enough to affect ΔE per mole percent by an amount large enough to be significant.

III. EXPERIMENTAL RESULTS

Repeated measurements of the electromotive force at 20° C for each cell are given in table 2. The constancy of the electromotive force of each of the 12 cells is shown by the small average deviation of single observations given in the last column. In no case is the average deviation more than 0.6 microvolt. The scattering of the mean values of individual cells in their respective subgroups is not more than 1.4 microvolts. The constancy and reproducibility of the cells, as indicated by the close agreement of the electromotive force values for each isotopic concentration, are important indications of the validity of the effect of the D_2O.

The mean electromotive force at 20° C of each subgroup is plotted in figure 1 with respect to the D_2O mole percent of the water in the saturated solution. The relation of electromotive force to the D_2O content is evidently linear within the range of the present work. The slope of the line indicates a decrease of electromotive force amounting to 2.9 microvolts per mole percent.[3]

The electromotive forces at 20 and 28° C are compared in table 3. No significant difference was found in the temperature coefficients for

[3] In contrast with our results, Yoneda reported to the Comité Consultatif d'Electricité, 1937, a decrease of 27 microvolts for 1/50 percent of D_2O. His results on three cells will probably be published in volume 18 of the Procès Verbaux, Comité International des Poids et Mesures.

the various D_2O concentrations. The mean change in electromotive force going from 28 to 20° C, 374.0 microvolts, lies between the value

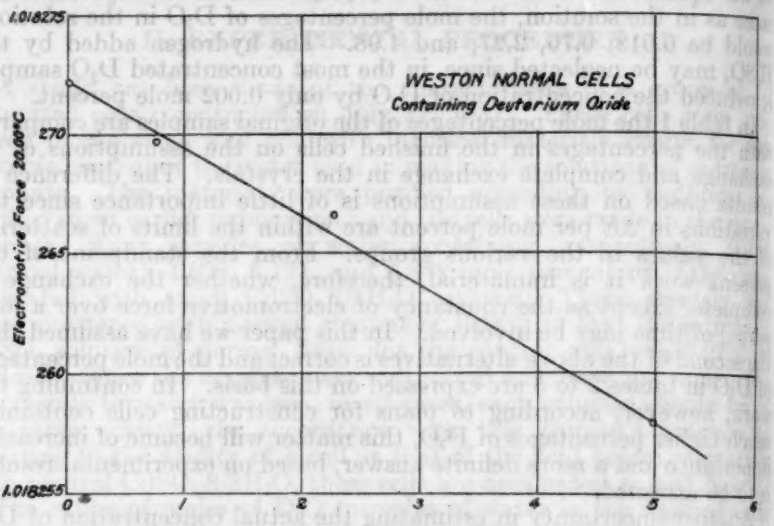

FIGURE 1.—*Relation of electromotive force to mole percent of* D_2O

380.5 calculated from the international temperature formula [4] and 370.1 calculated from the formula of Vigoureux and Watts.[5]

[4] Report of London Conference on Electrical Units and Standards, schedule C (1908).
[5] Proc. Phys. Soc. (London) 45, 172 (1933).

TABLE 2.—*Electromotive force of individual cells at 20.00° C*

TABLE 2.—*Electromotive force of individual cells at 20.00° C*

Cell No.	Mole percent of D_2O	International volts; measurements made during September–November 1937										Average deviation of single observations
		Sept. 9	Sept. 15	Sept. 23	Oct. 2	Oct. 8	Oct. 18	Oct. 28	Nov. 15	Nov. 19	Mean	
												μV
956	0.018	1.018272$_8$	1.018272$_7$	1.018272$_3$	1.018272$_9$	1.018272$_1$	1.018272$_2$	1.018273$_5$	1.018273$_0$	1.018273$_1$	1.018272$_8$	0.4
957	.018	70$_0$	72$_4$	72$_4$	72$_2$	71$_9$	71$_7$	72$_7$	72$_7$	72$_4$	72$_4$	.6
958	.018	71$_6$	72$_4$	72$_1$	71$_6$	71$_8$	71$_2$	72$_3$	71$_4$	72$_2$	71$_8$	.5
Mean		71$_8$	72$_5$	72$_3$	72$_2$	71$_8$	71$_7$	72$_9$	72$_4$	72$_8$	72$_3$	
959	0.76	69$_1$	68$_4$	69$_0$	69$_3$	68$_1$	68$_9$	69$_1$	69$_0$	69$_2$	68$_9$	0.3
960	.76	71$_6$	70$_7$	70$_3$	68$_6$	69$_3$	70$_0$	70$_3$	70$_5$	70$_3$	70$_3$	.5
961	.76	70$_7$	70$_7$	71$_1$	70$_3$	68$_4$	69$_4$	69$_3$	69$_4$	69$_4$	70$_0$	.6
Mean		70$_3$	69$_9$	70$_4$	69$_3$	68$_9$	69$_5$	69$_9$	69$_8$	69$_8$	69$_7$	
962	2.27	66$_5$	66$_4$	67$_0$	66$_7$	65$_8$	65$_8$	66$_6$	66$_0$	66$_1$	66$_3$	0.3
963	2.27	66$_8$	66$_3$	67$_6$	66$_2$	65$_3$	66$_3$	66$_4$	66$_0$	66$_3$	66$_3$	.4
964	2.27	66$_9$	67$_5$	68$_5$	67$_1$	66$_2$	66$_0$	67$_0$	67$_0$	66$_0$	66$_6$	.6
Mean		66$_7$	66$_8$	67$_7$	66$_7$	65$_8$	66$_0$	66$_5$	66$_3$	66$_2$	66$_4$	
965	4.98	58$_6$	58$_7$	58$_4$	58$_2$	57$_2$	57$_6$	58$_0$	57$_9$	58$_2$	58$_1$	0.4
966	4.98	56$_7$	57$_2$	58$_4$	57$_6$	57$_0$	57$_1$	57$_8$	57$_3$	57$_2$	57$_4$	.4
967	4.98	57$_1$	58$_3$	59$_4$	58$_6$	58$_0$	57$_3$	58$_0$	58$_2$	58$_4$	58$_2$	.6
Mean		57$_6$	58$_2$	58$_7$	58$_1$	57$_4$	57$_4$	57$_9$	57$_8$	58$_0$	57$_9$	

TABLE 3.—*Change in electromotive force with temperature*

Cell No.	Mole percent of D_2O	Emf at 28.00° C (mean values)	Emf at 20.00° C (mean values)	Difference	Mean difference
		v	v	μV	μV
956	0.018	1.017899$_1$	1.018272$_8$	373.7	
957	.018	97$_5$	72$_1$	374.4	374.1
958	.018	97$_6$	71$_8$	374.2	
959	.76	95$_1$	68$_9$	373.8	
960	.76	95$_8$	70$_3$	374.5	373.8
961	.76	96$_5$	70$_9$	373.5	
962	2.27	92$_8$	66$_3$	373.5	
963	2.27	91$_9$	66$_5$	374.4	374.1
964	2.27	92$_8$	66$_9$	374.4	
965	4.98	84$_4$	58$_1$	373.7	
966	4.98	83$_8$	57$_4$	373.4	373.7
967	4.98	84$_3$	58$_2$	373.9	

The results of measurements of the hysteresis of these cells are shown in table 4. In the first test, the cells were moved from a bath at 20° C to another at 28° C. The electromotive forces were measured after 2 hours in the 28° bath and compared with the mean of the equilibrium values subsequently observed at that temperature. In the second test, the cells were transferred back to the 20° bath and again measurements made after 2 hours at the new temperature were compared with the mean of the equilibrium values at 20° C. The hysteresis is somewhat less for cells containing added D_2O than for the cells made with normal water.

The internal resistances of the cells at 20 and 28° C and the ratio of the values at the two temperatures are shown in table 5. The internal resistances, R, were calculated from the relation, $R=\frac{E-E'}{E'}\times 10^7$, where E is the electromotive force and E' the terminal voltage observed when the cell was discharging through an external resistance of 10^7 ohms.

TABLE 4.—*Hysteresis measurements 20 to 28 to 20° C*

[The cells were measured 2 hours after abruptly changing the temperature 8° C.]

Cell No.	Mole percent of D_2O	20 to 28° C			28 to 20° C		
		Emf 2 hr after change	Equilibrium emf at 28°	Difference	Emf 2 hr after change	Equilibrium emf at 20°	Difference
		v	v	μV	v	v	μV
956	0.018	1.017899$_7$	1.017899$_1$	+0.6	1.018268$_1$	1.018272$_8$	−4.7
957	.018	900$_0$	897$_5$	+2.5	256$_8$	272$_1$	−15.3
958	.018	899$_8$	897$_6$	+2.2	259$_0$	271$_8$	−12.8
Mean				+1.7			−10.9
959	0.76	896$_3$	895$_1$	+1.2	266$_3$	268$_9$	−2.6
960	.76	896$_9$	895$_8$	+0.9	269$_0$	270$_3$	−1.3
961	.76	895$_7$	896$_5$	−.8	269$_3$	270$_9$	−0.7
Mean				+0.3			−1.5
962	2.27	894$_9$	892$_8$	+1.2	264$_7$	266$_3$	−1.6
963	2.27	890$_8$	891$_8$	−1.2	262$_0$	266$_5$	−4.4
964	2.27	892$_0$	892$_5$	−0.5	263$_3$	266$_9$	−3.6
Mean				−0.2			−3.2
965	4.98	885$_5$	884$_4$	+1.1	256$_8$	258$_1$	−1.3
966	4.98	884$_2$	883$_8$	+0.4	255$_8$	257$_4$	−2.1
967	4.98	885$_0$	884$_3$	+.7	256$_0$	258$_3$	−2.3
Mean				+0.4			−1.9

TABLE 5.—*Internal resistance of the cells*

Cell No.	Mole percent D_2O	Resistance		Ratio R_{20}/R_{28}	Mean ratio R_{20}/R_{28}
		20.00° C	28.00° C		
		Ohms	*Ohms*		
956	0.018	758	602	1.259	
957	.018	737	594	1.241	1.250
958	.018	673	539	1.249	
959	.76	839	679	1.236	
960	.76	727	588	1.236	1.240
961	.76	816	654	1.248	
962	2.27	845	682	1.238	
963	2.27	799	640	1.248	1.241
964	2.27	825	666	1.238	
965	4.98	805	655	1.228	
966	4.98	800	645	1.240	1.233
967	4.98	769	624	1.232	

IV. CONCLUSIONS

Aside from the theoretical interest in the effect of deuterium oxide on the electromotive force of the cells, there are practical reasons for continuing the investigation. The results given in this paper indicate that the cells containing D_2O are fully as reproducible and constant as those made with normal water. With respect to hysteresis they may be superior. Observations over a longer period of time are needed to determine whether the cells are less subject to the troublesome formation of gas over the amalgam terminal. We believe the results so far obtained are sufficiently promising to justify extending the work to cover a wider range of concentrations of the deuterium oxide.

The authors thank Dr. E. R. Smith, who furnished the deuterium oxide, for helpful suggestions and in particular for standardizing the samples.

Washington, December 23, 1937.

[AUTHOR'S NOTE.—Because of the time which has elapsed since the manuscript of this paper was completed, it is desirable to state that subsequent measurements on these cells show them to maintain substantially the same relative differences. Slight increases in electromotive force have been observed in all cells, but the average increase for those made with ordinary water, 2.3 microvolts, exceeds that of the other cells, 1.7 microvolts, which argues against the likelihood of long continued exchange of D_2O between the crystals and solution. March 25, 1938.]

U. S. Department of Commerce National Bureau of Standards

RESEARCH PAPER RP1095

Part of Journal of Research of the National Bureau of Standards, Volume 20, May 1938

ANALYSIS OF PHOSPHATE ROCK

By James I. Hoffman and G. E. F. Lundell

ABSTRACT

The methods used at the National Bureau of Standards in the analysis of the two Standard Samples of Phosphate Rock, 56a and 120, are described, and a summary of the results obtained by nine cooperating analysts is given. The usual chemical analysis is supplemented by a qualitative spectrochemical examination, and one constituent, boric oxide, has been quantitatively determined by chemical and spectrochemical methods.

CONTENTS

	Page
I. Introduction	608
II. General discussion	608
1. Moisture	608
2. Phosphoric anhydride	608
3. Ferric oxide and alumina	609
4. Calcium oxide	610
5. Magnesia	610
6. Fluorine	610
7. Silica	611
8. Manganese oxide	611
III. Methods of analysis	612
1. Determination of moisture	612
2. Phosphoric anhydride	612
(a) Preparation of the solution	612
(b) Determination of phosphoric anhydride	612
3. Total ferric oxide	613
(a) Preparation of the solution	613
(b) Determination of total ferric oxide	614
4. Total alumina	614
(a) Preparation of the solution	614
(b) Determination of total alumina in the presence of less than 0.5 percent of magnesia	615
(c) Determination of total alumina in materials containing more than 0.5 percent of magnesia	616
5. Soluble ferric oxide and alumina	616
(a) Preparation of the solution	616
(b) Determination of soluble ferric oxide and alumina	616
6. Total calcium oxide	616
(a) Preparation of the solution	616
(b) Determination of total calcium oxide	616
7. Determination of magnesia	617
8. Determination of fluorine	619
9. Determination of silica	621
10. Determination of manganese oxide (MnO)	622
11. Determination of the alkalies	622
12. Determination of sulfur	622
13. Spectrochemical analysis (boron)	623
(a) Qualitative examination	623
(b) Quantitative determination of boron	623
IV. Summary of the results obtained in the cooperative analysis of phosphate rocks	624

I. INTRODUCTION

In analyzing the Standard Samples of Phosphate Rocks, 56a and 120, issued by the National Bureau of Standards, a number of improvements in old methods were made, and some new ones were developed. Most of the methods that were used when the first Standard Sample of Phosphate Rock was issued are still in use, but many of them have been modified to such an extent that the publication of the new and revised methods seems desirable. This paper brings the previous methods[1] up-to-date, but the discussion given in the former paper is not repeated. Certain modifications and suggestions by the analysts who cooperated in this work are incorporated in the discussion, but only the methods used at this Bureau are given in section III, Methods of Analysis.

II. GENERAL DISCUSSION

1. MOISTURE

The moisture content of air-dried samples of finely ground phosphate rock may vary considerably with changes in atmospheric conditions. All of the present work was therefore done on samples dried for 1 hour at 105° C, so that the results reported by all the analysts might have a common basis. Tests at this Bureau indicated that a variation of ±5° C in the temperature is permissible in the case of these particular rocks, and that even if a sample is exposed for 40 hours in an atmosphere of carbon dioxide saturated with water and then dried, its weight is practically the same as it would have been if it had been dried without this severe exposure.[2]

2. PHOSPHORIC ANYHDRIDE

Most of the cooperating analysts used either the alkalimetric or the gravimetric method recommended by the Association of Official Agricultural Chemists.[3] The alkalimetric method involves precipitating the phosphate as ammonium phosphomolybdate in acid solution, dissolving the precipitate in an excess of a standard solution of sodium hydroxide, and then titrating the excess with standard nitric acid. In the gravimetric method the ammonium phosphomolybdate is dissolved in dilute ammonium hydroxide, and the phosphate is then precipitated as magnesium ammonium phosphate and ignited to the pyrophosphate, $Mg_2P_2O_7$. The volumetric method is used almost exclusively in control laboratories and yields fairly accurate results in a very short time if conditions are closely controlled, especially if the sodium hydroxide is standardized by means of a standard sample of phosphate rock. The gravimetric method, involving only one precipitation with magnesia mixture, yields results that are slightly high, usually about 0.2 percent.

In the standardization of Samples 56a and 120, only gravimetric methods involving two precipitations with magnesia mixture were

[1] *The analysis of phosphate rock*, J. Assn. Official Agr. Chem. 8, 184 (1924).

[2] In a private communication, W. H. MacIntire, chemist of the Tennessee Valley Authority, Knoxville, Tenn., states that more uniform results are obtained if their superphosphates and "metaphosphates" are dried at room temperature for 24 to 48 hours over sulfuric acid in a partially evacuated desiccator, than if they are dried in an oven at 105° C.

[3] Official and Tentative Methods of Analysis of the Association of Official Agricultural Chemists, pp 18-22, 4th ed. (1935), published at Washington, D. C.

used at this Bureau, because previous work [4] showed that such a procedure is necessary if accurate results are desired. Two such methods were employed. One involves a precipitation of the phosphate as ammonium phosphomolybdate, followed by two precipitations with magnesia mixture, and is described in detail elsewhere.[5] The other is the recently published method [6] in which two precipitations with strong magnesia mixture in the presence of ammonium citrate serve to separate the phosphate from all the other constituents of the phosphate rock without the preliminary precipitation with molybdate reagent.

For comparison, the results obtained at this Bureau by the official gravimetric method of the Association of Official Agricultural Chemists are included in the Summary (tables 2 and 3).

3. FERRIC OXIDE AND ALUMINA

Total ferric oxide and alumina are seldom determined. The manufacturers of fertilizers are usually interested only in "soluble iron and alumina." To keep the results on a common basis, the cooperating analysts have agreed that the percentages of soluble Fe_2O_3 and Al_2O_3 shall represent the amounts dissolved by transferring a 2.5-g sample to a 250-ml flask, adding 50 ml of diluted hydrochloric acid (1+1) containing 1 g of boric acid, covering the neck of the flask with a watch glass, and boiling for 30 minutes. Tests have shown that the boric acid has practically no effect on the results, but that attack on the glassware by the fluorine in the rock is somewhat lessened.

By analysis of synthetic solutions containing known amounts of alumina, the method for soluble alumina described in the succeeding pages has been found to yield accurate results. Some of the cooperating analysts obtained satisfactory results by shorter methods, usually of an empirical nature. Such methods are not objectionable, especially if the general type of the rock to be analyzed is known. The preparation of the solution is probably the most important part of this determination, because it is essential that all the analysts start with solutions containing the same amount of dissolved material.

Considerable quantities of alumina are retained by the precipitate obtained with sodium hydroxide if this reagent is used for separating iron and other elements from aluminum in materials containing appreciable quantities of magnesium.[7] The error caused by this retention may become serious in the analysis of some of the newer fertilizers of high magnesia content.

In the determination of total ferric oxide and alumina a mixture of perchloric, hydrochloric, and nitric acids is recommended for decomposing the material, because this mixture effects a rapid and fairly complete decomposition of phosphate rocks, and at the same time eliminates fluorine, which might cause errors in the determination of iron.[8] Nitric acid should *always* be used with perchloric acid in this attack because, without its use, serious explosions may occur as a result of the rapid interaction of perchloric acid and the organic matter contained in most phosphate rocks.

---

[4] BS J. Research 5, 279 (1930) RP200.
[5] J. Assn. Official Agr. Chem. 8, 194 (1924).
[6] *Determination of phosphoric anhydride in phosphate rock, superphosphate and "metaphosphate."* J. Research NBS 19, 59 (1937) RP1010.
[7] G. E. F. Lundell, J. I. Hoffman, and H. A. Bright, Chemical Analysis of Iron and Steel, p. 545 (J. Wiley & Sons, New York, N. Y., 1931).
[8] W. F. Hillebrand and G. E. F. Lundell, Applied Inorganic Analysis, p. 775-776 (J. Wiley & Sons, New York, N. Y., 1929).

4. CALCIUM OXIDE

Total calcium oxide was determined by precipitating the calcium as oxalate in a slightly acid (pH, 3 to 4) solution. Bromphenol blue was used as the indicator in adjusting the acidity, and two precipitations were made to free the calcium oxalate from phosphate, iron, and aluminum.

5. MAGNESIA

Most of the analysts determined magnesia by the method[9] published at this Bureau in 1932 or by some slight modification of it. In this method calcium is removed by precipitating it as sulfate in alcoholic solution, and the magnesia is then determined in the filtrate (after evaporating the alcohol) by precipitating it with phosphate in the presence of ammonium citrate, and igniting the magnesium ammonium phosphate to magnesium pyrophosphate, $Mg_2P_2O_7$.

6. FLUORINE

If a phosphate rock is fused with sodium carbonate and the cooled melt is leached with water, much fluorine remains in the insoluble residue.[10] For example, by such a treatment of 0.5-g samples of Phosphate Rocks 56a and 120, 1.4 and 1.6 percent of fluorine out of a total of 3.5 and 3.8 percent, respectively, were retained by the insoluble residue. The work of Reynolds and Jacob shows that three fusions and extractions usually do not yield more than 90 percent of the fluorine. As it is obviously impracticable to separate it by such a procedure, analysts who determine fluorine in phosphatic materials almost always resort to a method involving distillation.

All the analysts who determined fluorine distilled it by the method of Willard and Winter [11] or by some modification of it. Perchloric acid was used by cooperating analysts 7 and 9 (tables 2 and 3). Egbert Janes and H. H. Edwards maintained temperatures between 135 and 140° C in the distilling flask, by dropping water into the solution during the distillation. A flask fitted with a dropping funnel and thermometer similar to that shown in figure 1 was used. The analysts of the U. S. Department of Agriculture maintained temperatures between 120 and 150° C by passing steam into the flasks during the distillation.[12] It was observed in both of the laboratories mentioned that free sulfur or pyritic sulfur in the phosphate rock causes high results for fluorine if the distillate is titrated with thorium nitrate. In the laboratory of the Department of Agriculture this difficulty is overcome by redistillation. Janes and Edwards state that this interference can be prevented by igniting the sample at a low temperature in a silica dish before transferring it to the distilling flask.

Because of the dangers attending the use of perchloric acid for decomposing materials containing organic matter,[13] especially if nitric acid can not be used as a preliminary oxidizer during the heating, it was deemed advisable to develop a method in which perchloric acid is not used. At the National Bureau of Standards the fluorine was

[9] *The determination of magnesia in phosphate rock*, BS J. Research **9**, 487 (1932) RP484.
[10] See also, D. S. Reynolds and K. D. Jacob, Ind. Eng. Chem. Anal. Ed. **3**, 366 (1931).
[11] H. H. Willard and O. B. Winter, Ind. Eng. Chem. Anal. Ed. **5**, 7 (1933).
[12] D. S. Reynolds, J. B. Kershaw, and K. D. Jacob, J. Assn. Official Agr. Chem. **19**, 156 (1936).
[13] Practically all phosphate rocks contain organic carbon. See K. D. Jacob, W. L. Hill, H. L. Marshall, and D. S. Reynolds, Tech. Bul. 364, p. 51 (1933) U. S. Department of Agriculture, Washington, D. C.

therefore distilled from a sulfuric acid [14] solution and determined in the distillate by the lead chlorofluoride method.[15] At the temperature used in this distillation (160 to 170° C), a little sulfuric acid passes into the distillate, but this does not interfere in the lead chlorofluoride method.

Willard and Winter indicated that they obtained complete recovery of fluorine from fluorite (CaF_2), phosphate rock, or cryolite by direct decomposition and distillation with perchloric acid. By the method described in the succeeding pages, using the apparatus shown in figure 1, complete recovery of fluorine from fluorite was not obtained by the use of either sulfuric or perchloric acid. By first fusing the sample with sodium carbonate and then distilling, complete recovery was obtained. The difference (0.1 to 0.2 percent) between the results obtained with fused and unfused samples of phosphate rock is probably too small to warrant the introduction of this extra step in the method. For routine work, fusion probably is never necessary, but since it is not definitely known how the fluorine is combined in all types of phosphate rock, the analyst should make determinations with and without preliminary fusions to find out whether direct treatment with acid and distillation will yield satisfactory recovery in the type of material being analyzed.

7. SILICA

Owing to the difficulty of separating all the fluorine from the insoluble residue that is left when the cooled melt of a sodium carbonate fusion of a phosphate rock is leached with water, the determination of silica is even more difficult in this case than in glasses, enamels, or other materials that contain little or no phosphorus. In fact, no reasonably rapid and accurate method is available. The one here described, although somewhat of a makeshift, is the best expedient available. The determination of silica therefore remains the most difficult and least satisfactory in the entire analysis.

In the method described, two fusions with sodium carbonate and leachings of the cooled melts with water serve to separate most of the fluorine from the insoluble residue, which still contains some of the silica.

The silica in the alkaline solutions is separated from the fluorine in the usual way,[16] by first precipitating most of it with zinc nitrate and then the remainder with zinc oxide dissolved in ammonium hydroxide. The silica in the insoluble residue is obtained by adding boric acid to lessen the effect of the fluorine which is still retained, and then dissolving the residue in hydrochloric acid and dehydrating in the usual manner.

8. MANGANESE OXIDE

By far the most satisfactory method for the determination of manganese oxide in phosphate rock is that in which it is determined colorimetrically after oxidation to permanganic acid by sodium or potassium periodate in strong acid solution.

[14] The use of phosphoric acid has also been suggested for this distillation.
[15] J. I. Hoffman and G. E. F. Lundell, *Determination of fluorine and of silica in glasses and enamels containing fluorine*, BS J. Research **3**, 581 (1929) RP110.
[16] BS J. Research **3**, 581 (1929) RP110.

III. METHODS OF ANALYSIS

1. DETERMINATION OF MOISTURE

Place 5.00 g of sample in a glass-stoppered weighing bottle of such diameter that the depth of the sample does not exceed 0.5 cm. Dry for 1 hour at 105° C in a well-ventilated oven. At the end of 1 hour, loosely stopper the bottle, and cool in a desiccator. Momentarily raise the stopper, again put it in place, and weigh. The loss in weight is regarded as moisture.

2. PHOSPHORIC ANHYDRIDE

(a) PREPARATION OF THE SOLUTION

Method A.—Transfer 2.500 g of the dried material to a 300-ml Erlenmeyer flask, add 30 ml of hydrochloric acid and 10 ml of nitric acid. Place a small watch glass over the mouth of the flask, and boil gently for 30 minutes. Rinse the glass, add 50 ml of water, heat to boiling, and filter through a paper of close texture, catching the filtrate in a 250-ml volumetric flask. Wash the paper [17] and the Erlenmeyer flask thoroughly with diluted hydrochloric acid [18] (1+4), cool the contents of the volumetric flask to the proper temperature, and add water until the flask is filled to the mark. Mix thoroughly and transfer 50.00 ml of the solution (representing 0.5000 g of sample) to a 300-ml Erlenmeyer flask.

Method B.—Transfer 0.5000 g of the dried material to a 300-ml Erlenmeyer flask and add 15 ml of hydrochloric acid and 3 ml of nitric acid. Place a small watch glass over the mouth of the flask, and boil gently for 30 minutes. Rinse and remove the watch glass, and without filtering, proceed with the addition of ammonium citrate, hydrochloric acid, and magnesia mixture.

This method obviates the use of volumetric glassware and requires less time than method *A*. The results obtained are equally accurate if the material contains no appreciable amount of compounds of phosphorus insoluble in this mixture of acids.

(b) DETERMINATION OF PHOSPHORIC ANHYDRIDE [19]

To the solution in the 300-ml Erlenmeyer flask, add 30 g of ammonium citrate, 10 ml of hydrochloric acid, and 100 ml of strong magnesia mixture.[20] Neutralize the solution with ammonium hydroxide, using litmus paper as indicator, and add 3 ml of ammonium hydroxide in excess. Dilute the solution to 225 to 250 ml with water, add a few glass beads, stopper the flask tightly, shake on a shaking

[17] By applying the treatment prescribed, no phosphorus is volatilized, and only 0.03 percent of P_2O_5 remained in the insoluble residue in the case of the National Bureau of Standards Sample 56, and less than 0.005 percent in Samples 56a and 120. Unless it is known that no phosphorus remains insoluble, ignite the paper and insoluble residue in platinum, fuse with a small quantity of sodium carbonate, and leach the cooled melt with hot water. Filter, acidify the filtrate with hydrochloric acid, and add the solution to the contents of the volumetric flask. Or, if the filtrate is acidified with nitric acid, the phosphorus may be precipitated with molybdate reagent, separately determined, and the percentage found added to that obtained in the main determination.

[18] This denotes 1 volume of concentrated hydrochloric acid (sp gr 1.18) diluted with 4 volumes of water. Diluted ammonium hydroxide (1+19) denotes 1 volume of ammonium hydroxide (sp gr 0.90) diluted with 19 volumes of water. If no dilution is specified, the concentrated reagent is meant. This system of specifying dilution is used throughout this paper.

[19] This method is described in detail in J. Research NBS **19**, 59 (1937) RP1010.

[20] Prepare the strong magnesia mixture as follows: Dissolve 400 g of $MgCl_2.6H_2O$ and 300 g of ammonium chloride in 1,500 ml of warm water. When solution is complete, add ammonium hydroxide until the solution is alkaline to litmus. Allow to stand for about 1 hour, filter, and add hydrochloric acid to the filtrate until the solution is acid to litmus. If properly prepared, the volume of the solution will be almost exactly 2 liters.

machine for about 30 minutes and allow to stand overnight. Filter through a paper of close texture, and wash the flask and paper once with a small quantity of diluted ammonium hydroxide (1+19). Discard the filtrate.

Dissolve any magnesium ammonium phosphate remaining in the flask in about 50 ml of warm diluted hydrochloric acid (1+4) and pour the solution through the paper to dissolve the phosphate that was transferred to the filter, and to separate any insoluble residue that may have remained if method *B* was used for the preparation of the solution. Wash the paper and flask with more of the same acid, and add 0.3 g of citric acid and 1 ml of magnesia mixture to the solution, which should have a volume of about 100 ml. While stirring, add ammonium hydroxide until the solution is alkaline to litmus, and then add 5 ml in excess. Stir occasionally during 30 minutes, and allow to stand for 4 hours or overnight.

Collect the precipitate on a 9-cm paper of close texture, wash with cool diluted ammonium hydroxide (1+19), and transfer the paper and precipitate to a weighed platinum or porcelain crucible. Char the paper without flaming, burn off the carbon below 900° C, and finally ignite to constant weight, preferably in a muffle furnace with pyrometric control, at 1,050 to 1,100° C.

The weight of the magnesium pyrophosphate, $Mg_2P_2O_7$, multiplied by 63.79 and divided by the weight of the sample, yields the percentage of P_2O_5.

Tests have shown that in the analysis of phosphate rock the time of standing in the first precipitation can be reduced to 3 hours and in the second to 2 hours, if the solutions are chilled before shaking or stirring and then allowed to stand in ice water or in a refrigerator at 5 to 10° C. With small quantities (less than 10 mg of P_2O_5), the longer time of standing is essential, and even then it is best to chill and shake alternately two or three times.

An alternative umpire method involving a preliminary precipitation of the phosphate with molybdate, followed by two precipitations with magnesia mixture is described in a previous publication.[20a]

3. TOTAL FERRIC OXIDE

(a) PREPARATION OF THE SOLUTION

Transfer 2.000 g of the dried sample to a 300-ml Erlenmeyer flask, and add 30 ml of diluted nitric acid (1+2), 5 ml of hydrochloric acid, and 10 ml of 60-percent perchloric acid. Place the uncovered flask on the hot plate, evaporate until fumes of perchloric acid appear, and heat just below its boiling point until nearly all the acid has been volatilized. Do not evaporate quite to dryness. Cool somewhat, and drench the residue with 5 ml of hydrochloric acid. Add 30 ml of warm water, and heat until salts are in solution. Remove the insoluble residue by filtering through a paper of loose texture, wash thoroughly with hot diluted hydrochloric acid (1+19) and reserve the solution. Ignite the paper and residue in platinum, treat with hydrofluoric and sulfuric acids to eliminate the silica, and fuse the nonvolatile residue with a little sodium pyrosulfate. Dissolve the cooled melt in 25 ml of diluted hydrochloric acid (1+19), and precipitate the iron in the solution by adding a slight excess of ammonium

[20a] *The analysis of phosphate rock.* J. Assn. Official Agr. Chem. 8, 194 (1924).

hydroxide. Collect the precipitate on a small filter, and wash once or twice with water.[21] Dissolve the precipitate in hot diluted hydrochloric acid (1+19), and add the solution to the reserved solution.

(b) DETERMINATION OF TOTAL FERRIC OXIDE

To the combined solutions add a few drops of a saturated solution of potassium permanganate, boil to expel chlorine, and then add stannous chloride dropwise until the iron is reduced, as is indicated by the disappearance of the yellow color. Avoid any large excess. Wash the inside surface of the beaker with a jet of water, cool rapidly, and add at one stroke 10 ml of a saturated solution of mercuric chloride. Agitate the solution for 1 minute, and then pour it into a 1-liter porcelain casserole containing 20 ml of manganese sulfate solution[22] and 450 ml of water. Titrate with a solution of potassium permanganate, not stronger than 0.1 *N*, and correct the result by subtracting the volume of permanganate required in a titration of the reagents alone. Calculate the percentage of Fe_2O_3.

In most cases it is not necessary to filter and to recover the iron in the insoluble residue. The iron can be reduced with stannous chloride as soon as the salts have been dissolved in dilute hydrochloric acid after the evaporation with perchloric acid, *provided* that no brown or black particles remain undissolved. Mere visual observation will easily show whether it is necessary to recover iron from the insoluble residue.

The percentages of iron oxide in the insoluble residues from eight phosphate rocks were as follows: NBS Standard Tennessee Phosphate Rock 56, 0.05; NBS Standard Tennessee Phosphate Rock 56a, 0.007; NBS Standard Florida Phosphate Rock 120, 0.007; Florida pebble rock, 0.005; Florida hard rock, 0.005; Tennessee blue rock, 0.01; Wyoming phosphate rock, 0.01; and Idaho phosphate rock, 0.01. It is evident that the recovery of iron is of consequence in only one of the eight insoluble residues. The amount of iron in the insoluble residue may depend on the fineness of the sample.

4. TOTAL ALUMINA

(a) PREPARATION OF THE SOLUTION

Transfer 2.500 g of the dried sample to a platinum dish, and add 30 ml of diluted nitric acid (1+1) and 10 ml of hydrofluoric acid. Evaporate to dryness on the steam bath, then add 30 ml of diluted nitric acid (1+1), 5 ml of hydrofluoric acid, and 15 ml of 60-percent perchloric acid. Evaporate nearly to dryness on the hot plate, cool, wash the inside surface of the dish with a jet of water, and add 5 ml of 60-percent perchloric acid. Again evaporate nearly to dryness, cool somewhat, and add 30 ml of diluted hydrochloric acid (1+2). Heat the solution on the steam bath, and if a residue remains, collect it on a small tight filter paper. Ignite the paper in a platinum crucible, and treat the residue with a drop of sulfuric acid and about 0.5 ml of hydrofluoric acid. Evaporate to dryness, ignite for 1 minute at 600 to 800° C, and fuse the residue with about 0.5 g of sodium carbonate. Dissolve the cooled melt in the original acid solution of the sample.

[21] The precipitation with ammonium hydroxide is made to eliminate traces of platinum which would otherwise interfere in the determination of iron.

[22] Dissolve 200 g of $MnSO_4.4H_2O$ in 1,000 ml of H_2O, and add a cooled mixture of 400 ml of H_2SO_4, 1,200 ml of H_2O, and 400 ml of approximately 85-percent phosphoric acid.

(b) DETERMINATION OF TOTAL ALUMINA IN THE PRESENCE OF LESS THAN 0.5 PERCENT OF MAGNESIA

Nearly neutralize the warm solution (60° C) having a volume of about 200 ml, with a 25-percent solution of sodium hydroxide, and pour this solution slowly while stirring into 100 ml of a 25-percent solution of sodium hydroxide containing 0.5 g of sodium carbonate. Transfer the solution and precipitate to a 500-ml volumetric flask, allow to cool, fill the flask to the mark with cool water, and mix thoroughly. Filter through a dry filter into a dry 200-ml volumetric flask. Two 200-ml portions may be collected if duplicate determinations are to be made.

Determine the alumina in a 200-ml portion of the filtrate, representing 1.000 g of sample, by the phosphate method as follows: Acidify the solution with hydrochloric acid, add 10 ml of the concentrated acid in excess, and then 1.0 g of diammonium phosphate. Dilute to 350 to 400 ml, add methyl orange indicator, make just alkaline with ammonium hydroxide, and restore the pink color with several drops of diluted hydrochloric acid (1+5). Heat the solution to boiling, and add 15 ml of a 50-percent solution of ammonium acetate. Continue the boiling for 5 minutes, and then collect the precipitate on an 11-cm filter of close texture (No. 42 Whatman or No. 589 S&S blue ribbon), and allow the precipitate to drain. Without washing, transfer the paper and precipitate to the beaker in which the precipitation took place, and stir the paper to a pulp. Add 10 ml of hydrochloric acid and 1.0 g of diammonium phosphate, and dilute the solution to 300 ml. Add methyl orange indicator, and precipitate the aluminum as before. Filter, and wash with a hot 5-percent solution of ammonium nitrate until 5 ml of the washings gives at most a barely distinguishable opalescence with an acidified solution of silver nitrate. Usually, 150 ml of wash solution is sufficient.

Ignite the paper and precipitate in platinum or porcelain. Heat at a low temperature until the carbon is gone, then at about 1,000° C until constant weight is obtained. Weigh as $AlPO_4$ and multiply by 0.418 to convert to the weight of Al_2O_3. A blank should be carried through all steps of the method and the weight of the $AlPO_4$ corrected accordingly.

In routine analyses two steps of the method may be omitted. (1) In decomposing most phosphate rocks the residue that remains undissolved after the treatments with nitric, hydrofluoric, and perchloric acids contains only a negligible amount of alumina and no calcium oxide. It therefore is usually permissible to ignore the insoluble residue, and, without filtering, to proceed with the sodium hydroxide precipitation. (2) Results are only slightly higher if only a single phosphate precipitation is made. For routine work it is therefore permissible to omit the second precipitation with phosphate. Macerated paper must, however, be added, and the washing with a solution of ammonium nitrate must be thorough.

The percentages of alumina in the insoluble residues were determined in eight phosphate rocks as follows: NBS Standard Tennessee Phosphate Rock 56, 0.03; NBS Standard Tennessee Phosphate Rock 56a, 0.02; NBS Standard Florida Phosphate Rock 120, 0.02; Florida pebble rock, 0.01; Florida hard rock, 0.005; Tennessee blue rock, 0.005; Wyoming phosphate rock, 0.005; and Idaho phosphate rock, 0.005.

(c) DETERMINATION OF TOTAL ALUMINA IN MATERIALS CONTAINING MORE THAN 0.5 PERCENT OF MAGNESIA

To avoid low results for alumina when 0.5 percent or more of magnesia is present, separate most of the magnesium from the aluminum as follows: To the perchloric acid solution of the sample add 50 ml of hydrochloric acid, and dilute to 400 ml. Add methyl orange indicator solution and then ammonium hydroxide until the indicator just turns yellow. Restore the pink color by adding hydrochloric acid dropwise, heat the solution nearly to boiling, and add 15 ml of a 50-percent solution of ammonium acetate. Boil for 5 minutes, filter, and wash the precipitate a few times with a 5-percent solution of ammonium nitrate. Dissolve the precipitate in 30 ml of hot diluted hydrochloric acid (1+2), and proceed with the neutralization and precipitation with sodium hydroxide.

The magnitude of the error caused by magnesium is illustrated by the following determinations of magnesia in a synthetic standard prepared by mixing 2.500 g of National Bureau of Standards Argillaceous Limestone [23] 1A with 1.5 g of P_2O_5. Three determinations by the method in which magnesia is not removed, (4 (b), p. 615) indicated 3.84, 3.90, and 3.91 percent of alumina, respectively, in the limestone, whereas 4.14 and 4.17 percent, respectively, were obtained by the method in which magnesia is removed before the alumina is separated by means of sodium hydroxide (4 (c).

5. SOLUBLE FERRIC OXIDE AND ALUMINA

(a) PREPARATION OF THE SOLUTION

Transfer 2.500 g of sample to a 250-ml flask, add 50 ml of diluted hydrochloric acid (1+1) containing 1 g of boric acid, cover the neck of the flask with a watch glass, and boil moderately for 30 minutes. Remove the flask from the source of heat, add 20 ml of water, and remove the insoluble matter by filtration. Catch the filtrate in a 250-ml volumetric flask, cool the solution, and dilute to the mark. Mix well, and remove suitable aliquot portions for the determinations of soluble ferric oxide and alumina.

(b) DETERMINATION OF SOLUBLE FERRIC OXIDE AND ALUMINA

Determine soluble ferric oxide in an aliquot portion of the prepared solution by the procedure described for total ferric oxide under 3 (b), p. 614.

Determine soluble alumina in an aliquot portion of the prepared solution by the procedure described for total alumina under 4 (b) p. 615 or 4 (c), p. 616.

6. TOTAL CALCIUM OXIDE

(a) PREPARATION OF THE SOLUTION

Prepare the solution as directed for total alumina under 4 (a) p. 614.

(b) DETERMINATION OF TOTAL CALCIUM OXIDE

Transfer an aliquot portion of the prepared solution, representing 0.5000 g of sample, to a 400-ml beaker, add 50 ml of a saturated solution of ammonium oxalate (about 4 g of $(NH_4)_2C_2O_4.H_2O$ in 100 ml of

[23] This limestone contains 14.11 percent of SiO_2, 1.63 percent of Fe_2O_3, 4.16 percent of Al_2O_3, 0.16 percent of TiO_2, 41.32 percent of CaO, and 2.19 percent of MgO.

water) and dilute the solution to 200 ml. Add 2 drops of brom phenol blue indicator solution,[24] and heat to 80 to 90° C, and then add ammonium hydroxide until the color in the hot solution changes from yellow to a light green but not to a distinct blue. This yields a solution having a pH value between 3 and 4. Digest on the steam bath for 1 to 2 hours, cool, filter through a paper of close texture, and wash the precipitate in the beaker and on the paper two or three times with ammonium oxalate-oxalic acid wash solution (2 g of $(NH_4)_2C_2O_4.H_2O$ and 1 g of $H_2C_2O_4.2H_2O$ dissolved in 1 liter of water). Actual determinations of the pH of the solutions by means of a Coleman Model 3D pH Electrometer showed that satisfactory results can be obtained at pH values between 3 and 4.4, but that low results are obtained if the acidity is increased to a pH of 2.0 to 2.4.

Transfer the paper and the precipitate to the beaker in which the calcium was precipitated, stir the paper to a pulp, and add 20 ml of diluted hydrochloric acid (1+1). Heat on the steam bath until the calcium oxalate is dissolved, add 25 ml of a saturated solution of ammonium oxalate, dilute to 200 ml, and repeat the precipitation as previously described. Collect the precipitate on a paper of close texture, and wash with ammonium oxalate-oxalic acid wash solution. Transfer the paper and precipitate to a platinum crucible with cover, and heat in the uncovered crucible until carbon has been destroyed. Cover the crucible, ignite at 1,200° C, and weigh as $CaO+Mn_3O_4$. The crucible should be reheated and the weight checked because of possible absorption of moisture during the first weighing.

Part of the manganese in the original sample will be found in the ignited calcium oxide. To correct for this, dissolve the ignited residue in 50 ml of diluted nitric acid (1+4), add 5 ml of 85-percent phosphoric acid to the solution, and determine the manganese colorimetrically by the periodate method described under determination of manganese oxide (p. 622). Calculate the manganese to Mn_3O_4, and subtract from the weight of the ignited residue. The amount of Mn_3O_4 that accompanied the calcium oxide in the case of Sample 56a (MnO=0.18 percent) was only 0.1 mg, and with Sample 120 (MnO=0.027) it was only 0.03 mg. Therefore, no serious error is introduced if the correction for manganese is neglected in the analysis of materials containing less than 0.2 percent of manganese oxide. The averages of four closely checking results obtained by this method for total CaO in Samples 56, 56a, and 120 were 44.9, 45.62, and 49.67 percent, respectively, as compared with the certificate values, 44.8, 45.55, and 49.62 percent, respectively.

The proper conditions for the precipitation of calcium in dilute acid solutions can also be obtained by the method previously described by the authors.[24a]

7. DETERMINATION OF MAGNESIA

Transfer 2.00 g of the sample to a 250-ml beaker, cover, add 15 ml of diluted hydrochloric acid (2+1) and 5 ml of nitric acid, and boil gently for 10 to 15 minutes. Remove the beaker from the source of heat, add 6 ml of diluted sulfuric acid (1+1), remove the cover, and evaporate until fumes of sulfuric acid appear. Cool slightly,

[24] Prepared by dissolving 0.10 g of brom phenol blue reagent in 1.5 ml of 0.1 *N* sodium hydroxide and diluting to 25 ml.

[24a] *The Analysis of Phosphate Rock*, J. Assn. Official Agr. Chem. 8, 203 (1924).

wash down the inside surface of the beaker with a jet of water, and again evaporate until fumes of sulfuric acid appear. Cool, add 10 ml of water, stir thoroughly, and digest on the steam bath for 10 to 15 minutes. Remove from the steam bath, add 100 ml of 95-percent alcohol, stir so that the calcium sulfate is well dispersed throughout the liquid, and then allow to stand for 30 minutes or longer. Filter by means of suction through a tight plug of filter-paper pulp, using a Gooch crucible, carbon funnel, or Büchner funnel, and wash five times with 5-ml portions of 95-percent alcohol containing 1 ml of sulfuric acid per 100 ml.

Evaporate the alcoholic filtrate as far as possible on the steam bath. Transfer the solution to a 300-ml Erlenmeyer flask, dilute to 75 to 100 ml, and add 2 g of citric acid and 15 ml of a 25-percent solution of diammonium phosphate, $(NH_4)_2HPO_4$. Add ammonium hydroxide until the solution is alkaline to litmus, and then add 10 ml in excess. Add 5 to 10 glass beads, tightly stopper the flask, and shake on a shaking machine for at least 1 hour. Allow to stand in a cool place for 4 hours or preferably overnight. Filter through a tight paper containing a little paper pulp, and wash thoroughly with diluted ammonium hydroxide (1+19), containing 50 g of diammonium phosphate per liter. Pass 25 ml of hot diluted hydrochloric acid (1+19) through the paper into the flask in which the precipitation took place, transfer the solution to a 150-ml beaker, and wash the paper and flask thoroughly with more of the diluted acid. To the solution in a volume of 50 to 75 ml and containing no glass beads, add 0.5 ml of a 25-percent solution of diammonium phosphate, cool, and then add ammonium hydroxide, while stirring, until the solution is alkaline to litmus. Stir for a few minutes, then add 3 to 4 ml of ammonium hydroxide and allow to stand for 4 hours or overnight. Transfer the precipitate to a small filter, and wash with diluted ammonium hydroxide (1+19). Transfer the paper and precipitate to a platinum crucible, ignite slowly at a temperature below 900° C until the carbon is burned, preferably in a muffle furnace with pyrometric control, and then at about 1,100° C for 1 to 2 hours. Cool and weigh.

The residue consists of $Mg_2P_2O_7$ and possibly $Mn_2P_2O_7$ and $Ca_3(PO_4)_2$. If the alcoholic filtrate was clear, the tricalcium phosphate will not exceed 0.3 mg and can be neglected unless very accurate results are desired.[25] The correction for manganese is made as follows: Dissolve the residue in 10 ml of diluted sulfuric acid (1+9), transfer the solution to a 300-ml Erlenmeyer flask, and add 50 ml of diluted nitric acid (1+3), 2 ml of 85-percent phosphoric acid, and 0.5 g of potassium periodate, KIO_4. Boil for 15 to 20 minutes, cool, and dilute to a convenient volume. In another flask containing the same amounts of the reagents treated in a similar way, match the color by adding a standard solution of potassium permanganate. From the volume of the solution of permanganate required, calculate the weight of $Mn_2P_2O_7$ in the residue. Subtract this weight from the total weight, and regard the difference as $Mg_2P_2O_7$, which contains 36.2 percent of MgO.

[25] If a correction for calcium is to be made, dissolve the residue in 10 ml of diluted sulfuric acid (1+19), evaporate to about 5 ml, and then add 25 ml of 95-percent alcohol. Allow to stand for 1 to 2 hours, filter on a small paper, and wash with alcohol. Dry the paper in the funnel, and dissolve the precipitate of calcium sulfate in 20 ml of hot diluted hydrochloric acid (1+99). Add a few crystals of ammonium oxalate, heat, render the solution faintly ammoniacal, and allow to stand for about 1 hour. Filter, ignite, and weigh as CaO. Calculate to tricalcium phosphate, $Ca_3(PO_4)_2$, and subtract from the apparent weight of $Mg_2P_2O_7$.

If calcium is determined in this way, the alcoholic filtrate is used for the determination of manganese. Before applying the periodate oxidation, this filtrate must be evaporated and heated until fumes of sulfuric acid appear, and then treated with nitric acid to make sure that reducing substances are absent.

8. DETERMINATION OF FLUORINE

Fuse 0.50 to 1.00 g of sample with 4.0 g of sodium carbonate in a platinum crucible. Keep the molten mass at a red heat for 5 minutes, then grasp the hot crucible with tongs, and immediately immerse the lower half in cold water. Tap the cold crucible to loosen the solidified mass, and transfer the cooled melt to a 125-ml Claissen flask (see fig. 1). Scrub the crucible and cover with a policeman and a little hot water, and transfer the washings to the flask, which rests in a 4-cm hole in an asbestos gauze *E*, and is fitted with rubber stoppers, a delivery bulb *A* for admitting acid and water, a thermometer *D*, and a condenser *B*, which delivers the distillate into a 400-ml beaker *C*. The end of the condenser is immersed in 20 ml of a 20-percent solution of sodium hydroxide contained in the beaker *C*.

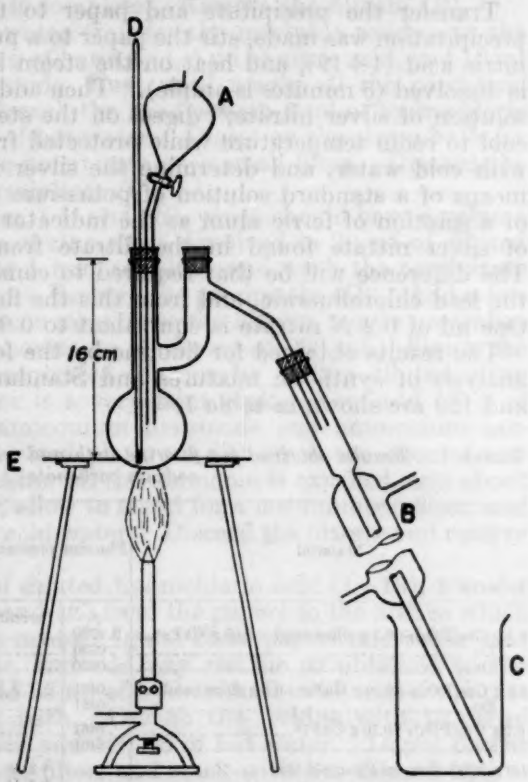

FIGURE 1.—*Apparatus for distilling fluorine.*

Add 0.05 to 0.1 g of 20- to 40-mesh flake graphite or granulated coke to prevent bumping,[26] close the flask with the stopper containing the thermometer and the delivery tube *A*, admit 30 ml of diluted sulfuric acid (1+1), and cautiously heat the contents of the flask until frothing ceases. A good Tirrill or similar burner is a satisfactory source of heat. Increase the heat until the liquid in the flask boils vigorously, and continue the boiling until the temperature of the liquid has risen to 160° C. Then without removing the source of heat, admit water through the tube *A* at such a rate that the temperature of the liquid in the flask remains between 160 and 170° C. Collect 300 ml of distillate between these temperatures.

Evaporate the *alkaline* distillate to a volume of 250 ml, and add 3 ml of a 10-percent solution of sodium chloride and 2 drops of bromphenol blue indicator.[27] Add dilute nitric acid until the color changes to yellow, and then sodium hydroxide until the color changes just to blue.

[26] This means of preventing bumping was suggested by W. E. Dickinson, Chief Chemist of the International Agricultural Corporation, Norfolk, Va.

[27] Prepared by dissolving 0.10 g of bromphenol blue reagent in 1.5 ml of 0.1 *N* sodium hydroxide and diluting to 25 ml.

Now add 2 ml of diluted hydrochloric acid (1+1) and 5.0 g of solid lead nitrate, $Pb(NO_3)_2$, and heat on the steam bath. As soon as the lead nitrate is in solution, add 5.0 g of solid sodium acetate, $NaC_2H_3O_2.3H_2O$, stir vigorously, and digest on the steam bath for 30 minutes with occasional stirring. Allow to stand overnight at room temperature, and decant the solution through a paper of close texture (589 *S* & *S* blue ribbon or 42 Whatman). Wash the precipitate, beaker, and paper once with cold water, then four to five times with a cool saturated solution of lead chlorofluoride,[28] and then once more with cold water.

Transfer the precipitate and paper to the beaker in which the precipitation was made, stir the paper to a pulp, add 100 ml of diluted nitric acid (1+19), and heat on the steam bath until the precipitate is dissolved (5 minutes is ample). Then add a slight excess of a 0.2 *N* solution of silver nitrate,[29] digest on the steam bath for 30 minutes, cool to room temperature while protected from the light, filter, wash with cold water, and determine the silver nitrate in the filtrate by means of a standard solution of potassium thiocyanate,[30] using 5 ml of a solution of ferric alum as the indicator.[31] Subtract the amount of silver nitrate found in the filtrate from that originally added. The difference will be that required to combine with the chlorine in the lead chlorofluoride, and from this the fluorine may be computed. One ml of 0.2 *N* nitrate is equivalent to 0.00380 g of fluorine.

The results obtained for fluorine by the foregoing procedure in the analysis of synthetic mixtures and Standard Phosphate Rocks 56a and 120 are shown in table 1.

TABLE 1.—*Results obtained for fluorine with and without preliminary fusion with sodium carbonate*

Material	Fluorine present		Fluorine found by procedure described. (Preliminary fusion with Na_2CO_3)		Fluorine found by direct distillation without fusion with Na_2CO_3	
	g	*Percent*	*g*	*Percent*	*g*	*Percent*
0.5 g $Ca_3(PO_4)_2$+0.1 g silica sand +0.05 g CaF_2 [a]	0.0230				0.0163	
Do	.0230		0.0224			
Do	.0230		.0225			
0.9 g $Ca_3(PO_4)_2$+0.10 g CaF_2 [a]+0.2 g silica sand	.0461				.0365	
Do	.0461		.0458			
0.9 g $Ca_3(PO_4)_2$+0.10 g CaF_2 [a]	.0461		.0464			
Do	.0461				.0366	
1.0 g NBS Standard Sample 56a		[b] 3.56		3.45		
Do		[b] 3.56		3.52		
Do		[b] 3.56				3.38
Do		[b] 3.56				3.44
1.0 g NBS Standard Sample 120		[b] 3.76		3.73		
Do		[b] 3.76		3.75		
Do		[b] 3.76				3.55
Do		[b] 3.76				3.50

[a] NBS Standard Sample 79 containing 94.8 percent of CaF_2.
[b] Certificate value.

[28] To prepare lead chlorofluoride wash solution: (a) Dissolve 10 g of lead nitrate in 200 ml of water; (b) dissolve 1.0 g of sodium fluoride in 100 ml of water, and add 2 ml of hydrochloric acid; and, (c) mix solutions (a) and (b). Allow the precipitate to settle and decant the supernatant liquid. Wash four or five times with 200 ml of water by decantation, and then add about 1 liter of cold water to the precipitate and allow to stand for 1 hour or longer with occasional stirring. Pour through a filter and use the clear filtrate. By adding more water to the precipitate of lead chlorofluoride in the beaker and stirring, more wash solution may be prepared as needed.

[29] Standardized by precipitating a measured portion with hydrochloric acid and weighing the silver chloride.

[30] Standardized by comparing with the standard solution of silver nitrate under the same conditions as obtain in the method. A convenient concentration is 0.1 *N*.

[31] A cold saturated water solution of ferric alum (free from chlorides) to which has been added sufficient colorless nitric acid to bleach the brown color of the water solution.

9. DETERMINATION OF SILICA

Fuse 0.500 g of the dried sample with 5 g of sodium carbonate, transfer the cooled melt to a platinum dish, leach with hot water, and filter when disintegration is complete. Return the insoluble residue to the dish by means of a jet of hot water, add 50 ml of a 2-percent solution of sodium carbonate, boil for a few minutes, filter, and wash thoroughly with hot water. Reserve the combined filtrates (*A*). Transfer the insoluble residue to a platinum crucible, ignite, fuse with 3 g of sodium carbonate, leach the cooled melt with hot water, and filter when disintegration is complete. Reserve the filtrate (*B*).

By means of a jet of water transfer the insoluble residue to the platinum dish, then add 1 g of boric acid, 5 ml of nitric acid, and 10 ml of 60-percent perchloric acid. Heat until nearly all the perchloric acid is volatilized, cool, drench the residue with 5 ml of hydrochloric acid, and then add 50 ml of hot water. Digest on the steam bath for 5 minutes, and collect the precipitate on a small filter. Discard the filtrate and reserve the precipitate (*C*).

To the combined filtrates, (*A*) and (*B*), which should have a volume of about 300 ml, add 1 g of zinc oxide dissolved in 20 ml of diluted nitric acid (1+4), boil for 1 minute, filter, and wash the precipitate thoroughly with hot water. Reserve the precipitate (*D*). Add a few drops of methyl red indicator solution to the filtrate, nearly neutralize with nitric acid, and evaporate to a volume of 200 ml. Finish the neutralization of the concentrated solution by adding diluted nitric acid (1+9) until the color is a very faint pink. Now add 1.0 g of zinc oxide dissolved in ammonium hydroxide and ammonium carbonate,[32] and boil in a covered platinum dish until the odor of ammonia is entirely gone. After all the ammonia is expelled, add about 50 ml of warm water, stir, allow to stand for a few minutes, filter, and wash the precipitate with cold water. Discard the filtrate and reserve the precipitate (*E*).

With the aid of a jet of diluted hydrochloric acid (1+19), transfer the precipitates (*C*), (*D*), and (*E*) from the papers to the dish in which the last precipitation was made. Ignite these papers and those used in the previous filtrations, and add any residue so obtained to the contents of the dish. Add 25 ml of hydrochloric acid, and evaporate to dryness on the steam bath. Drench the residue with 10 ml of hydrochloric acid, and then add 100 ml of hot water. Digest on the steam bath for 15 minutes, filter, and wash with hot diluted hydrochloric acid (1+19), and then with hot water. Return the filtrate and washings to the dish in which the evaporation was made, add 10 ml of sulfuric acid, and evaporate until fumes of sulfuric acid are evolved. Allow to cool, add 100 ml of water, digest for 5 minutes on the steam bath, filter, and wash with hot water.

Place the two papers containing the silica in a platinum crucible, char the paper without flaming, and finally ignite at 1,200° C. Cool in a desiccator, weigh, and determine the silica by treatment with hydrofluoric and sulfuric acids in the usual manner.

Synthetic mixtures consisting of 0.5000 g of National Bureau of Standards Limestone 1A+0.050 g of fluorspar (CaF_2)+0.25 g of tri-

[32] Transfer 1.0 g of zinc oxide and 2.0 g of ammonium carbonate to a small beaker, add 20 ml of water and 2 ml of ammonium hydroxide (sp gr 0.90), and digest on the steam bath until a clear solution is obtained.

calcium phosphate were prepared and analyzed for silica by the foregoing procedure. Two determinations yielded 0.0713 and 0.0709 g of silica, respectively. The total content of silica was 0.0714 g. In the analysis of Standard Samples of Phosphate Rocks 56a and 120, 7.7 and 11.0 percent were obtained, as compared with the certificate values 7.6 and 11.0 percent, respectively.

10. DETERMINATION OF MANGANESE OXIDE (MnO)

Transfer 0.500 g of sample to a 300-ml Erlenmeyer flask and add 5 ml of nitric acid and 15 ml of 60-percent perchloric acid. Heat to boiling, and continue the boiling until fumes of perchloric acid begin to be evolved. Remove from the source of heat, cool somewhat, and add 10 ml of diluted hydrochloric acid (1+1). Now boil the solution until most of the perchloric acid has been volatilized. Reduction of the volume to about 5 ml is satisfactory.

Cool the solution and add 50 ml of warm diluted nitric acid (1+4) in which 0.5 g of boric acid has been dissolved. Digest for a few minutes, cool, filter through a paper of loose texture, and wash the flask and paper a few times with warm water. To the filtrate and washings in a 300-ml Erlenmeyer flask add 5 ml of 85-percent phosphoric acid and 0.5 to 1.0 g of potassium periodate. Boil for 10 minutes, cool, dilute if necessary, and determine the amount of manganese in the solution by comparing the color with that obtained by dissolving and similarly treating a material of known manganese content. It is obvious that it is desirable, but not necessary, to select a standard whose manganese content is approximately that of the unknown. The National Bureau of Standards Standard Samples of Phosphate Rocks 56, 56a, and 120 are satisfactory standards for materials containing up to 0.5 percent of MnO.

No significant quantity of manganese remains in the insoluble residue if the National Bureau of Standards Standard Samples 56, 56a, and 120 are decomposed by this procedure.

11. DETERMINATION OF THE ALKALIES

Determine the alkalies by the J. Lawrence Smith method.[33]

12. DETERMINATION OF SULFUR

Sulfur is seldom determined. Detailed directions are therefore not given.

Total sulfur was determined by (1) digesting a 2-g sample with concentrated nitric acid containing bromine; (2) evaporating with hydrochloric acid to remove the nitric acid; (3) digesting the residue with hydrochloric acid (1+1) and filtering; (4) adjusting the acidity to 1 to 2 ml of hydrochloric acid in 100 ml of solution; (5) precipitating the sulfate by adding barium chloride; (6) filtering and washing; (7) igniting the barium sulfate; and (8) correcting for sulfate obtained from reagents. No sulfur was found in the siliceous residue resulting from the evaporation with hydrochloric acid.

[33] W. F. Hillebrand and G. E. F. Lundell, Applied Inorganic Analysis, p. 786 (J. Wiley & Sons, New York N. Y., 1929 ed.); G. E. F. Lundell and J. I. Hoffman, Outlines of Methods of Chemical Analysis, p. 73 and 185 (J. Wiley & Sons, New York, N. Y., 1938 ed.).

The percentages of total sulfur (as SO_3) found in Phosphate Rocks 56a and 120 were 0.73 and 0.32, respectively.

Pyritic sulfur was determined by transferring a 5-g sample to an Erlenmeyer flask, adding 40 ml of diluted hydrochloric acid (1+1), boiling for 5 minutes, filtering, washing the residue thoroughly with diluted hydrochloric acid (1+99), discarding the filtrate and washings, and then treating the residue as was done for *total sulfur*.

No significant amount of pyritic sulfur (less than 0.005 percent of S) was found in Phosphate Rock 56a and only 0.01 percent in Phosphate Rock 120.

Soluble sulfide sulfur, that is, sulfide sulfur that can be evolved by treatment with hydrochloric acid, was determined by the method that is used for this determination in cements.[34] The sample is treated with hydrochloric acid and stannous chloride in a suitable flask, and the evolved gases are passed into an ammoniacal solution of zinc sulfate. The stannous chloride prevents oxidation of sulfides by the oxidized constituents of the rock during the evolution. The sulfide which is absorbed in the ammoniacal zinc sulfate is determined by acidifying the solution with hydrochloric acid, and titrating with a standard solution of iodine.

Only 0.01 percent of sulfide sulfur (as S) was found in Phosphate Rock 56a and 0.05 percent in Phosphate Rock 120. The foregoing results indicate that most of the sulfur in these two rocks is present as soluble sulfates.

13. SPECTROCHEMICAL ANALYSIS (BORON)

(a) QUALITATIVE EXAMINATION

Spectrochemical analyses of the two samples were made by B. F. Scribner of the spectroscopy section of this Bureau. The arc spectra were photographed in the region 2470 to 3300 A, using carbon electrodes, and in the region 3200 to 4600 A, using copper electrodes. The spectra were examined for the sensitive lines of Ag, Al, As, Au, B, Ba, Be, Bi, Ca, Cb, Cd, Ce, Co, Cr, Cu, Fe, Ga, Ge, Hf, Hg, In, Ir, K, Li, Mg, Mn, Mo, Na, Ni, Os, Pd, Pb, Pt, Rh, Ru, Sb, Sc, Si, Sn, Sr, Ta, Th, Ti, Tl, U, V, W, Y, Zn, and Zr. No special effort was made to detect such elements as fluorine or sulfur, since other tests had already shown their presence. The elements found are as follows:

Tennessee Phosphate Rock 56a.

Major constituents: Ca, Al, Fe, Mg, Si.
Minor constituents: Mn, Na, K, Cr, Sr, Cu, Ti.
Traces ..... Pb, B, Sn, Ni.

Florida Phosphate Rock 120.

Major constituents: Ca, Al, Fe, Mg. Si.
Minor constituents: Mn, Na, K, Cr, Sr, Cu, Ti, Mo, Ni, V.
Traces ..... Pb, Sn, B.

(b) QUANTITATIVE DETERMINATION OF BORON

Boron is the only constituent that was quantitatively determined by the spectrochemical method. This was done by comparison of the spectra of the two samples with the spectra of a set of standard mixtures photographed under comparable conditions. The standards

[34] H. A. Bright, J. Research NBS 18, 137 (1937) RP968.

were prepared to give a graded series of known concentrations of boron, using as a base a sample of tricalcium phosphate practically free from boron. The sensitivity of the test for boron is approximately 0.0001 percent. The precision of the method decreases as the concentration decreases, being within ±10 percent of the amount present for concentrations above 0.005 percent of boron and within ±20 percent below 0.005 percent. The boron reported as B_2O_3 was as follows:

Tennessee Phosphate Rock 56a: 0.005 percent of B_2O_3.
Florida Phosphate Rock 120: Less than 0.001 percent of B_2O_3.

It is interesting to note that the spectrochemical tests indicated higher percentages of manganese, copper, and boron in the Tennessee Rock than in the Florida Rock, and higher percentages of nickel, molybdenum, vanadium, tin, and chromium in the Florida than in the Tennessee Rock. This is in agreement with the following percentages of these constituents found by chemical methods.[35]

Tennessee Rock 56a: MnO, 0.18; CuO, 0.002; B_2O_3, 0.005; NiO, 0.0005; MoO_3, 0.0002; V_2O_5, none found; SnO_2, 0.001; Cr_2O_3, 0.001.

Florida Rock 120: MnO, 0.027; CuO, 0.001; B_2O_3, 0.002; NiO, 0.003; MoO_3, 0.002; V_2O_5, 0.015; SnO_2, 0.002; Cr_2O_3, 0.01.

The ability to distinguish between such small percentages suggests the possibility of determining these and other minor constituents quickly and accurately by spectrochemical methods, provided that suitable standards are available.

IV. SUMMARY OF THE RESULTS OBTAINED IN THE COOPERATIVE ANALYSIS OF PHOSPHATE ROCKS

Tables 2 and 3 give a summary of the results obtained in the analysis of the National Bureau of Standards Phosphate Rocks 56a and 120. The analysts mentioned in this tabulation have rendered valuable assistance in this work, and the authors express their deep appreciation to them.

[35] The boron was determined chemically by Lewis F. Rader, Jr., and W. L. Hill, Fertilizer Research Division, Bureau of Chemistry and Soils, U. S. Department of Agriculture, by the use of a method involving distillation and titration. The method will be published in the Journal of Agricultural Research. (Now in press.)

TABLE 2.—*Results obtained in the cooperative analysis of the National Bureau of Standards Standard Sample of Phosphate Rock 56a*

[All results are based on a sample dried for 1 hour at 105° C.[a]]

Analyst[a] (by number)	P_2O_5	Total Fe_2O_3	Total Al_2O_3	Soluble Fe_2O_3	Soluble Al_2O_3	CaO	MgO	F	SiO_2	MnO	Na_2O	K_2O	Total sulfur as SO_3	TiO_2
	%	%	%	%	%	%	%	%	%	%	%	%	%	%
1	[b]32.90 [c]32.88 [c]32.96	2.14	2.03	2.14	1.77	45.62	0.14	3.49	11.02	0.18	0.30	0.25	0.73	0.09
2	[d]33.20			4.20		45.36	.18							
3	[b]32.85	2.24	2.12			45.49	.10		11.50					
4	[c]33.15			2.11	1.88									
5	[c]33.26			2.17	1.90	45.56								
6	[d]33.12			2.11	1.87	45.48	.12							
7	[f]32.82	2.14	1.98			45.48	.12	3.53	10.92	.18	.24	.31	.73	.08
8	[b]32.90 [d]32.83					45.85	.18							
9	[d]33.17	2.23	2.04	2.12	1.94	45.55	.13	3.66	10.60	.19	.31	.29	.72	.07
10	[c]33.05	2.16	1.93				.12							
Averages	[g]33.01	2.18	2.02	2.13	1.87	45.55	.14	3.56	[h]11.01	.18	.28	.28	.73	.08

[a] Seven analysts reported an average of 0.53% of moisture, obtained by drying for 1 hour at 105° C. The results varied from 0.36 to 0.64%. Not much significance is to be attached to these values because the moisture content changes with atmospheric conditions.

[b] Gravimetric.—Precipitation with molybdate followed by two precipitations with magnesia mixture (J. Assn. Official Agr. Chem 8, 195 (1924).

[c] Gravimetric.—Two precipitations with magnesia mixture without preliminary precipitation with molybdate (J. Research NBS **19**, 59 (1937) RP1010).

[d] AOAC, volumetric.

[e] AOAC, gravimetric.

[f] Gravimetric.—Single precipitation with magnesia mixture after molybdate precipitation (J. Assn. Official Agr. Chem. 8, 194 (1924)).

[g] Special work at the National Bureau of Standards, and a careful consideration of all the methods employed indicate that 32.90 should be regarded as the most probable percentage of P_2O_5 in this sample.

[h] Special work at the National Bureau of Standards indicates that an uncertainty of at least ±0.2% should be assigned to this value.

Analyst 1 also found 0.002% of CuO, 0.0005% of NiO, 0.0002% of MoO_3, 0.001% of SnO_2, 0.001% of Cr_2O_3, and no V_2O_5 in a 10-g sample.

Analyst 7 also reported 0.005% of B_2O_3. B. F. Scribner of the spectroscopy section of the National Bureau of Standards found 0.005% of B_2O_3, spectrochemically. Analyst 9 also reported 1.56% of CO_2, 0.26% of organic matter, 0.0021% of As_2O_3, and 0.39% of combined water.

*ANALYSTS, BY NUMBER, AS LISTED IN TABLE 2

1. James I. Hoffman, National Bureau of Standards, Washington, D. C.
2. E. W. Magruder, Chief Chemist, and W. A. Ryder, F. S. Royster Guano Co., Norfolk, Va.
3. W. Catesby Jones, Chief Chemist, John H. Elder, and James R. Lindsay, Commonwealth of Virginia, Department of Agriculture and Immigration, Richmond, Va.
4. C. A. Butt, Chief Chemist, and C. M. Cartledge, International Agricultural Corporation, East Point, Ga.
5. W. E. Dickinson, Chief Chemist, International Agricultural Corporation, Norfolk, Va.
6. P. McG. Shuey, Shuey & Co., Savannah, Ga.
7. W. L. Hill, L. F. Rader, Jr., T. H. Tremearne, H. L. Marshall, and D. S. Reynolds, phosphate section, Fertilizer Research Division, Bureau of Chemistry and Soils, U. S. Department of Agriculture, Washington, D. C.
8. John B. Smith, Chief Chemist, W. L. Adams, and E. J. Deszyck, Rhode Island State College Agricultural Experiment Station, Kingston, R. I.
9. Egbert Janes, Chief Chemist, and H. H. Edwards, International Agricultural Corporation, Mulberry, Fla.
10. L. E. Dupont, Chief Chemist, International Agricultural Corporation, Wales, Tenn.

TABLE 3.—*Results obtained in the cooperative analysis of the National Bureau of Standards Standard Sample of Phosphate Rock 120*

[All results are based on a sample dried for 1 hour at 105° C.[a]]

Analyst* (by number)	P_2O_5	Total Fe_2O_3	Total Al_2O_3	Soluble Fe_2O_3	Soluble Al_2O_3	CaO	MgO	F	SiO_2	MnO	Na_2O	K_2O	Total sulfur as SO_3	TiO_2
	%	%	%	%	%	%	%	%	%	%	%	%	%	%
1	[b] 35.17 [c] 35.17 [e] 35.38	0.87	0.85	0.87	0.75	49.67	0.13	3.74	7.70	0.027	0.14	0.08	0.32	0.06
2	[d] 35.30			1.40		49.70								
3	[b] 35.24	.90	.89			49.32	.13							
4	[c] 35.46			.92	.73									
5	[c] 35.40			.92	.84	49.80								
6	[d] 35.43			.85	.82	49.55								
7	[f] 35.25	.89	.82			49.66	.13	3.71	7.47	.026	.12	.09	.32	.06
8	[b] 35.16 [d] 35.50			1.58		49.80	.18							
9	[d] 35.43	.87	.89	.86	.84	49.44	.15	3.82	7.03	.045	.17	.11	.33	.06
10	[c] 35.37	.92	.92				.09							
Averages	[g] 35.33	.89	.87	.89	.80	49.62	.14	3.76	[h] 7.40	.033	.14	.09	.32	.07

[a] Seven analysts reported an average of 0.53% of moisture, obtained by drying for 1 hour at 105° C. The results varied from 0.43 to 0.66%. Not much significance should be attached to these values, because the moisture content changes with atmospheric conditions.

[b] Gravimetric.—Precipitation with molybdate followed by two precipitations with magnesia mixture (J. Assn. Official Agr. Chem. 8, 195 (1924)).

[c] Gravimetric.—Two precipitations with magnesia mixture without preliminary precipitation with molybdate (J. Research NBS 19, 59 (1937) RP1010).

[d] AOAC, volumetric.

[e] AOAC, gravimetric.

[f] Gravimetric.—Single precipitation with magnesia mixture after molybdate precipitation (J. Assn. Official Agr. Chem. 8, 194 (1924)).

[g] Special work at the National Bureau of Standards, and a careful consideration of all the methods employed indicate that 35.20 should be regarded as the most probable percentage of P_2O_5 in this sample.

[h] Special work at the National Bureau of Standards indicates that 7.6 represents more nearly the true silica content of this material, and that an uncertainty of at least ±0.2 percent should be assigned to this value.

Analyst 1 also found 0.061% of CuO, 0.003% of NiO, 0.002% of MoO_3, 0.015% of V_2O_5, 0.002% of SnO_2 and 0.01% of Cr_2O_3. Analyst 7 also reported 0.001% of B_2O_3. B. F. Scribner of the spectroscopy section of the National Bureau of Standards found (0.001% of B_2O_3, spectrochemically. Analyst 9 also reported 1.96% of CO_2, 0.32% of organic matter, 0.0018% of As_2O_3, and 0.12% of combined water.

*ANALYSTS, BY NUMBER, AS LISTED IN TABLE 3

1. James I. Hoffman, National Bureau of Standards, Washington, D. C.
2. E. W. Magruder, Chief Chemist, and W. A. Ryder, F. S. Royster Guano Co., Norfolk, Va.
3. W. Catesby Jones, Chief Chemist, John H. Elder, and James R. Lindsay, Commonwealth of Virginia, Department of Agriculture and Immigration, Richmond, Va.
4. C. A. Butt, Chief Chemist, and C. M. Cartledge, International Agricultural Corporation, East Point, Ga.
5. W. E. Dickinson, Chief Chemist, International Agricultural Corporation, Norfolk, Va.
6. P. McG. Shuey, Shuey & Co., Savannah, Ga.
7. W. L. Hill, L. F. Rader, Jr., T. H. Tremearne, H. L. Marshall, and D. S. Reynolds, phosphate section, Fertilizer Research Division, Bureau of Chemistry and Soils, U. S. Department of Agriculture, Washington, D. C.
8. John B. Smith, Chief Chemist, W. L. Adams, and E. J. Deszyck, Rhode Island State College Agricultural Experiment Station, Kingston, R. I.
9. Egbert Janes, Chief Chemist, and H. H. Edwards, International Agricultural Corporation, Mulberry, Fla.
10. L. E. Dupont, Chief Chemist, International Agricultural Corporation, Wales, Tenn.

WASHINGTON, February 18, 1938.

U. S. Department of Commerce National Bureau of Standards

RESEARCH PAPER RP1096

Part of Journal of Research of the National Bureau of Standards, Volume 20, May 1938

MAXIMUM USABLE FREQUENCIES FOR RADIO SKY-WAVE TRANSMISSION, 1933 TO 1937[1]

By Theodore R. Gilliland, Samuel S. Kirby, Newbern Smith, and Stephen E. Reymer

ABSTRACT

Graphs are presented to indicate the maximum usable frequencies for sky-wave transmission from June 1933 to December 1937. The graphs are given for March, June, and December to show equinoctial, summer, and winter conditions for each year. The factors which must be considered in deriving these graphs from vertical-incidence ionosphere measurements are outlined briefly. The principal factors are Snell's law, variation of virtual height of the ionosphere with frequency, the curvature of the ionosphere, and the effect of the earth's magnetic field.

The method of applying these graphs to simple and complex transmission paths is indicated.

The effects of sporadic *E* reflections, absorption, and scattered reflections are discussed briefly.

It is pointed out that the graphs and the ionosphere data from which they were derived may be used to estimate future diurnal, seasonal, and long-time variations of maximum usable frequencies.

CONTENTS

	Page
I. Introduction	627
II. Relation of vertical to oblique-incidence transmission	628
III. Transmission path	631
IV. Graphs of maximum usable frequencies	637
V. Other transmission characteristics	638
1. Sporadic *E*	638
2. Absorption	638
3. Scattered reflections	639
VI. Conclusions	639

I. INTRODUCTION

The graphs of maximum usable frequencies for radio sky-wave transmission presented here were prepared from the vertical-incidence ionosphere measurements made by the National Bureau of Standards at Washington.[2] These graphs, for any particular month, are derived from the average condition of the ionosphere for that month. The graphs give results representative of the winter, summer, and equinoctial periods from June 1933 to December 1937, inclusive.

[1] A preliminary version of this paper was presented as paper C6 of the meeting in London in November 1937 of the special committee on radio-wave propagation.

[2] Theodore R. Gilliland, Samuel S. Kirby, Newbern Smith, and Stephen E. Reymer, *Characteristics of the ionosphere and their application to radio transmission.* J. Research NBS 18, 645 (1937) RP1001; Proc. Inst. Radio Engrs. 25, 823 (1937), and a series of monthly reports beginning in Proc. Inst. Radio Engrs. 25, 1174 (September 1937).

The maximum usable frequency for any distance is defined as the highest frequency which can be used for radio sky-wave transmission over the given distance. Waves of frequencies higher than this penetrate through the ionosphere and are not returned to the earth; waves of lower frequencies are reflected and may be used for transmission over this distance. Graphs of maximum usable frequencies in terms of distance also give skip distances as a function of frequency. The maximum usable frequencies give more directly than skip distances information usually desired in connection with radio transmission; i. e., determination of the maximum frequency which can be used over a given distance is of more general value to an engineer than the minimum distance over which communication can be had on a given frequency.

II. RELATION OF VERTICAL TO OBLIQUE-INCIDENCE TRANSMISSION

Radio waves incident obliquely upon the layers of the ionosphere are more easily reflected than those incident vertically, that is, they can be reflected from regions of smaller ionization density. In general, for a given frequency of the transmitted wave, the larger the angle of incidence, the less is the ionization density required for reflection. Thus, if a given layer will reflect waves up to a certain frequency at vertical incidence, it will reflect waves of considerably higher frequencies at oblique incidence.

The angle of incidence is the angle between the ray and the normal to the lower boundary of the ionosphere at the point where the ray enters the ionosphere. The angle of incidence should not be confused with the angle of departure, which is the angle above the horizontal at which the ray is projected from the transmitting station. Although, in general, a transmitting station may radiate energy at all angles above the horizontal, only certain ray-paths, corresponding to a few definite angles of departure, are useful for transmission over a given distance at a given time. At vertical incidence the angle of incidence is zero, and increases for oblique incidence.

The angle of incidence depends on (1) the distance of transmission for one reflection from the ionosphere, and (2) the height of the layer. Given these two quantities, therefore, the angle of incidence may be calculated. The maximum usable frequency is given roughly, from this angle and the vertical-incidence critical frequency, by the following relation, known as the "secant law":

$$f' = f_c \sec \theta_1$$

where

f' = maximum usable frequency,
f_c = critical frequency or highest frequency reflected at vertical incidence from a given layer, and
θ_1 = angle of incidence.

The given distance will be within the "skip-zone" for all higher frequencies.

The secant law does not take several important factors into account. The first and most important of these is the fact that the virtual

height of a given layer of the ionosphere increases with frequency, especially near the critical frequency. As a result, it is difficult to choose the proper height to be used in calculating the angle of incidence for a given distance. A method whereby, for a flat ionosphere, this difficulty may be overcome has been described by Smith.[3]

The second factor which must be considered is the curvature of the ionosphere. This introduces another modification in the calculation of the angle of incidence for a given distance and a given height of reflection. This results in a higher maximum usable frequency over a given distance than would be calculated on the basis of a flat ionosphere.

Still another factor that must be taken into account is the effect of the earth's magnetic field. In the presence of the earth's field a radio wave in the ionosphere is split into two components known as the

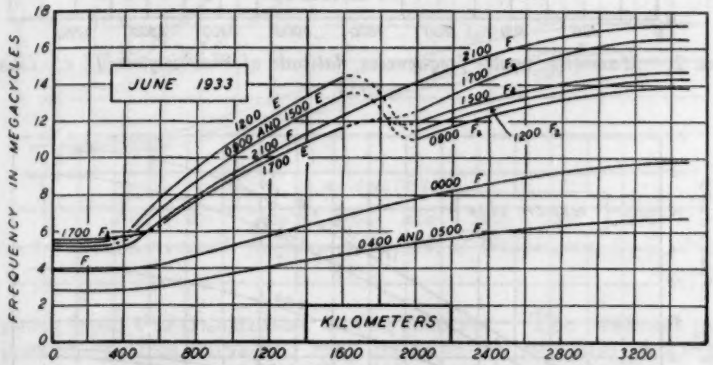

FIGURE 1.—*Maximum usable frequencies, latitude of Washington, D. C., June 1933.*

ordinary ray and the extraordinary ray. These components are reflected from different levels in the ionosphere, and consequently have different critical frequencies. At Washington, the vertical-incidence critical frequency for the extraordinary ray is about 800 kc/s higher than for the ordinary ray, for frequencies in the neighborhood of 5,000 kc/s, and the separation is greater for lower frequencies. At oblique incidence the effect of the earth's magnetic field complicates the calculation of maximum usable frequencies. The maximum usable frequency for the extraordinary ray is always greater than for the ordinary ray. Except for short distances, the difference is not great, and decreases with increasing frequency and distance. For practical communication problems it is sufficiently accurate to make the calculations for the ordinary ray.

Methods of obtaining maximum usable frequencies, taking into account the earth's magnetic field and the curvature of the ionosphere, have been presented by Smith.[4] These methods have been used in preparing figures 1 to 14.

[3] Newbern Smith, *Extension of normal-incidence ionosphere measurements to oblique-incidence radio transmission.* J. Research NBS **19**, 89 (1937) RP1013.

[4] Newbern Smith, *The application of vertical-incidence ionosphere measurements to oblique-incidence radio transmission.* J. Research NBS **20**, 683 (1938) RP1100; Proc. Inst. Radio Engrs.

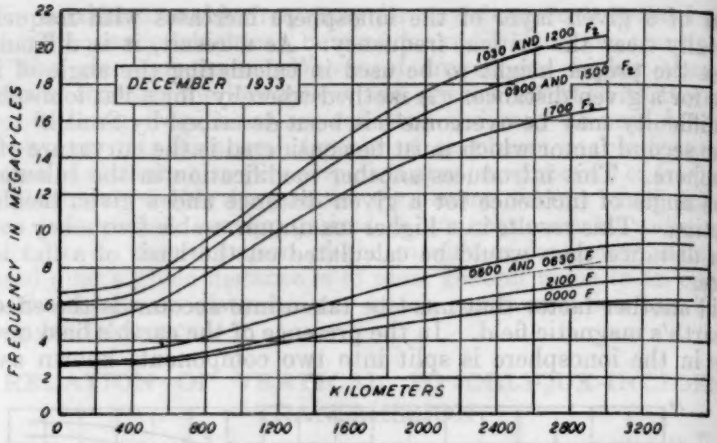

FIGURE 2.—*Maximum usable frequencies, latitude of Washington, D. C., December 1933.*

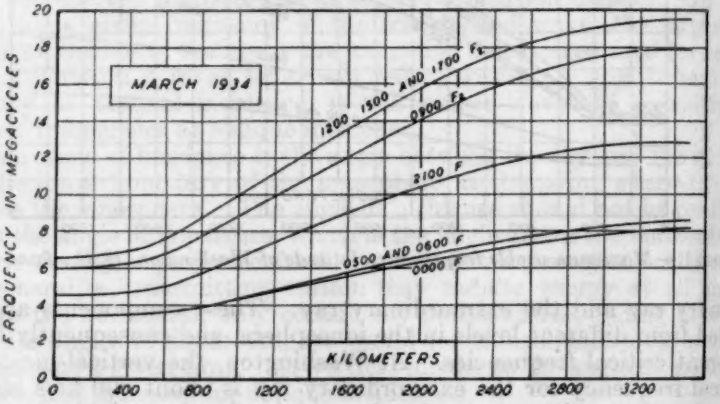

FIGURE 3.—*Maximum usable frequencies, latitude of Washington, D. C., March 1934.*

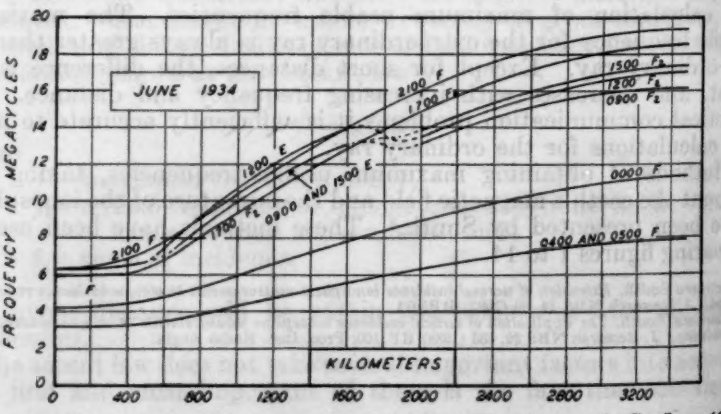

FIGURE 4.—*Maximum usable frequencies, latitude of Washington, D. C., June 1934.*

III. TRANSMISSION PATH

The geographical part of the ionosphere which controls long-distance high-frequency radio transmission is that part traversed by the wave

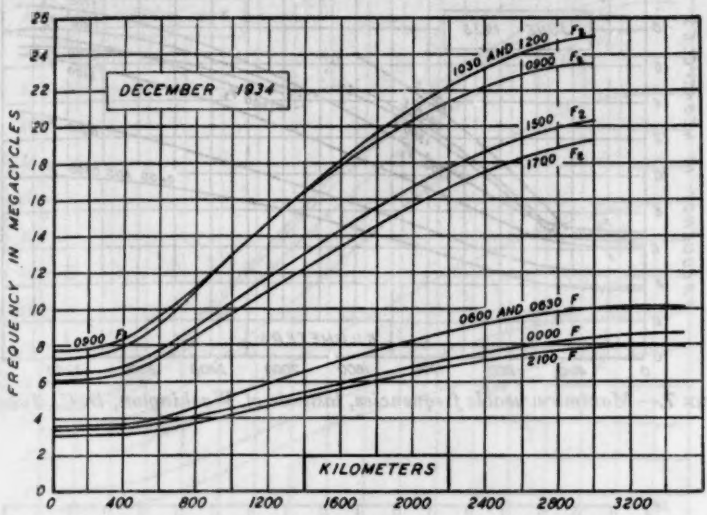

FIGURE 5.—*Maximum usable frequencies, latitude of Washington, D. C., December 1934.*

in passing from the transmitter to the receiver. The neareast part of the ionosphere thus traversed may be as much as 1,000 to 2,000 km from the transmitter, and a similar distance from the receiver. Iono-

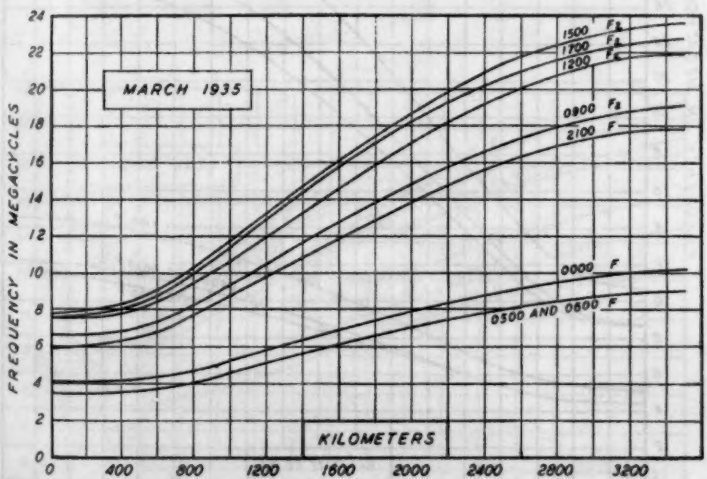

FIGURE 6.—*Maximum usable frequencies, latitude of Washington, D. C. March 1935.*

sphere conditions at this point may be considered to be the same as conditions at the transmitter or receiver, at the same local time, provided no great differences of latitude exist. Consequently, depending

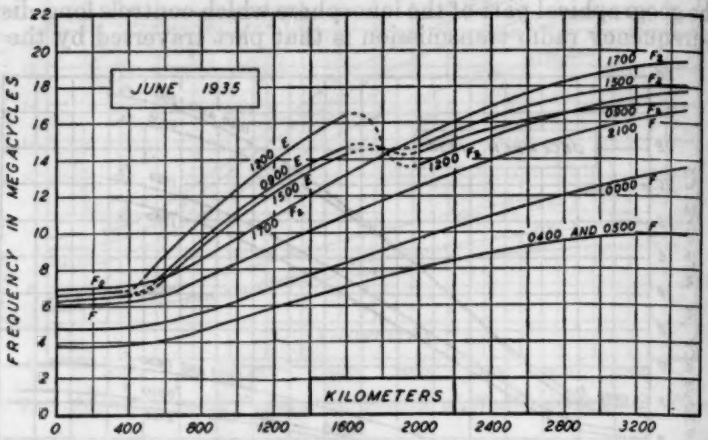

FIGURE 7.—*Maximum usable frequencies, latitude of Washington, D. C., June 1935.*

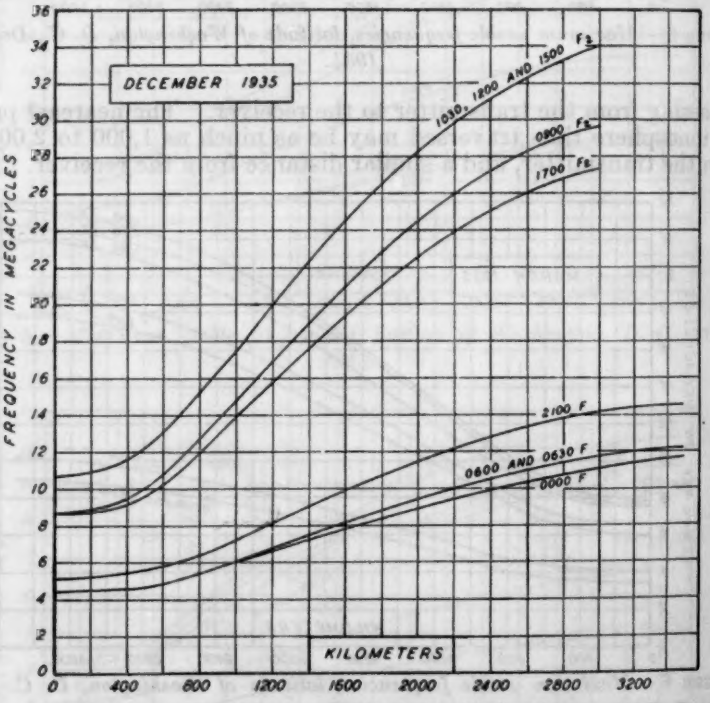

FIGURE 8.—*Maximum usable frequencies, latitude of Washington, D. C., December 1935.*

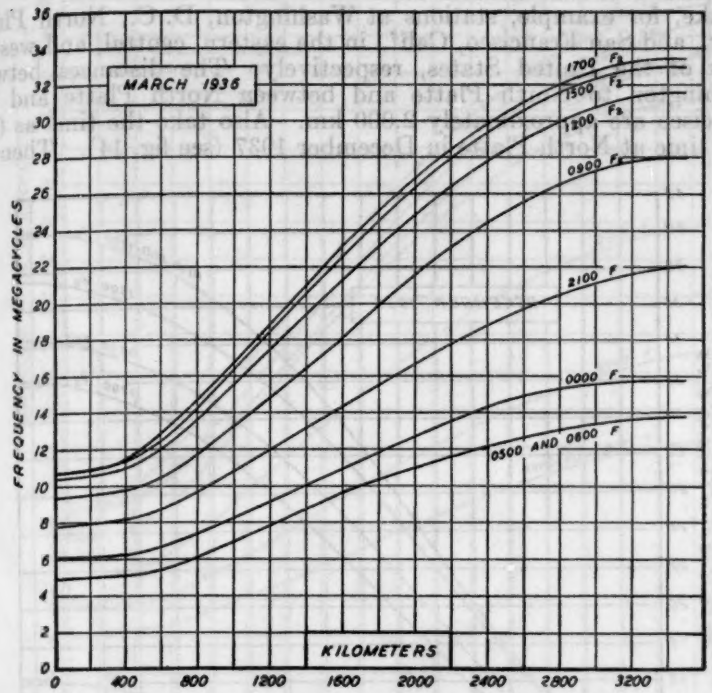

FIGURE 9.—*Maximum usable frequencies, latitude of Washington, D. C., March 1936.*

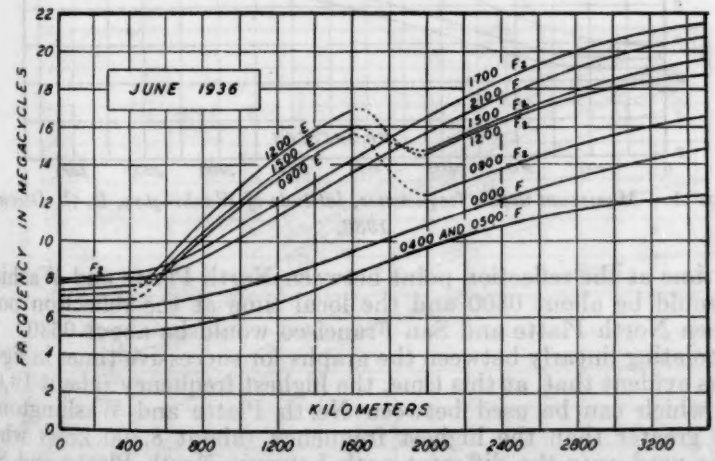

FIGURE 10.—*Maximum usable frequencies, latitude of Washington, D. C., June 1936.*

on the time of day, different frequencies might be necessary for transmission in different directions.

Take, for example, stations at Washington, D. C., North Platte, Nebr., and San Francisco, Calif., in the eastern, central, and western parts of the United States, respectively. The distances between Washington to North Platte and between North Platte and San Francisco are approximately 2,000 km. Also take the time as 0715 local time at North Platte in December 1937 (see fig. 14). Then the

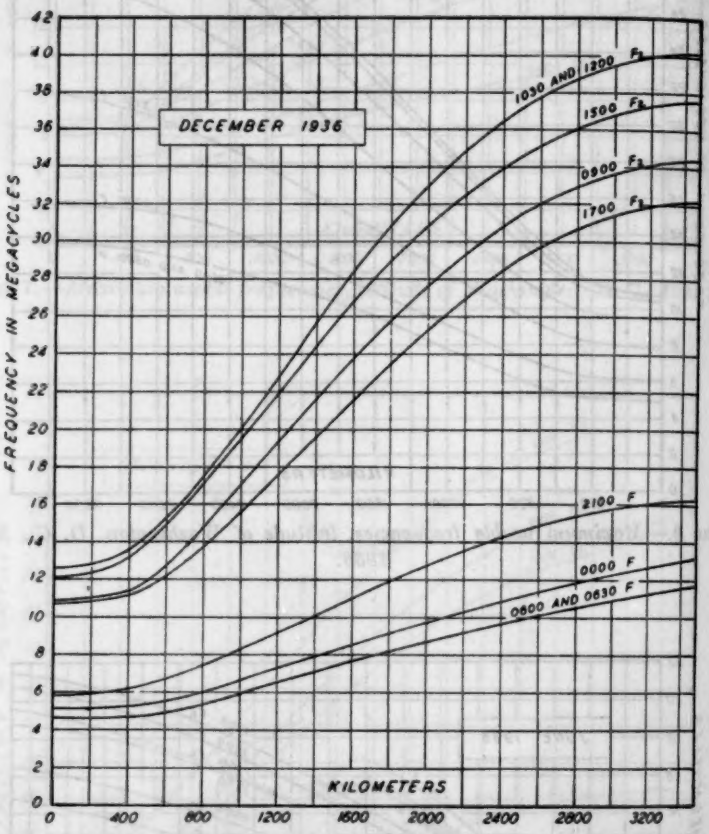

FIGURE 11.—*Maximum usable frequencies, latitude of Washington, D. C., December 1936.*

local time at the reflection point between North Platte and Washington would be about 0800 and the local time at the reflection point between North Platte and San Francisco would be about 0630. By interpolating linearly between the graphs for successive times in figure 14 it is evident that, at this time, the highest frequency (about 19,000 kc/s) which can be used between North Platte and Washington is much greater than the highest frequency (about 8,300 kc/s) which can be used over the different path between North Platte and San Francisco. This does not mean, however, that different frequencies should be used for two-way communication over the same path, such as North Platte to Washington and Washington to North Platte,

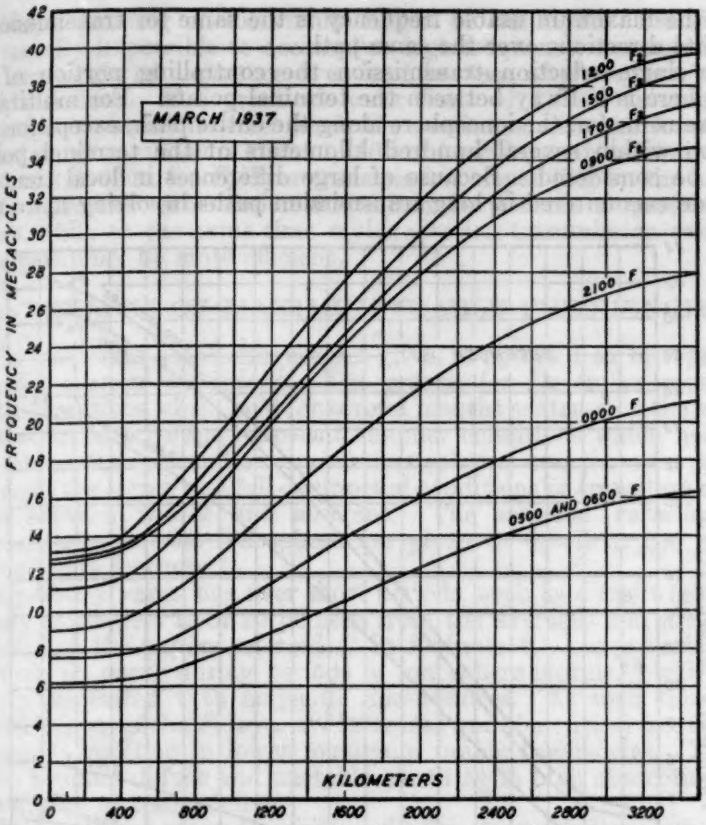

FIGURE 12.—*Maximum usable frequencies, latitude of Washington, D. C., March 1937.*

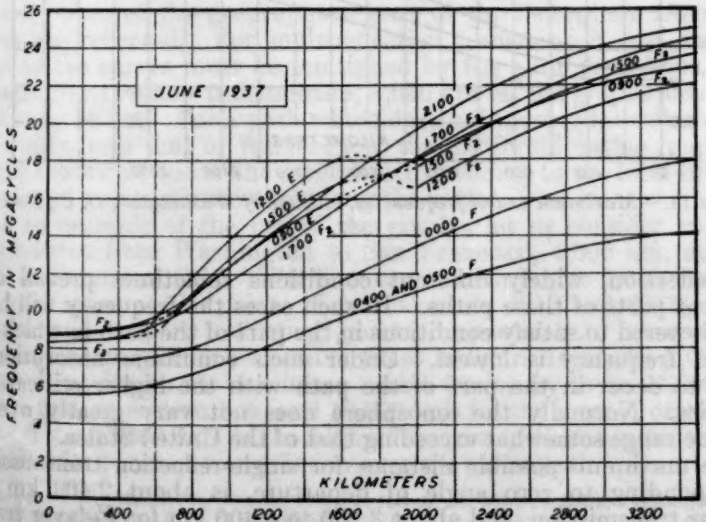

FIGURE 13.—*Maximum usable frequencies, latitude of Washington, D. C., June 1937.*

since the maximum usable frequency is the same for transmission in opposite directions over the same path.

For single-reflection transmission the controlling portion of the ionosphere is halfway between the terminal points. For multireflection transmission the ionosphere along the entire path, except for that portion within several hundred kilometers of the terminal points, must be considered. Because of large differences in local time and latitude encountered in long transmission paths involving more than

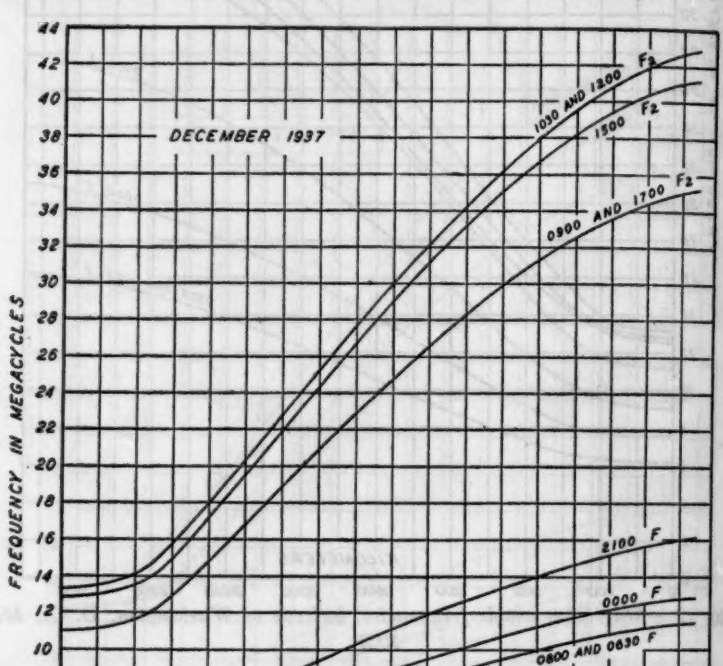

FIGURE 14.—*Maximum usable frequencies, latitude of Washington, D. C., December 1937.*

one reflection, widely different conditions sometimes prevail over different parts of these paths. In such cases the frequency will have to be lowered to satisfy conditions in the part of the path in which the critical frequency is lowest. Under such conditions absorption is likely to occur in the part of the path with the higher critical frequencies. Normally the ionosphere does not vary greatly over a latitude range somewhat exceeding that of the United States.

The maximum possible distance for single-reflection transmission, corresponding to zero angle of departure, is about 2,400 km for *E*-layer transmission, and about 3,500 to 4,400 km for F_2-layer trans-

mission, depending on the virtual height of the layer. Practically, it is usually impossible to accomplish high-frequency transmission at this zero angle of departure over land because of absorption at the earth's surface. If a practical lower limit of 3½° is assumed for the angle of departure over land, the maximum distance for single-reflection transmission is about 1,700 km for *E*-layer transmission and 2,800 to 3,600 km for F_2-layer transmission, depending on the height. Single-reflection transmission may often be possible at greater distances, while at the same time multireflection transmission over the same path may be more efficient.

IV. GRAPHS OF MAXIMUM USABLE FREQUENCIES

The maximum usable frequencies given in figures 1 to 14 represent monthly average conditions. The graphs for December represent winter conditions which hold for several months centered on the winter solstice, those for June represent summer conditions which hold for several months centered on the summer solstice, and those for March represent the spring and fall equinoctial conditions or transition conditions between winter and summer. The seasonal variations in characteristics of the ionosphere are given in detail in the papers referred to in footnote 1.

Day-to-day variations over short periods, such as a few weeks, are usually small (less than 10 percent from the average) and are given in detail in the papers referred to in footnote 1. Large variations, however, do occur during periods of ionosphere storms,[5,6] which are usually associated with magnetic disturbances. At such times the virtual heights of the F_2 layer are increased and the critical frequencies decreased, resulting in lower maximum usable frequencies. The F_2 region becomes diffuse and unstable, resulting in high absorption and poor quality of transmission.

The graphs are given for single-reflection transmission at the latitude of Washington. Linear interpolations may be made between graphs for successive times. The conditions given in the curves are for local time at the geographical part of the ionosphere where the waves are reflected. For multireflection transmission, the distance scale on the curves must be multiplied by the number of hops. For example, for two-hop transmission, 3,000 km on the graphs should be read as 6,000 km. For a path which does not involve latitudes differing widely from that of Washington, the maximum usable frequency is then the lowest one of the several corresponding to the local times at the several points of reflection along the path.

As an example of the use of the graphs, let us consider two-hop transmission from Washington to San Francisco, 4,000 km, at 0900 EST in December 1937. The distance of each hop is 2,000 km, and the local times at the points of reflection are 0815 and 0645, at the eastern and western reflecting points, respectively. Interpolating between the graphs for successive times in figure 14 at the 2,000-km distance, we obtain the maximum usable frequency to be 21,000 kc/s for the first, or eastern hop, and 10,000 kc/s for the second, or western hop. Thus 10,000 kc/s is the highest frequency that can be used at this time for two-hop transmission over the given path.

[5] Samuel S. Kirby, Theodore R. Gilliland, Elbert B. Judson, and Newbern Smith, *The ionosphere, sunspots, and magnetic storms.* Phys. Rev. 48, 849 (1935).
[6] Samuel S. Kirby, Theodore R. Gilliland, Newbern Smith, and Stephen E. Reymer, *The ionosphere solar eclipse, and magnetic storm.* Phys. Rev. 50, 258 (1936).

The graphs for June show that both the E and F layers are effective in determining the maximum usable frequencies. For example, at noon the F_2 layer will be effective out to a short distance, say 500 km, because of its higher critical frequency; then the E layer will be effective out to 1,600 km because of its lower height and resulting larger angles of incidence. Beyond about 1,600 km the intensity of single-hop E-layer transmission decreases because of the necessarily small angles of departure at the transmitting station. The maximum usable frequency is then that which will be transmitted by two-hop E-, or single-hop F_2-layer propagation. Either of these conditions gives a maximum usable frequency lower than does the single-hop E-layer transmission at about 1,600 km. Of the two conditions, the F_2 layer gives the higher maximum usable frequency for average conditions at Washington as indicated on the graphs. A similar decrease of maximum usable frequency occurs when the F-layer transmission must change from one-hop to two-hop propagation at about 3,500 km.

V. OTHER TRANSMISSION CHARACTERISTICS

1. SPORADIC E

Reflections from the E region are often found at frequencies considerably in excess of the maximum daytime critical frequency for the E layer. These differ in character from the regular refraction phenomena of the normal E layer and occur at all seasons, but they are more prevalent during the summer months in Washington, sometimes persisting for several hours. Sporadic E reflections seem to be of the nature of reflections from a sharp boundary, as suggested by Kirby and Judson,[7] rather than of regular refraction from a region of intense ionization. Because of the sporadic nature of these reflections their effect has not been included in the graphs. Sporadic E, however, accounts for good transmission at higher frequencies than those indicated by the graphs for a small percentage of the time and at irregular intervals. Reports of long-distance transmission at frequencies as high as 56 megacycles, which occur mostly during the summer, appear to be by way of the sporadic E layer.

2. ABSORPTION

In contrast to the sharply defined maximum usable frequencies shown by the present graphs, there are less well defined minimum usable frequencies for practical high-frequency sky-wave transmission for various distances. These lower frequency limits are determined by absorption. The absorption varies in general with time of day, season, frequency, and length of path. Absorption occurs mainly in the lower ionosphere, that is, in the E layer and below. The absorption is greater during the summer day than during the winter day. It is greater for the lower high frequencies, that is, those frequencies which are close to or below the maximum usable frequency for the E layer for a given distance. It is usually greater during the day than during the night, especially for these lower high frequencies. A high-frequency wave at large angles of incidence, corresponding to long distances, is absorbed like a much lower frequency wave at small angles of incidence, corresponding to short distances.

[7] Samuel S. Kirby and Elbert B. Judson, *Recent studies of the ionosphere*. J. Research NBS 14, 409 (1935); Proc. Inst. Radio Engrs. 23, 733 (1935).

3. SCATTERED REFLECTIONS

Usually, complex scattered reflections are observed at frequencies considerably higher than the F_2-critical frequencies.[8] These reflections provide weak, poor-quality transmissions much above the maximum usable frequencies for F-layer transmissions over distances of several hundred kilometers.

VI. CONCLUSIONS

For practical applications the principal value of these graphs is to estimate transmission conditions in the future either diurnally, seasonally, or over longer periods. The ionosphere data of reference 1, from which these graphs were derived, indicate that the diurnal and seasonal characteristics are regular and may in general be predicted. In addition, there is a large variation of ionization densities with the 11-year sunspot cycle, as indicated by the increase of maximum usable frequencies from 1933 to 1937. At the end of the year 1937 the sunspot cycle was near a maximum and is expected to return to a minimum about 1944. In a rough way these graphs may be used for corresponding times on the descending part of the sunspot cycle. Current ionosphere data are given by the National Bureau of Standards in its weekly ionosphere bulletins broadcast from station WWV each Wednesday, and in reports on the characteristics of the ionosphere at Washington, D. C., published each month in the Proceedings of the Institute of Radio Engineers.

WASHINGTON, February 11, 1938.

[8] Samuel S. Kirby and Elbert B. Judson, *Recent studies of the ionosphere.* J. Research NBS 14, 469 (1935); Proc. Inst. Radio Engrs. 23, 733 (1935).

U. S. DEPARTMENT OF COMMERCE NATIONAL BUREAU OF STANDARDS

RESEARCH PAPER RP1097

Part of Journal of Research of the National Bureau of Standards, Volume 20, May 1938

BOILING POINTS OF BENZENE, ETHYLENE CHLORIDE, *n*-HEPTANE, AND 2,2,4-TRIMETHYLPENTANE OVER THE RANGE 660- TO 860-MM PRESSURE

By Edgar Reynolds Smith and Harry Matheson

ABSTRACT

By the comparative ebulliometric method, using water as the reference standard and ebulliometers of the Świętosławski type, data were obtained from which were developed the following equations expressing the relation between temperature and vapor pressure from 660 to 860 mm:

For benzene

$$t=80.094+0.042683(p-760)-0.00002199(p-760)^2+0.0000000250(p-760)^3,$$

and

$$p=760+23.429(t-80.094)+0.2804(t-80.094)^2-0.000383(t-80.094)^3;$$

for ethylene chloride

$$t=83.483+0.042037(p-760)-0.00002201(p-760)^2+0.0000000180(p-760)^3,$$

and

$$p=760+23.789(t-83.483)+0.2946(t-83.483)^2+0.00156(t-83.483)^3;$$

for *n*-heptane

and $t=98.413+0.044849(p-760)-0.00002344(p-760)^2+0.0000000145(p-760)^3,$

and

$$p=760+22.297(t-98.413)+0.2599(t-98.413)^2+0.00246(t-98.413)^3;$$

for 2,2,4-trimethylpentane (isooctane)

$$t=99.234+0.046511(p-760)-0.00002374(p-760)^2+0.0000000182(p-760)^3,$$

and

$$p=760+21.500(t-99.234)+0.2348(t-99.234)^2+0.00126(t-99.234)^3.$$

In these equations, t is the temperature in degrees centigrade at which the substance exerts the vapor pressure p in standard millimeters of mercury. The use of these substances as reference standards for boiling-point measurements is discussed. Equations for the relative volatilities of the two pairs, benzene-ethylene chloride and *n*-heptane-2,2,4-trimethylpentane, are given. The data show that Dühring's rule and the corresponding reciprocal temperature relationship hold accurately over a limited range of pressures, even for substances of different types.

CONTENTS

	Page
I. Introduction	641
II. Apparatus and materials	643
III. Experimental results and conclusions	644

I. INTRODUCTION

The comparative method of measuring vapor pressures of liquid substances requires a primary standard reference liquid for which the

relation between temperature and pressure is known with satisfactory precision. Undoubtedly, water is the best available liquid for a primary standard, for reasons which have been discussed by Świętosławski.[1,2] Recent measurements of the temperature-pressure relations of water between 660 and 860 standard mm pressure [3] are of adequate precision for a reference standard, and cover a most convenient and useful range of pressures for ebulliometric measurements. According to these measurements the boiling point of water between 660- and 860-mm pressure is given by the equation

$$t=100+0.0368578(p-760)-0.000020159(p-760)^2+ 0.00000001621(p-760)^3, \quad (1)$$

in which t is expressed in degrees centigrade (Int.) and p in millimeters of mercury (standard). This equation is in excellent agreement with the data of the National Bureau of Standards [4] as well as with those obtained recently by Zmaczynski [5] at the Physikalisch-Technische Reichsanstalt, and is apparently reliable to better than 0.001° on the International Temperature Scale for nearly 4° above and below the fixed reference point of 100°.

For comparative measurements of pressure, it is desirable to have an equation in which pressure is an explicit function of temperature. To obtain such an equation, the data of Beattie and Blaisdell were treated by the method of least squares to obtain the constants in the following equation

$$p=760+27.1313(t-100)+0.40083(t-100)^2+0.003192(t-100)^3, \quad (2)$$

which is valid over the same range of pressures. Equation 2 reproduces the 38 experimental points from which it was obtained with an average deviation of 0.012 mm and a greatest deviation of 0.031 mm, and agrees with the NBS data with equal precision over the range in which the two sets of data overlap. It may be well to mention that the equation fails rapidly above and below the range for which it was obtained.[6]

In the experimental procedure, successive measurements were made of the boiling point of one of the substances under investigation and the boiling point of water, in ebulliometers connected to the same manostat, by means of which the pressure was varied in steps from 660 to 860 mm. The pressures were calculated from the measured boiling points of water by eq 2 and tabulated with the corresponding boiling points of the substance. From the data tabulated for each substance, the constants were evaluated, by the method of least squares, for equations of the type

$$t=t_B+a(p-760)+b(p-760)^2+c(p-760)^3 \quad (3)$$

and

$$p=760+q(t-t_B)+r(t-t_B)^2+s(t-t_B)^3, \quad (4)$$

[1] W. Świętosławski, Comptes Rendus de la XII Conférence de l'Union Internationale de Chimie, p. 69 (1936).
[2] W. Świętosławski and E. R. Smith, J. Research NBS 20, 549 (1938) RP1088.
[3] J. A. Beattie and B. E. Blaisdell, Proc. Am. Acad. Arts Sci. 71, 361 (1937).
[4] N. S. Osborne and C. H. Meyers, J. Research NBS 13, 1 (1934) RP691.
[5] Zmaczynski's data over this range are given in the reference under footnote 2.
[6] In the reference of footnote 2, there is given an alternative equation involving the logarithm of the pressure, which is valid over a greater range. The additional alternative of interpolation from the table of Osborne and Meyers, footnote 4, is also pointed out.

in which a, b, c, q, r, and s are constants, t is the temperature in degrees centigrade at which the vapor pressure is p, and t_B is the normal boiling point, which is determined as one of the computed constants.

II. APPARATUS AND MATERIALS

For the determination of boiling points two ebulliometers were used. One of these was a simple barometric ebulliometer containing redistilled water for the reference standard. The other was a standard differential ebulliometer containing the substance under investigation. These ebulliometers were of the Świętosławski type [7] and have been described in other papers from this laboratory.[8] They were connected through drying tubes to a manostat, which was an 18-liter carboy placed in an insulated wooden case to insure uniformity of temperature. The pressure in the system was increased by the addition of nitrogen from a cylinder connected through a stopcock to the manostat, and decreased by evacuating through the same stopcock. The changes in pressure were adjusted roughly according to the levels of mercury in an open-arm manometer, also connected to the manostat through a stopcock, final adjustments being made as indicated by observations of the boiling point of water. The procedure involved the approximate adjustment of the pressure to a desired value, say about 660 mm, followed by three temperature measurements. The temperature of the water boiling in one ebulliometer was first measured. The thermometer was then transferred, at equal short time intervals, from the ebulliometer containing water to the one containing the substance under examination and then back to the water, a temperature measurement being made in each position. Averaging the temperature readings of the water corrects for any possible slight drift in pressure in the manostat during the operation. Thus when water boils at this average temperature, t_w, the substance boils at the measured temperature, t_s, under the same pressure. This pressure is calculated from eq 2, and thus there are obtained a series of temperatures and corresponding vapor pressures for the substance relative to water, as the primary standard.

A calibrated platinum resistance thermometer (coiled-filament type)[9] and a calibrated Mueller thermometer bridge were used to measure the temperatures.

Water.—For the ebulliometric reference standard, distilled water from the laboratory supply was distilled from alkaline permanganate and again distilled shortly before use.

Benzene.—The initial material was benzene which conformed to the specifications adopted by the American Chemical Society for the reagent grade of this substance.[10] Two liters of this material was distilled fractionally in a 40-bulb vacuum-jacketed column of the Świętosławski type [11] equivalent to about 25 theoretical plates. The distillate was collected in eight fractions, each of about 250 ml. The normal boiling points of the third and fifth fractions were meas-

[7] W. Świętosławski, Ebulliometry, p. 7 and 16. (Chemical Publishing Company of New York, Inc., 1937).
[8] M. Wojciechowski, J. Research NBS 17, 453 (1936) RP921.
E. R. Smith and M. Wojciechowski, J. Research NBS 17, 841 (1936) RP947.
[9] C. H. Meyers, BS J. Research 9, 807 (1932) RP508.
[10] Ind. Eng. Chem., Anal. Ed. 4, 347 (1932).
[11] W. Świętosławski, Ebulliometry, p. 27 (Chemical Publishing Company of New York, Inc., 1937).

ured by the comparative method and found to be 80.093 and 80.094°, in agreement with the value of 80.094° reported by Wojciechowski [12] for benzene of high purity. The difference between the boiling point and the temperature of condensation of these fractions, measured in the differential ebulliometer, was 0.001°, which also indicated high purity. Since these fractions were of satisfactory purity, they were used for the measurements and the other fractions were not tested.

Ethylene chloride.—About 2 kg of this substance, obtained from Eastman Kodak Co., was distilled in the 40-bulb column and collected in a series of fractions, each of about 150 ml. Fractions 5, 7, and 10 had normal boiling points of 83.478, 83.481, and 83.482° C, respectively, according to single measurements, and each showed in the differential ebulliometer a difference of 0.002° between boiling point and temperature of condensation. Fraction 7 was used for the measurements.

n-Heptane.—The initial material obtained from the Eastman Kodak Co. showed in the differential ebulliometer a difference between boiling-point and condensation temperature of 0.04°. After fractionation in the 40-bulb column, this difference was reduced to 0.001° for fraction 3, which was used for the measurements. A preliminary measurement of its boiling point gave 98.413° C. Since this result is slightly higher than the value of 98.365° obtained by Wojciechowski,[13] and lower than the value of 98.52° found by Beattie and Kay,[14] a sample of synthetic *n*-heptane made by the California Chemical Co., was obtained through the kindness of F. W. Rose, Jr., Research Associate of Project 6 of the American Petroleum Institute. This sample had been prepared by fractionation of the initial synthetic material through a 2.5-m locket-chain column, equivalent to about 60 theoretical plates. The difference between its boiling point and condensation temperature was 0.001°, and its boiling point in the differential ebulliometer was 98.413°, in complete agreement with the sample used for this work.

2,2,4-Trimethylpentane (*isooctane*).—The sample used for measurement was a portion of material made by Röhm and Haas, which was further purified by successive fractional distillation. The sample was kindly supplied by D. B. Brooks, of the automotive power plant section of this Bureau, who will describe its preparation and properties in detail in a subsequent paper. This sample had a freezing point of −107.31° C, and a difference of 0.001° between boiling point and condensation temperature in the differential ebulliometer.

III. EXPERIMENTAL RESULTS AND CONCLUSIONS

Benzene.—The comparative boiling point data for benzene and water are given in table 1. The boiling point of benzene is shown in column 1, and the corresponding boiling point of water in column 2. The corresponding pressure, calculated from the boiling point of water by eq 2, is given in column 3.

[12] M. Wojciechowski, J. Research NBS **19**, 347 (1937) RP1029.
[13] M. Wojciechowski, J. Research NBS **17**, 453 (1936) RP921. The material used in Wojciechowski's determination had a difference of 0.013° between boiling point and temperature of condensation.
[14] J. A. Beattie and W. C. Kay, J. Am. Chem. Soc. **59**, 1586 (1937).

TABLE 1.—*Boiling points of benzene between 660- and 860-mm pressure*

Boiling point		Pressure
Benzene	Water	
°C	°C	mm
75.532	96.053	658.96
76.261	96.685	674.35
76.841	97.188	686.81
77.430	97.697	699.60
78.015	98.204	712.55
78.606	98.714	725.77
79.201	99.230	739.35
79.796	99.744	753.08
80.299	100.178	764.84
80.822	100.628	777.20
81.417	101.140	791.46
82.022	101.662	806.21
82.606	102.163	820.59
83.285	102.745	837.56
84.079	103.427	857.82

The expression obtained for the boiling point of benzene as a function of pressure is

$$t=80.094+0.042683(p-760)-0.00002199(p-760)^2+0.0000000250(p-760)^3 \quad (5)$$

The average deviation of the 15 measurements from this equation is 0.001° and the greatest deviation is 0.003°. The normal boiling point is 80.094°, in agreement with a previous determination in this laboratory by Wojciechowski.[15] It is interesting that the value obtained by Wojciechowski is an average for several samples of benzene purified by different methods and measured at pressures within a few millimeters of normal, while in this work the boiling point is obtained as a constant to fit the equation according to measurements on one sample from 100 mm below to 100 mm above normal pressure. The expression obtained for pressure as a function of temperature is

$$p=760+23.429(t-80.094)+0.2804(t-80.094)^2-0.000383(t-80.094)^3, \quad (6)$$

which reproduces the measurements with an average deviation of 0.03 mm and a greatest deviation of 0.05 mm. General expressions for the values of dt/dp and dp/dt may be obtained easily from eq 5 and 6.

Ethylene chloride.—The data for ethylene chloride are given in table 2. The equations for the temperature-pressure relations of this substance are

$$t=83.483+0.042037(p-760)-0.00002201(p-760)^2+0.0000000180(p-760)^3 \quad (7)$$

with an average deviation of 0.001° and a greatest deviation of 0.002°, and

$$p=760+23.789(t-83.483)+0.2946(t-83.483)^2+0.00156(t-83.483)^3 \quad (8)$$

with an average deviation of 0.01 mm and a greatest deviation of 0.04 mm from the experimental values.

[15] M. Wojciechowski, J. Research NBS 19, 347 (1937) RP1029.

TABLE 2.—*Boiling points of ethylene chloride between 660- and 860-mm pressure*

Boiling point		Pressure
Ethylene chloride	Water	
°C	°C	mm
79.325	96.129	660.80
79.628	96.613	672.57
80.100	97.029	682.84
80.644	97.509	694.85
81.209	98.004	707.42
81.556	98.309	715.24
82.273	98.939	731.66
82.808	99.487	746.19
83.487	100.004	760.11
83.494	100.011	760.30
84.065	100.511	773.97
84.638	101.012	787.86
85.198	101.504	801.72
85.782	102.014	816.29
86.358	102.518	830.90
86.912	103.000	845.10
87.486	103.502	860.06

n-Heptane.—The equations for *n*-heptane, based on the data given in table 3, are

TABLE 3.—*Boiling points of n-heptane between 660- and 860-mm pressure*

Boiling point		Pressure
n-Heptane	Water	
°C	°C	mm
93.432	95.893	655.11
94.046	96.400	667.38
94.675	96.920	680.15
95.341	97.468	693.82
95.650	97.725	700.31
96.005	98.018	707.83
96.634	98.536	721.13
96.946	98.795	727.88
97.251	99.046	734.48
97.748	99.456	745.36
99.020	100.500	773.67
99.672	101.034	788.49
100.480	101.696	807.18
100.870	102.016	816.35
101.504	102.537	831.46
102.121	103.045	846.42
102.740	103.551	861.54

$$t=98.413+0.044849\ (p-760)-0.00002344\ (p-760)^2+0.0000000145\ (p-760)^3 \quad (9)$$

which reproduces the 17 experimental values with an average deviation of 0.001° and a greatest deviation of 0.003°, and

$$p=760+22.297\ (t-98.413)+0.2599\ (t-98.413)^2+0.00246\ (t-98.413)^3 \quad (10)$$

with an average deviation of 0.02 mm and a greatest deviation of 0.07 mm.

2,2,4-Trimethylpentane (isooctane).—The data for 2,2,4-trimethylpentane are given in table 4.

TABLE 4.—*Boiling points of 2,2,4-trimethylpentane between 660- and 860-mm pressure*

Boiling points		Pressure
2,2,4-Trimethylpentane	Water	
°C	°C	mm
94.318	96.090	659.86
94.949	96.592	672.08
95.471	97.007	682.31
96.088	97.501	694.64
96.706	97.992	707.10
97.111	98.318	715.47
97.860	98.912	730.94
98.598	99.496	746.44
99.310	100.061	761.65
99.869	100.503	773.74
100.501	101.003	787.61
101.117	101.491	801.36
101.768	102.003	815.99
102.404	102.506	830.57
103.005	102.980	844.50
103.642	103.481	859.45

The equations obtained from the data are

$$t=99.234+0.046511(p-760)-0.00002374(p-760)^2 +0.0000000182(p-760)^3 \quad (11)$$

with average and greatest deviations of 0.001 and 0.003°, respectively, and

$$p=760+21.500(t-99.234)+0.2348(t-99.234)^2 +0.00126(t-99.234)^3 \quad (12)$$

with average and greatest deviations of 0.02 and 0.07 mm, respectively.

In table 5 are listed the normal boiling points and the values of $(dt/dp)_{760}$ for the four substances studied. It is noteworthy that these values have not been obtained from single measurements in the vicinity of normal pressure, but have been calculated as constants in the equations which reproduce 15 to 17 experimental values over the range 660- to 860-mm pressure. Of these four substances, benzene is the only one which would be suitable for a secondary ebulliometric reference standard. On prolonged boiling ethylene chloride undergoes a slight hydrolysis if a trace of water is present, while *n*-heptane and 2,2,4-trimethylpentane have boiling points within the range where a secondary standard is superfluous.

TABLE 5.—*Normal boiling points and values of dt/dp*

Substance	Normal boiling point	$(dt/dp)_{760}$
	°C	°C/mm Hg
Benzene	80.09_4	0.0426_8
Ethylene chloride	83.48_9	$.0420_4$
n-Heptane	98.41_3	$.0448_5$
2,2,4-Trimethylpentane	99.23_4	$.0465_1$

Relative volatility.—For calculating the number of theoretical plates required in a fractionating column to obtain a given separation of an ideal two-component mixture, the equation [16]

$$n=\frac{\log \frac{x_0(1-x_n)}{x_n(1-x_0)}}{\log R} \tag{13}$$

is often useful. In this equation, n is the number of plates, R is the ratio, assumed constant, of the vapor pressures of the two pure constituents, and x_0 and x_n are the mole fractions corresponding to $n=0$ and $n=n$, x_0 being greater than x_n. Beatty and Calingaert have shown that the mixture n-heptane-2,2,4-trimethylpentane is very nearly ideal from the standpoint of vapor pressure, and also that in any case where R is nearly unity, a change in the value of R creates a marked difference in the calculated value of n, but that in such a case the boiling range is small, so that the absolute change in R is also small over the boiling range. The effect on n of a change in R is thus considered negligible. The values of R at the normal boiling points of n-heptane (98.413°) and 2,2,4-trimethylpentane (99.234°) can be calculated accurately by eq 10 and 12 to be 1.02356 and 1.02432, respectively, for this pair. The corresponding values of n, from eq 13, for a change in mole fraction from 0.05 to 0.95 are 252.9 and 245.1, respectively, the difference over this range of temperature being negligible for practical purposes. Values of R for the systems n-heptane-2,2,4-trimethylpentane and benzene-ethylene chloride over a range of temperature are given in table 6. For these two pairs the relative volatilities are expressed by the following equations:

TABLE 6.—*Values of R*

n-Heptane-2,2,4-trimethylpentane		Benzene-ethylene chloride	
Temperature	$R=\frac{p(n\text{-heptane})}{p(2,2,4\text{-trimethylpentane})}$	Temperature	$R=\frac{p(\text{benzene})}{p(\text{ethylene chloride})}$
°C		°C	
94.5	1.01995	79.0	1.11464
95.5	1.02089	80.0	1.11334
96.5	1.02181	81.0	1.11203
97.5	1.02272	82.0	1.11071
98.5	1.02364	83.0	1.10935
99.5	1.02456	84.0	1.10796
100.5	1.02550		
101.5	1.02647		
102.5	1.02746		

For n-heptane and 2,2,4-trimethylpentane between 94.5 and 102.5° C

$$R=1.02088-0.0008783t+0.000009198t^2,$$

where $R=p(n\text{-heptane})/p(2,2,4\text{-trimethylpentane})$. For benzene and ethylene chloride between 79.0 and 84.0° C

$$R=1.14596+0.0004845t-0.000011152t^2,$$

where $R=p(\text{benzene})/p(\text{ethylene chloride})$.

[16] H. A. Beatty and G. Calingaert, Ind. Eng. Chem. **26**, 504 (1934).

Dühring's rule.—An empirical relationship between the temperatures at which two liquids have equal vapor pressures, known as Dühring's rule, has found considerable use for the interpolation of data. The relationship is expressed by the equation

$$T_A = k_1 T_B + C_1, \tag{14}$$

where k_1 and C_1 are constants, and T_A and T_B are the temperatures at which the liquids A and B have the same vapor pressure. A similar relationship with a better claim to some theoretical basis involves the reciprocal temperatures

$$1/T_A = (k_2/T_B) + C_2 \tag{15}$$

Although these two relations have been tested before,[17] the relative vapor pressure data of this investigation afford a more precise comparison than has hitherto been made, over the short range of 200 mm, of the relative validities of eq 14 and 15.

In preference to an algebraic elimination between equations of type 3, the temperatures at which water, benzene, ethylene chloride, *n*-heptane, and isooctane exert the 11 vapor pressures of 660, 680, 700, ... 840, 860 mm were calculated from eq 1, 5, 7, 9, and 11. From these 11 sets of values the constants of eq 14 and 15 were found for each of the 10 possible pairs of the 5 substances. The accuracy with which these linear equations of types 14 and 15 hold is illustrated by the example of benzene and water given in table 7.

TABLE 7.—*Comparison of temperatures calculated from eq 12 and 13 for the pair benzene-water*

Pressure	Temperature of—			Δt eq 1—eq 16	Temperature of water, eq 17	Δt eq 1—eq 17
	Benzene, eq 5	Water, eq 1	Water, eq 16			
mm	°C	°C	°C	°C	°C	°C
660	75.581	96.096	96.102	−0.006	96.098	−0.002
680	76.526	96.914	96.917	−.003	96.916	−.002
700	77.448	97.712	97.713	−.001	97.714	−.002
720	78.350	98.492	98.491	+.001	98.494	−.002
740	79.231	99.255	99.251	+.004	99.255	.000
760	80.094	100.000	99.995	+.005	99.999	+.001
780	80.939	100.729	100.724	+.005	100.728	+.001
800	81.767	101.443	101.439	+.004	101.441	+.002
820	82.581	102.142	102.141	+.001	102.141	+.001
840	83.380	102.828	102.830	−.002	102.829	+.001
860	84.167	103.500	103.509	−.009	103.505	−.005
Average deviation				0.004		0.002
Greatest deviation				0.009		0.005

The equations for this pair are

$$t_w = 0.86268 t_s + 30\ 900, \tag{16}$$

in which t is expressed in degrees centigrade, and

$$\frac{1}{T_w} = (0.772945/T_s) + 0.00049175, \tag{17}$$

[17] For example, see E. F. Linhorst. J. Am. Chem. Soc. **51**, 3262 (1929); A. M. White. Ind. Eng. Chem. **22**, 230 (1930); J. H. Perry and E. R. Smith. Ind. Eng. Chem. **25**, 195 (1933).

in which $T=t+273.160$. Without tabulating the results of the tests with the other nine pairs, an idea of the relative accuracy of eq 14 and 15 can be gained from the statement that for all pairs the average of the average and greatest deviations was found to be 0.002 and 0.004° from eq 14, and 0.001 and 0.003° from eq 15, respectively. Thus, in regard to accuracy there is very little choice between the two, though the reciprocal temperature relation seems to be slightly better, on the average, for the 10 pairs that were tested.

WASHINGTON, January 18, 1938.

U. S. DEPARTMENT OF COMMERCE NATIONAL BUREAU OF STANDARDS

RESEARCH PAPER RP1098

Part of Journal of Research of the National Bureau of Standards, Volume 20, May 1938

SUITABILITY OF VARIOUS PLASTICS FOR USE IN AIRPLANE DOPES

By Gordon M. Kline and Cyrus G. Malmberg

ABSTRACT

A number of different cellulose derivatives of potential interest as film-forming constituents for airplane dopes have recently become available commercially. An investigation has been undertaken at the National Bureau of Standards to determine the fundamental factors involved in the formulation of dopes containing these new derivatives to obtain optimum tautness and durability. Data are presented in this paper relative to the effect of varying the acyl or ethoxyl content and the viscosity of cellulose esters and ethers on the tautness of fabrics doped with them. It is concluded that the solvents and diluents govern to a large extent the tautening properties of the dope and the durability of the film deposited on the fabric.

CONTENTS

	Page
I. Introduction	651
II. Details of test materials and measurements	652
1. Properties of the plastics	652
2. Composition of the dopes	654
3. Method of preparing the doped panels	655
4. Methods of testing the fabrics	655
5. Results of tests on the doped panels	657
III. Effect of various factors on initial tautness of doped fabrics	666
1. Type of plastic	666
2. Acyl or alkyl substitution	666
3. Viscosity	667
4. Solvent composition	667
IV. Effect of weathering on tautness of doped fabrics	668
V. Effect of weathering on flexibility of the dope film	669
VI. Summary and conclusions	670

I. INTRODUCTION

The problem of producing a fire-resistant doped fabric to replace the hazardous cellulose nitrate product was investigated in 1933 at the National Bureau of Standards for the National Advisory Committee for Aeronautics, and the results were reported in this journal.[1] It was established that none of the synthetic resins then available would produce films of satisfactory tautness when used alone on the fabric, and that their addition to either cellulose nitrate or cellulose acetate dope resulted in a corresponding lowering of the fabric tension. Data were also obtained on the comparative rates of burning of fabrics doped with various cellulose nitrate and cellulose acetate compositions, both with and without the addition of fire-retarding salts to the fabric. It was shown that cellulose acetate dope yields a relatively nonhazardous product when applied to untreated fabric,

[1] G. M. Kline, *Fire-resistant doped fabric for aircraft*, J. Research NBS **14**, 575–587 (1935) RP788.

and that when it is applied to fabric treated with boric-acid-borax mixture, a product which is nonflammable under ordinary conditions is obtained. However, the investigation was not continued at that time to include a study of the effect of varying the ingredients of a cellulose acetate dope on the tautening characteristics and particularly on the moisture sensitivity of the doped fabric.

Cellulose acetate has now become available commercially in several grades, representing materials of different degrees of acetylation and viscosity. Likewise, other cellulose derivatives, possessing characteristics which indicate that they might make satisfactory dope bases, are being manufactured. Among these more recently developed products are ethylcellulose, cellulose acetobutyrate, cellulose acetopropionate, and cellulose nitroacetate. These products are also available in various grades denoting differences in chemical composition and in viscosity. The proper formulation of dopes based on these new materials to obtain the requisite balance of solvents, diluents, and plasticizers, both as to types and amounts, can be accomplished only by a thorough laboratory study of the various factors involved. The Bureau of Aeronautics of the U. S. Navy Department has, therefore, requested the National Bureau of Standards to undertake such an experimental study in order to develop a dope, based on these comparatively nonflammable cellulose derivatives, which will compare favorably with or surpass cellulose nitrate dope with respect to the effect of high relative humidity on the tautness of the doped fabric.

In the first phase of this work a variety of cellulose derivatives and synthetic resins were applied to airplane fabric to study the relation of tautness to the type of plastic base used in the dope, the percentage of acyl or alkyl substitution in the various cellulose derivatives, and the viscosity [2] of these derivatives. These panels are also providing data on the relative resistance to weathering of the various doped fabrics, while tests are in progress to determine the effect of solvents, diluents, and plasticizers on the tautening property and to establish the moisture relations of the various doped fabrics.

II. DETAILS OF TEST MATERIALS AND MEASUREMENTS

1. PROPERTIES OF THE PLASTICS

The materials tested were furnished by various manufacturers whose interest and cooperation in this investigation have been very helpful. They also supplied data regarding the viscosity and chemical composition of the compounds, shown in table 1. In the manufacturers' reports the chemical composition was expressed as percentages. The number of equivalents of each substitution group present in the compounds and also of free hydroxyl groups were calculated from these percentage figures. These latter values are listed in table 1 and indicate immediately the degree of hydrolysis, which is closely related to the solubility [3] and moisture-absorbing [4] properties of the cellulose derivative.

[2] The term "viscosity" is used in this paper to denote certain flow characteristics of solutions of the various plastics as measured in the manner described in the footnote to table 1.

[3] W. Coltof, *Solubility properties of certain highly polymeric substances.* J. Soc. Chem. Ind. **56**, 363T-377T (1937).

[4] S. E. Sheppard and P. T. Newsome, *The sorption of water vapor by cellulose and its derivatives.* J. Phys. Chem. **33**, 1817-35 (1929).

TABLE 1.—*Viscosity and composition of test materials*

Material	Sample designation	Viscosity [a]	Composition	
			Percentage basis	Equivalents basis
Cellulose acetate	CA-a1	9.4 sec.	39.1 acetyl	2.38 acetyl; 0.62 hydroxyl.
Do	CA-a2	6.2 sec.	40.0 acetyl	2.48 acetyl; 0.52 hydroxyl.
Do	CA-a3	10.5 sec.	40.9 acetyl	2.57 acetyl; 0.43 hydroxyl.
Do	CA-a4	28 sec.	40.4 acetyl	2.51 acetyl; 0.49 hydroxyl.
Do	CA-a5	44 sec.	40.0 acetyl	2.48 acetyl; 0.52 hydroxyl.
Do	CA-a6	56 sec.	38.4 acetyl	2.32 acetyl; 0.68 hydroxyl.
Do	CA-a7	81 sec.	38.7 acetyl	2.35 acetyl; 0.65 hydroxyl.
Do	CA-a8	83 sec.	38.4 acetyl	2.32 acetyl; 0.68 hydroxyl.
Do	CA-a9	94 sec.	39.1 acetyl	2.38 acetyl; 0.62 hydroxyl.
Do	CA-a10			ca.3 acetyl.
Do	CA-b1	2 sec.	39.0 acetyl	2.37 acetyl; 0.63 hydroxyl.
Do	CA-b2	33 sec.	40.3 acetyl	2.51 acetyl; 0.49 hydroxyl.
Do	CA-b3	64 sec.	39.2 acetyl	2.39 acetyl; 0.61 hydroxyl.
Do	CA-b4	77 sec.	38.1 acetyl	2.29 acetyl; 0.71 hydroxyl.
Cellulose acetopropionate	CAP-a1	31 sec.	17.1 acetyl; 26.9 propionyl	1.13 acetyl; 1.34 propionyl; 0.53 hydroxyl.
Do	CAP-b1	34.5 cp [b]	15.5 acetyl; 31.3 propionyl	1.08 acetyl; 1.64 propionyl; 0.28 hydroxyl.
Do	CAP-b2	470 cp.	15.5 acetyl; 31.3 propionyl	1.08 acetyl; 1.64 propionyl; 0.28 hydroxyl.
Do	CAP-b3	650 cp.	15.5 acetyl; 31.3 propionyl	1.08 acetyl; 1.64 propionyl; 0.28 hydroxyl.
Do	CAP-c1	35 cp.	14.0 acetyl; 34.0 propionyl	1.00 acetyl; 1.83 propionyl; 0.17 hydroxyl.
Do	CAP-c2	42 cp.	11.0 acetyl; 34.0 propionyl	0.74 acetyl; 1.72 propionyl; 0.54 hydroxyl.
Do	CAP-c3	90 cp.	9.0 acetyl; 33.0 propionyl	0.58 acetyl; 1.60 propionyl; 0.82 hydroxyl.
Cellulose acetobutyrate	CAB-b1	36 cp.	32.5 acetyl; 15.4 butyryl	2.31 acetyl; 0.66 butyryl; 0.03 hydroxyl.
Do	CAB-b2	315 cp.	32.2 acetyl; 15.2 butyryl	2.27 acetyl; 0.65 butyryl; 0.08 hydroxyl.
Do	CAB-b3	665 cp.	32.0 acetyl; 16.1 butyryl	2.28 acetyl; 0.69 butyryl; 0.03 hydroxyl.
Cellulose nitroacetate	CNA-b1	Medium		
Cellulose nitrate	CN-c1	0.5 sec.		
Do	CN-c2	10.5 sec.		
Do	CN-c3	84 sec.		
Methylcellulose	MC-b1	Low		
Ethylcellulose	EC-b1	6.2 sec.	47.5 ethoxyl	2.43 ethoxyl; 0.57 hydroxyl.
Do	EC-b2	22 sec.	47.7 ethoxyl	2.44 ethoxyl; 0.56 hydroxyl.
Do	EC-b3	66 sec.	48.2 ethoxyl	2.48 ethoxyl; 0.52 hydroxyl.
Do	EC-d1	20 cp.	48.3 ethoxyl	2.49 ethoxyl; 0.51 hydroxyl.
Do	EC-d2	30 cp.	52.0 ethoxyl	2.77 ethoxyl; 0.23 hydroxyl.
Do	EC-d3	35 cp.	48.7 ethoxyl	2.52 ethoxyl; 0.48 hydroxyl.
Do	EC-d4	75 cp.	48.0 ethoxyl	2.47 ethoxyl; 0.53 hydroxyl.
Do	EC-d5	150 cp.	48.3 ethoxyl	2.49 ethoxyl; 0.51 hydroxyl.
Do	EC-d6	210 cp.	49.5 ethoxyl	2.58 ethoxyl; 0.42 hydroxyl.
Benzylcellulose	BC-b1	Medium		
Chlorinated rubber	CR-b1	125 cp.		
Methyl methacrylate	MM-c1			

[a] The viscosity values were obtained in the manufacturers' laboratories by the following variety of methods (all parts by weight unless otherwise noted):

Cellulose acetate series CA-a: ASTM falling-ball method, using 20-percent solutions in acetone. (See ASTM Standards, 1936, part II, Nonmetallic Materials, published by the American Society for Testing Materials, Philadelphia, Pa.)

Cellulose acetate series CA-b: ASTM falling-ball method, using 20-percent solutions in a mixture of 90 parts of acetone and 10 parts of ethyl alcohol.

Cellulose acetopropionate series CAP-a: ASTM falling-ball method, using 20-percent solutions in acetone.

Cellulose acetopropionate series CAP-b: capillary viscometer, using 10-percent solution in acetone at 25° C.

Cellulose acetopropionate series CAP-c: Same as above.

Cellulose acetobutyrate series CAB-b: Same as above.

Cellulose nitrate series CN-c: ASTM falling-ball method.

Ethylcellulose series EC-b: ASTM falling-ball method, using a 20-percent solution in a mixture of 80 parts of toluene and 20 parts of ethyl alcohol.

Ethylcellulose series EC-d: Capillary viscometer method, using a 5-percent solution in a mixture of 80 parts of toluene and 20 parts of absolute ethyl alcohol by volume at 25° C.

Chlorinated rubber CR-b: Capillary viscometer, using a 20-percent solution in toluene at 25° C.

[b] cp=centipoise.

2. COMPOSITION OF THE DOPES

Inasmuch as it was desired to compare the behavior of various cellulose derivatives with one another, the same solvent mixture and plasticizer, triphenyl phosphate, were employed in a majority of the dopes. In most cases the proportions of the latter were one part of plasticizer to nine parts of cellulose derivative. Preliminary tests indicated that varying the concentration of the cellulose base in the solvent mixture between the limits of 5 and 10 percent had comparatively little effect on the tautness produced. A concentration of about 6.4 percent was, therefore, used for most samples, although it was necessary to dilute some of the aluminum-pigmented dopes to obtain a solution of suitable viscosity for brushing. Complete data concerning the formulas of the dopes are shown in table 2. Formula I was used in general for the cellulose esters and formula VI for the ethylcelluloses. The other formulas were introduced because of the special solubility characteristics of certain derivatives, such as cellulose triacetate, or to compare with those above solvent compositions recommended in the literature or by the manufacturer.

TABLE 2.—*Formulas of experimental dopes*

Formula	Plastic base	Plasticizer	Aluminum powder	Solvent	Composition of solvent (parts by weight)
	Percent	*Percent*	*Percent*	*Percent*	
I, clear	6.4	0.6 triphenyl phosphate	None	93.0	Acetone 48, ethyl acetate 20, methyl ethyl ketone 20, diacetone alcohol 5.
I, pigmented	6.0	1.2 triphenyl phosphate	4.8	88.0	Acetone 50, ethyl acetate 15, methyl ethyl ketone 15, diacetone alcohol 8.
IA, clear	6.4	None	None	93.6	Acetone 48, ethyl acetate 20, methyl ethyl ketone 20, diacetone alcohol 5.
IA, pigmented	6.0	do	4.8	89.2	Acetone 50, ethyl acetate 15, methyl ethyl ketone 15, diacetone alcohol 8.
II, clear	6.4	0.6 triphenyl phosphate	None	93.0	Acetone 50, ethyl alcohol 10, toluene 40.
II, pigmented	6.0	1.2 triphenyl phosphate	4.8	88.0	Do.
IIA, clear	6.4	0.3 triphenyl phosphate	None	93.3	Do.
IIA, pigmented	6.0	do	4.8	88.9	Do.
IIB, clear	6.4	None	None	93.6	Do.
IIB, pigmented	6.0	do	4.8	89.2	Do.
III, clear	10.4	1.0 benzyl alcohol	None	88.6	Acetone 16.5, ethyl alcohol 8.5, benzene 36.6, toluene 18.0, xylene 9.0.
III, pigmented	6.0	0.6 benzyl alcohol	4.8	88.6	Do.
IV, clear	6.4	do	None	93.0	Do.
IV, pigmented	6.0	do	4.8	88.6	Do.
VI, clear	6.4	None	None	93.6	Acetone 25, ethyl acetate 70, toluene 45, diacetone alcohol 10.
VI, pigmented	6.0	do	4.8	89.2	Do.
VIA, clear	6.4	0.6 Dow No. 6	None	93.0	Do.
VIA, pigmented	6.0	1.2 Dow No. 6	4.8	88.0	Do.
VII, clear	6.4	0.6 triphenyl phosphate	None	93.0	Ethyl acetate 25, methyl ethyl ketone 25, butyl acetate 25, Methyl Cellosolve 25.
VII, pigmented	6.0	1.2 triphenyl phosphate	4.8	88.0	Do.
VIIA, clear	6.4	None	None	93.6	Do.
VIIA, pigmented	6.0	do	4.8	89.2	Do.
VIII, clear	6.4	0.6 triphenyl phosphate	None	93.0	Methyl Cellosolve.
VIII, pigmented	6.0	1.2 triphenyl phosphate	4.8	88.0	Do.
IX, clear	3.8	0.4 triphenyl phosphate	None	95.8	Chloroform 70, tetrachlorosethane 30.
IX, pigmented	2.4	do	1.9	95.2	Do.

TABLE 2.—*Formulas of experimental dopes*—Continued

Formula	Plastic base	Plasticizer	Aluminum powder	Solvent	Composition of solvent (parts by weight)
	Percent	*Percent*	*Percent*	*Percent*	
X, clear	7.7	None	None	92.3	Toluene.
X, pigmented	6.0	do	4.8	89.2	Do.
XI, clear	7.6	do	None	92.4	Toluene 33.1, xylene 22.3, Cellosolve 22.3, methyl amyl ketone 22.3.
XI, pigmented	6.0	do	4.8	89.2	Toluene 26.8, xylene 24.4, Cellosolve 24.4, methyl amyl ketone 24.4.
XII, clear	4.5	do	None	95.5	Water.
XII, pigmented	4.5	do	3.6	91.9	Do.

3. METHOD OF PREPARING THE DOPED PANELS

Wooden frames (fig. 1), constructed in accordance with specification SP–16 of the U. S. Naval Aircraft Factory, were used in these tests. Cotton airplane fabric, weighing approximately 4 oz/yd², was placed over the frame and a 50-pound weight was attached to each side. In this way uniform tension in both directions of the weave of the cloth was produced. The fabric was tacked to the frame with

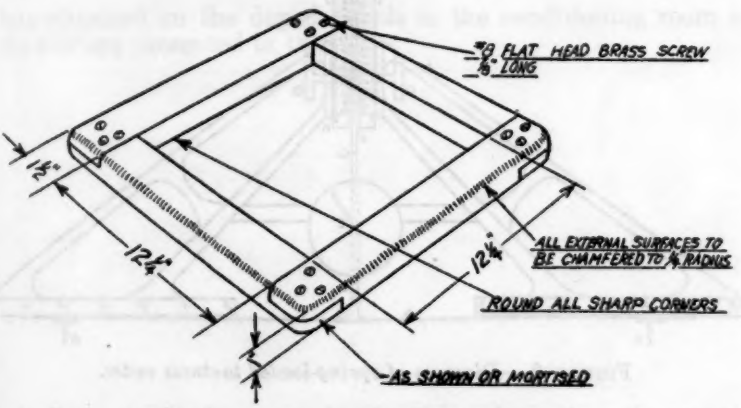

FIGURE 1.—*Construction of exposure panel.*

No. 4 upholsterer's tacks, spacing them approximately 1 inch apart. Four coats of clear dope and, in the case of the pigmented panels, two coats of aluminum-pigmented dope were brushed on the panels. The average weight of the clear doped fabrics after drying was 7.2 oz/yd² and of the pigmented doped fabrics was 8.7 oz/yd².

4. METHODS OF TESTING THE FABRICS

The measurements of tautness of the fabric were made with a spring-loaded tautness meter, the construction of which is shown in figure 2. The instrument is essentially a Schiefer Compressometer,[5] modified to adapt it to measuring the deflection of a doped fabric instead of the thickness and compressibility of textile fabrics and similar materials.

[5] H. F. Schiefer, BSJ. Research 10, 705–13, (1933) RP561. The assistance of Dr. Schiefer in designing the tautness meter and in preparing figure 2 is gratefully acknowledged.

For measuring tautness, the instrument is placed upon the fabric, *A*, of a panel or wing section with the foot, *C*, midway between the two ribs, *B*. The foot, *C*, is of spherical shape with a 0.5-inch radius of curvature. It is fastened to the bottom of the spindle, *D*, of the lower dial micrometer, *E*. The rod, *F*, is fastened to the top of the spindle, *D*, at *G* and to the top of a helical spring, *H*, at *I*. The bottom of the spring is fastened to the tube, *J*, at *K*. The upper dial micrometer, *L*, is fastened to the top of the tube at *M*. The spindle, *N*, of the upper dial micrometer is attached to the rod, *F*, at *O* by a ball and socket union. The tube may be moved up or down relative to the frame, *P*, by turning the knob, *Q*, of the rack and pinion, *R*. The frame, *P*, consists of an aluminum beam having a three-point support which rests on the framework of the panel or on any two

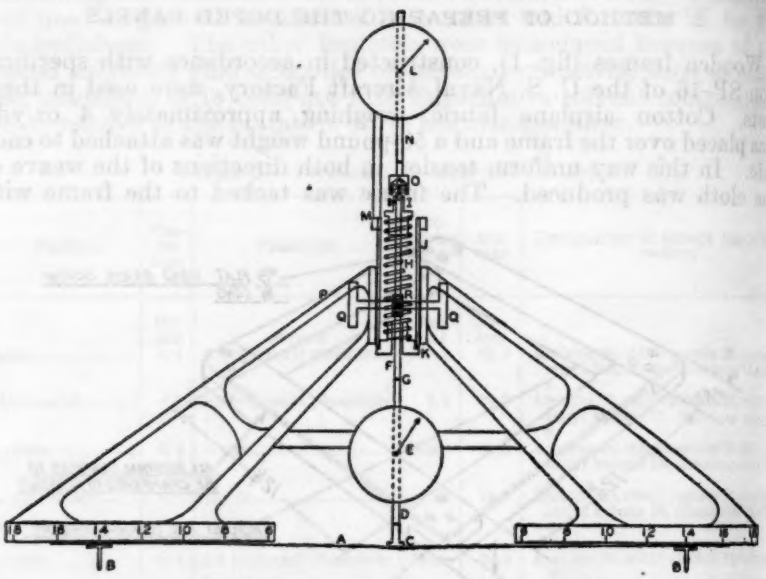

FIGURE 2.—*Diagram of spring-loaded tautness meter.*

adjacent ribs of a wing. Graduations on the beam indicate the width of the rib spacing so that the instrument may be centered quickly and conveniently. By turning the knob the foot may be lowered upon the doped fabric. The load which is applied to the specimen by the foot may be ascertained from the upper dial reading, which indicates the elongation of the spring, and a calibration curve of the spring. The amount of deflection of the doped fabric when loaded is indicated on the lower dial, which is graduated to read directly to 0.001 inch.

For the estimation of tautness of doped fabrics, the foot is lowered upon the specimen by means of the rack and pinion until the load on the fabric is 3 ounces, as indicated by the upper dial. A reading of the lower dial is taken at this load. Then the load on the fabric is increased to 19 ounces and a second reading of the lower dial is taken. The difference between these two readings of the lower dial is the deflection in thousandths of an inch of the fabric under one pound load,

as tested. The less the deflection under a given load, the greater is the tautness.

Tautness measurements were made on the fabrics conditioned at approximately 70° F. and 65-percent relative humidity. For the cloth alone a 2-ounce loading is employed instead of 1 pound in order to avoid excessive stretching. The average deflection observed for the undoped fabrics with the 2-ounce load was 45 mils with an average variation of ±2.5 and a maximum difference of ±6 mils. A 1-pound load deflects such fabrics approximately 260 mils.

After drying for at least 1 week in the laboratory, the doped panels were placed in a room kept at 70° F and 65-percent relative humidity. Three measurements of tautness were made in this room at intervals during a period of 1 week. The panels were placed upon the roof of the Industrial Building of the National Bureau of Standards on August 14, 1937, on racks inclined at an angle of 45° and facing south. Measurements of tautness and brittleness were made at intervals under prevailing conditions of temperature and humidity. Brittleness of the film, i. e., tendency to "ringworm", was determined by pressing the thumb firmly into the fabric covering at each corner of the panel.

5. RESULTS OF TESTS ON THE DOPED PANELS

Data obtained on the doped panels in the conditioning room and on the roof are presented in table 3.

TABLE 3.—*Tautness and flexibility data obtained in aging tests of doped fabrics*

[Tautness values are reported as the number of mils deflection of the fabric under a 1-pound load; brittleness, i. e., "ringworming," of the film is indicated by the letter *R;* deterioration of the film leading to surface cracking is indicated by the letter *c; S* indicates slackness of the fabric, in which condition deflection values are meaningless; *W* indicates removal of the film by rain. Panels were placed on the roof on August 14, 1937]

Panel number				1	2	3	4	5	6	7	8	9	10	11	12
Material				CA-a1	CA-a1	CA-a2	CA-a2	CA-a3	CA-a3	CA-a4	CA-a4	CA-a4	CA-a5	CA-a5	CA-a5
Formula				I	I	I	I	I	I	I	I	VII	I	I	IA
Pigmentation				Clear	Al	Clear	Al	Clear	Al	Clear	Al	Al	Clear	Al	Al
Exposure conditions															
Temperature	Relative humidity	Number of days on roofs	Prevailing weather												
°F	*Percent*														
74	64	(•)	(•)	100	83	107	88	100	85	104	84	73	109	85	79
73	64	(•)	(•)	101	83	110	88	101	84	104	84	72	108	84	79
73	63	(•)	(•)	100	83	109	88	101	84	105	84	72	108	84	79
90	40	2	Sunshine	94	83	106	96	105	93	92	90	79	107	87	88
94	52	5	do	93	84	103	85	95	98	93	88	78	101	92	80
63	97	9	Rain	120	106	115	92	127	106	106	92	112	130	110	107
65	99	11	do	127	116	128	102	135	106	108	102	115	130	115	108
92	52	17	Sunshine	93	87	110	84	95	88	95	86	78	100	90	68
74	35	31	do	94	84	109	92	101	95	105	94	84	100	88	74
52	63	56	Cloudy	113	94	130	99	110	97	120	94	90	113	92	90
50	90	67	Rain	136	125	145	112	140	115	114	110	117	140	120	120
54	41	78	Sunshine	92	79	113	100	94	89	115	90	78	104	84	75
52	43	93	Cloudy	*R*	82	116	87	*R*	86	101	83	84	108	88	80
54	96	105	Rain	----------	*S*	*S*	*S*	----------	*S*	*S*	*S*	*S*	*S*	*S*	*S*
30	56	121	Cloudy	----------	103	138	116	----------	102	142	115	86	125	100	88
43	43	128	Sunshine	----------	67	92	74	----------	70	86	74	69	87	70	62

Panel number				13	14	15	16	17	18	19	20	21	22	23	24
Material				CA-a5	CA-a5	CA-a6	CA-a6	CA-a7	CA-a7	CA-a8	CA-a8	CA-a9	CA-a9	CA-a10	CA-a10
Formula				VII	VIII	I	I	I	I	I	I	I	I	IX	IX
Pigmentation				A1	A1	Clear	A1	Clear	A1	Clear	A1	Clear	A1	Clear	A1
74	64	(*)	(*)	71	67	104	86	98	86	112	85	101	87	78	61
73	64	(*)	(*)	73	68	105	86	96	87	110	85	100	87	78	60
73	63	(*)	(*)	72	67	105	87	97	87	110	85	100	87	78	60
90	40	2	Sunshine	68	63	102	87	101	87	116	90	98	89	100	73
94	52	5	do	77	67	94	84	99	87	105	87	90	83	98	75
63	97	9	Rain	113	110	95	91	117	104	140	107	100	92	101	80
65	99	11	do	111	110	97	101	118	112	120	106	107	98	108	80
92	52	17	Sunshine	72	68	104	78	100	90	105	82	104	87	*R*	80
74	35	31	do	73	*R*	117	100	104	85	105	85	111	95	----------	75
52	63	56	Cloudy	80	----------	140	98	121	90	122	88	130	98	----------	75
50	90	67	Rain	110	----------	120	100	135	116	137	116	114	110	----------	93
54	41	78	Sunshine	70	----------	128	107	105	82	110	84	125	100	----------	75
52	43	93	Cloudy	71	----------	125	83	107	89	123	87	115	88	----------	73
54	96	105	Rain	*S*	----------	*S*	*S*	*S*	*S*	*S*	*S*	*S*	*S*	----------	120
30	56	121	Cloudy	83	----------	152	118	124	98	130	99	170	117	----------	69
43	43	128	Sunshine	58	----------	95	82	84	69	93	69	94	78	----------	63

(*) Exposed in laboratory conditioning room.

TABLE 3.—*Tautness and flexibility data obtained in aging tests of doped fabrics*—Continued

Panel number				25	26	27	28	29	30	31	32	33	34	35	36
Material				CA-b1	CA-b1	CA-b2	CA-b2	CA-b3	CA-b3	CA-b4	CA-b4	CAP-a1	CAP-a1	CAP-a1	CAP-b1
Formula				I	I	I	I	I	I	I	I	I	I	VII	I
Pigmentation				Clear	Al	Clear	Al	Clear	Al	Clear	Al	Clear	Al	Al	Clear
Exposure conditions															
Temperature	Relative humidity	Number of days on roof	Prevailing weather												
°F	*Percent*														
74	64	(a)	(a)	107	90	98	82	99	90	104	84	112	92	79	116
73	64	(a)	(a)	107	90	96	83	103	89	104	86	112	93	80	116
73	63	(a)	(a)	107	90	96	82	102	89	105	85	112	92	79	117
90	40	2	Sunshine	114	99	97	89	102	91	104	84	123	109	89	12
94	52	5	do	106	95	97	88	90	87	96	82	122	107	100	130
63	97	9	Rain	118	110	118	116	120	120	125	103	114	110	107	120
65	99	11	do	124	118	109	104	108	117	130	110	125	100	108	125
92	52	17	Sunshine	120	104	105	97	92	90	96	83	131	109	106	135
74	35	31	do	118	97	107	99	106	90	100	81	130	115	100	140
52	63	56	Cloudy	143	104	140	105	115	96	116	92	135	101	108	*R*
50	90	67	Rain	125	116	130	100	120	120	135	117	130	107	105	----------
54	41	78	Sunshine	*R*	90	111	99	112	98	99	80	132	108	98	----------
52	43	93	Cloudy	----------	94	116	95	108	95	104	80	127	98	92	----------
54	96	105	Rain	----------	*S*	*S*	*S*	*S*	*S*	*S*	*S*	*S*	*S*	*S*	----------
50	56	121	Cloudy	----------	112	143	120	142	120	125	96	146	111	98	----------
43	43	128	Sunshine	----------	80	85	80	80	76	83	68	107	80	85	----------

Panel number				37	38	39	40	41	42	43	44	45	46	47	48
Material				CAP-b1 I A1	CAP-b2 I Clear	CAP-b2 I A1	CAP-b3 I Clear	CAP-b3 I A1	CAP-c1 I Clear	CAP-c1 I A1	CAP-c2 I Clear	CAP-c2 I A1	CAP-c3 I Clear	CAP-c3 I A1	CAB-b1 I Clear
Formula															
Pigmentation															
74	64	(*)		90	103	89	109	90	110	76	116	90	122	92	95
73	64	(*)		93	104	89	107	90	110	76	118	94	128	93	94
73	63	(*)		93	104	89	107	90	110	76	118	93	129	93	95
90	40		2	Sunshine	125	112	120	103	126	89	132	107	140	102	110
94	52		5	do	123	110	123	108	130	100	131	106	132	97	107
63	97		9	Rain	105	102	112	105	106	90	126	113	133	122	84
65	99		11	do	108	95	104	102	115	90	125	111	135	115	99
92	62		17	Sunshine	125	104	126	107	140	*R*	135	125	143	106	*R*
74	35		31	do	140	115	131	113	*R*	------	140	115	135	104	------
52	63		56	Cloudy	140	102	130	103	------	------	*R*	117	150	107	------
50	90		67	Rain	117	109	115	102	------	------	------	112	140	121	------
54	41		78	Sunshine	*R*	115	145	103	------	------	------	112	140	105	------
52	43		93	Cloudy	------	100	125	100	------	------	------	108	*R*	103	------
54	96		105	Rain	*S*	120	*S*	*S*	------	------	------	*S*	------	*S*	------
50	56		121	Cloudy	108	110	142	108	------	------	------	112	------	112	------
43	43		128	Sunshine	88	99	108	87	------	------	------	91	------	84	------

(*) Exposed in laboratory conditioning room.

TABLE 3.—*Tautness and flexibility data obtained in aging tests of doped fabrics*—Continued

Panel number				49	50	51	52	53	54	55	56	57	58	59	60
Material				CAB-b1	CAB-b2	CAB-b2	CAB-b2	CAB-b3	CAB-b3	CNA-b1	CNA-b1	CN-c1	CN-c1	CN-c2	CN-c2
Formula				I	I	I	VII	I	I	I	I	I	I	I	I
Pigmentation				Al	Clear	Al	Al	Clear	Al	Clear	Al	Clear	Al	Clear	Al
Exposure conditions															
Temperature	Relative humidity	Number of days on roof	Prevailing weather												
°F	Percent														
74	64	(a)	(a)	79	91	76	65	96	75	98	82	122	94	107	85
73	64	(a)	(a)	79	90	76	65	97	77	97	83	124	95	108	87
73	63	(a)	(a)	79	90	76	65	96	76	97	83	123	95	108	86
90	40	2	Sunshine	92	101	90	74	105	90	107	90	150	120	134	109
94	52	5	do	94	100	90	75	106	91	96	87	150	114	135	115
63	97	9	Rain	78	82	72	84	80	71	108	110	120	112	110	107
65	99	11	do	83	101	83	85	102	87	108	107	118	109	115	94
92	52	17	Sunshine	*R*	106	90	83	107	91	110	97	*R*	133	140	120
74	35	31	do	----------	114	98	80	116	105	105	97	----------	123	*R*	105
52	63	56	Cloudy	----------	110	90	*R*	122	92	*R*	94	----------	115	----------	94
50	90	67	Rain	----------	111	96	----------	127	96	----------	117	----------	105	----------	102
54	41	78	Sunshine	----------	117	108	----------	114	105	----------	90	----------	114	----------	98
52	43	93	Cloudy	----------	103	84	----------	109	88	----------	85	----------	112	----------	96
54	96	105	Rain	----------	135	110	----------	140	120	----------	*S*	----------	130	----------	114
30	56	121	Cloudy	----------	133	104	----------	130	108	----------	120	----------	118	----------	102
43	43	128	Sunshine	----------	94	80	----------	100	85	----------	75	----------	110	----------	84

Panel number				61	62	63	64	65	66	67	68	69	70	71	72
Material				CN–c2	CN–c3	CN–c3	MC–b1	MC–b1	EC–b1	EC–b1	EC–b2	EC–b2	EC–b3	EC–b3	EC–d1
Formula				VII	I	I	XII	XII	VI	VI	VI	VI	VI	VI	VI
Pigmentation				Al	Clear	Al	Clear	Al	Clear	Al	Clear	Al	Clear	Al	Clear
74	64	(•)	(•)	60	105	90	138	100	109	90	106	86	104	84	110
73	64	(•)	(•)	61	104	90	138	96	112	90	108	86	105	83	111
73	63	(•)	(•)	61	105	90	138	96	111	90	108	86	105	83	111
90	40	2	Sunshine	75	133	113	83	55	130	104	128	101	130	99	122
94	52	5	do	80	128	116	71	45	127	100	128	107	122	104	120
63	97	9	Rain	78	116	116	*W*	*W*	120	100	112	105	115	99	138
65	99	11	do	80	115	106	----------	----------	126	110	111	110	110	101	150
92	52	17	Sunshine	86	125	125	----------	----------	135	111	136	104	135	105	*R*
74	35	31	do	83	*R*	122	----------	----------	*R*	112	*R*	110	*R*	112	----------
52	63	56	Cloudy	76	----------	110	----------	----------	----------	113	----------	110	----------	107	----------
50	90	67	Rain	88	----------	116	----------	----------	----------	118	----------	118	----------	116	----------
54	41	78	Sunshine	75	----------	112	----------	----------	----------	109	----------	108	----------	107	----------
52	43	93	Cloudy	76	----------	108	----------	----------	----------	107	----------	104	----------	106	----------
54	96	105	Rain	97	----------	120	----------	----------	----------	*S*	----------	*S*	----------	*S*	----------
30	56	121	Cloudy	69	----------	115	----------	----------	----------	114	----------	112	----------	116	----------
43	43	128	Sunshine	70	----------	96	----------	----------	----------	98	----------	95	----------	97	----------

(•) Exposed in laboratory conditioning room.

TABLE 3.—*Tautness and flexibility data obtained in aging tests of doped fabrics*—Continued

Panel number				73	74	75	76	77	78	79	80	81	82	83	84
Material				EC-d1	EC-d2	EC-d2	EC-d3	EC-d3	EC-d4	EC-d4	EC-d5	EC-d5	EC-d5	EC-d5	EC-d5
Formula				VI	VIA	VIA	VI	VI	VI	VI	IIB	IIB	IIA	IIA	II
Pigmentation				Al	Clear	Al	Clear	Al	Clear	Al	Clear	Al	Clear	Al	Clear
Exposure conditions															
Temperature	Relative humidity	Number of days on roof	Prevailing weather												
°F	*Percent*														
74	64	(*)	(*)	95	114	91	110	85	115	88	107	92	111	96	118
73	64	(*)	(*)	95	115	88	108	86	114	88	109	95	110	97	116
73	63	(*)	(*)	95	115	87	110	85	114	88	109	95	111	97	117
90	40	2	Sunshine	112	135	102	125	92	129	110	120	103	130	108	130
94	52	5	do	110	137	106	120	101	126	109	114	101	121	110	135
63	97	9	Rain	122	114	100	141	107	145	120	128	106	137	115	115
65	99	11	do	130	115	101	145	122	140	125	115	107	135	109	122
92	52	17	Sunshine	120	*R*	125	125	108	137	110	*R*	*R*	*R*	*R*	*R*
74	35	31	do	125	----------	112	125	106	135	107	----------	----------	----------	----------	----------
52	63	56	Cloudy	*R*	----------	*R*	*R*	105	*R*	107	----------	----------	----------	----------	----------
50	90	67	Rain	----------	----------	----------	----------	104	----------	102	----------	----------	----------	----------	----------
54	41	78	Sunshine	----------	----------	----------	----------	100	----------	106	----------	----------	----------	----------	----------
52	43	93	Cloudy	----------	----------	----------	----------	96	----------	111	----------	----------	----------	----------	----------
54	96	105	Rain	----------	----------	----------	----------	*S*	----------	*S*	----------	----------	----------	----------	----------
50	56	121	Cloudy	----------	----------	----------	----------	102	----------	109	----------	----------	----------	----------	----------
43	43	128	Sunshine	----------	----------	----------	----------	87	----------	98	----------	----------	----------	----------	----------

Panel number			85	86	87	88	89	90	91	92	93	94	95	96	97
Material			EC–d5 II A1	EC–d5 VI Clear	EC–d5 VI A1	EC–d5 VII A1	EC–d6 VI Clear	EC–d6 VI A1	BO–b1 III Clear	BO–b1 IV A1	BO–b1 VII A1	BO–b1 III A1	CR–b1 X Clear	CR–b1 X A1	MM–e1 IX A1
Formula															
Pigmentation															
74	64	(*)	111	106	83	85	112	88	121	104	101	101	130	98	98
73	64	(*)	108	105	88	86	113	91	125	102	103	105	133	99	96
73	63	(*)	109	105	87	85	113	90	124	102	103	103	131	99	97
90	40	2	122	124	110	100	124	106	135	125	119	120	155	130	125
94	52	5	125	120	103	103	120	101	130	122	120	120	143	125	120
68	97	9	117	135	114	115	132	115	120	114	103	107	114	92	103
65	99	11	113	135	114	120	135	118	127	109	104	115	120	85	107
92	53	17	*R*	126	110	107	124	105	*R*	135	132	125	*S*	127	135
74	35	31	------	*R*	118	100	*R*	113	------	120	122	128	------	130	118
83	63	56	------	------	113	113	------	100	------	113	115c	113c	------	115c	103
80	90	67	------	------	120	115	------	124	------	109	110c	114c	------	93c	107
54	41	78	------	------	113	104	------	105	------	113	123c	120c	------	150c	107
82	43	93	------	------	109	103	------	98	------	113	120c	114c	------	130c	100
74	35	105	------	------	118	100	*R*	113	------	120	122	128	------	130	118
83	63	121	------	------	113	*S*	------	*S*	------	113	115c	113c	------	115c	103
80	90	128	------	------	120	107	------	104	------	112	112c	117c	------	101c	90
54	41	96	------	------	*S*	107	------	104	------	112	112c	117c	------	136c	90
82	43	43	------	------	114	100	------	93	------	105	118c	107c	------	134c	95
					100										

(*) Exposed in laboratory conditioning room.

III. EFFECT OF VARIOUS FACTORS ON INITIAL TAUTNESS OF DOPED FABRICS

1. TYPE OF PLASTIC

The tautness values of the fabrics doped with the different plastic materials, measured in the conditioning room at 70° F and 65-percent relative humidity, are summarized in table 4. It will be noted that most of the cellulose plastics produced tautnesses ranging between 82

TABLE 4.—*Summary of tautening properties of various types of plastics used in dopes containing aluminum pigment*

Material	Number of samples tested	Formula used	Average deflection under 1-lb. load	Variation
			Mils	*Mils*
Cellulose acetate (hydrolyzed)	13	I	86	82 to 90.
Cellulose triacetate	1	IX	60	
Cellulose acetopropionate	7	I	91	*89 to 92.
Cellulose acetobutyrate	3	I	77	76 to 79.
Cellulose nitroacetate	1	I	83	
Cellulose nitrate	3	I	90	86 to 95.
Methylcellulose	1	XII	97	
Ethylcellulose	8	II	88	83 to 95.
Benzylcellulose	1	III	103	Most panels slack.
Chlorinated rubber	1	X	99	
Methyl methacrylate resin	1	XI	97	

* One panel read 76.

and 97. Cellulose triacetate and the cellulose acetobutyrate, which was also practically a triester, had average tautness values of 60 and 77, respectively. Great difficulty was experienced in obtaining a taut fabric with benzylcellulose. Plasticizer was omitted from most of the ethylcellulose dopes because of the comparatively poor tautening qualities of this type of cellulose derivative and its reported characteristic of forming flexible films without it. However, it was necessary to add plasticizer to the high ethoxyl compound (panels 74 and 75) because the unplasticized films of this material ringwormed spontaneously 1 day after doping. The resinous materials, such as chlorinated rubber and methyl methacrylate polymer, did not tighten the fabric as well as did most of the cellulosic materials. Solutions of butyl methacrylate and Methyl Cellosolve methacrylate polymers failed to tighten the fabric when applied in the same solvent mixture used for the methyl derivative.

2. ACYL OR ALKYL SUBSTITUTION

The data in table 3 indicate that varying the acetyl content of cellulose acetate between the limits of 2.29 and 2.57 equivalents did not have an apparent effect on the ability of the compound to tighten the fabric. Likewise, the results obtained with ethylcellulose containing from 2.43 to 2.77 ethoxyl equivalents did not show a correlation between ethoxyl content and tautening property. There was not sufficient variation in the acyl composition of the cellulose acetopropionates and cellulose acetobutyrates to indicate its effect on

tautness. Tests to determine this relationship are now under way on materials of this type having a greater variation in acyl content.

3. VISCOSITY

The absence of any effect of the size of the cellulose molecules, as indicated by the viscosity of solutions of these materials, on the tautening property is shown by the data in table 3. Cellulose acetates varying in viscosity from 2 to 94 seconds, as measured by the falling-ball test, did not differ markedly in their tautening ability. The same was true for ethylcelluloses whose 5-percent solutions in a mixture of 80 parts of toluene and 20 parts of ethyl alcohol gave viscosity values of 20 to 210 centipoises.

4. SOLVENT COMPOSITION

The results obtained with the different solvent formulas which were tested in this investigation lead to the rather startling conclusion that the most important single factor involved in the tautening property of a dope is the solvent composition employed. In the term "solvent composition" are included those organic liquids which form colloidal solutions of the cellulose derivatives, those which have only cosolvent and swelling action, and those which are merely diluents in the blend. It has been the usual practice to formulate the solvent composition on the basis of such requirements as drying time, antiblushing characteristics, solvent property, and economy, without an adequate appreciation that the choice of the solvent composition governs not only the tautening property of the dope but also the flexibility (conversely the brittleness) of the film deposited on the fabric.

TABLE 5.—*Effect of various solvent compositions on the production of tautness by cellulose dopes containing aluminum pigment*

Formulas	Cellulose acetate	Cellulose acetopropionate	Cellulose acetobutyrate	Cellulose nitrate	Ethylcellulose
	Mils	*Mils*	*Mils*	*Mils*	*Mils*
No. I	84	92	76	86	
No. VII	72	79	65	61	85
Methyl Cellosolve	67				
No. II					94
No. VI					86

Table 5 presents the data obtained on the effect of various solvent compositions on the tautness of the doped fabric. It will be noted that the difference in the tautness values of the two cellulose nitrate panels listed in this table is much greater than the tautness differences shown in table 4 for the various types of cellulose derivatives or for compounds varying only in viscosity and percentage substitution. Since these panels were prepared, the effect of various solvents and mixtures of solvents and nonsolvents on the shrinkage and flexibility of films of cellulose derivatives has been studied in detail. The solutions are poured into glass Petri dishes with and without a Cellophane lining. The film in contact with the glass provides information on the adhesive property of the composition and is also used to follow the

rate of drying. The film in contact with Cellophane is used to obtain an estimate of the amount of shrinking characteristic of the dope; in only a few instances has tenacious adherence of the film to Cellophane been noted. These tests are still in progress, but it may be noted here that they indicate that in order to obtain a maximum tautening effect it is necessary to formulate a dope so that a minimum of active solvent will be present during the final drying stage. Some solvent action is necessary in this stage to prevent precipitation (blushing) of the cellulose derivative. The selection of this solvent is an important factor in avoiding the formation of a brittle film, which Sheppard and Newsome [6] found to be associated with the presence of large crystallites. Thus, cellulose acetate dissolved in Methyl Cellosolve gave the maximum tautness for this cellulose derivative (table 5), but reference to table 3 shows that the film is brittle and ringworms after a few days' exposure on the roof. Likewise, cellulose acetobutyrate in formula VII (panel 52), which contains 25 percent of Methyl Cellosolve, tautens well but yields a brittle film. However, although our tests have not yet been completed, present indications are that it will be possible to formulate dopes with these cellulose derivatives which will tauten the fabric satisfactorily without yielding brittle films.

IV. EFFECT OF WEATHERING ON TAUTNESS OF DOPED FABRICS

In order to obtain comparative information on the effect of variations in temperature and humidity on the tautness of fabrics doped with various cellulose derivatives, it would be desirable to have all the panels at about the same initial tautness. This was not achieved with the panel tests reported in table 3. However, the tautnesses obtained with the cellulose compounds, using the solvent blend listed as formula VII, were more nearly alike than with any other composition. The variation in the tautness values obtained for these panels under different weather conditions is shown in figure 3.

The cellulose acetate panels were not markedly affected by the heat of the sun, but did slacken during periods of rain to a greater extent than any of the other cellulose derivatives. The cellulose acetopropionate panels also showed marked slackening in rainy weather after 3 months of exposure on the roof. The cellulose acetobutyrate and cellulose nitrate panels behaved about alike, becoming less taut when removed from the conditioning room into the sunlight and, in general, showing a slight additional decrease in tautness in rainy weather. The ethylcellulose and benzylcellulose panels were considerably poorer in initial tautness than those covered with the cellulose esters. Both of the cellulose ethers underwent a decrease in tautness in sunlight. During periods of rain the ethylcellulose panels showed additional slackening, whereas the benzylcellulose panels had a tendency to tighten.

It should be emphasized that the behavior of these cellulose films under various weather conditions with respect to both tautness and moisture absorption is dependent to a large extent upon the type and amount of plasticizer employed. For the above tests triphenyl

[6] S. E. Sheppard and P. T. Newsome. *Film formation with cellulose derivatives*, J. Soc. Chem. Ind. 56, 256T–261T (1937).

phosphate, present to the extent of 10 percent of the total nonvolatiles, was used throughout. In the course of the phase of our investigation dealing with the effect of plasticizers on tautness, both initially and upon exposure, compositions should become available which will have greater uniformity of tension under varying weather conditions.

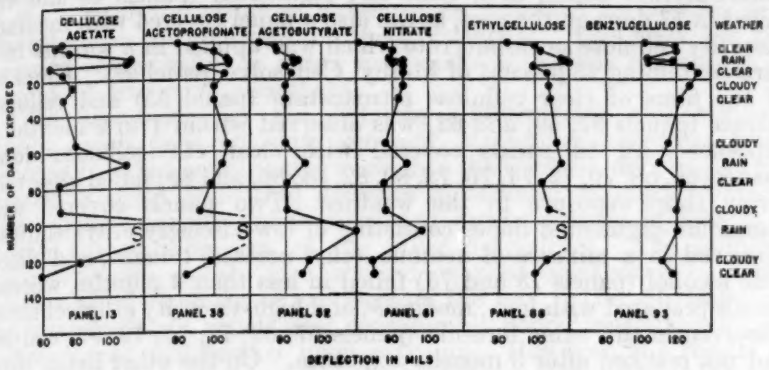

FIGURE 3.—*Variation in tautness of doped fabrics exposed on the roof.*

Formula VII was used for all of the dopes. "*S*" indicates slackness of the fabric. Weather conditions on the days when measurements were made were as follows:

Time on roof	Temperature	Relative humidity	Time on roof	Temperature	Relative humidity
Days	° *F.*	*Percent*	*Days*	° *F.*	*Percent*
2	90	40	31	74	35
5	94	52	56	52	63
9	63	97	67	50	90
10	64	98	78	54	41
11	65	99	93	51	43
13	86	62	105	54	96
17	92	52	121	30	56
24	72	74	128	43	43

V. EFFECT OF WEATHERING ON FLEXIBILITY OF THE DOPED FILM

The results of exposure tests on panels doped with the different cellulose derivatives, shown in table 3, must be considered as only tentative evidence of their relative stability. A formulation which yields a flexible and durable film with one derivative may produce a brittle and unstable film with another cellulose compound because of differences in their solubility. However, certain trends can be observed in the data in table 3. The cellulose acetate films are, in general, very stable to sunlight. The only panels which gave evidence of embrittlement were three covered with clear dope made from low-viscosity cellulose acetate (panels 1, 5, and 25), one panel covered with clear cellulose triacetate dope (panel 23), and one panel covered with aluminum-pigmented dope made by dissolving cellulose acetate of medium viscosity in Methyl Cellosolve (panel 14), in which case the embrittlement is directly attributable to the solvent employed. The clear dope films made with cellulose acetopropionates of various viscosities failed on five (panels 36, 38, 42, 44, and 46) of the seven

panels exposed. One panel covered with cellulose acetopropionate of low viscosity and containing aluminum pigment (panel 43) failed in 17 days on the roof. However, a sample of medium-viscosity cellulose acetopropionate of more recent manufacture than the rest showed good stability (panels 33, 34, and 35). The low-viscosity cellulose acetobutyrate dopes, both clear and pigmented (panels 48 and 49), failed in 17 days on the roof, as did also a panel covered with medium-viscosity cellulose acetobutyrate which was applied in a solvent mixture containing 25 percent of Methyl Cellosolve (panel 52). Cracking of the films of clear cellulose nitroacetate (panel 55) and cellulose nitrate (panels 57, 59, and 62) was observed within 1 to 2 months of exposure. All 12 panels covered with clear ethylcellulose dopes (panels 66, 68, 70, 72, 74, 76, 78, 80, 82, 84, 86, and 89) failed after relatively short exposure to the weather. Two panels covered with aluminum-pigmented dopes consisting of low-viscosity ethylcelluloses dissolved in a mixture of acetone, ethyl acetate, toluene, and diacetone alcohol (panels 73 and 75) failed in less than 2 months, whereas panels prepared with low-, medium-, and high-viscosity ethylcelluloses dissolved in this same formula (panels 67, 69, 71, 77, 79, 87, and 90) had not cracked after 3 months' exposure. On the other hand, three panels of pigmented medium-viscosity ethylcellulose applied in a mixture of toluene, ethyl alcohol, and acetone (panels 81, 83, and 85) failed in 17 days, which indicated that this particular formula apparently tends to lay down a film which is inherently brittle. The clear benzylcellulose film (panel 91) cracked and yellowed very soon after exposure. The pigmented benzylcellulose films (panels 92, 93, and 94) showed evidences of cracking after about 2 months of exposure, although the fabric was not tautened sufficiently for the typical "ringworm" type of failure to occur. The panels covered with methylcellulose (panels 64 and 65) showed remarkable tautness during the first week of exposure, but the methylcellulose was completely removed by the first rain. This action was, of course, anticipated, but the rapidity with which the aluminum-pigmented methylcellulose film was dissolved by the rain was rather surprising in view of the comparatively slow rate of solution of methylcellulose in the laboratory at ordinary temperature. The film of clear chlorinated rubber of low viscosity (panel 95) yellowed and disintegrated very rapidly upon exposure to sunlight. The pigmented film (panel 96) cracked in a manner similar to the benzylcellulose films after about 2 months' exposure. The pigmented methyl methacrylate film (panel 97) did not show any evidence of cracking after 3 months on the roof.

VI. SUMMARY AND CONCLUSIONS

1. The tautnesses of airplane fabric doped with various plastics dissolved in a variety of solvent mixtures were determined. It was observed that the most important single factor involved in the initial tautening property of a dope is the solvent composition. In order to obtain a maximum tautening effect, it is necessary to formulate a dope so that a minimum of active solvent will be present during the final drying stage. The selection of this solvent is also an important factor in avoiding the formation of a film which is initially brittle or which rapidly becomes brittle upon exposure out of doors.

2. The highest initial-tautness values were obtained with cellulose triesters, such as cellulose triacetate and a practically completely acylated cellulose acetobutyrate. Varying the acyl or ethoxyl content of partially hydrolyzed cellulose derivatives did not have a pronounced effect on the ability of the compounds to tighten the fabric. The initial tautening property is also apparently independent of the size of the cellulose molecule, as indicated by certain flow characteristics of solutions of these materials. The tests for the majority of the cellulose esters were made with films containing 10 percent of triphenyl phosphate.

3. In exposure tests the cellulose acetobutyrate and cellulose nitrate panels behaved quite similarly, slackening somewhat when removed from the conditioning room into the sunlight, and, in general, showing a slight additional decrease in tautness in rainy weather. The cellulose acetate panels slackened during periods of rain to a greater extent than any of the other derivatives. The cellulose acetopropionate panels also showed marked slackening in rainy weather after 3 months of exposure on the roof. The ethylcellulose and benzylcellulose panels were considerably poorer in initial tautness and slackened still further upon exposure. However, the results of these exposure tests must be considered as only exploratory and preliminary to the testing of dopes formulated to develop optimum tautness, flexibility, and moisture resistance. Before dopes having these characteristics can be formulated, it will be necessary to obtain detailed information on the effect of various solvents, diluents and plasticizers on the properties of the film-forming plastics.

This investigation was sponsored by the Bureau of Aeronautics, U. S. Navy Department, and the results are published by permission of the chief of that Bureau. The authors express their appreciation of the interest and suggestions during the course of this work of Lieut. Comdr. C. F. Cotton and J. E. Sullivan of the Bureau of Aeronautics, and of C. W. Woodrow of the Naval Aircraft Factory.

WASHINGTON, January 15, 1938.

U. S. Department of Commerce National Bureau of Standards

RESEARCH PAPER RP1099

Part of Journal of Research of the National Bureau of Standards, Volume 20, May 1938

MINIMUM PERCEPTIBLE COLORIMETRIC PURITY AS A FUNCTION OF DOMINANT WAVE LENGTH

By Irwin G. Priest and Ferdinand G. Brickwedde *

[Editorial Note.—In February 1926, Priest and Brickwedde presented the results of their study of colorimetric purity before the Optical Society of America and an abstract, carrying the title given above, appeared in the J. Opt. Soc. Am. and Rev. Sci. Instr. **13**, 306 (1926). The work had not been prepared for publication at the time of Mr. Priest's death, and Dr. Brickwedde is now working in another field. Therefore, at the suggestion of the Director of the National Bureau of Standards, the writer has undertaken the preparation of this article.—Deane B. Judd.]

ABSTRACT

A 4° square, two-part photometric field, symmetrical about a vertical division and viewed through a pupil 3 mm in diameter, is illuminated in both parts by artificial sunlight at a constant brightness of about 3 or 4 mL (retinal illumination, 70 to 90 photons) with a surrounding field of about 0.5 mL. Homogeneous light is added to one half, and sunlight simultaneously subtracted so that the field remains matched in brightness. Two adjustments of the mixture are made: (1) The least purity perceptible with certainty (p_{max}), and (2) the greatest imperceptible purity (p_{min}). The purity of these mixtures is then measured, increased accuracy being obtained by measuring a known large multiple of the homogeneous brightness. Values of p_{max} and p_{min} have been obtained as a function of the wave length of the homogeneous component; these values are reported in detail, and some discussion of their interpretation is given.

CONTENTS

	Page
I. Introduction	673
II. Procedure	674
1. Adjustment of the mixture	674
2. Photometric measurement of the components	674
3. Precautions and auxiliary studies	675
III. Results	676
IV. Discussion	679
1. Comparison with other work	679
2. Interpretation	681

I. INTRODUCTION

This work is undertaken as a part of a program of research on determination and correlation of the characteristics of vision outlined by Priest [1] in 1921 when he listed as one of the functions to be determined, "Saturation sensibility—the least change in purity perceptible as a change in saturation." This work deals with saturation sensibility near zero purity.[2] It is therefore of particular interest in the colorimetry of illuminants closely resembling sunlight in color

*Research Associate at the National Bureau of Standards, representing the Munsell Research Laboratory, July 1925 to June 1926.

[1] Irwin G. Priest, *The spectral distribution of energy required to evoke the gray sensation*, BS Sci. Pap. 17, 231 (1922) S417 (see Appendix, p. 260).

[2] For a definition of colorimetric purity, see Irwin G. Priest, *Apparatus for the determination of color in terms of dominant wave length, purity, and brightness*, J. Opt. Soc. Am. and Rev. Sci. Instr. 8, 173 (1924); Irwin G. Priest, *The computation of colorimetric purity*, J. Opt. Soc. Am. and Rev. Sci. Instr. 9, 503 (1924).

and in the colorimetry of nearly achromatic surface colors viewed under such illuminants; it bears importantly upon the question of tolerances in the specification of such colors and upon the determination of nearest color temperatures [3] by means of which such illuminants are customarily specified.

II. PROCEDURE

1. ADJUSTMENT OF THE MIXTURE

A 4° square, two-part photometric field, symmetrical about a vertical division and viewed through a pupil 3 mm in diameter, was illuminated in both parts by Abbot-Priest sunlight [4] at a constant brightness of about 3 or 4 mL (retinal illumination, 70 to 90 photons) with a surrounding field of about 0.5 mL.[5] Homogeneous light was added to the right half of the field and sunlight simultaneously subtracted so that the right half of the field remained matched in brightness with the unchanged left half. Two adjustments of the mixture in the right half-field were made. First the proportion (p) of homogeneous light in the mixture was increased until the observer perceived a definite chromaticity difference between the sunlight in the left half and the mixture in the right; this is called a setting of the least purity perceptible with certainty (p_{max}). The observer then decreased the proportion of homogeneous light in the mixture until the chromaticity difference just disappeared. This second adjustment is called the greatest imperceptible purity (p_{min}). The average between a setting of least perceptible difference and a setting of greatest imperceptible difference is thought to be a more reliable indication of sensibility than either one taken alone; it has sometimes been called the "doubtful difference." [6] Accordingly, this average has also been computed and is referred to as (p_{mean}).

2. PHOTOMETRIC MEASUREMENT OF THE COMPONENTS

After each adjustment (either of least perceptible or greatest imperceptible difference) the observer made a photometric measurement of the components of the mixture from which the purity (p_{max} or p_{min}) may be computed. One of two photometric methods was used.

In the equality-of-brightness method, the nonselective filter in the homogeneous beam was removed. Since this filter was usually either of 5- or 10-percent transmission, the homogeneous component by this operation was increased either twentyfold or tenfold. Then the observer decreased the sunlight component of the right half of the field until the brightness was again judged equal to that of the left half which remained unaltered throughout. The reduction in sunlight component was accomplished by increasing the distance of the lamp from a diffusing screen; it may therefore be expressed as a simple function of this distance (essentially the inverse-square law). This reduction is equal to a known multiple (usually about 19 or 9) of the homogeneous brightness, and thus permits the ratio of homogeneous

[3] R. Davis, *A correlated color temperature for illuminants*, BS J. Research 7, 659 (1931) RP365.

[4] Irwin G. Priest, *A precision method for producing artificial daylight*, Phys. Rev. [2] 11, 502 (1918); J. Opt. Soc. Am. and Rev. Sci. Instr. 12, 479 (1926). D. B. Judd, *Reduction of data on mixture of color stimuli*, BS J. Research 4, 525 (1930) RP163.

[5] Irwin G. Priest, *Apparatus for the determination of color in terms of dominant wavelength, purity, and brightness*, J. Opt. Soc. Am. and Rev. Sci. Instr. 8, 173 (1924).

[6] D. B. Judd, *Sensibility to color-temperature change as a function of temperature*, J. Opt. Soc. Am. 23, 7 (1933).

brightness component to brightness of the mixture to be computed. This ratio is the colorimetric purity of the mixture.

The equality-of-brightness method is convenient but it is open to two criticisms: First, the field size (4° square) is larger than that to which the standard luminosity function recommended by the International Commission on Illumination applies,[7] and second, the observer has to make the photometric match with a considerable chromaticity difference (sometimes amounting to 20 least perceptible differences) between the two halves of the field. Accordingly, for about half of the work, the brightnesses of the components of the mixture were obtained by flicker photometry.

In the flicker method a 2° diaphragm was substituted for the rectangular 2 by 4° opening constituting the mixture field. The nonselective filter in the homogeneous beam was removed, and the flicker disk interrupting the homogeneous beam with sunlight of brightness variable by an auxiliary photometer was set into rotation at a suitable speed. Adjustment of the auxiliary photometer for minimum flicker yields a measure of the brightness of this known multiple of the homogeneous component. From this brightness and the known constant brightness of the photometric field the purity of the mixture (p_{max} or p_{min}) was computed.

3. PRECAUTIONS AND AUXILIARY STUDIES

The wave-length scale was calibrated by reference to the lines of the helium emission spectrum. Stray light in the spectrum was measured and stray-light filters used in the extremes of the spectrum over the whole region within which stray light would introduce appreciable errors. This is particularly important for the short-wave region of the spectrum.

A special check was made (observer IGP) of the slit-width errors. These errors can be shown by computation to be negligible in comparison with the inherent uncertainty of liminal settings even for the rather large slit widths used (10 mμ). The experimental check corroborated the computations.

A special study was made (observer FGB) of the variation of p_{max} and p_{min} taken on different days over a period of 6 weeks. It was found that there was no regular variation from day to day, but the mean for a given day varied on the average from the mean on another day by more than would be expected from the theory of errors. This is probably to be ascribed to a change in criterion of what constitutes a "just perceptible" and a "just imperceptible" difference; such variations are common, and indeed, characteristic of liminal settings.[8] The conclusions from this study were used in a special determination of the wave length of the maximum value of p_{mean} (observer, FGB). This determination was carried out by making one setting only of p_{max} and p_{min} at one wave length (565.0 mμ) somewhat lower than that which preliminary determination indicated for the maximum, then a single determination approximately at the wave length of the maximum (567.5 mμ), and finally a single determination at a wave length (570.0 mμ) slightly above that for the maximum. After a rest

[7] K. S. Gibson and E. P. T. Tyndall, *The visibility of radiant energy*, BS Sci. Pap. 19, 131 (1923-24) S475. Proc. Int. Comm. on Illum., 6th meeting, Geneva, 1924 (University Press, Cambridge, England) p. 67 and 232 (1926).

[8] See, for example, D. B. Judd, *Precision of color temperature measurements under various observing conditions; a new color comparator for incandescent lamps*, BS J. Research 5, 1164 (1930) RP252.

period, the observer repeated the series starting with the higher wave length. In this way, changes in criteria were avoided (long-time fluctuations), and practice and fatigue effects (short-time fluctuations) reduced. From this work it was concluded that the wave length at which p_{mean} is a maximum is for this observer (FGB, left eye) 568.0± 1.0 mμ.

III. RESULTS

Figure 1 shows on a logarithmic scale as a function of wave length the result of every separate determination taken by IGP by the flicker method. Figure 2 similarly shows those taken by FGB.

Table 1 gives the average values of p_{mean} for each observer. These averages were obtained by plotting points representing the averages of the groups of points shown on figures 1 and 2 on a logarithmic scale together with similar points derived from data obtained with the equality-of-brightness method. Smooth curves were drawn among these points, greater weight being given to the flicker determinations. The flicker method is not open to the two criticisms of the equality-of-brightness method discussed in the previous section, and it has the further advantage of greater precision in the measurement of the smaller homogeneous brightnesses. This greater precision is particularly marked for the extremes of the spectrum (400 to 450 mμ, 630 to 680 mμ); in these regions it sometimes happened that the equality-of-brightness method even gave negative values for p_{min} in spite of the nature of the experiment, which insures that some amount of homogeneous component greater than zero must be added. It will be understood, however, that even when increased by ten- or twenty-fold these very small homogeneous brightnesses added to the sunlight component may fall below the differential limen for equality-of-brightness settings. It may therefore be concluded that the addition to sunlight of small amounts of light from the extremes of the spectrum are detectable as chromaticity differences long before they become detectable as brightness differences.

The only regular difference observed between the flicker and equality-of-brightness methods is that for the long-wave half of the spectrum the flicker method gave generally higher results. This is to be expected from the smaller field size, and since greater interest attaches to photometric results in accord with this smaller field size, the general course of the flicker determinations was followed closely in drawing the curve. The greater weight attached to the flicker determinations was therefore of two kinds: That attached to more representative photometric observing conditions, and that to determinations of higher precision.

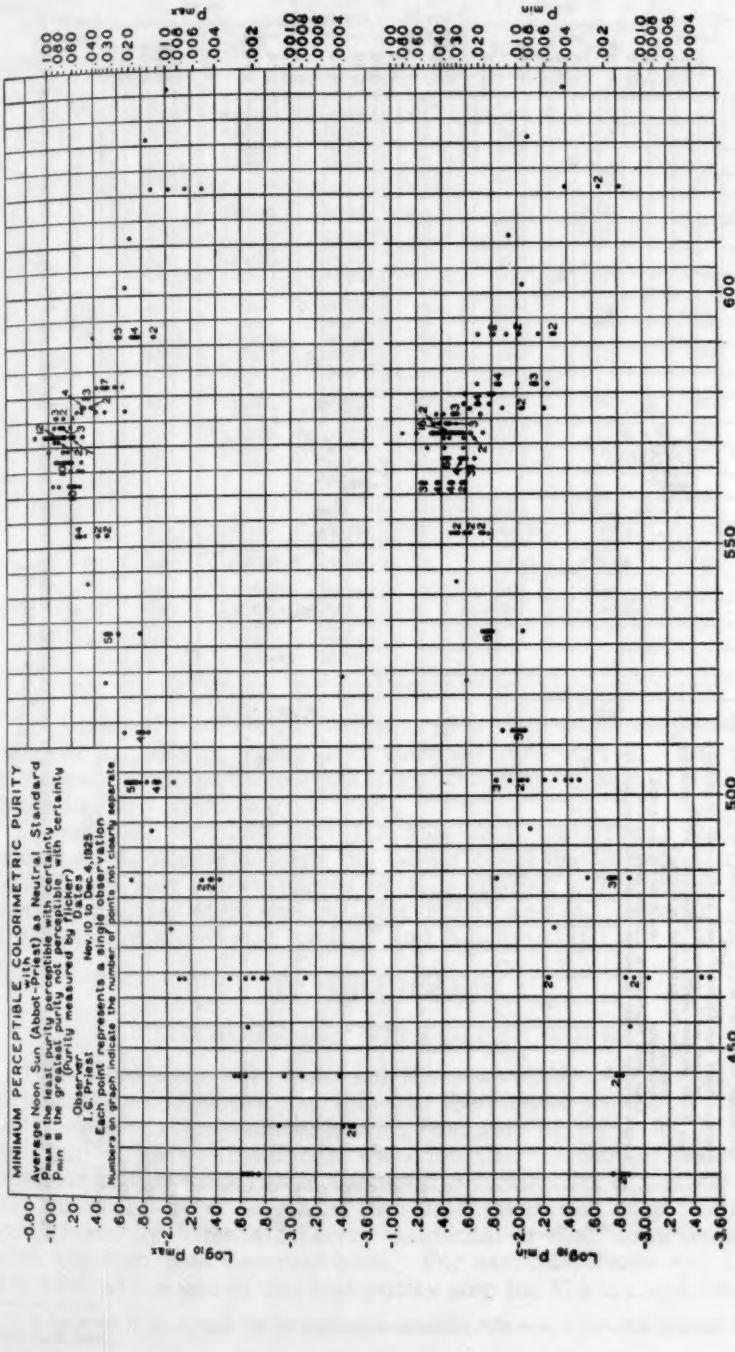

FIGURE 1.—*Individual observations of minimum perceptible colorimetric purity (observer IGP), mixture analyzed by flicker method.*

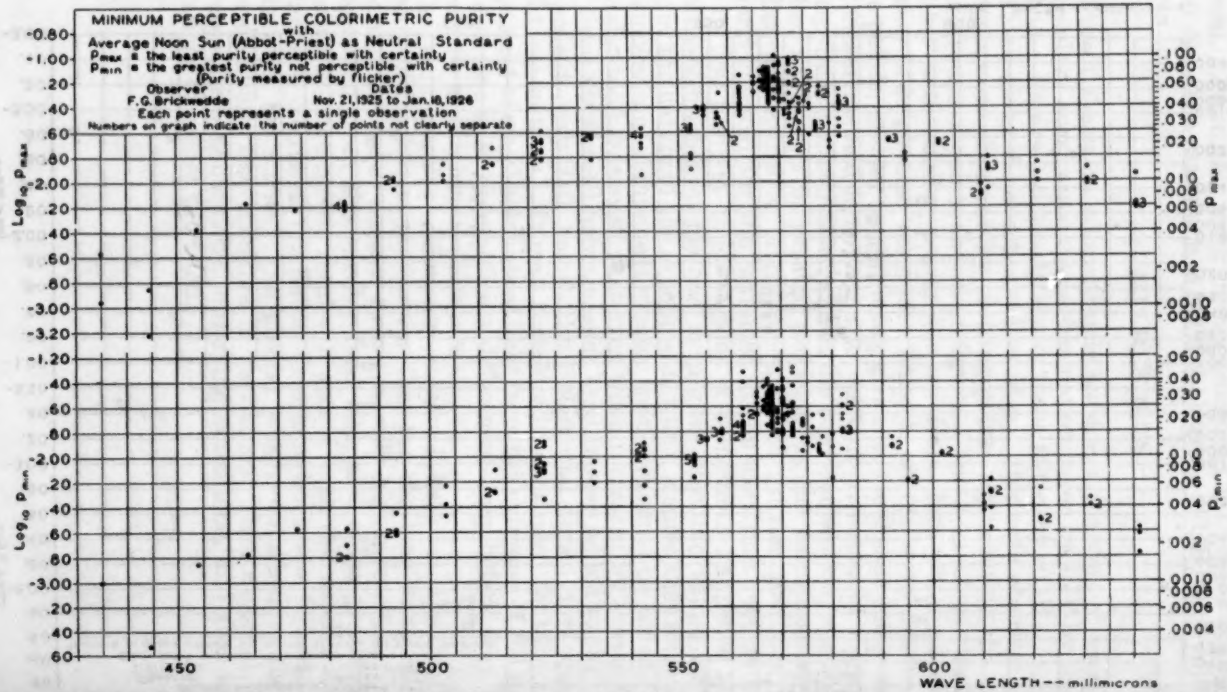

FIGURE 2.—*Individual observations of minimum perceptible colorimetric purity (observer FGB), mixture analyzed by flicker method.*

TABLE 1.—*Minimum perceptible colorimetric purity*

Wave length	p_{mean}		Average p_{mean}	Wave length	p_{mean}		Average p_{mean}
	IGP	FGB			IGP	FGB	
mμ				mμ			
405	0.00105	0.0013	0.00118	557.5	0.0340	0.0272	0.0306
10	.00105	.0015	.00128	60	.0387	.0322	.03545
20	.0011	.00195	.00152	62.5	.0454	.0374	.0414
30	.00115	.0024	.00178	65	.0516	.0422	.0469
35	.0012			67.5	.0564	.0447	.05055
40	.0013	.00305	.00218	568		.0447	
45	.0014			70	.0594	.0432	.0513
50	.0016	.00375	.00268	71.5		.0405	
55	.0019	.00405	.00298	72.1	.0604		
60	.00235	.0043	.00332	72.5	.0603	.0364	.04835
65	.00315	.0044	.00378	73.5	.0595	.0306	.04505
70	.0043	.0045	.0044	75	.0548	.0262	.0405
75	.00535	.0046	.00498	76	.0452		
80	.00635	.0047	.00552	77.5	.0340	.0229	.02845
85	.0074	.0050	.0062	78.5	.0289		
90	.0086	.00565	.00712	80	.0258	.0208	.0233
95	.00995	.0065	.00822	82.5	.0226		
500	.0115	.00755	.00952	85	.0206	.0176	.0191
05	.0131	.00875	.01092	90	.0176	.0150	.0163
10	.0149	.0102	.01255	600	.0137	.0114	.01255
15	.0169	.0118	.01435	10	.0111	.0087	.0099
20	.0190	.0132	.0161	20	.0090	.0073	.00815
25	.0214	.0143	.01785	30	.00745	.00685	.00715
30	.0238	.0148	.0193	40	.0062	.00655	.00638
35	.0264	.01495	.02068	50	.00545	.00635	.0059
40	.0286	.01505	.02182	60	.0051	.0062	.00565
45	.0300	.0152	.0226	70	.0049	.006125	.00551
50	.0308	.0166	.0237	80	.00485	.00605	.00545
52.5	.0312	.0189	.02505				
55	.0320	.0225	.02725				

The values of the first two columns in table 1 were computed from values of p_{max} and p_{min} read from these adopted curves. The values in the last column of table 1 are the arithmetical means of the values in the first two columns.

Figure 3 shows (solid curve) a plot on a logarithmic scale of a smooth curve drawn through the values given in the last column of table 1. It also shows curves of p_{max} (dotted curve, arithmetical mean of p_{max} for IGP and p_{max} for FGB) and p_{min} (dashed curve, arithmetical mean of p_{min} for IGP and p_{min} for FGB).

IV. DISCUSSION

1. COMPARISON WITH OTHER WORK

When these data were obtained there was only one investigation with which to compare them; this was the pioneer work of Jones and Lowry[9] on saturation scales extending from zero purity to the spectrum (unit purity) for eight different wave lengths. Although subsequent repetition of this work has in the main corroborated it, the variation with dominant wave length of the first saturation step from zero purity found by Jones and Lowry incidental to their main purpose is much less than that reported here. For example, Jones and Lowry give 0.035 as the size of the first purity step for 575 mμ and 0.025 for

[9] L. A. Jones and E. M. Lowry, *Retinal sensibility to saturation differences*, J. Opt. Soc. Am. and Rev. Sci. Instr. 13, 25 (1926).

440 mμ; this is a variation by a factor of about 1.4, while from table 1 the corresponding variation is by a factor of about 18.

Since 1926, however, p_{max} has been redetermined by no less than three independent investigations, those by Purdy,[10] by Martin, Warburton, and Morgan,[11] and by Wright and Pitt,[12] Purdy investigated the change in p_{max} with field brightness, and therefore extended the scope of his work over that of the present results in an important particular; but he used stimuli of relatively few wave lengths (8) over

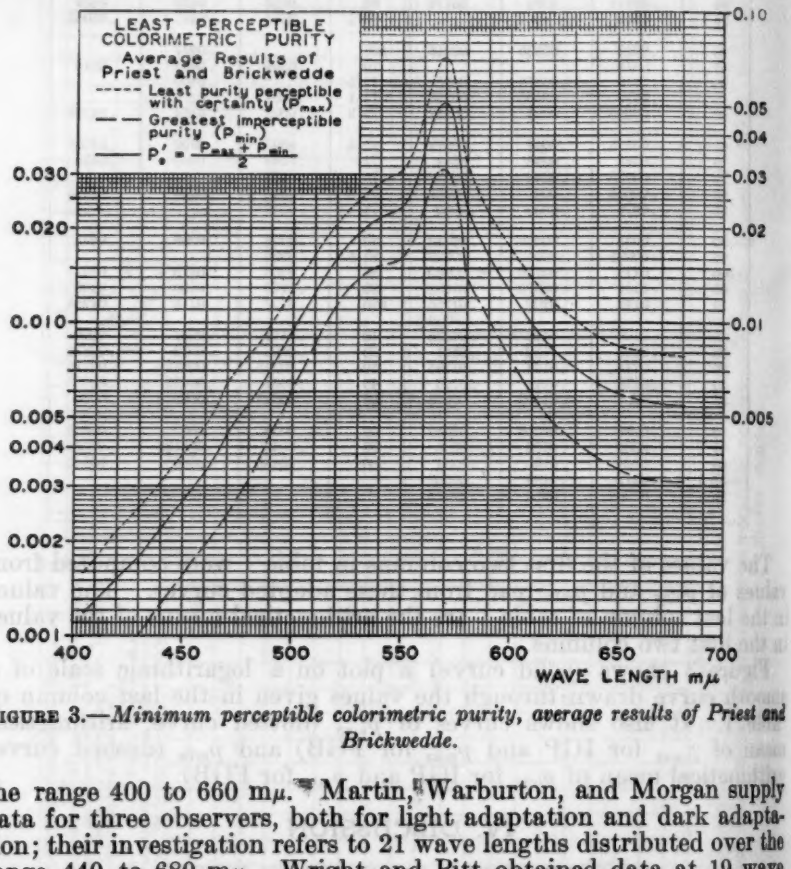

FIGURE 3.—*Minimum perceptible colorimetric purity, average results of Priest and Brickwedde.*

the range 400 to 660 mμ. Martin, Warburton, and Morgan supply data for three observers, both for light adaptation and dark adaptation; their investigation refers to 21 wave lengths distributed over the range 440 to 680 mμ. Wright and Pitt obtained data at 19 wave lengths distributed uniformly over the range 470 to 650 mμ. In each of these investigations the results completely corroborate within experimental error those previously obtained by Priest and Brickwedde, with exceptions arising only from the fact that the Priest-Brickwedde results cover a greater wave-length range more thoroughly than any other investigation.

[10] D. McL. Purdy, *On the saturations and chromatic thresholds of the spectral colours*, Brit. J. Psychol. (Gen. Sec.) **21** (pt. 3), 283 (1931).

[11] L. C. Martin, F. L. Warburton, and W. J. Morgan, Determination of the Sensitiveness of the Eye to Differences in the Saturation of Colours, Medical Research Council, Reports of the Committee upon the Physiology of Vision, XIII, Special Report Series, No. 188 (London, 1933).

[12] W. D. Wright and F. H. G. Pitt, *The saturation-discrimination of two trichromats*, Proc. Phys. Soc. (London) **49**, 329 (1937).

There can therefore be no doubt remaining as to the essential correctness of the data presented here completely for the first time.[13]

2. INTERPRETATION

Through the courtesy of Mr. Priest these data were, in advance of publication, placed at the disposal of Dr. Selig Hecht and the writer. By an extension of the Young three-component theory of vision Hecht has shown that these data are consistent with sensibility to wave-length change in the spectrum and roughly consistent with the mixture data of the OSA "excitation" curves, used for many years as a definition of normal vision.[14] These data have formed an important basis for Hecht's further theoretical papers, in which he has shown that they may be completely harmonized with the OSA curves.[15] Judd has shown by an empiric relation that these data are consistent with many other chromaticity-sensibility functions and are approximately consistent both with the mixture data and coordinate system of the OSA "excitation" curves,[16] and he has also shown by a special transformation of coordinates that these data are in precise agreement with the mixture data of the standard observer adopted in 1931 by the International Commission on Illumination.[17]

From their appearance in summarized form in these publications, the Priest-Brickwedde data have continued to spread [18] and in this way have already exerted a considerable influence on modern developments in visual theory.

It is probably worth noting that Priest for some time held the view that p_{mean} should duplicate very closely the luminosity function. This caused him to remark [19] "Least perceptible purity is largely dependent upon visibility; the relative amounts of *energy* required to introduce a hue difference show comparatively small variation with wave length," and to view with suspicion the presence (see fig. 3) of the marked maximum quite definitely removed (570 mμ) from the wave length of maximum spectral luminosity (555 mμ). He was inclined to the belief that if a truly achromatic stimulus were to be substituted for the rather greenish-yellow artificial sunlight then this pronounced maximum at 570 mμ would no longer be found. This belief led him to remark, "Further extensive investigation of least perceptible purity should be prefaced by a definite adoption of a neutral standard."

The present view of this maximum at 570 mμ is that it indicates sunlight to be more confusible in chromaticity with 570 mμ than with any

[13] Martin, Warburton, and Morgan (see footnote 11, p. 680) give a discussion of possible sources of unreliability of the Jones-Lowry data. See, also, D. B. Judd, *Chromaticity sensibility to stimulus differences*, J. Opt. Soc. Am. **22**, 95 (1932).

[14] Selig Hecht, *The development of Thomas Young's theory of color vision*, J. Opt. Soc. Am. **20**, 231 (1930). The tentative theoretical curves in this paper do not completely harmonize mixture data for the normal eye with the Priest-Brickwedde data; consult D. B. Judd, *The mixture data embodied in the tentative curves of Hecht's theory of vision*, J. Opt. Soc. Am. **20**, 647 (1930); this deviation has been taken care of in Hecht's subsequent formulation of Young's idea.

[15] Selig Hecht, *The interrelation of various aspects of color vision*, J. Opt. Soc. Am. **21**, 615 (1931); A Quantitative Formulation of Colour-Vision, Report of a Joint Discussion of Vision, The Physical and Optical Societies, June 1932; The Retinal Processes Concerned with Visual Acuity and Color Vision, Bulletin No. 4, Howe Laboratory of Ophthalmology, Harvard Medical School (Harvard University Press, Cambridge, Mass., August 1931.)

[16] D. B. Judd, *Chromaticity sensibility to stimulus differences*, J. Opt. Soc. Am., **22**, 72 (1932).

[17] D. B. Judd, *A Maxwell triangle yielding uniform chromaticity scales*, J. Research NBS **14**, 41 (1935); RP755; J. Opt. Soc. Am. **25**, 24 (1935).

[18] See, for example, J. F. Schouten, *Grundlagen einer quantitativen Vierfarbentheorie*. I, Proc. Konink Akad. Wetenschappen Amsterdam **38**, No. 6 (1935). Schouten, like Hecht, has shown an approximate correspondence between mixture data for the normal eye and the Priest-Brickwedde data by resort to a certain form of visual theory.

[19] I. G. Priest and F. G. Brickwedde, *The minimum perceptible colorimetric purity as a function of dominant wave length with sunlight as neutral standard*, J. Opt. Soc. Am. and Rev. Sci. Instr. **13**, 306 (1926).

other part of the spectrum. On the basis of this conclusion, a new coordinate system was derived,[20] which has not only been successful in coordinating chromaticity sensibility data of various sorts but has also proved to be useful in practical specification of color tolerances and in the estimation for practical purposes of nearest chromaticity from a chromaticity series.[21] The success of these colorimetric procedures can largely be traced to the Priest-Brickwedde data.

WASHINGTON, January 2, 1938.

[20] D. B. Judd, *A Maxwell triangle yielding uniform chromaticity scales*, J. Research NBS **14**, 41 (1935) RP758; J. Opt. Soc. Am. **25**, 24 (1935).

[21] D. B. Judd, *A method for determining whiteness of paper*, Paper Trade J., Tech. Sec. **100**, 266 (1935); **102**, 154 (1936); Tech. Assn. Papers, series 18, 392 (1935); series 19, 359 (1936).
H. J. McNicholas, *Color and spectral transmittance of vegetable oils*, J. Research NBS **15**, 90 (1935) RP818; Oil and Soap **12**, 167 (1935).
D. B. Judd, *Estimation of chromaticity differences and nearest color temperature on the standard 1931 ICI colorimetric coordinate system*, J. Research NBS **17**, 771 (1936) RP944; J. Opt. Soc. Am. **26**, 421 (1936).
H. J. McNicholas, *Selection of colors for signal lights*, J. Research NBS **17**, 955 (1936) RP956.
D. B. Judd, *Surface color*, J. Opt. Soc. Am. **25**, 44 (1935).
F. C. Breckenridge and W. R. Schaub, *Rectangular uniform-chromaticity-scale coordinates*, J. Opt. Soc. Am. **27**, 226 (1937).
D. L. MacAdam, *Projective transformations of ICI color specifications*, J. Opt. Soc. Am. **27**, 294 (1937).

U. S. DEPARTMENT OF COMMERCE NATIONAL BUREAU OF STANDARDS

RESEARCH PAPER RP1100

Part of Journal of Research of the National Bureau of Standards, Volume 20, May 1938

APPLICATION OF VERTICAL-INCIDENCE IONOSPHERE MEASUREMENTS TO OBLIQUE-INCIDENCE RADIO TRANSMISSION

By Newbern Smith

ABSTRACT

An extension of the transmission curves described in a previous paper is given. The effects of the earth's curvature and magnetic field are considered, as well as absorption or reflection from lower ionosphere layers. A chart is included for rapid calculation of transmission curves.

CONTENTS

		Page
I.	Introduction	683
II.	Effect of the earth's curvature	683
III.	Effect of the earth's magnetic field	698
IV.	Behavior of the wave below the point of reflection	702
V.	Angle of departure and arrival of the waves	704
VI.	Determination of sec ϕ_0	704
VII.	Transmission factors	705
VIII.	Conclusions	705

I. INTRODUCTION

In a recent number of this Journal[1] the author outlined a graphic method of obtaining, from vertical-incidence ionosphere measurements, the limiting frequencies and virtual heights of reflection of radio waves incident obliquely upon the ionosphere. In that paper was developed a type of "transmission curve" which, when superimposed on a curve of frequency against virtual height, measured at vertical incidence, gave directly the virtual height of reflection for a given frequency at a given distance. A logarithmic sec ϕ_0 transmission curve was also described by which, for a given distance, one curve could be used to determine the heights, to a fair approximation, at any frequency.

It is the purpose of the present paper to evaluate in more detail the effect of the earth's curvature upon the ray theory of ionosphere transmission, to indicate the modifications consequently necessitated in the application of the transmission curves, and to consider briefly how the earth's field may affect limiting frequencies and virtual heights.

II. EFFECT OF THE EARTH'S CURVATURE

The influence of the earth's magnetic field will be neglected in this section. In the next section the effect of the magnetic field on radio

[1] Newbern Smith. *Extension of normal-incidence ionosphere measurements to oblique-incidence radio transmission.* J. Research NBS **19**, 89 (1937) RP1013.

transmission will be considered for the case of the plane earth, and it will be assumed that the results hold approximately for the curved earth, also.

The elementary theory of propagation of electromagnetic waves in an ionized medium whose surfaces of equal ionic density are planes

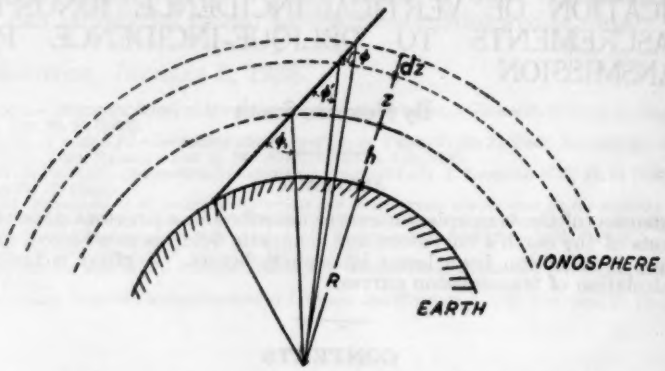

FIGURE 1.—*Variation, with height, of angle a straight line makes with the normal to the earth's surface.*

shows that, by Snell's law, the waves will penetrate the medium until the refractive index μ' is reduced to the value $\sin \phi_1$, where ϕ_1 is the angle of incidence of the waves upon the ionosphere, i. e., the angle the wave normal makes with the vertical on entering the ionosphere. To obtain the corresponding relation for a curved ionosphere it is necessary to consider the variation in the angle ϕ which a straight line makes with the vertical, or normal to the earth's surface, at various altitudes (z).

The geometry of figure 1 leads to the relation

$$\sin \phi' = \sin \phi \left(1+\frac{dz}{R+h+z}\right). \tag{1}$$

Assuming Snell's law to be valid for a ray traversing an infinitely thin layer of the ionosphere, of thickness dz, we can use this relation to obtain the differential equation:

$$\frac{d(\mu' \sin \phi)}{\mu' \sin \phi} = -\frac{dz}{R+h+z}$$

Integrating this from the lower boundary of the ionosphere, where $\mu'=1$, $\phi=\phi_1$, and $z=0$ (see fig. 2) up to the altitude z, we get

$$\mu' \sin \phi = \frac{\sin \phi_1}{1+\frac{z}{R+h}} \tag{2}$$

as the form of Snell's law appropriate to the curved earth.

This means that the wave will penetrate the curved ionosphere until the refractive index μ' is reduced to the value μ_0', given by

$$\mu_0' = \frac{\sin \phi_1}{1+\frac{z_0}{R+h}}, \tag{3}$$

where ϕ_1 is the angle of incidence of the wave on the lower boundary of the ionosphere and z_0 is the maximum height of penetration above this lower boundary.

From the geometry of figure 1, we have also

$$\sin \phi_1 = \sin \phi' \left(1+\frac{z}{R+h}\right). \tag{1a}$$

If we put $\phi' = \phi_0$ and $z = z_v$, the values which these quantities have at the top of the equivalent triangular path in figure 2, this becomes

$$\sin \phi_1 = \sin \phi_0 \left(1+\frac{z_v}{R+h}\right), \tag{4}$$

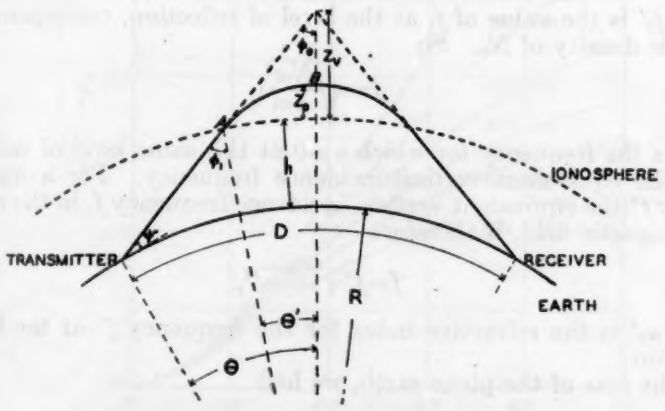

FIGURE 2.—*Transmission through curved ionosphere.*

z_v=height of equivalent triangular path; z_0=true height of reflection, at level where $\mu' = \sin \phi_1 \left(1-\frac{z_0}{R+h}\right)$, R=radius of earth; and D=distance of transmission.

and so the refractive index at the level of reflection must be

$$\mu_0' = \sin \phi_0 \frac{\left(1+\frac{z_v}{R+h}\right)}{\left(1+\frac{z_0}{R+h}\right)} \tag{5}$$

instead of $\mu_0' = \sin \phi_0$, as is the case for the plane earth.

If, as is usually the case, the penetration $z_0 << R+h$, we may write this condition

$$\mu_0' = \sin \phi_0 \left(1+\frac{z_v - z_0}{R+h}\right) \tag{5a}$$

The effect of the earth's curvature is thus to cause the radio wave to be reflected from a region of smaller ionization density than would be necessary were the earth flat.

In considering the problem of radio transmission over a distance, it will often be convenient to speak of an "equivalent vertical-incidence frequency" for the given wave frequency and transmission path. This is the frequency which is reflected at vertical incidence at the same height and undergoes approximately the same absorption as does the actual wave at oblique incidence. It will be denoted by f, and the actual wave frequency will be denoted by f'.

Since, for a frequency f',

$$\mu=\sqrt{1-\frac{Ne^2}{\pi m f'^2}}=\sqrt{1-\frac{f_0^2}{f'^2}},$$

where $f_0=\sqrt{\frac{Ne^2}{\pi m}}$,[2 3] it follows that reflection of this frequency will take place at a level where

$$\mu_0'=\sqrt{1-\frac{f_0'^2}{f'^2}},$$

where f_0' is the value of f_0 at the level of reflection, corresponding to an ionic density of N_0. So

$$f=\sqrt{\frac{N_0e^2}{\pi m}},$$

and f is the frequency for which $\mu=0$ at this same level of reflection, i. e., the equivalent vertical-incidence frequency. For a wave frequency f' the equivalent vertical-incidence frequency f, in the absence of a magnetic field, is therefore

$$f=f'\sqrt{1-\mu_0'^2}, \tag{6}$$

where μ_0' is the refractive index for the frequency f' at the level of reflection.

In the case of the plane earth, we had

$$\mu_0'=\sin\phi_1=\sin\phi_0,$$

which gives

$$f=\frac{f'}{\sec\phi_0},$$

the well-known secant law. In the case of the curved earth, however, we must use the values of μ_0' given by eq 3 or eq 5, and

$$\sqrt{1-\mu_0'^2}=\sqrt{1-\frac{\sin^2\phi_1}{\left(1+\frac{z_0}{R+h}\right)^2}}=\sqrt{1-\sin^2\phi_0\left(\frac{1+\frac{z_v}{R+h}}{1+\frac{z_0}{R+h}}\right)^2} \tag{7a}$$

Under practical conditions z_0 is almost always less than 400 km, and values of z_v greater than 600 km contribute nothing to trans-

[2] W. H. Eccles, Proc. Roy. Soc. (London) [A] 87, 79 (1912).
[3] J. Larmor, Jahrb. drahtlosen Telegraphie 25, 141 (1925).

mission over appreciable distances, so that we can always consider z_0 and $z_v \ll R+h$. Using this approximation, eq 7a becomes

$$\sqrt{1-\mu_0'^2}=\cos\phi_1\sqrt{1+\frac{2z_0}{R+h}\tan^2\phi_1}=\cos\phi_0\sqrt{1-\frac{2(z_v-z_0)}{R+h}\tan^2\phi_0} \quad (7b)$$

Figure 3 gives values of $\frac{1}{\sqrt{1-\mu_0'^2}}$ plotted against $\tan\phi_1$ for various

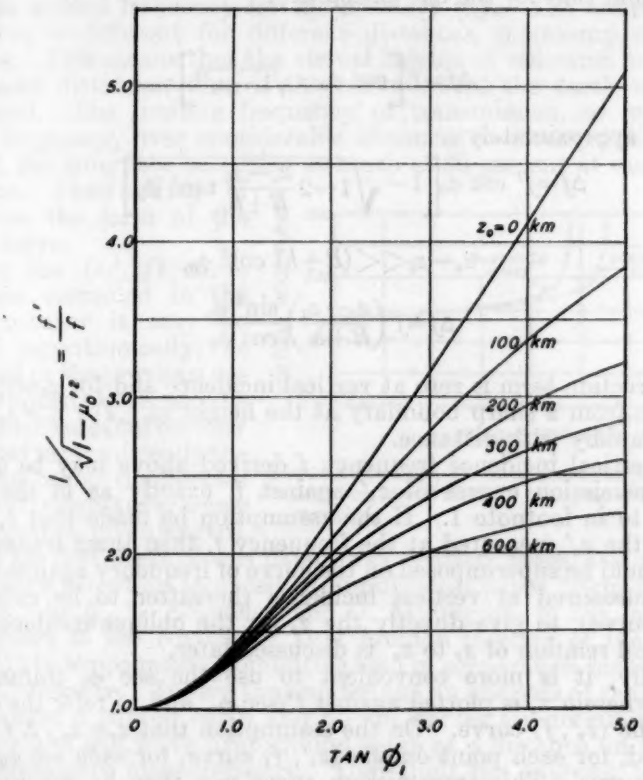

FIGURE 3.—*Variation of* $\frac{1}{\sqrt{1-\mu_0'^2}}$ *with* z_0 *and tan* ϕ_0.

values of z_0, assuming $h=100$ km (at the bottom of the E layer). These curves may be used to determine the relation of f to f' for various values of z_0 and ϕ_1. By substituting ϕ_0 for ϕ_1 and z_0-z_v for z_0, similar curves may also be plotted to determine the relation of f to f' for various values of z_0, z_v, and ϕ_0.

If, further, $z_0 \ll (R+h)\cot^2\phi_1$ or $(z_v-z_0) \ll (R+h)\cot^2\phi_0$ we may write eq 7b approximately,

$$\sqrt{1-\mu_0'^2}=\cos\phi_1\left[1+\frac{z_0}{R+h}\tan^2\phi_1\right]=\cos\phi_0\left[1-\frac{z_v-z_0}{R+h}\tan^2\phi_0\right] \quad (7c)$$

a form which it is convenient to use in some discussions. This approximation leads to results good to 1 percent or better for E-layer

transmission, where z_0 is less than 50 km, and for single-reflection F-layer transmission over distances less than 1,500 km, or multireflection F-layer transmission where each reflection covers less than 1,500 km. For transmission over distances greater than 1,500 km for each reflection it is necessary to use the more exact expression.

The correction term, or frequency Δf which it is necessary to subtract from $f'/\sec \phi_0$ in order to obtain f, is the amount by which the equivalent vertical-incidence frequency for the curved ionosphere differs from that for the flat ionosphere.

This is

$$\Delta f = f'\left[\cos \phi_0 - \sqrt{1-\mu_0'^2}\right],$$

which is approximately

$$\Delta f = f' \cos \phi_0 \left[1 - \sqrt{1 - 2\frac{z_s - z_0}{R+h}\tan^2 \phi_0}\right]$$

and, if

$$z_s - z_0 << (R+h)\cot^2 \phi_0,$$

$$\Delta f \doteq f'\left(\frac{z_s - z_0}{R+h}\right)\frac{\sin^2 \phi_0}{\cos \phi_0}$$

This correction term is zero at vertical incidence and for $z_0 = z_s'$, i. e., reflection from a sharp boundary at the height z_0. For $z_0 \neq z_s'$ it increases rapidly with distance.

The vertical incidence frequency f derived above may be used to plot transmission curves of z_s' against f, exactly as in the paper referred to in footnote 1. If the assumption be made that z_s is the same as the z_s' measured at the frequency f, then these transmission curves could be superimposed on the curve of frequency against virtual height, measured at vertical incidence (hereafter to be called the (z_s', f) curve), to give directly the z_s for the oblique-incidence case. The actual relation of z_s to z_s' is discussed later.

Actually, it is more convenient to use the sec ϕ_0 transmission curves, wherein z_s is plotted against $f'/\sec \phi_0$, and to refer the correction to the (z_s', f) curve. On the assumption that $z_s = z_s'$, Δf can be calculated, for each point on the (z_s', f) curve, for each sec ϕ_0 transmission curve. This transmission curve can then be superimposed on the (z_s', f) curve displaced toward the higher frequencies by the amount Δf, and the oblique-incidence values of z_s read off.

The calculation of Δf for each distance from z_s' and z_0, without any assumption as to z_s, and for a ϕ_0 calculated for an equivalent triangular path of height z_s', is discussed below. This value of Δf can be used in the same manner as was described in the preceding paragraph, and the sec ϕ_0 curves applied, ϕ_0 being calculated for an equivalent triangular path of height z_s' instead of z_s.

If the $(z_s' f)$ curve and the sec ϕ_0 curves are plotted logarithmically, as in the paper referred to,[4] we may calculate a factor $1+\Delta f/f$, as follows:

$$1 + \frac{\Delta f}{f} = \frac{\cos \phi_0}{\sqrt{1-\mu_0'^2}}$$

[4] *Extension of normal-incidence ionosphere measurements to oblique-incidence radio transmission.* J. Research NBS 19, 89 (1937) RP1013.

The frequencies on the (z_v', f) curve can then be easily multiplied by this factor by adding the factor logarithmically to the curve, and the log sec ϕ_0 curves can be applied to the resulting corrected (z_v', f) curve. It should be noted that in this expression the ϕ_0 refers only to an equivalent triangular path of height z_v', and not z_v. The z_v enters only into the expression for μ_0'.

A typical (z_v', f) curve corrected in this manner for a given distance (2,000 km) is shown in figure 4. The virtual heights are lower on the corrected curve and the curve extends out to frequencies higher than the critical frequency for the ordinary ray. The correction to the curve is different for different distances, increasing with the distance. This means that the virtual heights of reflection are lower, for greater distances, than if the curvature of the earth were not considered. The limiting frequency of transmission, or maximum usable frequency, over considerable distances is correspondingly increased, the difference becoming as much as 20 percent at the greater distances, depending of course on the form of the (z_v', f) curve.

When the (z_v', f) curve has been corrected in the above manner it may be plotted logarithmically, as described in the previous paper mentioned above, and the logarithmic sec ϕ_0 curves may be applied to give directly the maximum usable frequencies and virtual heights over transmission paths of given lengths.

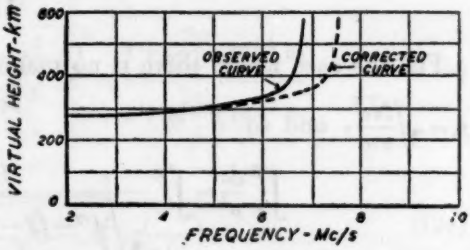

FIGURE 4.—*(z_v', f) curve corrected for a given distance (2,000 km) for the effect of the earth's curvature.*

Since the first draft of this paper was written there has come to the author's attention an excellent unpublished paper "Skip-Distance Analysis," by T. L. Eckersley and G. Millington, in the form of a contribution to the November 1937 London meeting of the Special Radio Wave Propagation Committee held in preparation for the Cairo Radio Conference. In this they undertake an analysis of radio transmission over a curved earth and obtain curves for determining the retardation of sky wave over ground wave at a distance, in terms of vertical-incidence measurements. They limit the analysis, however, to the case where z_0 is very small compared with h. The analysis can thus apply only to E-layer transmission, since for F-layer transmission, z_0 must be measured from the lower boundary of the ionosphere in order to include the effect of retardation in the E layer.

Their work, however, suggests a method of approximate analysis for larger values of z_0 and a means for easily estimating the error involved in the assumption made above that the z_v for a given frequency f' was equal to the vertical-incidence z_v' for the equivalent vertical-incidence frequency f.

The development given by Eckersley and Millington begins with the following relation, for the ray path shown in figure 2:

$$\theta' = \int_A^B d\theta = \int_A^B \frac{ds \sin \phi}{R+h+z'},$$

where ds is an element of the ray path making an angle with the vertical. Since, from eq 2

$$\sin\phi=\frac{1}{\mu'}\frac{\sin\phi_1}{1+\frac{z}{R+h}},$$

this becomes

$$\theta'=\frac{\sin\phi_1}{R+h}\int_A^B\frac{ds}{\mu'\left(1+\frac{z}{R+h}\right)^2}. \tag{8}$$

They also used the relation

$$\int_A^B\frac{ds}{\mu'}=\int_0^{z_0}\frac{dz}{\mu'\cos\phi}=\int_0^{z_0}\frac{dz}{\sqrt{\mu'^2-\frac{\sin^2\phi_1}{\left(1+\frac{z}{R+h}\right)^2}}}. \tag{9}$$

For the case where there is no magnetic field $\mu'=\sqrt{1-\frac{f_0^2}{f'^2}}$, where $f_0=\sqrt{\frac{Ne^2}{\pi m}}$, and so

$$\int_A^B\frac{ds}{\mu'}=\int_0^{z_0}\frac{f'dz}{\sqrt{f'^2-f_0^2-f'^2\frac{\sin^2\phi_1}{\left(1+\frac{z}{R+h}\right)^2}}}. \tag{10}$$

Putting into this expression the wave frequency f' in terms of the equivalent vertical-incidence frequency given above in eq 6.

$$\int_A^B\frac{ds}{\mu'}=\frac{1}{\sqrt{1-\mu_0'^2}}\int_0^{z_0}\frac{fdz}{\sqrt{\frac{f^2}{1-\mu_0'^2}\left(1-\frac{\sin^2\phi_1}{\left(1+\frac{z}{R+h}\right)^2}\right)-f_0^2}}. \tag{11}$$

At this point Eckersley and Millington assumed that they were dealing with a thin layer, and that in consequence (1) θ' was only slightly less than $\frac{\sin\phi_1}{R+h}\int_A^B\frac{ds}{\mu'}$, from eq 8, (2) $\int_A^B\frac{ds}{\mu'}$ was only slightly greater than $\frac{1}{\sqrt{1-\mu_0'^2}}\int_0^{z_0}\frac{fdz}{\sqrt{f^2-f_0^2}}$, from eq 11. This simplification is justified for E-layer transmission, but is unfortunately not justified for F_2-layer transmission, since the lower boundary of the ionosphere must be taken at the beginning of the E-layer in each case. We shall not, therefore, confine our discussion to this limited case. It must also be noted that the simplification introduced by assuming $z_0\ll(R+h)\cot^2\phi_1$ also is not valid except at comparatively short distances,

where $\phi_1=45°$ or less. For practical purposes, it is, however, justifiable to assume $z_0 << R+h$. Using this relation then, we obtain

$$\theta'=\frac{\sin\phi_1}{R+h}\int_A^B\frac{ds}{\mu'}\left(1-\frac{2z}{R+h}\right). \tag{12}$$

Eckersley and Millington combined the approximate forms of eq 8 and 11 and introduced the value of $\sqrt{1-\mu_0'^2}=\cos\phi_1$, to obtain $\theta'=\frac{\tan\phi_1}{R+h}\int_0^{z_0}\frac{f\,dz}{\sqrt{f^2-f_0^2}}$. We shall, however, combine eq 11 and 12 to obtain the more exact relation

$$\theta'=\frac{\sin\phi_1}{(R+h)\sqrt{1-\mu_0'^2}}\int_0^{z_0}\frac{f\,dz}{\sqrt{f^2(1-A)-f_0^2}}\left(1-\frac{2z}{R+h}\right), \tag{12a}$$

where

$$1-A=\frac{1-\dfrac{\sin^2\phi_1}{\left(1+\dfrac{z}{R+h}\right)^2}}{1-\mu_0'^2}=\frac{1+\dfrac{2z}{R+h}\tan^2\phi_1}{1+\dfrac{2z_0}{R+h}\tan^2\phi_1} \tag{12b}$$

If we let

$$1+B=\frac{1}{\sqrt{1-A\left(\dfrac{f^2}{f^2-f_0^2}\right)}}, \tag{12c}$$

$$\theta'=\frac{\sin\phi_1}{(R+h)\sqrt{1-\mu_0'^2}}\int_0^{z_0}\frac{dz}{\sqrt{1-\dfrac{f_0^2}{f^2}}}(1+B)\left(1-\frac{2z}{R+h}\right) \tag{13}$$

For values of z_0 considerably less than $(R+h)\cot^2\phi_1$ B is usually a small number, and for $z\to z_0$ (near the level of reflection) it is also usually small. It may attain, however, relatively large values.

In general, the evaluation of B involves a knowledge of the distribution of ionic density, and a precise evaluation of the quantity θ' involves graphic integration for each case considered. We shall for the present consider two principal cases, $z_0\to 0$ and $z_0=z_v'$, the virtual height at vertical incidence for the frequency $f=f'\sqrt{1-\mu_0'^2}$, and discuss some cases of linear distributions of ionic density, where $z/z_0=f_0^2/f^2$.

(*a*) $z_0 \ll (R+h)\cot^2\phi_1$. This case applies to *E*-layer transmission at any distance or to *F*-layer transmission at short distances (ϕ_1 small).

Combining eq 6 and 7 we get

$$f=f'\cos\phi_1\left[1+\frac{z_0}{R+h}\tan^2\phi_1\right], \tag{14b}$$

and from eq 12b

$$1-A=1+2\left(\frac{z-z_0}{R+h}\right)\tan^2\phi_1.$$

From eq 12c

$$1+B=1+\left(\frac{z_0}{R+h}\right)\frac{1-\frac{z}{z_0}}{1-\frac{f_0^2}{f^2}}\tan^2\phi_1,$$

if we assume that $(1-z/z_0)/(1-f_0^2/f^2)$ is nowhere so large as to make B comparable with unity. This is equivalent to assuming that f_0^2/f^2 does not approach 1 much more rapidly than does z/z_0, an assumption that is valid except quite close to a critical frequency. Transmissions involving equivalent vertical-incidence frequencies close to the critical frequency are of interest, however, only when the distance of transmission is short, and in this case ϕ_1 is small, so that B is a small number, anyhow.

Thus

$$\theta'=\frac{\tan\phi_1}{R+h}\left[1-\frac{z_0}{R+h}\tan^2\phi_1\right]\int_0^{z_0}\frac{dz}{\sqrt{1-\frac{f_0^2}{f^2}}}$$

$$\left\{1+\frac{z_0}{R+h}\tan^2\phi_1\frac{\left(1-\frac{z}{z_0}\right)}{\left(1-\frac{f_0^2}{f^2}\right)}-\frac{2z}{R+h}\right\}.$$

Now $\int_0^{z_0}\frac{dz}{\sqrt{1-\frac{f_0^2}{f^2}}}=z_v'$, the virtual height measured at vertical incidence for the equivalent vertical-incidence frequency f. Since the terms involving $z_0/R+h$ are small, we may write

$$\theta'=\frac{z_v'\tan\phi_1}{R+h}\left[1-\frac{z_0}{R+h}\tan^2\phi_1(1-C)-C'\right], \tag{14c}$$

where

$$C=\frac{1}{z_v'}\int_0^{z_0}\frac{dz}{\sqrt{1-\frac{f_0^2}{f^2}}}\left(\frac{1-\frac{z}{z_0}}{1-\frac{f_0^2}{f^2}}\right), \text{ and}$$

$$C'=\frac{2}{z_v'(R+h)}\int_0^{z_0}\frac{zdz}{\sqrt{1-\frac{f_0^2}{f^2}}}$$

For a linear distribution of ionic density

$$1-\frac{z}{z_0}=1-\frac{f_0^2}{f^2},\ z_v'=2z_0, \text{ and } C=1, \text{ and}$$

$$\theta'=\frac{\tan\phi_1}{R+h}\int_0^{z_0}\frac{dz}{\sqrt{1-\frac{z}{z_0}}}\left[1-\frac{2z}{R+h}\right],$$

$$=\frac{z_v'\tan\phi_1}{R+h}\left[1-\frac{2}{3}\left(\frac{z_v'}{R+h}\right)\right]. \tag{15}$$

For z_0 vanishingly small $C' \to 0$ and eq 14 reduces simply to

$$\theta' = \frac{z_v' \tan \phi_1}{R+h} \tag{15a}$$

(*b*) $z_0 \to z_v'$. This case applies to reflection from a fairly sharp boundary at the level z_0, the refractive index being nearly unity up to nearly this level. An example of this would be reflection from the sporadic E region. The angular distance of the part of the ray path where μ departs appreciably from unity is small and so the ionosphere can be considered as essentially flat. This is the condition assumed by the author in the paper already referred to (RP1013). Here $z_v = z_v'$ and

$$\tan \phi_0 = \frac{\sin \theta'}{\frac{z_v'}{R+h} + 1 - \cos \theta'}. \tag{16}$$

In this case

$$\sqrt{1-\mu_0'^2} = \cos \phi_0 \left(1 - \frac{z_v' - z_0}{R+h} \tan^2 \phi_0\right) \tag{16a}$$

For $z_v' - z_0$ vanishingly small compared with $(R+h) \cot^2 \phi_0$, this reduces to the case for the plane ionosphere, where

$$\sqrt{1-\mu_0'^2} = \cos \phi_0.$$

(*c*) $z_0 = \frac{1}{2} z_v'$, i. e., a linear distribution of ionic density. Here $1 - f_0^2/f^2 = 1 - z/z_0$ and eq 12a becomes

$$\theta' = \frac{\sin \phi_1}{(R+h)\sqrt{1-\mu_0'^2}} \int_0^{z_0} \frac{dz\left(1 - \frac{2z}{R+h}\right)}{\sqrt{1 - A - \frac{z}{z_0}}}$$

Putting in the value of $1-A$ and integrating

$$\theta' = z_v' \frac{\sin \phi_1 \sqrt{1 + \frac{2z_0}{R+h} \tan^2 \phi_1}}{(R+h)\sqrt{1-\mu_0'^2}} \left(1 - \frac{2}{3} \frac{z_v'}{R+h}\right). \tag{17}$$

Now since we may consider $z_0 \ll R+h$ we can write, as in eq 7b

$$\sqrt{1-\mu_0'^2} = \cos \phi_1 \sqrt{1 + \frac{2z_0}{R+h} \tan^2 \phi_1},$$

and thus eq 17 becomes

$$\theta' = \frac{z_v' \tan \phi_1}{R+h} \left[1 - \frac{2}{3} \frac{z_v'}{R+h}\right], \tag{15}$$

just as in the case where $z_0 \ll (R+h) \cot^2 \phi_1$. We must, however, write for the equivalent vertical-incidence frequency in this case

$$f = f' \cos \phi_1 \sqrt{1 + \frac{2z_0}{R+h} \tan^2 \phi_1} \tag{17a}$$

instead of the value

$$f=f' \cos \phi_1\left[1+\frac{z_0}{R+h} \tan^2 \phi_1\right], \tag{14b}$$

which we could use when $z_0 \ll (R+h) \cot^2 \phi_1$.

The three examples just treated give an idea of what happens on transmission through the ionosphere, and of the angular distance θ' the wave travels in the ionosphere as a function of angle of incidence ϕ_1 (or vertex angle of equivalent triangular path ϕ_0), of true height of reflection z_0 and of virtual height measured at vertical incidence z_v'. We must now consider the part of the path from the earth to the lower boundary of the ionosphere. If we consider the incident ray to traverse an angular distance $(\theta-\theta')$ in going from the earth to the lower boundary of the ionosphere, the geometry of figure 2 tells us that

$$\tan \phi_1=\frac{\sin (\theta-\theta')}{\frac{h}{R}+1-\cos (\theta-\theta')} \tag{18}$$

For a given ϕ_1, then, we may solve this equation for $(\theta-\theta')$, and, by adding this angle to the angle θ' already computed, we obtain the entire angular distance θ traversed by the wave from the ground to the point of reflection in the ionosphere. For $h=100$ km, as we are assuming, it is sufficiently accurate to replace $\sin (\theta-\theta')$ by $(\theta-\theta')$ and $1-\cos (\theta-\theta')$ by $\frac{1}{2}(\theta-\theta')^2$ in this equation. We can thus solve for $(\theta-\theta')$, obtaining

$$\theta-\theta'=\cot \phi_1-\sqrt{\cot^2 \phi_1-\frac{2h}{R}} \tag{18a}$$

We can now write the expression for the total distance of transmission D in terms of ϕ_1 (or ϕ_0) z_0 and z_v':

$$D=2R\left(\cot \phi_1-\sqrt{\cot^2 \phi_1-\frac{2h}{R}}\right)+\theta', \tag{19}$$

where θ' is computed as above, from eq 12a.

The time T required for the sky wave to travel from the transmitter to the receiver is, if c=velocity of the wave in vacuum,

$$T=\frac{2}{c}\left(R\frac{\sin (\theta-\theta')}{\sin \phi_1}+\int_A^B \frac{ds}{\mu}\right).$$

If we put in the value of $\int_A^B ds/\mu$ obtained on the basis of the above analysis, and replace $\sin(\theta-\theta')$ by its value in terms of ϕ_1, we may express T in terms of the quantities ϕ_1 (or ϕ_0), z_0 and z_v', as was done with D.

The relation between the height z_v of the equivalent triangular path and the virtual height z_v' measured at vertical incidence for the

equivalent vertical-incidence frequency $f=f'\sqrt{1-\mu_0'^2}$ can now be written. From the geometry of figure 2,

$$\tan\phi_0=\tan(\phi_1-\theta')=\frac{\sin\theta'}{\frac{z_v}{R+h}+1-\cos\theta'},$$

so that

$$z_v=(R+h)[\sin\theta'\cot(\phi_1-\theta')-1+\cos\theta'] \tag{20}$$

The relation between z_v, z_v', z_0, ϕ_1, ϕ_0, θ', D, f', and f may be summarized for the cases discussed here.

(a) $z_0<<\frac{1}{2}(R+h)\cot^2\phi_1$

$$f=f'\cos\phi_1\left[1+\frac{z_0}{R+h}\tan^2\phi_1\right],$$

$$\theta'=\frac{\tan\phi_1}{R+h}\left[1-\frac{z_0}{R+h}\tan^2\phi_1\right]\int_0^{z_0}\frac{dz}{\sqrt{1-\frac{f_0^2}{f^2}}}$$

$$\left\{1+\frac{z_0}{R+h}\tan^2\phi_1\left(\frac{1-\frac{z}{z_0}}{1-\frac{f_0^2}{f^2}}\right)-\frac{2z}{R+h}\right\},$$

$$T=\frac{2}{c}\left[\frac{R(\theta-\theta')}{\sin\phi_1}+\frac{1}{\cos\phi_1}\int_0^{z_0}\frac{dz}{\sqrt{1-\frac{f_0^2}{f^2}}}\left\{1-\frac{z_0}{R+h}\tan^2\phi_1\left(1-\frac{1-\frac{z}{z_0}}{1-\frac{f_0^2}{f^2}}\right)\right\}\right],$$

$$\theta-\theta'=\cot\phi_1-\sqrt{\cot^2\phi_1-\frac{2h}{R}},$$

$$D=2R\theta,$$

$$z_v=(R+h)[\sin\theta'\cot(\phi_1-\theta')-1+\cos\theta'],$$

$$z_v'=\int_0^{z_0}\frac{dz}{\sqrt{1-\frac{f_0^2}{f^2}}},$$

(a') $z_0=0$,

$$f=f'\cos\phi_1,$$

$$\theta'=\frac{z_v'\tan\phi_1}{R+h},$$

$$T=\frac{2}{c}\left[\frac{R(\theta-\theta')}{\sin\phi_1}+\frac{z_v'}{\cos\phi_1}\right],$$

$$\theta-\theta'=\cot\phi_1-\sqrt{\cot^2\phi_1-\frac{2h}{R}},$$

$$D=2R\theta, \text{ and}$$

$$z_v=(R+h)[\sin\theta'\cot(\phi_1-\theta')-1+\cos\theta'],$$

(*b*) linear gradient of ionic density $\left(z_0=\frac{1}{2}z_v'\right)$

$$f=f'\cos\phi_1\sqrt{1+\frac{z_v'}{R+h}\tan^2\phi_1},$$

$$\theta'=\frac{z_v'\tan\phi_1}{R+h}\left[1-\frac{2}{3}\frac{z_v'}{R+h}\right],$$

$$T=\frac{2}{c}\left[\frac{R(\theta-\theta')}{\sin\phi_1}+\frac{z_v'}{R+h}\right],$$

$$\theta-\theta'=\cot\phi_1-\sqrt{\cot^2\phi_1-\frac{2h}{R}},$$

$$D=2R\theta,$$

$$z_v=(R+h)[\sin\theta'\cot(\phi_1-\theta')-1+\cos\theta'],$$

(*c*) $z_0=z_v'$,

$$f=f'\cos\phi_0,$$

$$\tan\phi_0=\frac{\sin\theta'}{\frac{z_v'}{R+h}+1-\cos\theta'}=\frac{\sin\theta}{\frac{z_v'+h}{R}+1-\cos\theta},$$

$$T=\frac{2}{c}\frac{(R+h)\sin\theta}{\sin\phi_0}$$

$$D=2R\theta, \text{ and}$$

$$z_v=z_v'$$

Case (*a'*) corresponds to the special case treated by Eckersley and Millington, except that, for simplicity of analytical computation, they took $R+h=R$ in the expression for θ', which introduces an error of about $0.016h$ percent (h expressed in km)—not a serious error for $h=100$ km, as we have assumed. This error becomes appreciable, however, if it is attempted to extend this treatment, as they have done, to a height of 400 km or so.

Martyn's equivalence theorem,[5] developed for a plane ionosphere, tells us that

$$z_v=z_v',$$

$$T=\frac{2}{c}\frac{z_v'}{\cos\phi_0}=\frac{2}{c}\frac{z_v'}{\cos\phi_1},$$

$$D'=2z_v'\tan\phi_0=2z_v'\tan\phi_1, \text{ and}$$

$$f=f'\cos\phi_0=f'\cos\phi_1,$$

where

ϕ_1 = angle of incidence of waves upon the ionosphere,
ϕ_0 = half the vertex angle of the equivalent triangular path,
z_v = height of equivalent triangular path,
T' = time the wave spends in the ionosphere, and
D' = horizontal distance the wave travels in the ionosphere.

We see that the relation $z_v=z_v'$ is valid in case (*c*) but not in any other case. The relation $T=\frac{2}{c}\frac{z_v'}{\cos\phi_1}$ is valid in cases (*a'*) and (*b*), but is not valid in general. The relation $D'=2z_v'\tan\phi_1$ holds approximately only in case (*a'*). And finally, $f=f'\cos\phi_0$ in case (*c*), $f=f'$

[5] D. F. Martyn, Proc. Phys. Soc. (London) 47, 332 (1935).

cos ϕ_1 in case (a'), and f is a complicated function in every other case. It is therefore concluded that the equivalence theorem, in the form given, cannot be applied to the curved-earth problem.

Referring again to the summaries of cases (a'), (b), and (c), we may for a given value of z_v' take a set of values of z_0, for each of which can be calculated the variation of D with ϕ_1, in each of the three cases. We may also, for these values of z_v' and z_0, calculate the variation of f'/f with ϕ_1. By eliminating ϕ_1 graphically, we can determine the variation of f'/f with D for a given z_v' and z_0, or, what is the same thing, the variation of f'/f with z_v' for a given D and z_0. We can plot a family of transmission curves, with f as abscissas and z_v' as ordinates, for each value of D and several values of z_0, corresponding to each of these cases.

Such curves may be superimposed on the (z_v', f) curve obtained at vertical incidence, and the (z_0, f) curve deduced therefrom, to give directly the wave frequency f' corresponding to reflection at a given level z_0, which is characterized by a given z_v'. The value of z_0 appropriate to reflection at the given height determines which curve of the family for a given D is to be used, and the point of reflection is determined as the intersection of this transmission curve with the (z_v', f) curve.

The value of z_v depends only on D and ϕ_1, and so lines of equal z_v may be plotted on the curve sheet for each D, so that z_v, as well as f', may be read off directly.

Because of the approximations made in case (b) and the assumption of a linear variation of ionic density with height, this case is of only special significance. It will be assumed, until further investigation determines more precisely the variation of conditions with z_0, that the curves vary smoothly between those calculated for $z_0=0$ and those calculated for $z_0=z_v'$.

A family of curves for each distance is rather cumbersome for rapid use. It is, as was said above, more convenient to use the log sec ϕ_0 transmission curves, and apply a correction to the (z_v', f) curve by multiplying each vertical-incidence frequency by the factor $1+\Delta f/f$, where

$$1+\frac{\Delta f}{f}=\frac{\cos\phi_0}{\sqrt{1-\mu_0'^2}}.$$

This factor is obtained, for a given D, z_v' and z_0, by determining corresponding values of D and $\sqrt{1-\mu_0'^2}$ for arbitrary values of ϕ_0 or ϕ_1. It is unity for $z_v'=z_0$ and is quite easily obtained for $z_0=0$. For intermediate values of z_0 it will be assumed that the factor $1+\Delta f/f$ varies in a manner similar to that determined from the relation eq 7b with $z_v=z_v'$, i. e.,

$$\frac{\cos\phi_0}{\sqrt{1-\mu_0'^2}}=\sqrt{1-\frac{2(z_v'-z_0)}{R+h}\tan^2\phi_0},$$

but drawn through the values for $z_0=0$ and $z_0=z_v'$ determined in the more precise analysis, rather than those indicated on the assumption that $z_v=z_v'$. Cos ϕ_0 is here calculated for an equivalent triangular path of height z_v'.

Figure 5 gives the approximate factors by which f must be multiplied to give $f'/\sec \phi_0$ for values of z_v' from 200 to 500 km and for distances up to 4,000 km.

III. EFFECT OF THE EARTH'S MAGNETIC FIELD

The presence of the earth's magnetic field introduces some complications in the use of these transmission curves. These complications are often of minor importance compared with some of the unknown

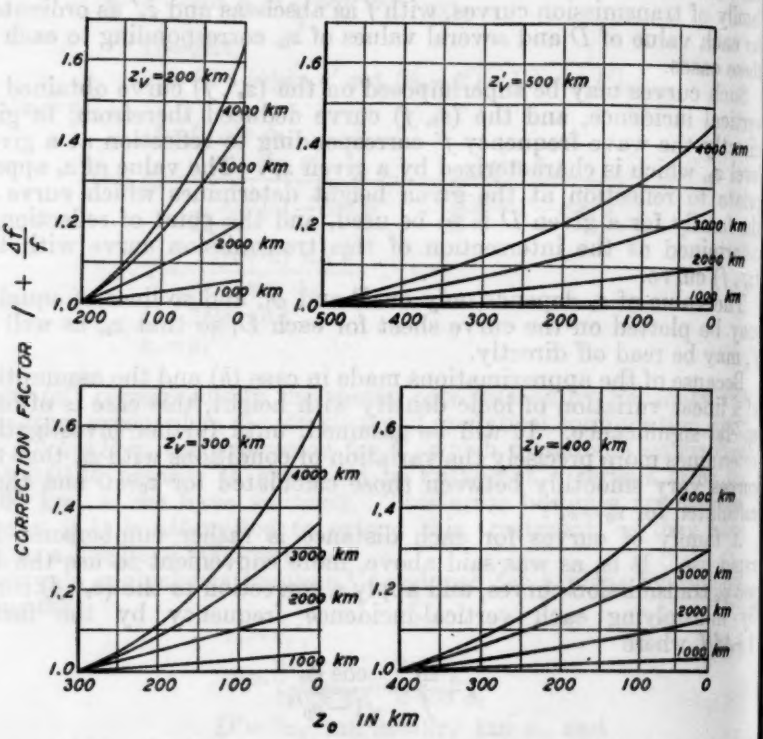

FIGURE 5.—*Approximate factors by which the equivalent vertical-incidence frequency f must be multiplied to give the frequency f'/sec ϕ_0 which is to be used in conjunction with the log sec ϕ_0 curves.*

factors (e. g., the geographic uniformity of the ionosphere over the transmission path), especially over long distances, but the effect of the earth's field must at times be taken into account. The anisotropy of the ionosphere due to this field causes the effect of the field on radio transmission to vary with the length, direction, and geographic location of the transmission path.

One effect of the field is to cause the received signal to be split in general into two main components, the one with the lower maximum usable frequency known as the "o" component and the other as the "x" component. The refractive index for a frequency f', in the presence of a magnetic field H, whose components along and trans-

verse to the direction of phase propagation are, respectively, H_L and H_T is given [6] by

$$\mu'^2=1-\frac{f_0^2}{f'^2-\frac{f'^2f_T^2}{2(f'^2-f_0^2)}\pm\sqrt{\left[\frac{f'^2f_T^2}{2(f'^2-f_0^2)}\right]^2+f'^2f_L^2}},$$

where

$$f_0=\sqrt{\frac{Ne^2}{\pi m}},$$

$$f_T=\frac{e}{2\pi mc}H_T,$$

$$f_L=\frac{e}{2\pi mc}H_L, \text{ and}$$

N=ionization density.
Upper sign refers to o-component; lower to x-component.

The frequency of the wave whose x-component is returned from a given ionization density, at a given height, is different from the frequency of the wave whose o-component is returned from the same level. This frequency separation is in general a function both of frequency and distance and may often become negligible at great distances.

For practical calculation, it may be assumed that only the field and direction of wave propagation in the region near the level of reflection will appreciably affect the propagation of the wave. This assumption is probably better for the o- than for the x-component, and is, it must be emphasized, only a good approximation.

With this limitation, therefore, the value of μ'^2 may be calculated for a given transmission frequency and transmission path. If we put $\mu'=\sin\phi_0$ and deduce z_r from $\sin\phi_0$ as was done in the previous paper, we may plot transmission curves, of virtual height against equivalent vertical-incidence frequency, for the o- and x-components. When these curves are applied to the corrected (z_r', f) curves, they may be expected to give reasonably good results. An example of this type of transmission curve is shown in figure 6. The one curve gives transmission conditions for the x-component, and the other for the o-component. The frequency used is well over the gyrofrequency $f_H=eH/2\pi mc$ so that the x-component is returned from a lower level than is the o-component and has a higher limiting frequency.

It is not now justifiable to plot the transmission curves logarithmically, since the form of the curves will vary with the transmission frequency f'. For practical purposes, however, a logarithmic curve may be used within a limited range of wave frequencies about the frequency f' for which the curve is plotted; a practical limit might be, say, within ± 15 percent of this frequency.

The logarithmic sec ϕ_0 transmission curves may be used in estimating the maximum usable frequency for each component over a given path by adding or subtracting the separation between the limiting frequencies for the two components, evaluated at that frequency and distance. This separation is in general a function only of the trans-

[6] E. V. Appleton. J. Inst. Elec. Engrs. (London), 71, 642 (1932).

mission frequency and the quantity sec ϕ_0, and may be estimated within the limits of experimental error in most cases.

Figure 7 gives the frequency to be added or subtracted from the maximum usable frequency given by the logarithmic sec ϕ_0 transmission curves for the cases $H_L=0$, $H_T \doteq 0$, and $H_T=H_L$. The $H_T=0$ case is uninteresting save for single-hop transmission over the magnetic equator, close to the magnetic meridian. For transmission in the continental United States H_L is much less than H_T and, indeed, is negligible over east-west paths, so that such transmission we may consider as essentially transverse transmission. In this case,

$$\mu'^2=1-\frac{f_0^2}{f'^2-\delta\frac{f'^2f_H^2}{f'^2-f_0^2}},$$

where $\delta=0$ for the o-component and 1 for the x-component, and the logarithmic sec ϕ_0 transmission curves give the correct maximum

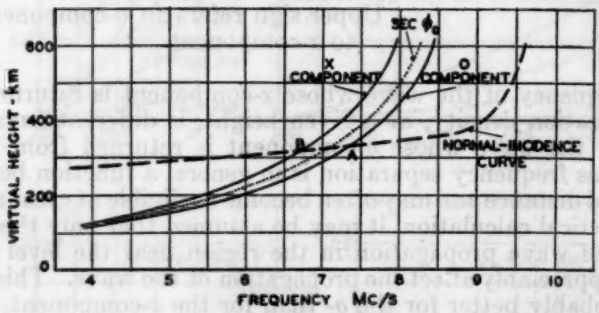

FIGURE 6.—*Transmission curve, including effect of earth's magnetic field at level of reflection.*

Dotted line=secant-law curve ($f'=f$ sec ϕ_0) for the given distance D and wave frequency f'. Dashed line=(z_r', f) curve for the o-component, this being the component which, at vertical incidence is a measure of the ionization density N. The o-component of the frequency f' over the given distance is reflected at A, and the x-component at B.

usable frequency for the o-component. For this reason the o-component lies along the sec ϕ_0 axis in the $H_L=0$ case in figure 7.

For a maximum usable frequency for the o-component below the gyrofrequency $f_H=\sqrt{f_T^2+f_L^2}$ the x-component always has a maximum usable frequency above f_H. This is only important for E-layer transmission and only in cases where the x-component is not too highly absorbed at frequencies near f_H. This case must not be confused with the case of a transmission frequency f' less than f_H, in which case the x-component is reflected from a level above the level where the o-component is reflected.

Another effect of the anisotropy of the ionosphere due to the earth's field is to cause a difference in the directions of phase and energy propagation in the medium. This results in the wave's being reflected, not at the level where the direction of phase propagation is horizontal, but where the direction of energy flow (group direction) is horizontal. This effect has not been considered in these curves, and is probably not important to the degree of accuracy to which these calculations are carried.

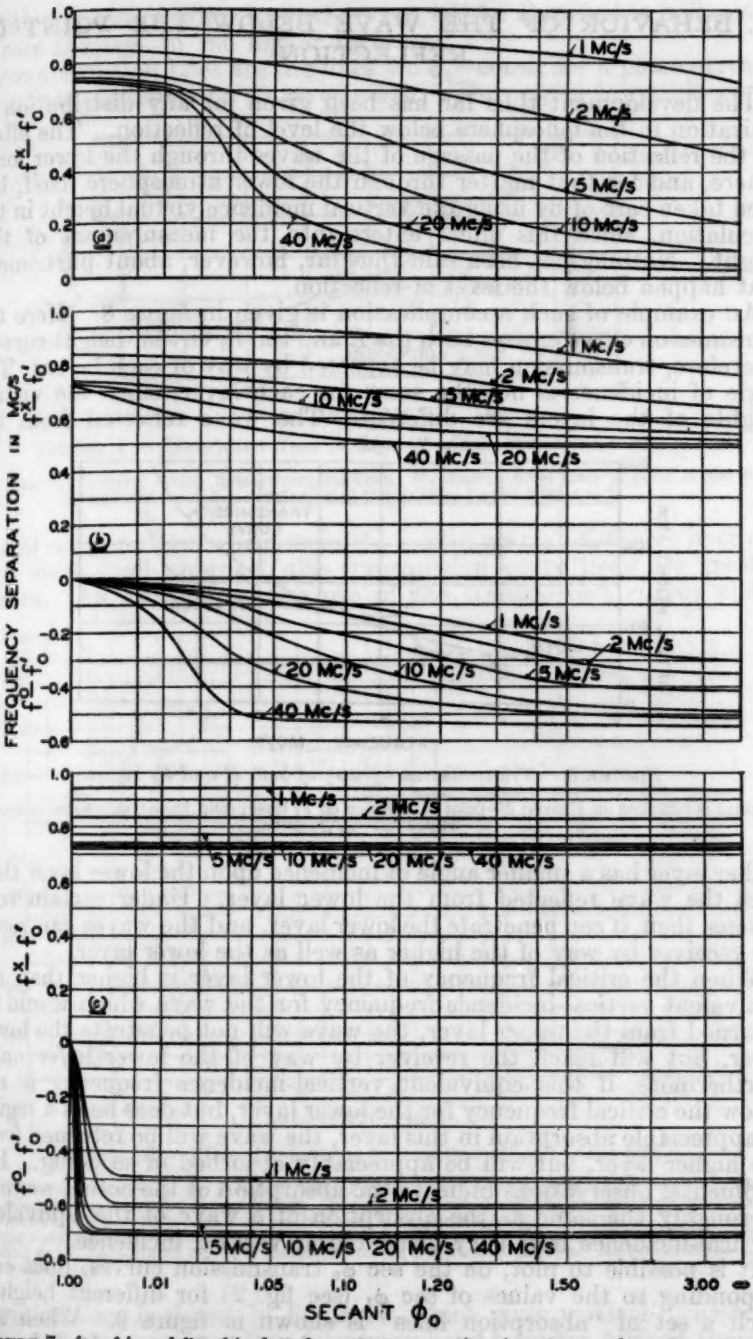

FIGURE 7. *$f^x - f_0'$ and $f^o - f_0'$ plotted against sec ϕ_0 f^x = frequency whose x-component is reflected at the same level as is the o-component of f^o.*

$f_0' = f' \cos \phi_0$

The value of f' is given, in Mc/s, on each curve. Curves (a) $H_L = 0$. Here $f^o - f_0' = 0$ and the curves for the o-component lie on the sec ϕ_0 axis. Curves (b) $H_L = H_T \neq 0$. Curves (c) $H_T \doteq 0$. Here $f^x - f_0'$ and $f^o - f_0'$ are independent of sec ϕ_0, save near sec $\phi_0 = 1$.

IV. BEHAVIOR OF THE WAVE BELOW THE POINT OF REFLECTION

The development thus far has been given for any distribution of ionization in the ionosphere below the level of reflection. The effect on the reflection of the passage of the waves through the lower ionosphere, and for that matter through the lower atmosphere itself, has been taken care of by using the vertical incidence virtual height in the calculation, since this effect enters into the measurement of this height. Nothing has been said thus far, however, about phenomena that happen below the level of reflection.

An example of such a complication is given in figure 8. Here the transmission curve crosses both the E and the F_2 virtual-height curves. Therefore, transmission may be expected by way of each layer. The angle of incidence is not the same for each layer, since the virtual heights of the layers are different. The wave reflected from the

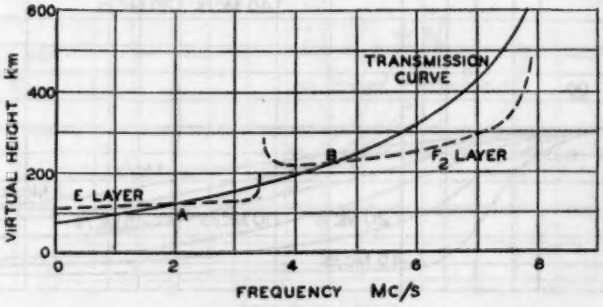

FIGURE 8.—*Transmission by way of both E and F_2 layers.*

A=point of reflection on *E* layer; *B*=point of reflection on F_2 layer; solid line=transmission curve; and dashed line=(z_v', f) curve.

higher layer has a smaller angle of incidence upon the lower layer than does the wave reflected from the lower layer. Under certain conditions, then, it can penetrate the lower layer, and the waves can reach the receiver by way of the higher as well as the lower layer.

When the critical frequency of the lower layer is higher than the equivalent vertical-incidence frequency for the wave which would be returned from the upper layer, the wave will not penetrate the lower layer, but will reach the receiver by way of the lower layer only. Furthermore, if this equivalent vertical-incidence frequency is not below the critical frequency for the lower layer, but does lie in a region of appreciable absorption in this layer, the wave will be returned from the higher layer, but will be appreciably absorbed in so doing. Experimental observations indicate the absorption of the actual wave to be roughly the same as the absorption of a wave of the equivalent vertical-incidence frequency measured at vertical incidence.

It is possible to plot, on the sec ϕ_0 transmission curves, lines corresponding to the values of sec ϕ_1 (see fig. 2) for different heights. Such a set of "absorption lines" is shown in figure 9. When the transmission curve is superimposed on the (z_v', f) curve the behavior of a wave below the reflection level may be estimated by the region of the (z_v', f) curve sheet through which the absorption line through the reflection point passes. If this line passes through a region of

absorption or cuts a lower layer the wave will be absorbed or will not penetrate through to the higher layer.

These absorption lines are the lines sec ϕ_1=const. for a plane earth and for short distances on a curved earth. They curve toward larger

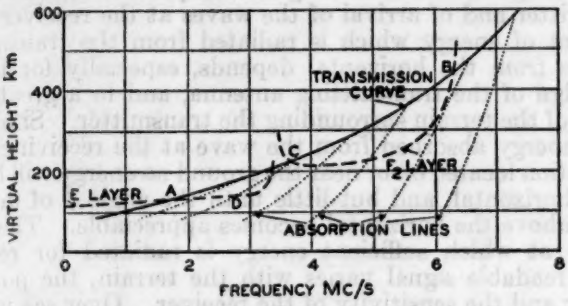

FIGURE 9.—*Absorption lines on logarithmic transmission curve.*

Dashed line=(z', f) curve; dotted lines=absorption lines. *E* reflection takes place at point *A* and F_2 reflection at point *B*. F_2 reflection at *C* is shielded by the *E* layer at *D*.

values of sec ϕ_1 for lower heights in the case of greater distances over a curved earth, and approach the transmission curve itself for great distances. An example of the use of the transmission curves and

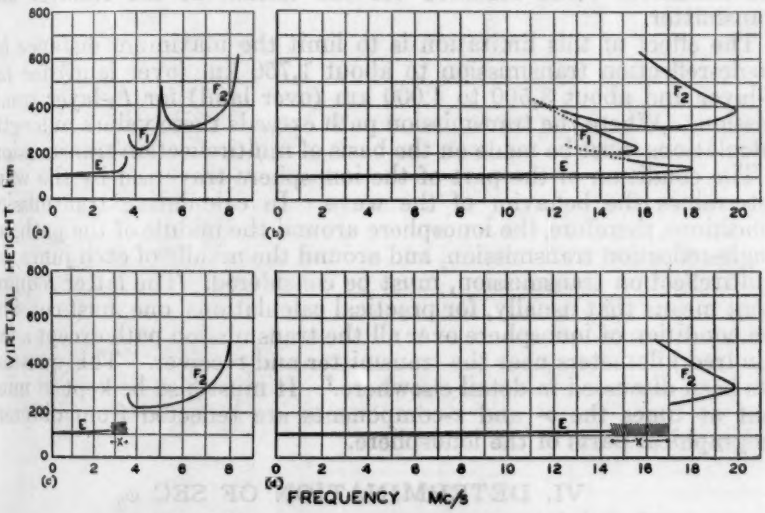

FIGURE 10.—*Virtual heights at vertical and oblique incidence.*

(a) (z', f) curve showing *E*, F_1, and F_2 layers. (*b*) oblique-incidence heights corresponding to (*a*). Dotted lines show parts of curves shielded by *E* layer. Note transmission of some frequencies by several layers. This shows how the F_1-layer reflections are relatively unimportant for transmission. (*c*) (z', f) curve showing absorption (×) above critical frequency for the *E* layer. (*d*) oblique-incidence heights corresponding to (*c*). Absorption here (×) completely blocks out some frequencies. All curves are for the o-component.

absorption lines is shown in figure 10, which gives vertical-incidence curves and the corresponding frequency-height curves derived therefrom for the transmitted wave over a distance. From these latter curves can be deduced, of course, the equivalent paths or group retardation of the waves over the transmission path.

V. ANGLE OF DEPARTURE AND ARRIVAL OF THE WAVES

Disregarding any possible asymmetry of the wave trajectory due to the earth's magnetic field, the angles of departure of the waves from the transmitter and of arrival of the waves at the receiver are equal. The amount of energy which is radiated from the transmitter at a given angle from the horizontal depends, especially for low angles, on the design of the transmitting antenna, and to a great extent on the nature of the terrain surrounding the transmitter. Similar factors affect the energy absorbed from the wave at the receiving station.

For a station located on or near the ground no energy will be radiated below the horizontal, and but little until the angle ψ of departure of the waves above the horizontal becomes appreciable. The minimum value of ψ at which sufficient energy is radiated (or received) to produce a readable signal varies with the terrain, the power of the transmitter and the sensitivity of the receiver. Over sea water ψ can be very nearly zero; over land the minimum value may be several degrees. A fair average approximation may be that ψ must exceed about 3.5°.

A simple geometrical calculation gives ψ in terms of sec ϕ_0 for various distances, and these may be noted on the transmission curves. The point of reflection must then correspond to an angle ψ greater than the minimum value assumed for the terrain at the receiver and transmitter.

The effect of this limitation is to limit the maximum distance for single-reflection transmission to about 1,750 km (over land) for the E-layer and about 3,500 to 4,000 km (over land) for F_2-layer transmission. Where the transmission path exceeds these values in length, calculations must be made on the basis of multireflection transmission.

The condition of the part of the ionosphere traversed by the wave determines the behavior of the wave. In calculating transmission conditions, therefore, the ionosphere around the middle of the path, for single-reflection transmission, and around the middle of each jump, for multireflection transmission, must be considered. The latter requirement means that usually, for practical calculations, one must consider the condition of ionosphere over all the transmission path except a few hundred kilometers near the transmitter and receiver. This question has been discussed in detail elsewhere.[7] It must also be kept in mind that at times the o- and x-components are reflected from different geographical parts of the ionosphere.

VI. DETERMINATION OF SEC ϕ_0

Figure 11 gives an alignment chart for the rapid determination of the factor sec ϕ_0 to be used in calculating the logarithmic transmission curves. To use the chart, place a straightedge so that it passes through the desired virtual height and the desired distance laid off on the distance scale at the lower left-hand edge of the chart (increasing distances lie to the left). The ordinate of the intersection of the straightedge with the vertical line corresponding to the same

[7] T. R. Gilliland, S. S. Kirby, N. Smith, and S. E. Reymer. *Characteristics of the ionosphere and their applications to radio transmission.* J. Research NBS 18, 645 (1937) RP1001; Proc. Inst. Radio Engrs. 25, 823 (1937).

The weekly radio broadcasts of the National Bureau of Standards on the ionosphere and radio-transmission conditions. Letter Circular LC499.

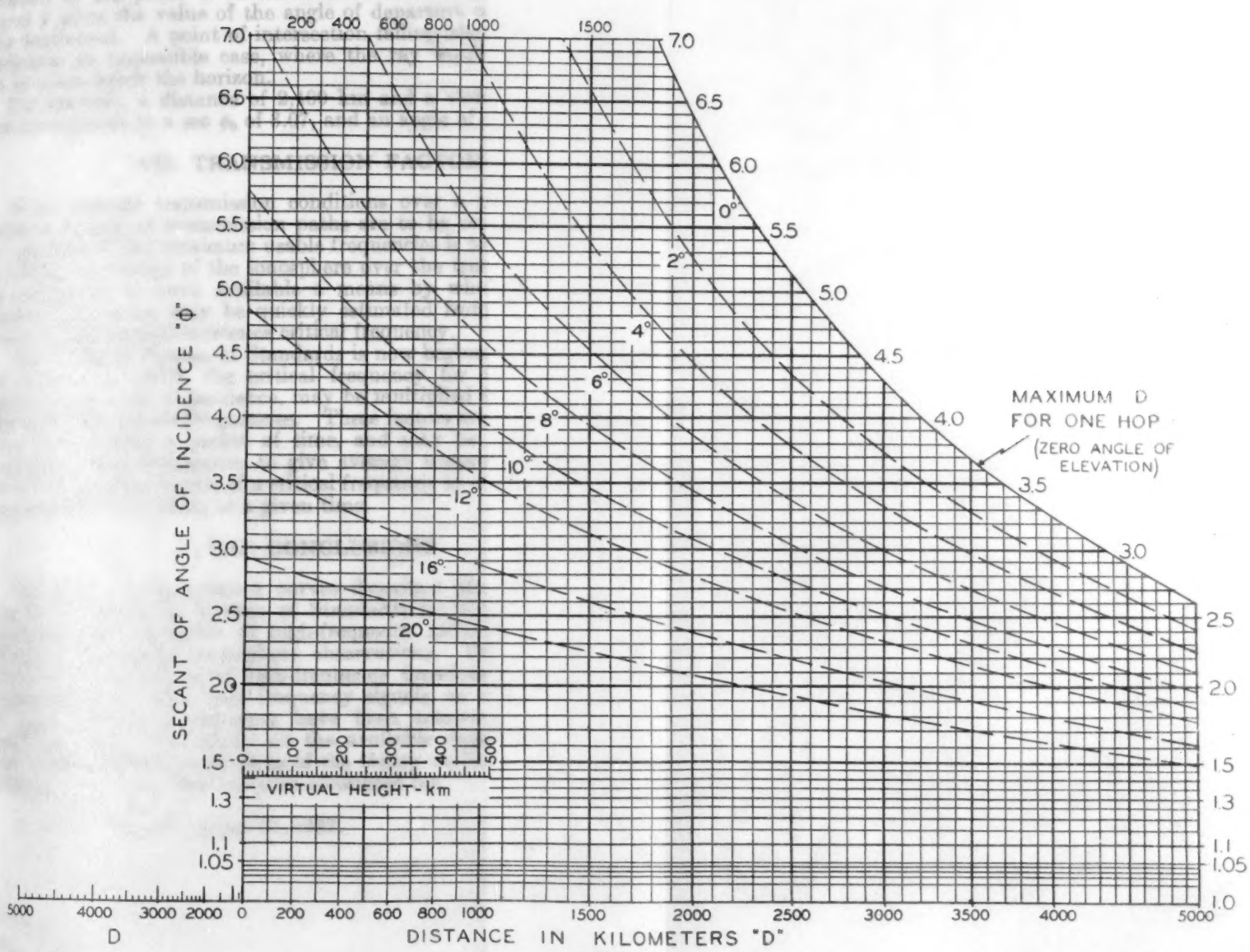

FIGURE 11.

57763—38 (Face p. 704)

UNIV. OF MICH.

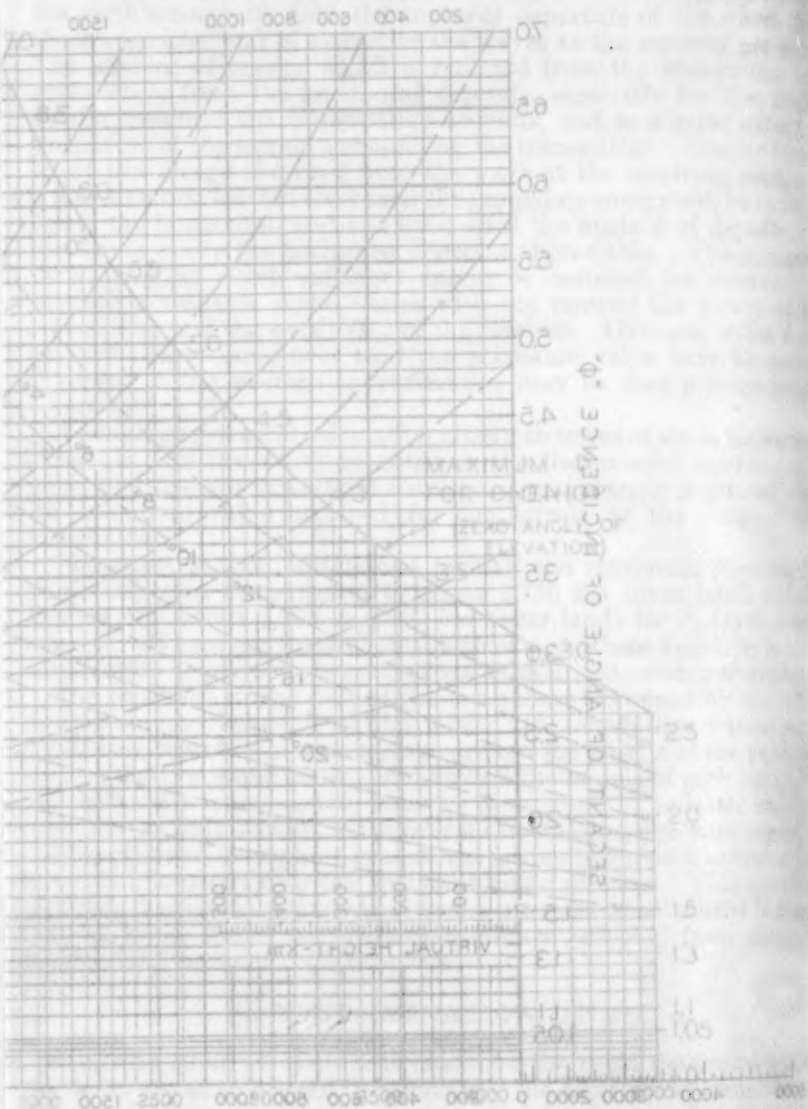
SECANT OF ANGLE OF INCIDENCE, Φ
VIRTUAL HEIGHT - Km
DISTANCE IN KILOMETERS

desired distance laid off on the main distance scale (increasing distances lie to the right) gives the value of sec ϕ_0. The relation of the point of intersection to the curved dashed lines of equal ψ gives the value of the angle of departure of the waves from the horizontal. A point of intersection falling above the $\psi=0°$ line indicates an impossible case, where the ray would have to depart at an angle below the horizon.

For example, a distance of 2,400 km and a virtual height of 300 km corresponds to a sec ϕ_0 of 3.07, and an angle of departure of 8.2°.

VII. TRANSMISSION FACTORS

When average transmission conditions over a period of time or when a variety of transmission paths are to be considered, or when an estimate of the maximum usable frequencies is to be made without a precise knowledge of the ionosphere over the transmission path, it is convenient to have available a means by which the maximum usable frequencies may be quickly estimated from an approximate value of the vertical-incidence critical frequency.

The National Bureau of Standards is now beginning a compilation of factors by which the critical frequency for the *o*-component, measured at vertical incidence, may be multiplied in order to obtain the maximum usable frequencies. These factors are based on average observations over a period of time, and may be applied either to average critical frequencies to give average transmission conditions, or to a given observation of a critical frequency to obtain approximate transmission conditions at a given time.

VIII. CONCLUSIONS

The type of transmission curves described above have been in use at the National Bureau of Standards for the past 2 years in studying the correlation of high-frequency radio-transmission conditions with regular ionosphere observations. The results of continuous measurements of high-frequency broadcasting stations and observations on other high-frequency signals, as well as the results of some specific experiments have been compared with vertical-incidence data. Practically all the available data agree with what would be expected on the basis of the theory outlined above, and the exceptions may in most cases be accounted for.

WASHINGTON, November 22, 1937.

sured distance laid off on the main distance scale (increasing stances lie to the right) gives the value of sec ϕ_0. The sition of the point of intersection to the curved dashed lines of qual ψ gives the value of the angle of departure of the waves from the horizontal. A point of intersection falling above the $\psi=0°$ line dicates an impossible case, where the ray would have to depart t an angle below the horizon.

For example, a distance of 2,400 km and a virtual height of 400 m corresponds to a sec ϕ_0 of 3.07, and an angle of departure of 6.2°.

VII. TRANSMISSION FACTORS

When average transmission conditions over a period of time or hen a variety of transmission paths are to be considered, or when n estimate of the maximum usable frequencies is to be made without precise knowledge of the ionosphere over the transmission path, it s convenient to have available a means by which the maximum sable frequencies may be quickly estimated from an approximate alue of the vertical-incidence critical frequency.

The National Bureau of Standards is now developing a tabulation f factors by which the critical frequency for the o-component, easured at vertical incidence may be multiplied in order to obtain he maximum usable frequencies. These factors are based on average bservations over a period of time, and may be applied either to verage critical frequencies to give average transmission conditions, r to a given observation of a critical frequency to obtain approximate ransmission conditions at a given time.

VIII. CONCLUSIONS

The type of transmission curves described above have been in se at the National Bureau of Standards for the past 2 years in aking the correlation of high-frequency radio-transmission resu tions with regular ionosphere observations. The results of con tinuous measurements of high-frequency broadcasting stations and bservations on other high-frequency signals, as well as the results f some specific experiments have been compared with vertical- ncidence data. Practically all the available data agree with what ould be expected on the basis of the theory outlined above, and the xceptions may in most cases be accounted for.

Washington, November 22, 1937.

U. S. DEPARTMENT OF COMMERCE NATIONAL BUREAU OF STANDARDS

RESEARCH PAPER RP1101

Part of Journal of Research of the National Bureau of Standards, Volume 20, May 1938

A PORTABLE APPARATUS FOR MEASURING VIBRATION IN FRESH CONCRETE

By George L. Pigman, Floyd B. Hornibrook, and Jesse S. Rogers

ABSTRACT

A portable vibrograph was designed and constructed for measuring vibration in fresh concrete during the process of placing by vibration. An electromagnetic type of pickup unit, submerged with definite orientation within the concrete, picks up the vibrations and conveys an electric response through either of three electric circuits, and then through an amplifier to a cathode-ray oscillograph. Particle displacements, velocities, or accelerations can be measured and displacement, velocity, or acceleration wave forms obtained, depending upon the circuit chosen. Frequencies which form simple ratios with 60 cycles can be measured accurately, and other frequencies can be estimated.

The integrating or differentiating circuit-amplifier-oscillograph system was found to cause a variation of less than 3 percent in the recording of a constant input for frequencies ranging from approximately 20 to 300 c/s.

The pickup unit was calibrated by use of microscope observations of amplitudes of vibration of a steel plate, vibrating in a horizontal direction at approximately 60 c/s, to which the pickup unit was attached. The amplitudes included in this calibration ranged from approximately 0.045 to 0.00035 in. Lower amplitudes were evaluated by extrapolation.

Calibrations of the acceleration and velocity scales were made by replacing the pickup unit with an audio-frequency oscillator supplying a sine wave of known frequency and voltage, corresponding to calibrated amplitudes. Accelerations ranging from approximately $\frac{1}{16}$ to 40 times gravity, and velocities ranging from 0.01 to 2.5 f/s were included in the calibration.

Typical curves are presented showing the variation of amplitude of vibration in concrete with distance from the vibrator. Photographs are given showing corresponding particle displacement, velocity, and acceleration wave forms produced by vibration of concrete with two different types of vibrators.

CONTENTS

	Page
I. Introduction	707
II. Design requirements	708
III. Theory and construction of electrical and mechanical systems	708
1. General considerations	708
2. Pickup unit	709
3. Integrating circuit	710
4. Differentiating circuit	713
5. Indicating system	714
IV. Calibration	715
V. Vibration measurements	716
VI. Conclusions	721

I. INTRODUCTION

Within the past decade, numerous studies have been made of the effects of the vibration of fresh concrete. Meager data, however, are available on the actual displacements, velocities, and accelerations,[1]

[1] Throughout this paper the terms amplitude, displacement, velocity, and acceleration refer to particle motion unless otherwise specifically stated.

within the concrete. It was thought that an apparatus capable of measuring these vibration characteristics at any point within the concrete could be of value in numerous studies. Such studies might include the effectiveness of various types and sizes of vibrators, the effect of size and rigidity of forms, and the effect of different mixes and C/W ratios on the propagation of vibrations within the concrete. Accordingly, an apparatus was designed and built at the National Bureau of Standards for measuring the foregoing vibration characteristics, as well as the frequencies and the propagation velocities of the vibrations.

This paper describes the apparatus in detail and also gives a brief description of various types of measurements which have been made.

II. DESIGN REQUIREMENTS

The following requirements were considered essential for an apparatus to be used for measuring vibration in fresh concrete over a wide range of both field and laboratory conditions.

1. The unit for picking up the vibrations should be small, light, portable, mechanically rugged, and adapted to being immersed to any desired depth in the concrete, with a definite orientation.
2. The indicating device should give a continuous indication which can be read rapidly.
3. The reading should be proportional to the actual displacement, velocity, or acceleration, as the case may be, at a given point and in a given direction in the concrete.
4. With proper adjustment, the pickup unit should be capable of registering vibrational motion in either a horizontal or the vertical direction.
5. The apparatus should respond accurately over the range of amplitudes [2] and frequencies encountered in the commercial vibration of concrete.
6. A means of obtaining wave forms should be provided.

III. THEORY AND CONSTRUCTION OF ELECTRICAL AND MECHANICAL SYSTEMS

1. GENERAL CONSIDERATIONS

An electrical method of measuring the vibration in the concrete appeared to be most promising in satisfying the requirements. There are a number of well-known methods through which vibrational motion may be detected by electrical means. The motion may be caused to affect an electrical circuit through change of resistance, capacitance, or inductance, or through electromagnetic or piezoelectric effects. While certain of these methods [3 4 5] have been utilized to measure one vibration characteristic (either displacement, velocity, or acceleration) it is desirable to measure all three characteristics with one detecting circuit.

It was found that all three of these vibration characteristics could be measured by using a pickup of the electromagnetic type, which has a voltage output proportional to the velocity, and by combining

[2] Amplitude refers to the maximum displacement from the position of rest.
[3] U. S. Bureau of Mines Tech. Paper 518 and 556.
[4] C. D. Greentree, Gen. Elec. Rev. 40, No. 9 (Sept. 1937).
[5] M. Mary, Ann. Ponts et Chaussées 106, 338 (March 1936).

this pickup with electrical circuits for integrating and for differentiating the voltage from the pickup. In addition, the electromagnetic type of pickup unit is adapted to the desired simple, compact, and rugged construction, and requires a minimum of adjustment and recalibration.

A similar method of utilizing an electromagnetic detecting system in conjunction with electrical circuits to obtain displacements, velocities, and accelerations has been used by Meyer and Böhm.[6] The principles of their circuits are considerably different, however, from those described in the present paper, a different frequency range was covered in their work, and less accurate results were considered satisfactory.

Beale and Stansfield[7] have described an electromagnetic pickup and a resistance-capacitance type of integrating circuit used in pressure studies of diesel-engine operation. Draper and Bentley[8] have described a similar pickup unit and integrating circuit used in studying aircraft vibration during flight.

The present apparatus uses a pickup and an integrating circuit similar to those used by the above-mentioned investigators. In addition, it contains a differentiating circuit, so that by a simple switching arrangement either the displacement, velocity, or acceleration as a function of time may be shown on the oscillograph screen.

2. PICKUP UNIT

The mechanical design of the pickup unit follows the general principles of seismic vibration measuring devices. The unit consists essentially of an electromagnet (the seismic element) coupled through a spring of low stiffness to the vibrating member, the mass of the electromagnet and the spring constant being adjusted so that the electromagnet remains relatively motionless throughout the frequency range to be covered. The pickup coil is rigidly attached to the vibrating member (the case). Hence, the relative motion between the electromagnet and the pickup coil causes an induced electromotive force in the coil which is proportional to the instantaneous velocity of the vibrating member.

The first instrument made was constructed so that with the proper adjustment, measurements could be made in either a horizontal or the vertical direction. During experimentation in the measurement of vibration in concrete, it became evident that for the most widely used types of vibrators, including the internal and form types which vibrate in a horizontal plane, it was sufficient for the instrument to respond only to horizontal vibrational motion. Hence a new instrument was constructed which, by making it suitable for horizontal measurement only, was made more compact and rugged.

This second instrument is shown diagramatically in figure 1. The external dimensions are approximately 2¼ by 2¼ by 2½ in. The weight of the pickup unit and supporting rod together is about 2½ lb. The bulk specific gravity of the pickup unit is approximately 3.2.

As shown in figure 1, the suspension of the stationary magnet in this instrument consists of two phosphor-bronze strips, about 0.005 in.

[6] Elek. Nachr. Tech. 12, 404 (1935).
[7] Engineer 160, 667 (1935).
[8] J. Aero. Sci. 3, 116 (1936); 4, p. 281 (1937).

in thickness. The width and thickness of the middle section of each strip was decreased to obtain a natural period of the magnet of about ¼ second. A phosphor-bronze leaf spring was adjusted to exert a light pressure upon the surface of the magnet in order to produce sufficient damping to minimize the effect of transient vibration.

A semiflexible joint between the pickup-unit case and the supporting rod (section *A–A'*, fig. 1) allows free movement of the unit in the direction of measurement, but simultaneously provides high strength

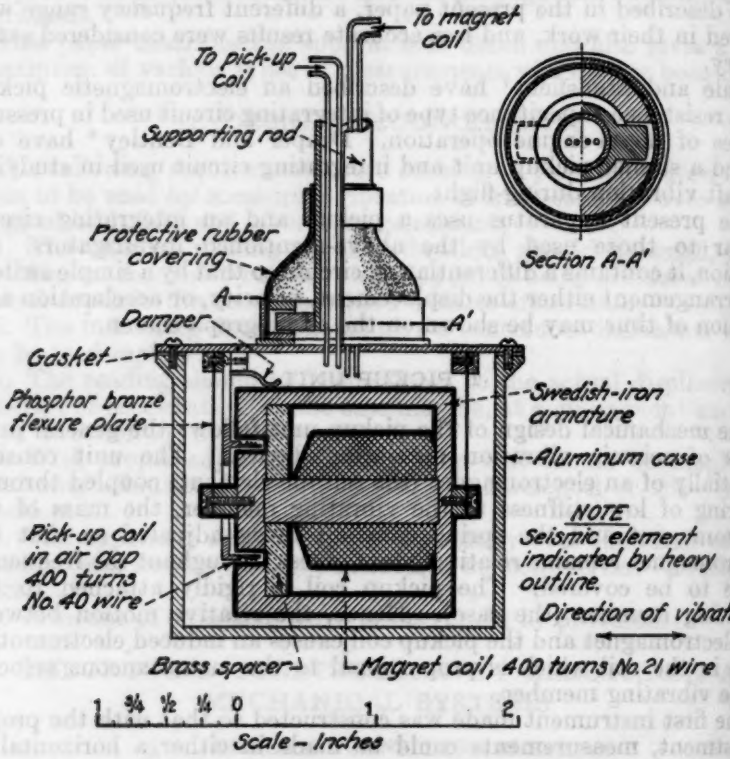

FIGURE 1.—*Schematic drawing of pickup unit.*

to allow the unit to be pushed, twisted, or pulled in any manner to permit rapid placement and alignment in the desired position in the concrete. The instrument is watertight, but its internal parts are readily accessible for any adjustment or repair.

3. INTEGRATING CIRCUIT

The integrating circuit [9] is shown in figure 2. The pickup coil, P, moving in a uniform magnetic field, has at any instant an induced electromotive force which is proportional to the pickup coil velocity, that is, $e=K(dx/dt)$, where x is the displacement of the coil from its

[9] For discussions of the theory involved, see Beale and Stansfield, Engineer **160**, 667 (1935); also Draper and Bently, J. Aero. Sci. **3**, 116 (1936); **4**, 281 (1937).

position of rest and K is a constant. For a single sinusoidal vibration of frequency $\omega/2\pi$ the current in the circuit will be

$$i=\frac{e}{\sqrt{R^2+(\omega L-1/\omega C)^2}}, \tag{1}$$

where R is the resistance, in ohms, in series with the condenser of capacitance C farads, and L is the inductance in henries of the pickup

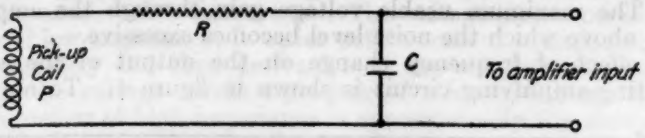

FIGURE 2.—*Diagram of integrating circuit.*

coil. If R and C are increased and L decreased sufficiently to make the term $(\omega L-1/\omega C)^2$ small compared with R^2, then approximately, $i=e/R=K(dx/dt)/R$.

In a complex wave the circuit introduces a phase distortion, due to the difference in phase lead of the various harmonic components.

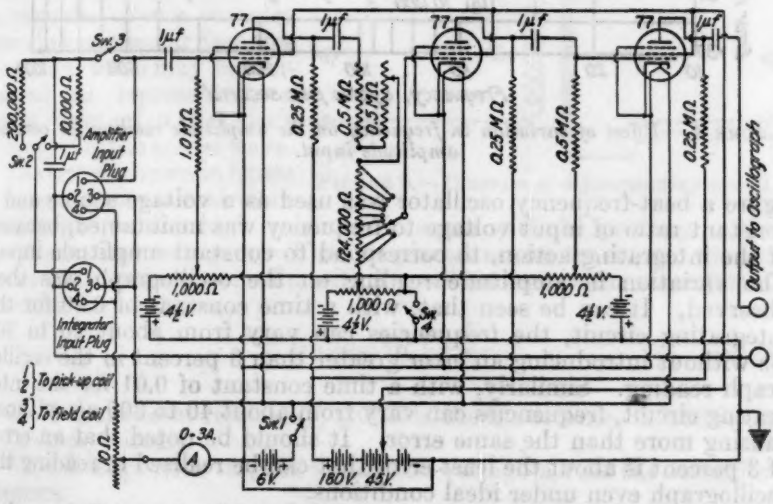

FIGURE 3.—*Diagram of integrating and amplifying circuits.*

Temporarily neglecting this phase distortion, the voltage across the condenser terminals at any instant, t, is then

$$E_c=\frac{1}{C}\int_0^t idt=\frac{K}{CR}\int_0^t\frac{dx}{dt}dt=\frac{K}{CR}x_t, \tag{2}$$

that is, E_c is proportional to the displacement at the time, t. If E_c then is applied through an amplifier to the deflecting plates of an oscillograph having a linear time axis, the trace on the oscillograph

screen will give an accurate picture of the displacement of the pickup as a function of time.

The integrating and amplifying circuits are shown in figure 3. The value of C used in the integrating circuit is 1 μf; two values of R are included, 10,000 and 200,000 ohms, respectively. Using the resistance of 10,000 ohms, making the time constant (CR) equal to 0.01, the sensitivity is approximately 20 times that when the resistance R equals 200,000 ohms ($CR=0.20$). The amplifier has three resistance-capacitance coupled stages using pentode tubes having high gain. The maximum usable voltage gain through the amplifier is 35,000, above which the noise level becomes excessive.

The effect of frequency change on the output of the complete integrating-amplifying circuit is shown in figure 4. To obtain this

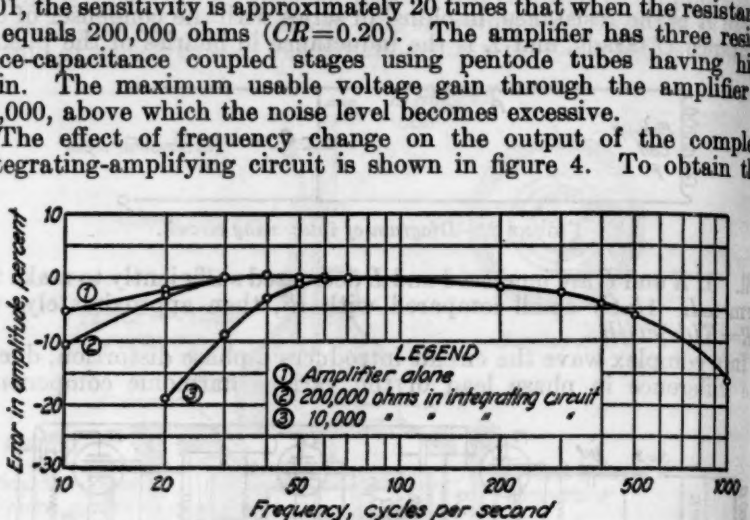

FIGURE 4.—*Effect of variation in frequency on the amplitude reading for constant amplitude input.*

figure a beat-frequency oscillator was used as a voltage source and a constant ratio of input voltage to frequency was maintained, because of the integrating action, to correspond to constant amplitude input. The variation in amplitude reading on the oscillograph was then observed. It can be seen that, with a time constant of 0.20 for the integrating circuit, the frequencies can vary from about 20 to 300 c/s without introducing an error greater than 3 percent in the oscillograph reading. Similarly, with a time constant of 0.01 for the integrating circuit, frequencies can vary from about 40 to 300 c/s without causing more than the same error. It should be noted that an error of 3 percent is about the least error that can be realized in reading the oscillograph even under ideal conditions.

Above 300 c/s the error increases, reaching 16 percent at 1,000 cycles. In commercial vibration of concrete, practically all vibrators operate in the frequency range of 50 to 150 c/s, and it is probable that most significant harmonics occur below 1,000 c/s.

The phase lead for a sinusoidal current of frequency $\omega/2\pi$ is $\theta=\tan^{-1} 1/\omega RC$, and represents the maximum phase error for any harmonic. Substituting the circuit constants in this expression, it is found that the phase distortion for the circuit with the time constant of 0.20 is negligible. In this case the angle θ is about 2.3 degrees at 20 cycles and decreases at higher frequencies. The circuit with the time constant of 0.01 (designed to be used only at frequencies above 100 c/s) gives a value of 9 degrees for the angle θ at 100 cycles. Even this maximum distortion, representing a shift of 1/40 wave length, is

normally insignificant, particularly as the higher harmonics are generally of comparatively low magnitude in the original wave and contribute even less proportionally to the shape of the integrated wave.

4. DIFFERENTIATING CIRCUIT

Several different electrical circuits may be used to perform what corresponds to a mathematical differentiating process and thus to convert an alternating voltage representing a velocity-time wave into its corresponding acceleration-time wave. The voltage measured across an inductor of low impedance, in series with a resistor of high resistance, is approximately the time derivative of the current in the circuit. Similarly, the voltage across a resistor of a low resistance in series with a capacitor of high impedance is approximately the time derivative of the voltage across the circuit. However, the circuit adopted as most satisfactory for the present purpose is shown in figure 5, wherein e_1 is an alternating voltage obtained from the pickup unit, and e_2 is the voltage output after passing through the differentiating circuit. For convenience, it may be assumed that $e_1=E \sin \omega t$, where E is a constant, $\omega=2\pi f$, f is the frequency in cycles per second, and t is the time in seconds. For a complex wave in a particular case this sinusoidal wave may be considered as representing a single term of a Fourier's series giving the actual wave.

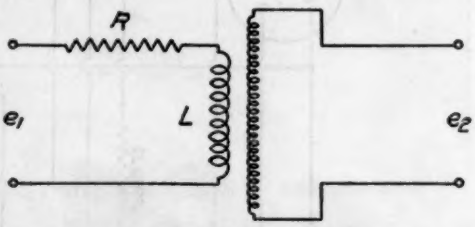

FIGURE 5.—*Diagram of differentiating circuit.*

The circuit shown in figure 5 is essentially an air-core transformer, with a high resistance in series with the primary. With the alternating voltage $e_1=E \sin \omega t$ placed across the input, the current i in the primary circuit, with a small current in the secondary, is given by the equation

$$E \sin \omega t = iR + L\frac{di}{dt}, \tag{3}$$

where R is the total resistance, and L is the inductance, in henries, of the primary circuit.

With R large with respect to $L\omega$, the voltage across the secondary becomes

$$e_2 = \frac{M}{R} E\omega \cos \omega t, \tag{4}$$

$$\text{or } e_2 = \frac{M}{R}\frac{de_1}{dt} = \frac{MK}{R}\frac{d^2x}{dt^2} \text{ (from eq 2)} \tag{5}$$

where d^2x/dt^2 is the acceleration at the time, t, and M is the mutual inductance, in henries, of the primary and secondary coils.

The phase distortion due to the difference in phase lag $\theta=\tan^{-1} L\omega/R$ is negligible with the given constants for all significant harmonics.

The present circuit has an advantage over the other differentiating circuits mentioned, in that the relation between the resistance and

the reactance of the coil in the input circuit is of small consequence, a condition which becomes of greater importance at low frequencies. Also, while a large voltage loss occurs in any of the three circuits, a portion of the loss may be regained in the present one by increasing the amount of winding on the secondary coil. The amount which the number of secondary turns may be increased is limited by the size of the coil and the amount of shielding required.

A diagram of the differentiating circuit with the constants and the switching arrangement used, is shown in figure 6. For the

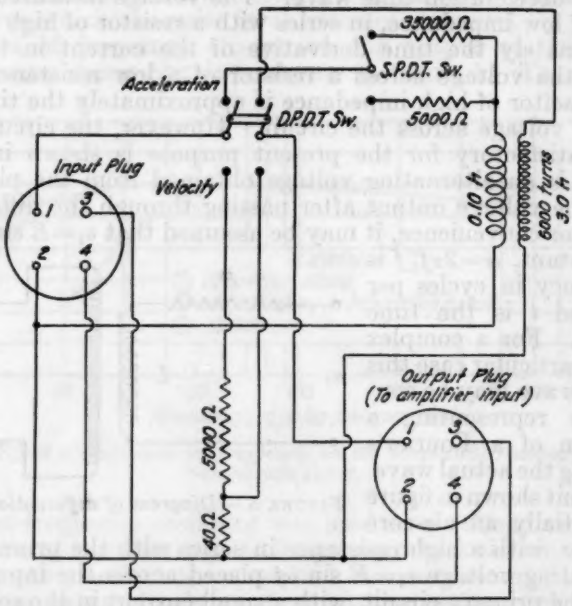

FIGURE 6.—*Diagram of the acceleration and velocity measuring circuits.*

constants chosen, as shown in the diagram, and with the input voltage corresponding to constant acceleration, the relation between acceleration reading on the oscillograph and the frequency follows the curve shown for the amplifier alone in figure 4.

Included in figure 6 is a voltage attenuating circuit with constants adjusted so that the desired range of velocity readings may be obtained to correspond to the displacement and acceleration scales.

5. INDICATING SYSTEM

A cathode-ray oscillograph with 5-in. screen serves as an indicating device, the screen being ruled in 0.10-in. divisions to permit rapid readings of the beam deflection. The oscillograph also contains a single-stage amplifier, which gives a voltage gain of about 25, making the total available voltage gain in the apparatus approximately 900,000.

For precise results, such high amplification might be undesirable. In the present case, variations of 5 percent are not considered excessive, and, with a simple rapid method of checking the calibration at any time having been devised, described in a later section, the magnitude of amplification used is not objectionable.

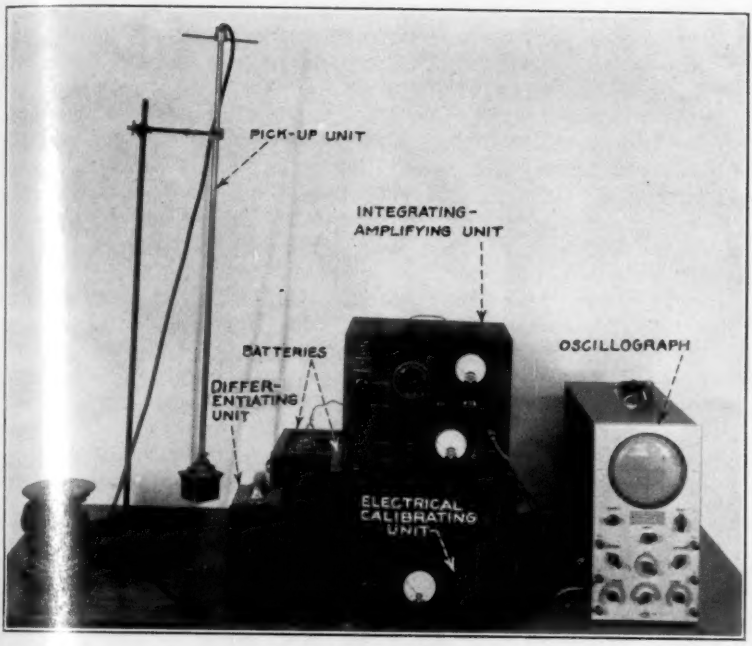

FIGURE 7.—*Assembled vibrograph.*

The oscillograph may be utilized to measure frequency of vibration, although it is often simpler to measure the frequency of the vibrator directly with some form of frequency meter. If the frequency to be measured, however, forms a simple ratio with 60 cycles, it can be determined directly through the patterns it forms on the oscillograph screen when the sweep circuit has been synchronized with the 60-cycle power supply. The accurate determination of any other frequency by means of the oscillograph required the use of a source of alternating voltage of known variable frequency.

Figure 7 shows the complete apparatus, assembled as it is used in making measurements.

IV. CALIBRATION

Calibration of the apparatus for displacement measurement was accomplished through the use of a steel plate (approximately 24 by 5 by $\frac{1}{16}$ in.) held in a vertical plane by being clamped at both ends to heavy concrete blocks. The pickup unit was bolted to the center of the plate, and the plate caused to vibrate horizontally by a rotating, motor-driven eccentric mass also attached to the center of the plate. The amplitude of vibration of the pickup unit was observed through a microscope, having a calibrated reticule in the eyepiece, sighted upon a fine crosshair on the top of the pickup unit. It was found that with the ends of the steel plate held in this manner, and the rotating eccentric driven at frequencies from 50 to 70 c/s, the vibration obtained was smooth and linear in character, and in general could be held to a very constant value. The amplitudes obtained for the calibration in this manner ranged from 0.045 in. to 0.00035 in.

During the calibration process, the various resistors in the tapped gain-control of the amplifier were adjusted in value to give the desired beam deflections on the oscillograph for the chosen amplitude ranges. A 3-in. total deflection of the oscillograph beam was obtained for amplitudes of approximately 0.045, 0.015, 0.0045, and 0.0015 in., respectively, with 200,000 ohms in the integrating circuit, and for amplitudes of approximately 0.0020 and 0.0010 in., respectively, with 10,000 ohms in the integrating circuit. For each range a linear relation was obtained between the optically measured amplitude and the oscillograph beam deflection.

Although in this scale calibration the frequency was maintained between 50 and 70 c/s, other tests were made at constant amplitude in which the frequency was varied from approximately 30 to 100 c/s (the frequency limits of the available vibration source) to check the linearity of the pickup unit output. No deviation from linearity was found in that range.

In order to utilize all of the available amplification, and to increase the range of the apparatus for the measurement of amplitudes too small to be conveniently observed by optical methods, an extrapolation was made. Observations were taken of the input voltages, at 60 c/s, necessary to give a definite oscillograph-beam deflection as the controls were set, first for each of the calibrated amplitude ranges, and then for each of the uncalibrated ranges. Assuming that the straight line relation found for the ranges covered by direct calibration still holds, the calibration can be extended for the evaluation of lower amplitudes. In this manner four additional ranges were obtained,

the lowest of which gives a 3-in. total oscillograph deflection for an amplitude of approximately 0.00002 in.

The calibration of the acceleration and velocity measuring circuits was accomplished through the use of a beat-frequency audio oscillator with an output wave containing a harmonic content of approximately 0.5 percent. With a constant voltage output from the oscillator, at a known frequency, the signal was applied to the calibrated integrating circuit and then to the uncalibrated acceleration and velocity measuring circuits, respectively, and corresponding readings were obtained under the three conditions. The amplitude corresponding to the given input signal was known from the first reading, and, with the signal being a sine wave of known frequency, the corresponding maximum velocity and acceleration could be accurately computed.

The acceleration scale was calibrated for six arbitrary ranges, covering accelerations from 2 to 1,250 f/s/s, or approximately $\frac{1}{16}$ to 40 times gravity. The velocity scale was calibrated for five ranges, covering velocities from 0.01 to 2.5 f/s.

In order to detect any changes in calibration which might appear, due to variations in the integrating, amplifying, or oscillograph circuits, a portable calibration checking device was constructed. This consists of an attenuator, supplied with 60-cycle alternating current, with which a known voltage may be supplied to the input of the integrating circuit. Immediately after calibration in each range, oscillograph beam deflection readings were taken with this attenuator in the circuit. A volume control, incorporated in the amplifier, permits the amplification to be adjusted at any time to obtain these standard readings. With this device, the calibration may be rapidly checked for any range before that range is used.

In the calibration of the integrating circuit, observations were made of the oscillograph reading obtained with the pickup unit being vibrated with large amplitude at right angles to the direction in which the unit is designed to respond. It was found that even such large transverse vibration apparently had no effect on the reading. In concrete, the pickup unit should thus respond only to vibrational motion in the direction of its axis.

V. VIBRATION MEASUREMENTS

A short laboratory study was made to test the adaptability of the vibrograph to the purposes for which it was designed. Two commercial internal vibrators,[10] of rotating eccentric weight type, the outside diameters of the vibrating shafts being 1 and $2\frac{3}{4}$ in., respectively, were used for vibrating the concrete. The small vibrator is directly driven by a $\frac{1}{3}$-hp electric motor, and operates at frequencies from 9,000 to 14,000 rpm. This vibrator is of a type designed to compact laboratory specimens, and was not intended for field work. The large vibrator is hydraulically operated, being driven by a 3-hp electric motor and can be operated at any frequency below 6,500 rpm. The amplitudes of vibration of the two vibrators when suspended in air were approximately 0.012 and 0.050 in., respectively. There was no appreciable diminution in vibrator amplitude when either vibrator was immersed in concrete, according to measurements made just above the immersed section of the vibrator.

[10] The vibrators were generously lent to the Bureau for these studies by the Viber Co., Ltd., and by the Electric Tamper and Equipment Co.

For most of the study a clay concrete was used, proportioned 1:2.2:3.8 parts by weight of clay, sand, and graded aggregate, respectively. The form used was 4 by 4 by 2 ft. high, inside dimensions, having rigid 4-in. concrete walls and base. During vibration of the concrete, almost no vibration was perceptible in the walls of the form.

With the limited data obtained, no attempt was made to evaluate the effects upon amplitude distribution in the concrete of such variables as size and shape of vibrator, size, shape, and rigidity of form, the frequency of vibration and variations in mix. However, several typical curves are presented in which some of these factors are varied.

Figure 8 shows the variation of amplitude of horizontal vibration at different depths in the concrete at various distances from the

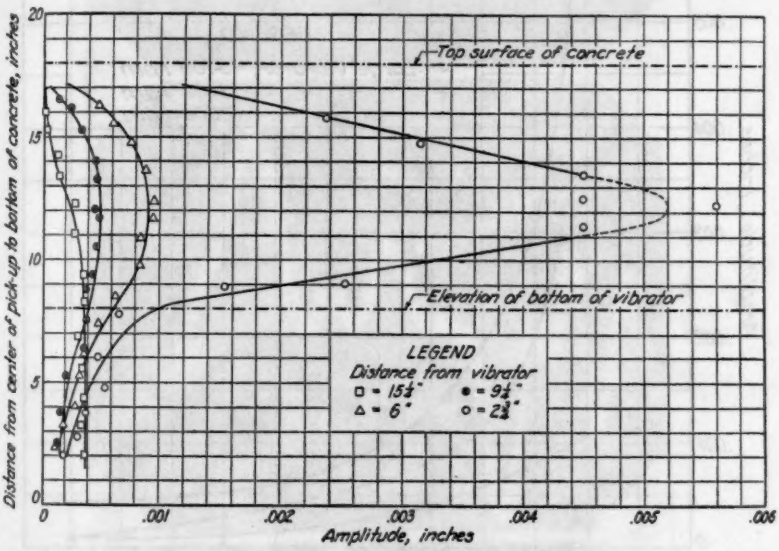

FIGURE 8.—*Variation of displacement amplitudes of vibration with depth in concrete at various distances from the vibrator.*

vibrator. The latter was held in the same position throughout (near the midpoint of the concrete) while the pickup unit was moved along the diagonal of the form. This figure indicates the necessity for carefully controlling the depth of immersion of the pickup unit during measurements, especially near the vibrator.

Figure 9 shows the variation of horizontal amplitude with distance from the vibrator for two different speeds of the large vibrator and one speed of the small vibrator. In obtaining these data, the vibrator was moved towards the pickup unit, the latter being maintained in one position at approximately the midpoint of the immersed section of the vibrator.

The accuracy of the points shown in figure 9 depends upon the degree in which the pickup unit will follow the actual motion of the concrete which surrounds it. This in turn depends upon (1) the ratio of the wave length of the vibratory wave in the concrete to the size of the pickup unit, (2) the change in amplitude in the concrete over the

length of the pickup unit, (3) the density of the pickup unit, and (4) the ease with which the concrete will flow around the unit, or the "internal friction" of the concrete. It is probable that in this respect the pickup unit acts as a piece of aggregate of the same approximate dimensions.

It will be shown later that with the frequencies ordinarily used in vibrating concrete the wave length is large with respect to the length of the pickup unit. The average specific gravity of the entire pickup unit is about 3.2, which is somewhat higher than the average value

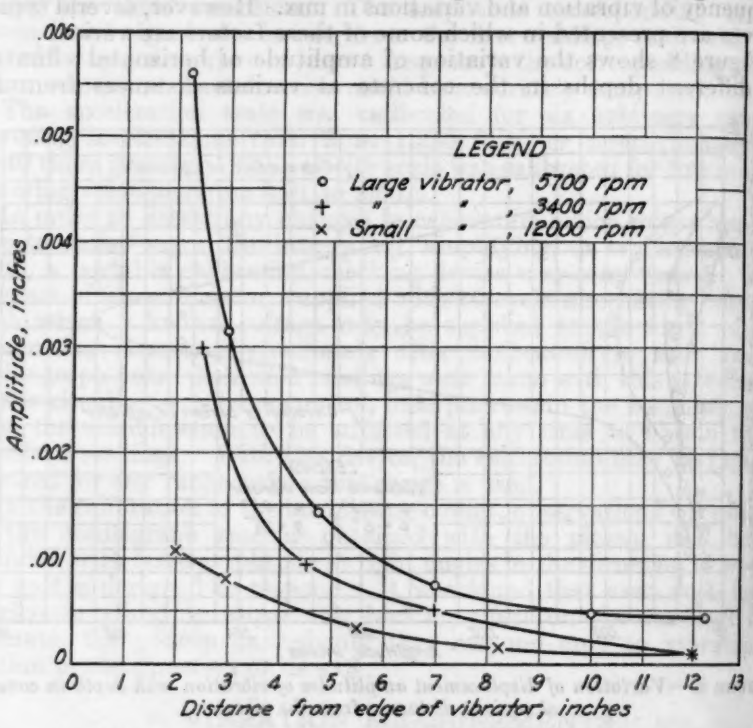

FIGURE 9.—*Variation of displacement amplitude with distance from vibrator for clay concrete contained in rigid concrete form.*

for concrete. However, as the seismic element remains nearly stationary, the mass being accelerated is less than the total mass of the pickup unit, and unduly large inertia forces are not expected to be present. The "internal friction" of concrete is considerable, even with relatively large amounts of water present, and in the dry concretes generally best adapted to placement by vibration is probably particularly great in magnitude. The amplitude-distance curves given in figure 9 for the large vibrator show that for distances from the source of vibration greater than 4 or 5 in. the amplitude gradient is not excessively large. Considering all of these factors it may be assumed that beyond 4 or 5 in. the pickup unit registers some average value of the amplitudes distributed over its surface. For distances less than about 4 in. the absolute value of the amplitude reading is to be questioned. However, from consideration of the regularity of the points

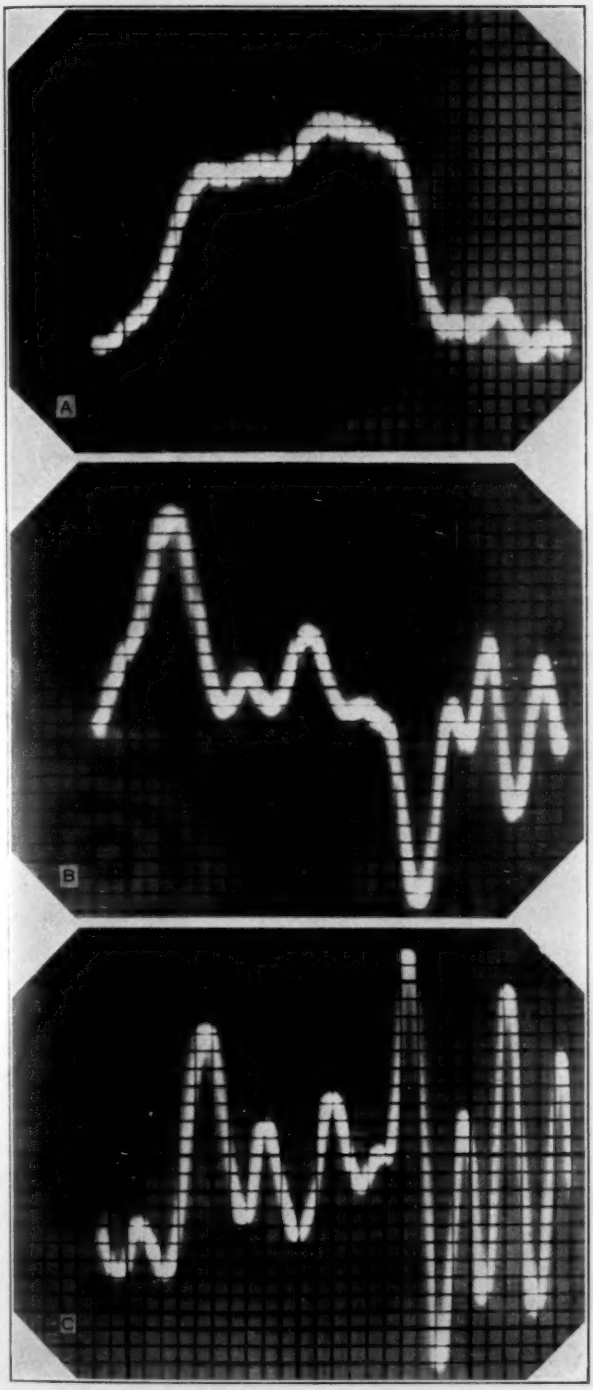

FIGURE 11.—*Corresponding displacement, velocity, and acceleration wave forms, A, B, and C, respectively, with correct phase relations maintained, of vibration produced in concrete with a compressed-air vibrator.*

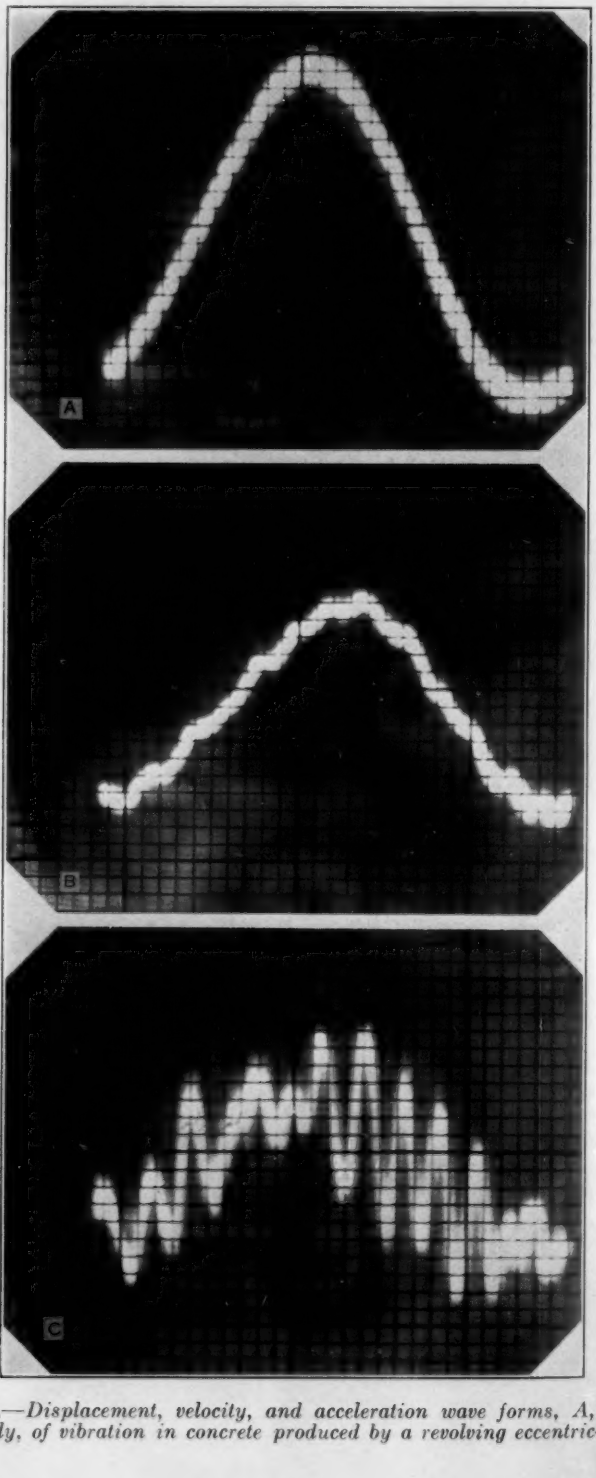

FIGURE 12.—*Displacement, velocity, and acceleration wave forms, A, B, and C, respectively, of vibration in concrete produced by a revolving eccentric-weight type vibrator.*

in figure 9 and their relation to the amplitude of the freely suspended vibrator, it is probable that even in this region the readings give a fair approximation of the true amplitudes in the concrete.

Figure 10 shows the variation of horizontal amplitude in portland cement concrete contained in a heavy wooden form, 2⅔ by 4½ ft. by 2 ft. high inside dimensions. In this case, although the vibrator was moved along the middle line of the box, the form itself vibrated very perceptibly, and the concrete was affected much more by the vibrator than was the clay concrete contained in the rigid concrete form (see fig. 9). (The clay concrete in the rigid form appeared, in general, to be compacted only 4 to 7 in. from the vibrator; the cement concrete in the wooden form was nearly all compacted in a short time.)

For the purpose of obtaining typical wave forms of several types of concrete vibrators, and to demonstrate qualitatively the actions of the integrating and differentiating circuits, records were made of the oscillograph traces obtained with the pickup unit immersed in clay

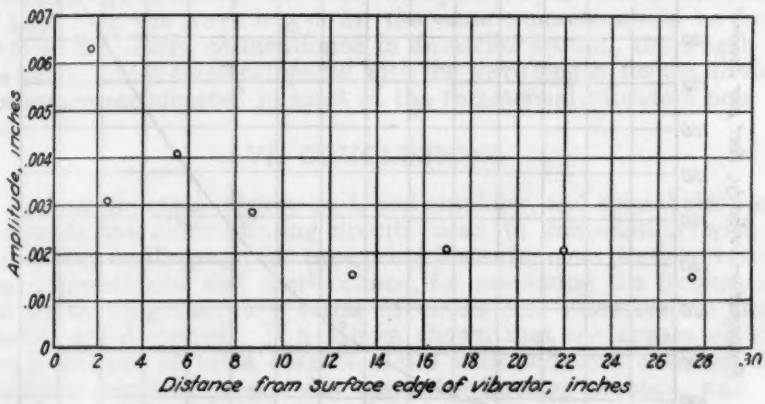

FIGURE 10.—*Variation of displacement amplitude with distance in portland cement concrete contained in heavy wooden form.*

concrete to which vibration was being applied. Figure 11 shows wave forms obtained with a reciprocating compressed-air vibrator applied to the form, *A*, *B*, and *C* being respectively the displacement, velocity, and acceleration waves. The correct phase relation was maintained between the photographs by synchronizing the oscillograph sweep circuit with the vibrator frequency by means of a second pickup unit. The fundamental wave of *A* has a frequency of approximately 110 c/s. A close inspection of the three waves will reveal that, going from *A* to *B* to *C* in that order, for the same abscissa the ordinate of each succeeding wave is proportional to the slope of the preceding one. Thus the maximum peak of velocity wave *B* corresponds precisely to the region of maximum slope of the displacement wave *A*.

As a further check on the validity of the relation indicated in the sequence of the three curves, the areas under the acceleration and velocity curves were measured with a planimeter and the corresponding velocity and displacement wave forms plotted (with arbitrary adjustment of scale). The plotted wave forms agreed closely with the pictured forms, although lack of linearity of the time base (oscillograph

sweep circuit) prevented precise superposition of the plotted wave on the picture.

The predominant part played in the velocity and acceleration waves by the high-frequency components, which are relatively unimportant in the displacement wave, is to be particularly noted, and appears to be characteristic of the vibration produced by piston-type vibrators.

Figure 12 gives the corresponding wave forms obtained with the large internal vibrator described in an earlier section, operating at a frequency of approximately 3,600 rpm. As before, *A*, *B*, and *C* are respectively the displacement, velocity, and acceleration waves, but in this case the correct phase relation was not maintained between the three traces. It may be noted that, although the displacement wave is superficially sinusoidal, high-frequency components, again,

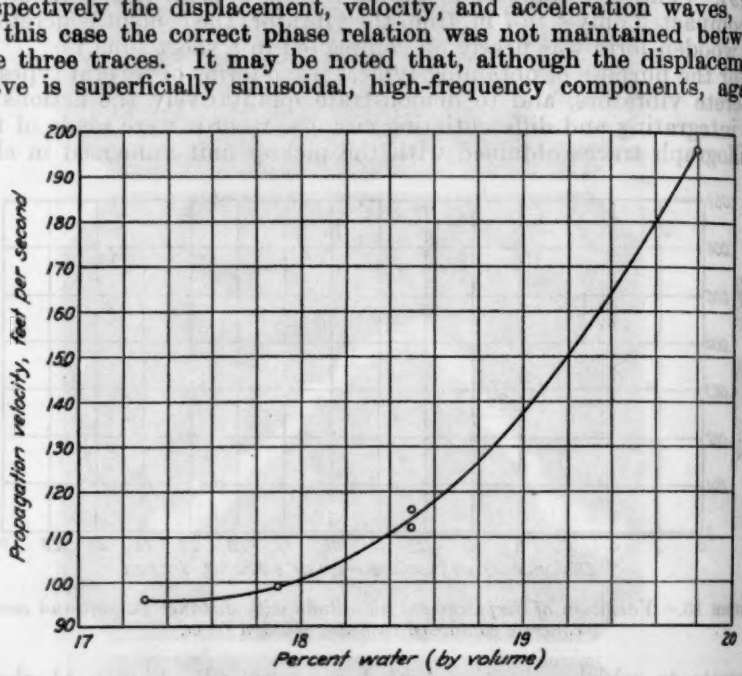

FIGURE 13.—*Variation of the velocity of propagation of vibration through concrete, proportioned 1:2.2:3.8 by weight, with change of water content of the concrete.*

are very evident in the acceleration wave form. The maximum acceleration associated with the harmonic waves alone, shown in figure 12 (*A*), is of the same order of magnitude as the maximum acceleration associated with the fundamental wave alone. It seems probable, therefore, that attempts to correlate efficacy of vibration with acceleration may yield misleading results when the values for acceleration are obtained by computations from amplitude and frequency data under the assumption that no harmonics are present. Unless the absence of appreciable harmonics is demonstrated (i. e., a truly sinusoidal displacement wave obtained), the possible effects of the harmonics should be considered.

Another type of measurement that can be made with this instrument is illustrated by figure 13, which shows the variation of velocity of propagation of vibration with change in the water content of portland cement concrete proportioned 1:2.2:3.8 by weight. When two pickup

units, one at the source of vibration and one several feet away in the concrete are used, and the oscillograph sweep is synchronized with the closest pickup unit, then as the second pickup unit is moved toward or from the vibrator, a phase shift occurs in the oscillograph pattern which is equal to the phase shift within the concrete over the distance moved. From this the wave length in the concrete can be determined. Knowing the frequency f and the wave length λ, the velocity can be calculated according to the relation $v=f\lambda$.

The technique used in making these particular measurements was not refined and accordingly the values given are first approximations only.[11]

The trend indicated in figure 13 was found to hold for concretes having much greater water content than shown, and measurements of the velocity in water gave results within 15 percent of the accepted value of the velocity of sound in water.

For the velocities indicated in figure 13 the wave lengths varied between 8 and 16 in., the frequency being 9,000 rpm. At a frequency of 3,600 rpm, the wave length for the same concrete would be from 20 to 40 in. Thus, as mentioned in an earlier section, the length of the pickup unit is small compared with the wave length, for the driving frequencies encountered in most of the commercial vibrators now in use.

VI. CONCLUSIONS

An electromagnetic pickup unit, and amplifier, and special electrical integrating and differentiating circuits used in conjunction with a cathode-ray oscillograph for measuring instantaneous particle velocities, displacements, and accelerations, for measuring the frequencies and for showing the wave forms of mechanical vibrations in fresh concrete are described. It has been shown that the apparatus will give a measure of these characteristics with sufficient accuracy for conditions found in present-day concrete-vibration practice, and, in addition, is adapted to a variety of more precise laboratory tests.

Appreciation is expressed to members of the Bureau's sound section, particularly to W. F. Snyder, for their assistance in the development and calibration of some of the electrical circuits.

WASHINGTON, March 4, 1938.

[11] Wave velocities as low as 260 f/s in peat and 360 f/s in fine sand have been reported. R. Koehler and A. Ramspeck, Veröffent Inst. Deut. Forschungsges. Bodenmechanik. 4, 9 (1936).

○